

Thomas Höfler, BSc

## **Chemical Reactions and Modifications of Lignin**

### **MASTER'S THESIS**

to achieve the university degree of

Diplom-Ingenieur

Master's degree programme: Technical Chemistry

submitted to

**Graz University of Technology**

Supervisors

Ao. Univ.-Prof. Dr.phil. Martin Mittelbach  
Dr.rer.nat. Sigurd Schober

Renewable Resources Group  
Institute of Chemistry, University of Graz

## **Eidesstattliche Erklärung**

### ***AFFIDAVIT***

Ich erkläre an Eides statt, dass ich die vorliegende Arbeit selbstständig verfasst, andere als die angegebenen Quellen/Hilfsmittel nicht benutzt, und die den benutzten Quellen wörtlich und inhaltlich entnommenen Stellen als solche kenntlich gemacht habe. Das in TUGRAZonline hochgeladene Textdokument ist mit der vorliegenden Masterarbeit identisch.

*I declare that I have authored this thesis independently, that I have not used other than the declared sources/resources, and that I have explicitly indicated all material which has been quoted either literally or by content from the sources used. The text document uploaded to TUGRAZonline is identical to the present master's thesis.*

---

Date

---

Signature

## Abstract

Lignin is the second most abundant biopolymer on earth and by far the biggest carrier of aromatic moieties. Yet, most of this potential remains unused, as the majority of lignin produced from the pulp and paper industry is burned to supply heat and power to the mill.

This master's thesis had two aims. Firstly, commercial lignin samples and samples from paper mills of the sulfate and sulfite pulping processes were characterized. The second and main aim was the production of valuable aromatic compounds from these samples with two depolymerization strategies. The electrochemical oxidation of the lignin feedstocks, carried out with a boron-doped diamond (BDD) anode, only led to the generation of low molecular mass organic acids and CO<sub>2</sub>. This led to a decrease in organic matter of the molecule, as confirmed via size-exclusion chromatography (SEC) and a decreasing chemical oxygen demand (COD). Thus, the BDD anode is not suitable for the electrochemical generation of aromatic moieties from lignin. A more promising way to generate valuable products was presented via a high-pressure reduction at elevated temperatures. This reduction could generate up to 65 % of a product oil, containing valuable products, mainly consisting of phenolic compounds. It was possible to extract up to 16.8 % of phenols from the different lignin feedstocks with this method. Besides that, a relatively high amount of resin components, like dehydroabietic acid methyl ester and various fatty acids, could also be found.

Analysis of depolymerization educts and products was mainly carried out by gas chromatography/ mass spectrometry (GC-MS), aided by SEC, Fourier-transform infrared (FTIR) spectroscopy and liquid chromatography/ mass spectrometry with time of flight detection (LC-TOF-MS). Important parts of the feedstock characterization were solubility tests with aqueous and organic solvents, FTIR spectroscopy, CHNOS analysis and the determination of moisture and ash content.

## Kurzfassung

Lignin, das weltweit zweithäufigste Biopolymer, beinhaltet mit Abstand den größten Anteil an aromatischen Bestandteilen in der Natur. Jedoch bleibt der Großteil dieses Potentials ungenutzt, da das in der Zellstoff- und Papierindustrie hergestellte Lignin meist verbrannt wird, um die Fabrik mit Wärme und Energie zu versorgen.

Dieser Masterarbeit lagen zwei Ziele zugrunde. Einerseits sollten käufliche Lignine und Lignine aus Papierfabriken, denen das Sulfat- und Sulfitverfahren zugrunde lagen, charakterisiert werden. Andererseits war das Hauptziel die Depolymerisierung dieser Lignine zu wertvollen, aromatischen Verbindungen. Die erste dieser Methoden, die elektrochemische Oxidation der Proben, wurde mit einer Bor-dotierten Diamantelektrode (BDD) durchgeführt. Diese Methode führte jedoch nur zur Erzeugung organischer Säuren und CO<sub>2</sub>, wodurch sich der Anteil organischen Materials im Molekül verringerte, was durch Größenausschlusschromatographie (SEC) und einen verringerten chemischen Sauerstoffbedarf (CSB) bestätigt werden konnte. Damit ist die BDD Anode nicht für die elektrochemische Erzeugung aromatischer Verbindungen aus Lignin geeignet. Eine vielversprechendere Methode für die Erzeugung wertvoller Verbindungen war die Hochdruck- und Hochtemperaturreduktion, mit der bis zu 65 % eines Produkt-Öls erzeugt werden konnten, welches hauptsächlich phenolische Komponenten enthielt. Dadurch war es möglich, bis zu 16.8 % an Phenolen aus den Ligninen zu gewinnen, wobei jedoch auch eine relativ große Anzahl an Harzsäuren und Derivaten, zum Beispiel der Methylester der Dehydroabietinsäure und Fettsäuren, identifiziert werden konnte.

Die Analyse der Edukte und Produkte wurde hauptsächlich mit Gaschromatographie, gekoppelt mit Massenspektrometrie (GC-MS), ausgeführt. Als weitere Analysemethoden wurden SEC, Fourier-Transformations Infrarotspektroskopie (FTIR Spektroskopie) und Flüssigchromatographie, gekoppelt mit einem Flugzeitmassenspektrometer (LC-TOF-MS), angewandt. Die Ausgangsmaterialien wurden auf ihre Löslichkeit in wässrigen und organischen Lösungsmitteln untersucht und mittels FTIR Spektroskopie, Elementanalyse, dem Feuchtigkeits- und Aschegehalt charakterisiert.

# Contents

Abstract .....	III
Kurzfassung.....	IV
1 Introduction .....	1
2 Theoretical Background .....	2
2.1 Wood .....	2
2.2 Wood pulping .....	7
2.3 Industrial lignins .....	12
2.4 Usage of lignins .....	15
2.5 Analytical methods .....	19
2.6 Lignin depolymerization.....	25
3 Experimental Section .....	46
3.1 Chemicals .....	46
3.2 Instruments .....	47
3.3 Lignin precipitation .....	49
3.4 Characterization.....	50
3.5 Soxhlet extraction of alkali lignin .....	54
3.6 Electrochemical oxidation (VTU) .....	55
3.7 Reactor Reactions .....	60
4 Results and Discussion.....	71
4.1 Lignin precipitation .....	71
4.2 Characterization.....	73
4.3 Soxhlet extraction of alkali lignin .....	94
4.4 Electrochemical oxidation .....	97
4.5 Reactor reactions .....	124
5 Conclusions and Outlook .....	166
List of Figures .....	168
List of Tables.....	171
References .....	174

# 1 Introduction

Lignocellulose is the most abundant form of biomass worldwide with a production of 170 billion tons per year in 2009.<sup>1</sup> In lignocellulose, lignin has the second highest percentage, thereby being the second most abundant natural polymer. Further, lignin is by far the biggest source of aromatic moieties in nature.

The main source of lignin is the pulp and paper industry, where it is a byproduct of the paper production from cellulose. From pulp industry alone, an estimated amount of 50 million tons<sup>2</sup> of lignin are produced each year.

Nevertheless, this potential is widely unused, as only 2 % of this lignin is recovered for further usage. Most of the lignin is directly burned at the pulp mill to generate heat and power for the process.

The aim of this thesis was to characterize lignin and lignin containing flows, commercial as well as real samples, from two different pulping processes, the kraft and the sulfite processes. Furthermore, the potential of generating potentially valuable low molecular products like phenols should be investigated. For that, two depolymerization methods, electrochemical oxidation and high-pressure reduction, were applied.

The lignin samples were analyzed for their solubility in various aqueous and organic solvents. Further, Fourier-Transform Infrared (FTIR) spectroscopy was applied for basic structural investigations on the lignins, while the molecular weight was analyzed via size exclusion chromatography (SEC). Other applied methods were elemental analysis and the determination of sulfur, water and ash content.

The electrochemical oxidation was carried out at VTU Engineering.<sup>3</sup> As electrode material, boron-doped diamond (BDD) was used at current densities of 200 and 1000 A/m<sup>2</sup>. Educts and products were analyzed for their chemical oxygen demand (COD), their molecular weight via SEC and for their structural features and compounds via FTIR spectroscopy and gas chromatography/ mass spectrometry (GC-MS). Additionally, liquid chromatography/ mass spectrometry with time of flight detection (LC-TOF-MS) was applied.

A method using high-pressure reduction at elevated temperatures was applied to yield valuable compounds from the lignin samples. The reaction was carried out in a batch reactor with and without the usage of hydrogen. Identification of the products was done solely with GC-MS analysis, with which also the amount of phenols in the product mixture was quantified.

## 2 Theoretical Background

### 2.1 Wood

Wood cell walls mainly consist of three components: Cellulose, hemicellulose and lignin.<sup>2,5,6</sup> A representation of this can be seen in Figure 1. The percentage of these components is mainly depending on the type of wood, but also varies between different species. Softwood, the wood from gymnosperm trees like conifers, contains about 40–44 % cellulose, 20–32 % hemicellulose and 26–34 % lignin. Compared to that, hardwood, the wood from angiosperm trees like deciduous trees, generally contains also 40–44 % cellulose, but a lower hemicellulose content of 15–35 % and 23–30 % lignin. The rest of the tree is made up of inorganics and extractives.<sup>1,5</sup> Table 1 sums up the composition of different plant resources, including softwoods, hardwoods, agricultural residues and grasses:

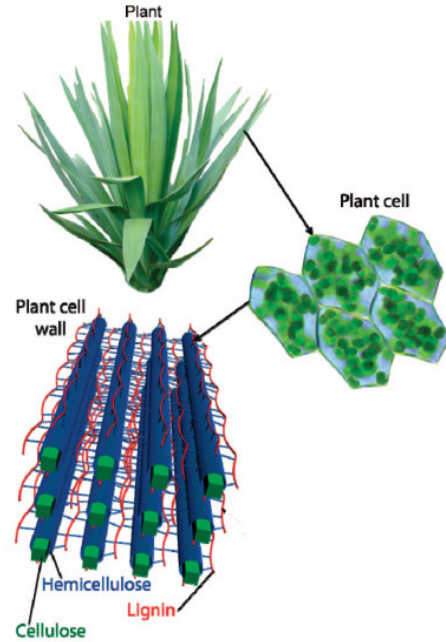


Figure 1: Schematic representation of the location of lignocelluloses in a plant (Adapted from Zakzeski et al.)<sup>4</sup>

Table 1: Biomass compositions of different plant resources

Type	Plant	Cellulose	Hemicellulose	Lignin
Softwood	White spruce <sup>7</sup>	40	31	28
	Pine <sup>8</sup>	46	23	28
Hardwood	River red gum <sup>7</sup>	45	19	31
	Poplar <sup>8</sup>	42–48	16–22	21–27
	Eucalyptus <sup>8</sup>	39–46	24–28	29–32
Agricultural residues	Rice straw <sup>7</sup>	39	24	36
	Corn stalks <sup>7</sup>	61	19	7
	Corn stover <sup>8</sup>	37	31	18
Grasses	Wheat straw <sup>9</sup>	33–40	20–25	15–20
	Miscanthus <sup>8</sup>	45–52	24–33	9–13
	Switchgrass <sup>8</sup>	32–37	26–33	17–18

Cellulose is the most abundant polymer on earth<sup>2,8</sup>, and is composed of  $\beta$ -d-glucopyranose units which are linked via 1→4 glycosidic bonds.<sup>10</sup> One cellulose molecule is made up of about 7000–15,000 monomer units, alternately rotated by 180°. <sup>11</sup> Cellulose shows a mostly crystalline structure, due to the intra- and intermolecular hydrogen bonds formed by the large number of hydroxyl groups in the chain.<sup>10</sup> The average degree of crystallinity of woody cellulose is about 50–70 %. These bonds also lead to the formation of microfibrils, which stiffen the chain and lead to aggregation, due to their highly-ordered nature.<sup>5</sup> The microfibrils do not solely show crystalline phases, which are mainly of I<sub>β</sub> type in wood compared to I<sub>α</sub> in algal and bacterial

cellulose, but also paracrystalline and amorphous regions.<sup>12</sup> The degree of polymerization (DP) of cellulose is between 3500 and 5000, depending on the type of wood and even the type of tree.<sup>10</sup>

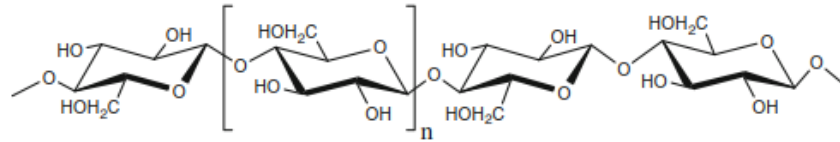


Figure 2: Molecular structure of cellulose ( $n = DP$ )<sup>5</sup>

Hemicellulose is generally composed of C5 and C6 polysaccharides<sup>13</sup>, whereas galactoglucomannans and arabinoglucuronoxylans are the main hemicelluloses in softwood and glucuronoxylans are the major hemicelluloses in hardwood.<sup>5</sup> As can be seen in Figure 3, arabinoglucuronoxylans and glucuronoxylans show the same backbone, only with varying branches and substituents. The biggest

difference in this case is the fact that the hardwood hemicellulose is acetylated, while the softwood hemicellulose is not.<sup>5</sup> Compared to cellulose, hemicelluloses show much shorter chain lengths, with only 500–3000 monomer units.<sup>11</sup> Other characteristics are a much lower DP than cellulose, with only 50–300, a large number of side chain groups and that they are generally amorphous.<sup>5</sup>

### 2.1.1 Lignin

Lignin, the second most abundant natural polymer on earth, provides structural support, a mechanical barrier against chemical and biological attacks and accelerates water movement within plants, enabling transport of nutrients into the plant and preventing it from destroying the polysaccharide-protein matrix.<sup>1,2,6,8,13–17</sup> Generally, it is a heterogeneous polyphenolic, amorphous biopolymer, which consists of three subunits: p-coumaryl alcohol/ p-hydroxyphenyl (H), coniferyl alcohol/ guaiacyl (G) and sinapyl alcohol/ syringyl (S) units, linked via different C-O-C (about 2/3)<sup>1</sup> and C-C bonds.<sup>1,4–7,13–18</sup>

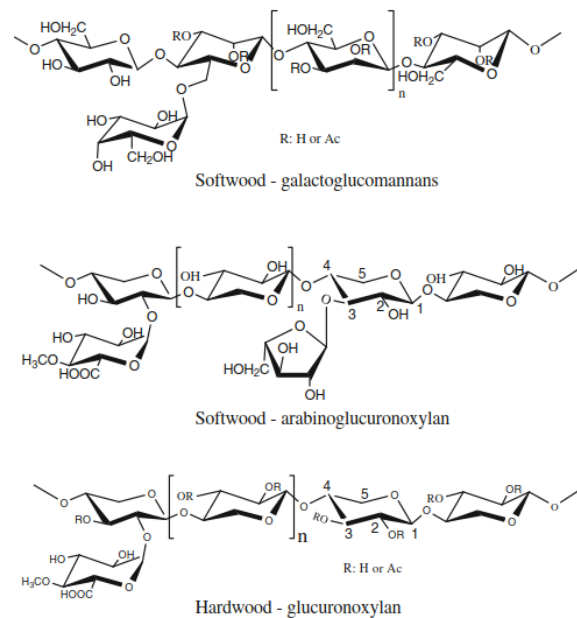


Figure 3: Structures of the main hemicelluloses in wood<sup>5</sup>



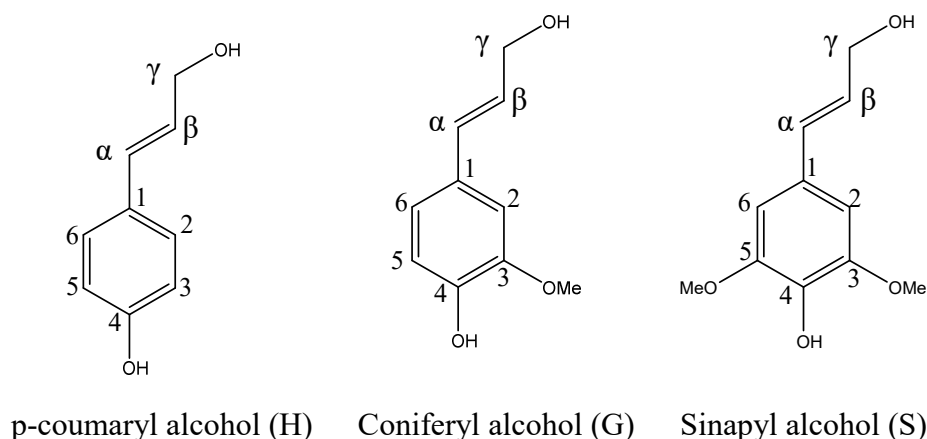


Figure 4: Structures of the monolignols (adapted from Li et al.)<sup>1</sup>

The proportion of these units varies strongly between plant species, but it can also vary in lignins from the same source, depending on the growing location and also the method of extraction.<sup>7</sup> But generally, softwood lignin consists of G units with a small amount of H units, hardwood lignin mainly contains S and G units in about the same proportions, while grass lignin contains all three units and additionally p-coumarates and ferulates. Due to that, softwood lignins are called G-lignins, hardwood ones are called GS-lignins while grass lignins are GSH-lignins.<sup>1,4-6,8,14,15,17</sup> These units are linked together by various bonding linkages, of which over 20 are known.<sup>13</sup> The main linkages between these units are  $\beta$ -O-4,  $\beta$ - $\beta'$ ,  $\beta$ -5,  $\alpha$ -O-4, 4-O-5, 5-5,  $\alpha$ -O- $\gamma$  and  $\beta$ -1'.<sup>1,4,5,7,14,15,17</sup> These and some other possible linkages are depicted in Figure 5.

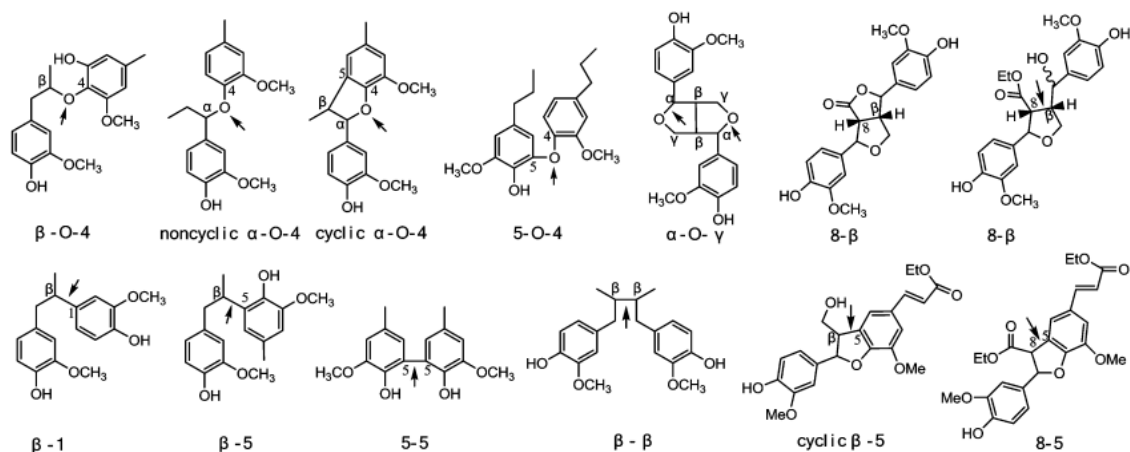


Figure 5: Linkages between monolignol units<sup>1</sup>

From these linkages, the  $\beta$ -O-4 linkage is the most abundant, with about 40 to 50 % in softwood and 50 to 65 % in hardwood lignin.<sup>1,4,16</sup> Furthermore, softwood lignin contains more  $\beta$ -5 and 5-5 linkages, which are more resistant, leading to a higher degree of condensation through cross-linking and branching in softwood than in hardwood lignin.<sup>1,7,16</sup> Table 2 sums up the percentages of the different linkages in hardwood and softwood lignin:

Table 2: Percentage of linkages in softwood and hardwood lignins<sup>1,4,7,18,19</sup>

Linkage	Abundance per 100 units [%]	
	Softwood	Hardwood
$\beta$ -O-4	35–60	50–70
$\beta$ - $\beta'$	2–6	3–7
$\beta$ -5	9–12	4–9
$\alpha$ -O-4	2–8	4–8
4-O-5	4–8	6–9
5-5	10–27	3–10
$\beta$ -1	1–10	1–7
Spirodienone	1–4	2–5
Dibenzodioxocin	5–7	1–2

Lignin carries various functional groups, like hydroxyl, methoxy, carboxyl and carbonyl groups. The most abundant of them are methoxyl and hydroxyl groups, which can be ranked in the order of aliphatic OH  $\gg$  phenolic OH > carboxylic OH.<sup>1,7,18</sup> Only 10–13 % of the phenolic OH (at the 4-position) are free phenolic groups, which means that most of them form ether bonds.<sup>19</sup> The methoxy group on the S units also leads to a favoring of linear structural forms in hardwood lignin.<sup>1</sup>

The three lignin units, H, G and S, are formed together from the three monolignols, p-coumaryl alcohol, coniferyl alcohol and sinapyl alcohol, by radical polymerization, leading to an irregular structure and optical inactivity.<sup>4-6,8,13-16</sup> The monolignols themselves are biosynthesized by three subsequent pathways: First the Shikimate pathway, producing phenylalanine, secondly the phenylpropanoid pathway, converting phenylalanine into p-coumaroyl-CoA and finally the three specific monolignol pathways. Figure 6 shows the whole monolignol biosynthesis pathway.<sup>5,14</sup>

## 2 Theoretical Background

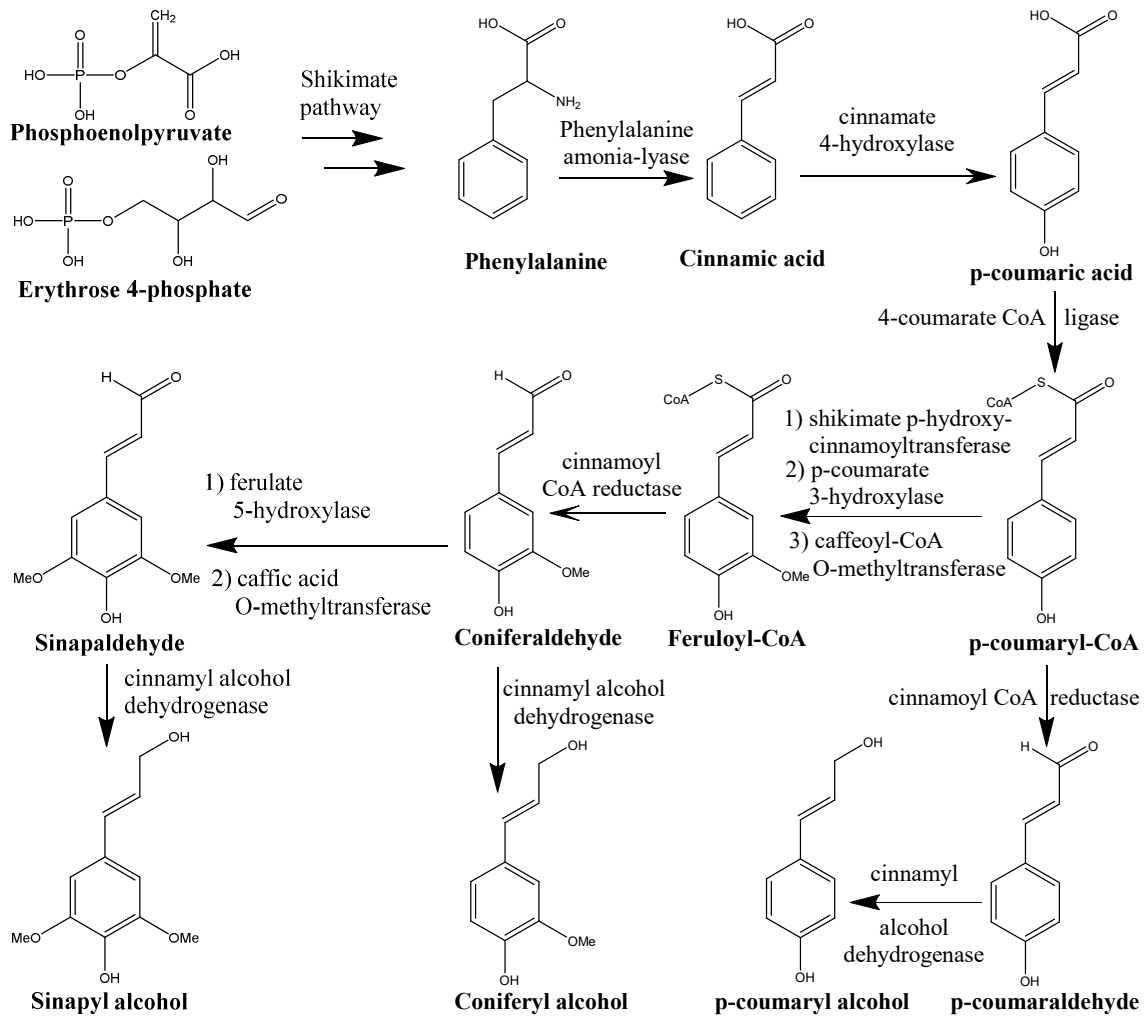
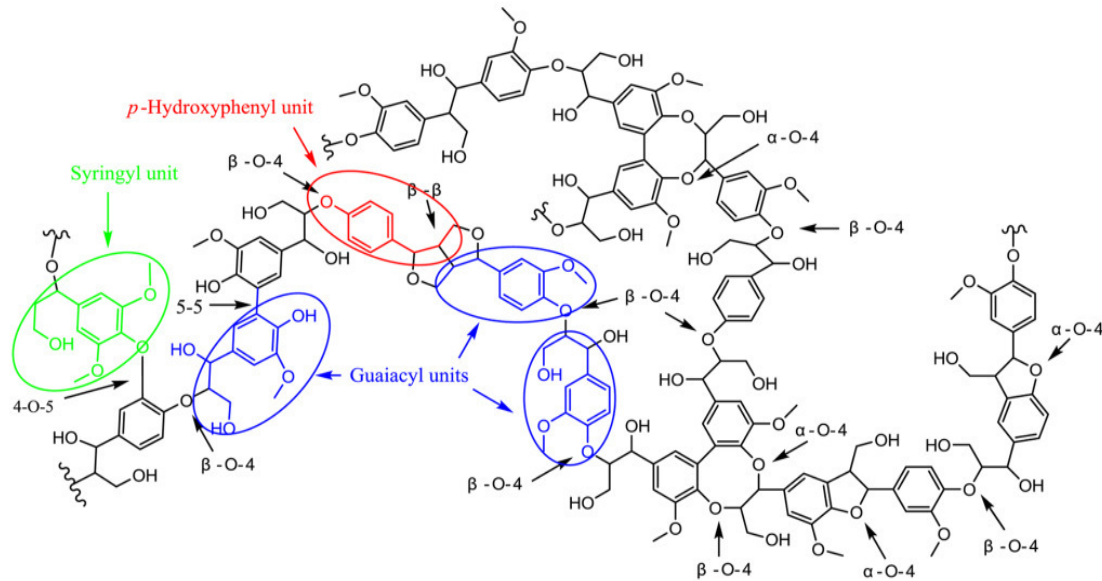


Figure 6: Biosynthesis pathway of the three monolignols (adapted from Guragain et al)<sup>14</sup>

Lignin monomers can also form covalent bonds with xylan molecules of hemicellulose in the cell wall, either via ether, ester or glycosidic linkages.<sup>6,8,14</sup> This leads to complex three-dimensional networks, also known as lignin-carbohydrate complexes (LCC).<sup>6,7,16</sup>

The structure of lignins is irregular and highly heterogeneous and depends strongly on the type of biomass, the botanical species and also the part of the plant.<sup>1,4-6,16</sup> Thus, there are no real structures for lignin, but only models, schematic representations, which show the main types of units and linkages prevalent in lignin molecules. Such a model can be seen in Figure 7.

Figure 7: Structural model of lignin (Li et al.)<sup>1</sup>

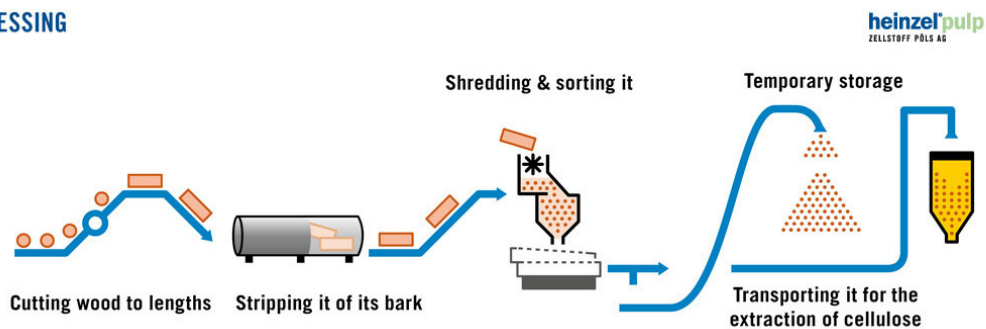
## 2.2 Wood pulping

Wood pulping is the process of removing lignin from wood fibers to use these fibers for paper production. This means that pulping is a delignification process. The two most important pulping processes are the sulfate process, also called kraft process, and the sulfite process.<sup>4,7</sup> By 2000, the sulfate process made up 89 % of the total production capacity, while the sulfite process only had a share of 3.7 %.<sup>16</sup> In Austria, most wood used for pulping is softwood. For example, Zellstoff Pöls AG mainly uses Spruce, Pine and Larch for pulp production.<sup>20</sup>

### 2.2.1 Sulfate process

The kraft process is the main process in wood pulping in the world.<sup>4,18</sup> Before processing, the wood needs to be cut, stripped of its bark and then shredded into wood chips. In this form, the wood chips can be stored until they are needed for pulping.<sup>21,22</sup>

#### WOOD PROCESSING

Figure 8: Wood processing prior to pulping<sup>22</sup>

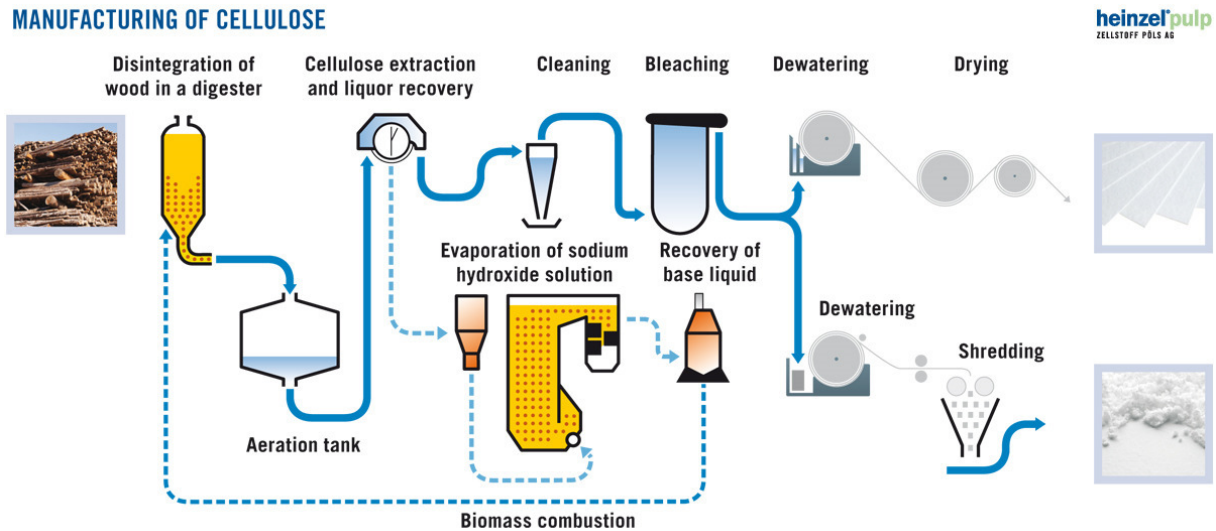
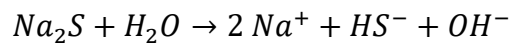


Figure 9: Kraft process (example: Zellstoff Pöls AG)<sup>22</sup>

The wood chips are then fed into a digester, in which they are mixed with white liquor, an aqueous solution of NaOH and Na<sub>2</sub>S, thus reacting at alkaline conditions.<sup>16,17</sup> The mixture is heated to 170°C and cooked at this temperature for two hours.<sup>18</sup>



During cooking, hydroxide and hydrosulfide anions are formed, as can be seen above.<sup>23</sup> These anions fragment the lignin molecule into smaller fragments by cleaving the ether linkages between the lignin subunits, generating free phenolic hydroxyl groups and decreasing the number of β-O-4 linkages<sup>19</sup>, increasing the solubility in the cooking liquor. The C-C linkages tend to survive the process.<sup>18</sup> By that, the cellulose pulp, which is solid, can be separated from the lignin. This cellulose pulp is then washed, bleached and dried before converting them into different paper products.<sup>19,22</sup> In contrast to that, the lignin and a large part of the hemicelluloses are dissolved in the liquor, now called black liquor due to its distinctive color.<sup>6,7,19</sup>

The black liquor has a pH of about 12 and is composed of about 2/3 organic and 1/3 inorganic material. It contains about 29–45 % lignin and 25–35 % hydroxy acids, originating from the peeling reaction of cellulose and hemicelluloses.<sup>7,19</sup> Figure 10 shows the main hydroxy acids in black liquor: glycolic, lactic, 2-hydroxybutyric, 2,5-dihydroxypentanoic, glucoisosaccharinic and xyloisosaccharinic acids<sup>24</sup>. The first three are α-hydroxy acids (AHAs), carboxylic acids with a hydroxyl group at the α-position of the carboxyl group, and the latter three are polyhydroxy acids (PHAs), carboxylic acids with two or more hydroxyl groups attached to carbon atoms.<sup>25</sup>

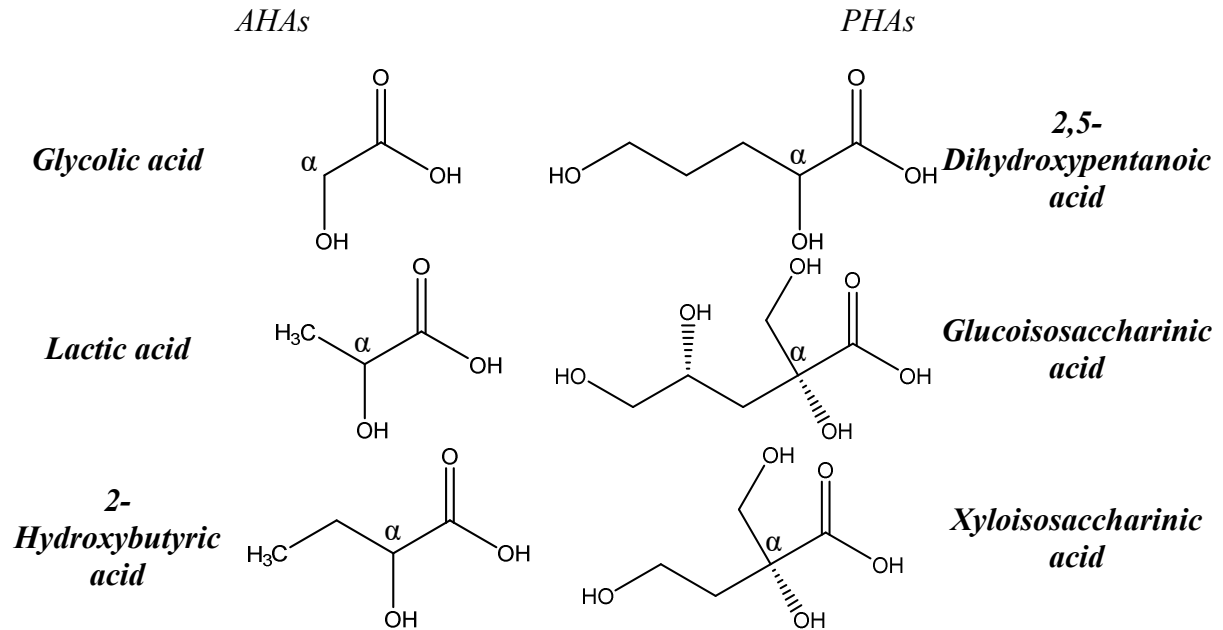


Figure 10: Structures of black liquor hydroxy acids

After evaporation of the sodium hydroxide solution, the base cooking liquors and the molten inorganic matter are separated from the concentrated black liquor as a smelt in the black liquor recovery boiler, while the organic matter is burned for process heating via steam or to generate electricity. The smelt, consisting of  $\text{Na}_2\text{S}$  and  $\text{Na}_2\text{CO}_3$ , is introduced into a dissolving tank filled with water, forming “green liquor”. The green liquor is mixed with lime,  $\text{Ca}(\text{OH})_2$ , converting  $\text{Na}_2\text{CO}_3$  to  $\text{NaOH}$ , while the  $\text{Na}_2\text{S}$  remains unchanged.  $\text{NaOH}$  and  $\text{Na}_2\text{S}$  are then reintroduced into the digester as white liquor.<sup>4,7,17,19,21,22,26,27</sup>

The delignification during kraft pulping generally proceeds in three phases:<sup>18,21</sup>

1. Initial phase: Up to 150 °C; controlled by diffusion, rapid removal of ~20 % lignin
2. Bulk phase: 150–170 °C, including the cooking phase; controlled by chemical reactions; removal of most of the lignin
3. Residual phase: After 90 % of lignin has been removed; marks the end of cooking, as further pulping would degrade the carbohydrates

About 4–5 % residual lignin still remains in the liquor after the cooking, which is removed later during bleaching.<sup>18</sup>

The chemical reactions during the kraft process can be assigned to the desired degradation or the condensation reactions. Degradation leads to liberation of lignin fragments and enhancement of their dissolution. The main reactions in this case are the cleavage of  $\alpha$ - and  $\beta$ -aryl ether linkages. In contrast to that, condensation leads to the formation of alkali-stable linkages, for example enol ethers<sup>21</sup>, via Michael addition of external and internal nucleophiles.<sup>18</sup>

During pulping, some new functional groups and linkages are formed in the lignin, for example stilbenes. Despite the use of  $\text{Na}_2\text{S}$ , a relatively low amount of sulfur can be found after degradation.<sup>4</sup>

### 2.2.1.1 Tall oil

In various kraft pulping mills, a subsequent tall oil production is connected to the process. In this production, the so-called tall oil soap is recovered during the classic evaporation step (at 20–30 wt% solids) via skimming/ decanting, as the soap becomes insoluble due to the common ion effect, precipitates and rises to the top. The efficiency of the decanter currently used is 60–90 %, highly depending on the process parameters and wood species. The tall oil soap is then transformed into crude tall oil by making it slightly acid, known as acidulation. This acidulation is carried out in batch reactors at pH 2.5–4 by adding 90–95 % sulfuric acid (200–300 kg/ton crude tall oil) or diluted sulfuric acid (~30 %) and boiling for 2 h at 98–108 °C. After settling overnight, the crude tall oil can be separated from the lignin and the aqueous phases due to their different densities. The crude tall oil can then be purified via distillation to yield resin acids and fatty acids.<sup>28,29</sup>

Crude tall oil is a viscous, sticky, dark brown tarlike liquid with an unpleasant smell from pulp processing, skimming and acidulation. It is composed of 38–53 % fatty acids, 30–53 % resin acids and 6.5–30 % unsaponified (neutral) compounds, like esters, sterols and hydrocarbons.<sup>28,29</sup>

The fatty acid fraction in crude tall oil is mainly made up of  $\text{C}_{18}$  fatty acids: oleic acid (10–20 %) and linoleic acid (11–17 %), followed by linolenic acid (1–5 %), palmitic acid (1.5–3 %), stearic and arachidic acid (both 0.5–1 %).<sup>28</sup>

Resin acids belong to the diterpenes, being comprised of four isoprene units, and have a molecular formula of  $\text{C}_{20}\text{H}_{30}\text{O}_2$ . The most important resin acids can be seen in Figure 11. The difference between the several resin acids is the position of the double bonds. In plants, levopimaric acid (double bonds at 12=13 and 8=14) is the most abundant isomer with 30–50 %. In tall oil, due to an isomerization reaction over 100 °C, abietic acid (7=8 and 13=14) has the highest content of these isomers with about 30 %, followed by dehydroabietic acid ( $\text{C}_{20}\text{H}_{28}\text{O}_2$ ) and dihydroabietic acid ( $\text{C}_{20}\text{H}_{32}\text{O}_2$ ) with 15–30 %, palustric acid (8=9 and 13=14) with 12 % and neoabietic acid (8=14 and 13=15).<sup>30</sup>

Crude tall oil also has a low moisture content of <2 % and ash and sulfur contents of under 0.3 %.<sup>28</sup>

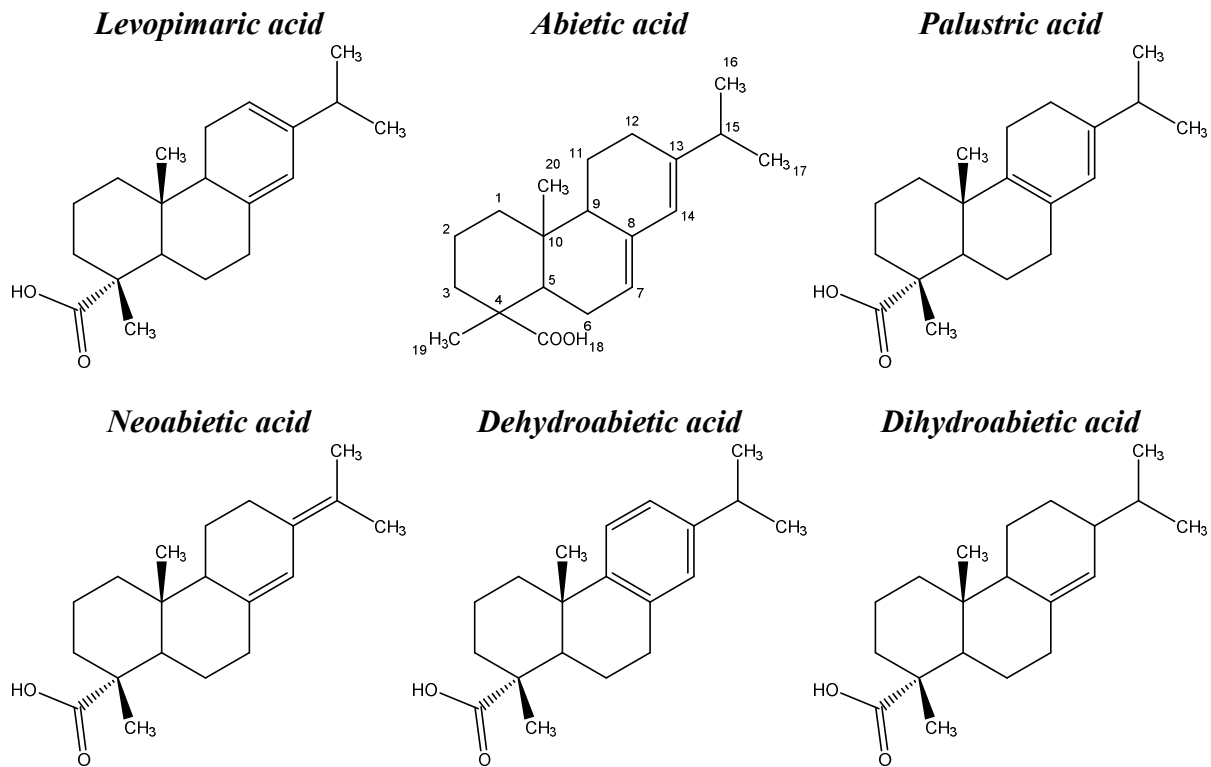


Figure 11: Structures of the most common resin acids (adapted from Fiebach; Grimm)<sup>30</sup>

### 2.2.2 Sulfite process

The sulfite process is the second biggest process in wood pulping. In general, sulfite pulping is composed of the usage of sulfites  $\text{SO}_3^{2-}$  or bisulfites  $\text{HSO}_3^-$ , depending on the process, and a counter ion, called base, which could be calcium, magnesium, sodium or ammonium. The pH ranges from 1 to 13 and temperatures from 50 up to 175 °C are applied, depending on the base, for 4 to 14 hours.<sup>4,6,7,17,21</sup>

Advantages of the sulfite process include brighter and easier refined pulps with less porous sheet than kraft pulps. Disadvantages could be the weaker pulp, difficult processes for some types of woods, long cooking times and complicated recovery of chemicals.<sup>7</sup>

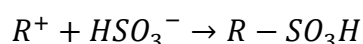
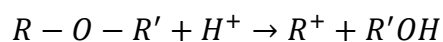
The delignification in sulfite pulping is composed of two stages, a first step with a high conversion rate, where the  $\text{SO}_2$  quickly penetrates the wood chips,<sup>7</sup> followed by a second step with a lower rate.<sup>21</sup> Then cellulose is separated from the other components by a sudden decompression from about 6 to 3 bar after the cooking time.<sup>7</sup>

The two most widely used sulfite processes are the acid magnesium bisulfite and the magnefite (= magnesium bisulfite) processes. The biggest difference between these two processes is the pH value used during pulping. While the acid bisulfite process needs a pH value in the range of



1.5, the magnesite process should have a pH of about 4.0, both sufficient to prevent the magnesium bisulfite from precipitating (pH 5–6).<sup>21</sup>

During the delignification process, depolymerization and degradation play a minor role, while the most important reaction can be assigned to the sulfonation. This reaction efficiently introduces charges along the lignin chain and breaks LCCs. In acidic conditions, slow hydrolyzing of  $\beta$ -O-4 ethers can be observed, while mechanisms similar to kraft pulping can be observed in alkaline conditions.<sup>21</sup> Undesirable side reactions would be hydrolysis of polysaccharides at lower pH, decreasing the strength of cellulose fibers, and cross-linking of lignin moieties with other aromatic structures under acidic conditions, when the  $\text{SO}_2$  level is too low.<sup>21</sup> The following reactions show the cleavage of ether bonds, resulting in sulfonate groups:<sup>1,7</sup>



## 2.3 Industrial lignins

The highest amount of commercially available lignins are, due to their role as pulping by-products, kraft lignins and lignosulfonates from the sulfate and sulfite processes, respectively. Apart from these, there are several other lignins available, like organosolv lignin, steam explosion lignin, pyrolysis lignin, milled wood lignin and enzymatic lignins. These lignins will be shortly presented in this chapter.<sup>1,2,4,6,7,15–17,31</sup>

### 2.3.1 Kraft lignin

The biggest part of commercially available lignin, about 85–95 %, is derived from the kraft process, due to its dominant abundance in global pulping.<sup>7,16</sup> Kraft lignin can be isolated from the black liquor by pH controlled precipitation to pH 9–10.5 with  $\text{CO}_2$  or to pH 1–2 with mineral acids with subsequent filtering, washing and drying to solid form.<sup>6,7,15,16,32</sup>

Sulfate pulping leads to a high structural modification of kraft lignin, resulting in lower number-average molecular weights, as  $M_n$  of about 1000–3000 Da have been reported with a dispersity between 2 and 4, sometimes also up to 8 or 9. The dispersity  $\mathcal{D}$ , defined as the ratio of the mass-average molar mass  $M_w$  to the number-average molar mass  $M_n$  ( $\mathcal{D}_M = M_w/M_n$ ), is a measure of how far away a distribution is from being uniform, represented by a dispersity of 1.0.<sup>33,34</sup> Thus, kraft lignins, like all other lignins, are highly non-uniform. The average monomer molecular weight equals 180 Da.<sup>1,15,17</sup> The sulfur content of kraft lignins is in the range of 1–3 %, with

ash contents between 0.5 and 3%.<sup>1,4,7,16,17</sup> Due to the extensive cleavage of  $\beta$ -aryl bonds, kraft lignin contains a high amount of phenolic hydroxyl groups and biphenyl and other condensed structures.<sup>7</sup> A model showing characteristics of kraft lignin can be seen in Figure 12.

Kraft lignin is hydrophobic, thus insoluble in water, but dissolves

readily in alkaline solutions over pH 10.5 and in other highly polar solvents.<sup>15,17</sup>

Mostly, commercially available kraft lignin is made water-soluble by sulfonation at 150–200 °C with Na<sub>2</sub>SO<sub>3</sub> or by sulfomethylation via reaction with Na<sub>2</sub>SO<sub>3</sub> and formaldehyde at 100 °C.<sup>6,16</sup> By that, a lignin structurally related to liginosulfonates is generated, which can be used to effectively replace liginosulfonates in their applications.<sup>17</sup>

### 2.3.2 Liginosulfonate

After stripping and sulfur recovery, liginosulfonate can be recovered from sulfite pulping liquor by the Howard process, where an excess of calcium hydroxide is added (95 % recovery)<sup>17</sup>, by treatment with a long-chain alkylamine followed by solvent extraction or also via ultrafiltration.<sup>15,16,31</sup> Depending on the sulfite process used, liginosulfonates can be obtained as magnesium, calcium, ammonium or sodium salts.<sup>16</sup>

As the sulfite process is less aggressive than the kraft process, the structure of liginosulfonates resembles the one of original lignin more closely.<sup>6</sup> The  $M_n$  of liginosulfonates can range from 1000 to 140,000 Da, while most of them are

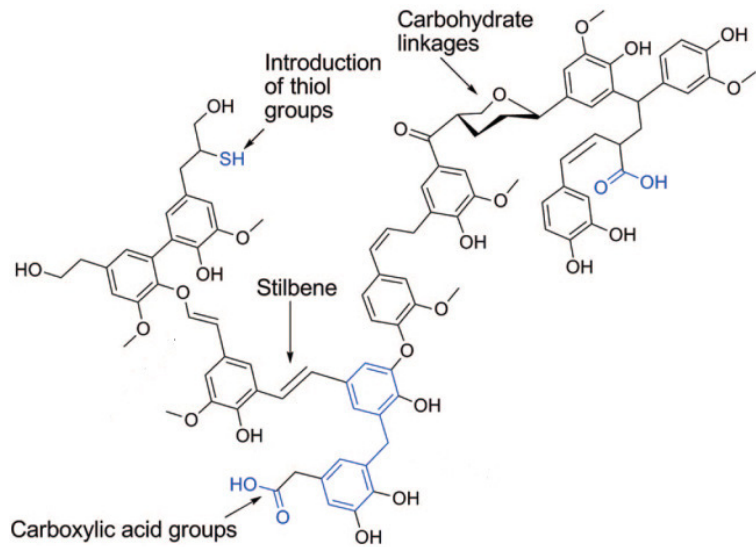


Figure 12: Model of kraft pine lignin (adapted from Zakzeski et al.)<sup>4</sup>

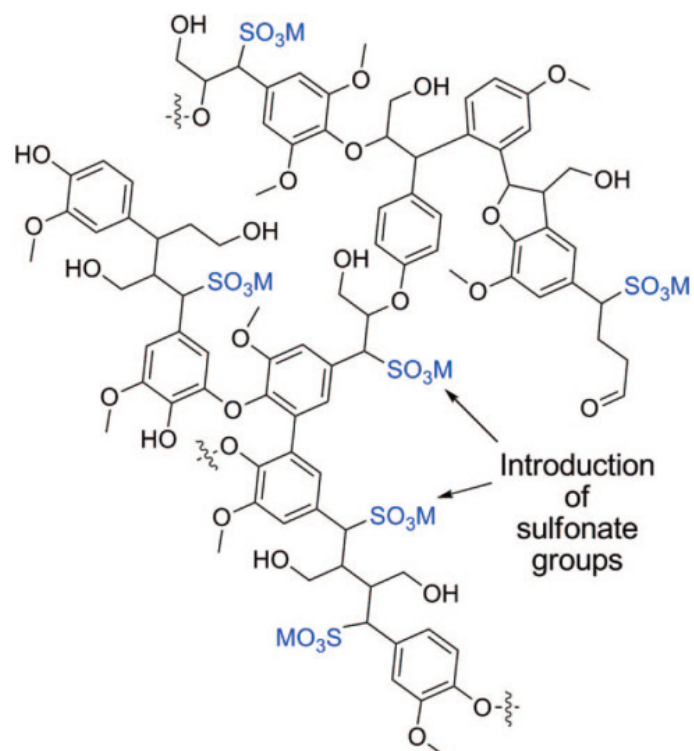


Figure 13: Model of liginosulfonate (Zakzeski et al.)<sup>4</sup>

between 5000 and 20,000 Da. The dispersity is also higher than in kraft lignin, with values ranging from 4 to 9. Monomer molecular weights are 188 Da for hardwood lignosulfonates and 215–254 Da for softwood lignosulfonates, respectively.<sup>15,17</sup> In the sulfite process, sulfonate groups are added to the benzylic carbon of the phenylpropane units, resulting in a sulfur content distinctly higher than for kraft lignins, with about 3–8 %.<sup>7,16,17</sup> The ash content is also higher, ranging from 4 to 8 %. A model for this lignosulfonate structure can be seen in Figure 13.

Lignosulfonates show hydrophobic and hydrophilic properties, are soluble in aqueous solutions on the whole pH range and in highly polar organic solvents.<sup>4,6,15,16</sup>

### 2.3.3 Other industrial lignins

Organosolv lignin is obtained from the organosolv pulping process, where a variety of solvents, mostly alcohols, and combinations, including alkaline and acidic aqueous components to enhance the pulping rate, can be used to extract lignin at high temperatures and pressures. The most well-known variant of these is the Alcell process, where ethanol or an ethanol-water mixture is used.<sup>6,15,17</sup> The organosolv lignin can be separated either by solvent removal and recovery or by precipitation with water coupled with solvent recovery via distillation.<sup>15</sup> This solvent recovery is also the biggest disadvantage of this process, as it is very cost intensive.<sup>4,17</sup> Organosolv lignins are less modified than kraft lignins, retaining most of the  $\beta$ -O-4 linkages,<sup>17</sup> and generally sulfur-free.<sup>6</sup> Ash contents are in the range of kraft lignins with 1.7 %.<sup>7</sup> Mostly, organosolv lignins are soluble in basic solutions and many polar solvents, but insoluble in acidic aqueous solutions between pH 2 and 7. The  $M_n$  of Organosolv lignins are normally below 1000 Da with a dispersity from 2.4 to 6.4 and a monomer molecular weight of 188 Da.<sup>15,17</sup>

Steam explosion lignins are derived from the steam explosion process, where biomass is first impregnated with steam at 180–230 °C under high pressures of 14–35 bar for 1–20 minutes after which the pressure is rapidly released.<sup>15</sup> This leads to a partial hydrolysis of aryl ether linkages in the lignin, while also homolytic cleavages occur.<sup>6,16</sup> Lignin can be recovered via extraction with organic solvents with high yield (90 %)<sup>15</sup> and a low amount of impurities like carbohydrates or wood extractives.<sup>6</sup> Steam explosion lignin shows similar molecular weights and properties as the organosolv lignin.<sup>4,17</sup> Thus, it has lower molecular weights and higher solubility in organic solvents than kraft lignin<sup>15</sup>, but is insoluble in water.<sup>6</sup> Steam explosion lignins are also sulfur-free.<sup>4</sup>

Pyrolysis lignins are a possibility for biorefinery processes. The process is characterized by high temperatures of 450–500 °C and short vapor residence times of up to two seconds to yield a bio-oil with char and gases as by-products. Pyrolysis lignins have a very low average

molecular weight, with  $M_n$  of 300 to 600 Da, indicating a high degree of depolymerization, with the presence of dimeric up to nonameric phenol units.<sup>15,17</sup> Pyrolysis lignin is structurally different from other lignins, due to the fact that rather C<sub>8</sub>- than C<sub>9</sub>-oligomers can be found.<sup>4</sup> The main disadvantage of pyrolysis is a high fuel consumption for the process, due to the relatively high temperatures.<sup>15</sup>

Milled wood lignin (MWL) is the lignin most similar to unaltered lignin due to the mild extraction conditions. This extraction is carried out by the Björkman process, where ball-milled wood is extracted by neutral solvents, mostly dioxane/water in a 9/1 volume ratio. Although, there is a possible depolymerization during the ball-milling, where  $\beta$ -aryl ether linkages could be cleaved, leading to generation of new free phenolic hydroxyl groups and increasing the amount of  $\alpha$ -carbonyl-groups by side-chain oxidation.<sup>1,15</sup>

Enzymatic lignins can be categorized into cellulolytic enzyme lignin (CEL) and enzymatic mild acidolysis lignin (EMAL): CEL is received by removing carbohydrate impurities from MWL via cellulolytic enzymes (85–88 % removal). This process increases the amount of  $\beta$ -O-4 linkages while decreasing the content of phenolic hydroxyl groups. CEL is characterized by a  $M_n$  of 1900 Da, a dispersity of about 6 and an average monomer molecular weight of 187 Da, while being structurally similar to MWL.<sup>1,15</sup> EMAL adds a mild acidolysis step (0.01 M HCl in dioxane/water) to CEL processing to improve carbohydrate removal. The  $M_n$  and average monomer molecular weight of EMAL are similar to the ones of CEL, but the dispersity is significantly improved, with 3 compared to 6 in CEL.<sup>1,15</sup>

## 2.4 Usage of lignins

While most of the lignin material recovered from pulping is directly burned at the mill, only about 2 % of lignin material are used for commercial applications. This is made up of about 1,000,000 t/a of liginosulfonates and 100,000 t/a kraft lignins.<sup>6</sup> This means, that most of the applications presented in this chapter have not been carried out on a larger scale, but rather present the huge potential of lignins.

### 2.4.1 Liginosulfonates

Only liginosulfonates possess real commercial applications so far, as they can be used as binders and dispersants<sup>2</sup>, emulsifiers<sup>16</sup>, heavy-metal sequestrants<sup>6</sup> and for the production of vanillin<sup>16</sup>.

About 45 %<sup>17</sup> to 50 %<sup>16</sup> of the liginosulfonates are used in concrete mixtures in proportions of 0.1–0.3 %<sup>16</sup>, to prevent lumping and settling of unsolved particles in suspension<sup>6</sup>, improving plasticity and flow of concrete<sup>17</sup>.

The second largest application, with about 15 %, is as additive in animal feed pellets as a binder for the pellets<sup>17</sup>, due to the low toxicity of lignosulfonates.<sup>6</sup> A maximum dose of 4 % ensures durability and abrasive resistance of the pellets.<sup>16</sup>

Another important application of lignosulfonates as binders is dust control as road binders of unpaved roads<sup>16</sup>, with about 11 %<sup>17</sup>, but also for public works, airports, sports facilities and racing circuits.<sup>6</sup> For this the concentrated crude spent liquor from sulfite pulping can be used.<sup>16,17</sup>

The major use of lignosulfonates as dispersants is as dye dispersants, with 12 %.<sup>17</sup> The lignosulfonates form solids in water dispersions due to their charged, polyelectrolyte nature,<sup>17</sup> allowing use in water-based paints and inks. Other usages as dispersants comprise addition to pesticides, with about 5 %<sup>17</sup>, to gypsum boards<sup>16</sup> and for the dispersion of water-based crop-protection chemicals<sup>2</sup>, keeping micronutrients in solution.<sup>6</sup>

Lignosulfonates are also capable of stabilizing oil-in-water interactions, reducing the tension at the oil-water interface. This leads to uses as emulsifier, for example as rheology-modifying agent for water-based systems.<sup>17</sup>

### 2.4.2 Materials

The main possibilities for materials produced from lignin are phenolic resins, epoxies, adhesives, polyolefins and other plastics.

In the production of phenol formaldehyde resins, lignin could be used as a substitute for phenols. Nevertheless, there are two limiting factors: Firstly, the chemical heterogeneity of lignins and secondly the increase of the  $M_w$ . However, these limitations can be countered by a chemical or biochemical modification of the lignin via phenolization or demethylation, by the addition of filler agents like starch or the usage of acetosolv or organosolv lignins. Furthermore, 50 % of kraft lignin or lignosulfonate can be added to binders instead of phenol. Lignins are not only a safer and more environmentally-friendly, but also a cheaper alternative for phenols and binders used in this process. Phenol formaldehyde resins are used as adhesives for plywood, chip-, fiber- and strand board and in the manufacturing of mineral wool, abrasives and rubber products.<sup>2,6,35</sup>

In epoxy resins, where epichlorohydrin reacts with molecules like bisphenol-A to linear polymers, lignin could be used as cross-linking agent, imparting the bulk properties. For that, the lignin must be free of impurities like salts, water and sugars. Thus, either industrial lignins have to be purified or impurity-free lignins, like organosolv lignin, have to be used. It is possible

to improve lignin reactivity in this reaction by introducing additional phenol moieties into lignosulfonate by reacting it with phenol and sulfuric acid.<sup>6,35</sup>

In the adhesives sector, lignin is also used for crosslinking reactions, mainly for the production of fiberboards.<sup>35</sup>

The mechanical and technical properties of polyolefins, like polyethylene or polypropylene, can be modified by adding about 30 % dry kraft lignin or epoxy-modified lignosulfonate to these materials. By that, the low biodegradability of polyolefins can be improved while also being a stabilizer against photo-oxidation by UV light, at the same time being cheaper as commercial UV stabilizers.<sup>6,35</sup> Other plastics achievable from lignins are polyester-lignin polymers from kraft lignin, an ecofriendly material with good thermal stability, stiff polyurethane sheets and foams for insulation from organosolv lignin or a bioplastic material from sulfur-free lignins, which is highly recyclable and looks like the plastics used in most household items.<sup>2,6</sup>

With better lignin recovery methods, yielding higher purity lignins with better physical properties on a constant level, lignins could be used as a precursor for carbon fiber production, replacing polyacrylonitrile. Lignin from future cellulose biorefineries could become an ideal feedstock for this application.<sup>2,6,8</sup>

Finally, lignin could function as raw material to produce active carbon/ carbon black materials by pyrolysis with subsequent physical activation. These materials could then be used in rubber reinforcements, for example.<sup>2,6</sup>

### **2.4.3 Chemicals and fuels**

As of now, vanillin is still the most important fine chemical produced from lignins, in this case lignosulfonate, even though most of this production was shut down in 1993 due to the lower cost production from petrochemicals. The main reason for this was the high amount of waste effluents produced in the process, leading to environmental issues due to the unsustainable costs of effluent treatment.<sup>6,7,16,17</sup> On the other side, Norwegian company “Borregaard” has developed an economically viable method for vanillin production from lignosulfonates via the usage of a copper catalyst. This process is also much more ecofriendly than the petrochemical process, due to 90 % less CO<sub>2</sub> emissions.<sup>6</sup> A proposed reaction mechanism for vanillin production from lignosulfonates, as carried out by “Borregaard”, can be seen in Figure 14. Though, this mechanism is not yet fully understood and subject of debate and research due to the complexity and heterogeneity of sulfite pulping products.<sup>36</sup>

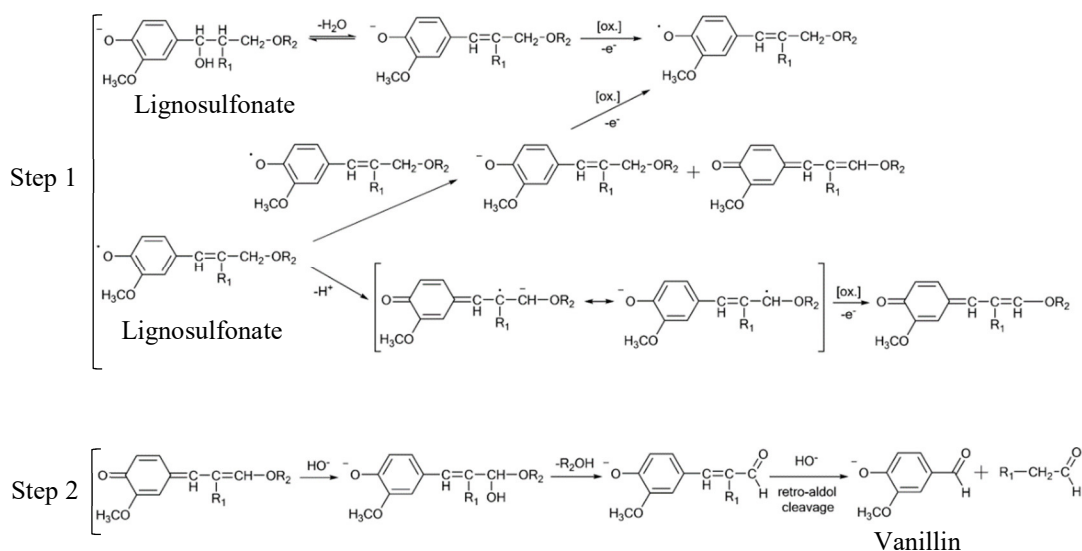


Figure 14: Proposed mechanism for vanillin production from lignosulfonates (adapted from Fache et al.)<sup>36</sup>

Another fine chemical produced from lignin was dimethyl sulfoxide (DMSO). To yield this colorless aprotic polar solvent, black liquor from the kraft process was mixed with sulfur and heated to over 200 °C, obtaining dimethyl sulfide (DMS). DMS can then be converted into DMSO by oxidation with  $N_2O_4$ . Like the vanillin production, this pathway was abandoned due to the lower cost of the petrochemical route, where methanol and  $CS_2$  or  $H_2S$  are used to produce DMS.<sup>6,16</sup>

In the future, reductive and oxidative processes can be used to produce fine chemicals as well as fuels. Hydrogenolysis and hydrodeoxygenation (HDO) of lignins could yield gasoline-range aromatics, as well as benzene, toluene, xylene, phenol, substituted coniferols, aromatic polyols and quinones.<sup>6,8</sup> Oxidation of lignins could lead to aromatic acids and aldehydes, but also ring-opened organic acids are possible products.<sup>8</sup> Another possibility are pyrolytic approaches, yielding low-molecular species in the vapor phase, which can be upgraded to fuels and chemicals with HDO catalysis.<sup>8</sup>

## 2.5 Analytical methods

### 2.5.1 Fourier transform infrared (FTIR) spectroscopy

One of the most important methods for the identification of different functional groups in molecules is infrared spectroscopy. The principal behind it is that the functional groups can be identified by the stretching and bonding of individual bonds and the energy needed for this is lying in the infrared, in wavelengths between 10 and 100  $\mu\text{m}$ . According to Hooke's law, the frequency  $\nu$  is proportional to the square root of the force constant  $f$ , similar to the strength of the bond, and inversely proportional to the square root of the reduced mass  $\mu$ .<sup>37</sup>

$$\nu = \frac{1}{2\pi c} \sqrt{\frac{f}{\mu}} ; \mu = \frac{m_1 * m_2}{m_1 + m_2}$$

where  $c$  is a constant and  $m_1$  and  $m_2$  are the masses of the atoms forming the bond.

This leads to the assumption that stronger bonds and lighter atoms vibrate faster and are thus found at higher frequencies. Although, not all bonds in a molecule are analyzed, but only the ones stretching much stronger or weaker or those comprising much heavier or lighter atoms than their neighbors, due to the high amount of vibrations.<sup>37</sup>

When measuring an IR spectrum, the sample is exposed to infrared radiation and the amount of infrared energy that passes through is plotted against the wavelength, which is depicted as "wavenumber" from values of  $4000\text{ cm}^{-1}$  (high frequency) to  $500\text{ cm}^{-1}$  (low frequency). This means that IR spectra are nothing else than absorption spectra. As hydrogen is much lighter than the other atoms in molecules, bonds to hydrogen are found at the highest wavenumbers. After bonds to hydrogen, other bonds are descending in order of their strength, from triple to double and single bonds, as seen in Table 3:<sup>37</sup>

Table 3: Regions of the IR spectrum (adapted from Clayden et al.)<sup>37</sup>

Wavenumber	Type of bonds	Examples
4000–2500 $\text{cm}^{-1}$	Bonds to hydrogen	O-H, N-H, C-H
2500–2000 $\text{cm}^{-1}$	Triple bonds	$\text{C}\equiv\text{C}$ , $\text{C}\equiv\text{N}$
2000–1500 $\text{cm}^{-1}$	Double bonds	$\text{C}=\text{C}$ , $\text{C}=\text{O}$ , $\text{NO}_2$
<1500 $\text{cm}^{-1}$	Single bonds	C-O, C-C, C-N, C-F, C-Cl

A large dipole moment leads to stronger absorption, while no IR absorption is observed within perfectly symmetrical bonds with no dipole moment. Another effect affecting the IR spectrum is the hydrogen bonding, as stronger H-bonds give broader peaks than weak ones.<sup>37,38</sup>



The IR spectra are measured with a spectrometer. The spectrometers used in FTIR are mainly composed of the following three parts.<sup>38,39</sup>

1. **IR source:** The ideal radiation source for FTIR spectroscopy are polychromatic, high temperature black bodies. Mostly, a so-called Globar is used, a resistively heated silicon carbide rod, which is normally operated at 1300–1500 °C.
2. **Michelson-Interferometer:** The Michelson interferometer is generally composed of a beam splitter, a moving and a stationary mirror. The beam splitter splits the beam from the light source into two beams, generating a path difference between them, when both beams are recombined again. Depending on the position of the moving mirror, either constructive or destructive interferences occur due to the varying path difference. Now the recombined beam is sent through the sample.
3. **Detector:** Generally, a detector transforms radiation into an electrical signal. For FTIR spectroscopy, pyroelectric bolometers are used as detectors. In this detector, ferroelectric materials, either deuterated triglycine sulfate (DTGS) or lithium tantalate, are used, which exhibit a change of polarization when the temperature is changed by the IR radiation. This polarization change can then be observed as an electrical signal.

A schematic diagram of a FTIR spectrometer is shown in Figure 15.

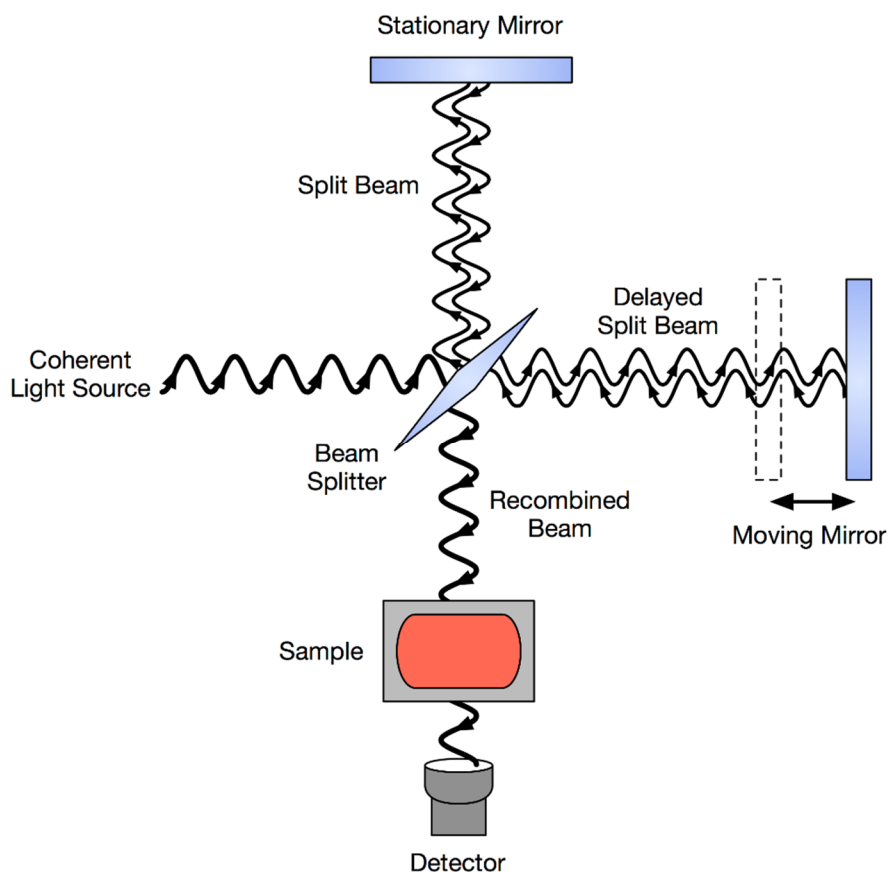


Figure 15: Schematic representation of a FTIR spectrometer<sup>40</sup>

The intensity variation of the beam from the Michelson-interferometer is measured as a function of the path difference by the detector, given by the movement of the mirror. So, after the signal is detected, it has to be converted into the wanted spectrum. For this, a Fourier-transformation is carried out by a PC directly connected to the detector.

The most widely used sampling technique in IR spectroscopy today is attenuated total reflection (ATR). Unlike many other IR techniques, in ATR the radiation is not transmitted through the sample, but only the surface of the sample is analyzed. This is carried out by total reflection at the interface between an optically dense medium  $n_1$  (ATR element) and an optically rare medium  $n_2$  (sample). The effect of total reflection, an internal reflection in the higher-refractive-index medium, can be observed when the angle of incidence is greater than the critical angle  $\theta_c$ , which is defined as

$$\sin \theta_c = \frac{n_1}{n_2}$$

Materials which exhibit this internal reflection are called internal reflection elements (IRE), widely used examples would be zinc selenide, diamond and germanium. The approximate depth of penetration of the beam are 0.50 to 2  $\mu\text{m}$ .<sup>39,41</sup>

## 2.5.2 Chromatography

According to the IUPAC definition, “chromatography is a physical method of separation in which the components to be separated are distributed between two phases, one of which is stationary (stationary phase) while the other (the mobile phase) moves in a definite direction.”<sup>42</sup> While the mobile phase is responsible for the transport of the particles, the separation of the sample is based on different retention times of its components in the stationary phase.<sup>43</sup>

Chromatographic methods can be classified according to their separation mechanism into adsorption chromatography, partition chromatography, ion-exchange chromatography, exclusion chromatography and affinity chromatography. The two methods used in this work, partition and exclusion chromatography, will be shortly described.

### 2.5.2.1 Partition Chromatography

In partition chromatography, the sample components are separated due to a difference in their solubilities in the mobile and the stationary phases. A prominent example for this is the high-performance liquid chromatography (HPLC), where a liquid mobile phase and mostly a solid stationary phase are used.<sup>42</sup>

A special case of partition chromatography is gas chromatography (GC), as the mobile phase, an inert carrier gas, is not used for interaction with the analyte. Thus, after vaporizing the sample and transporting it to the column by the carrier gas, the separation is solely carried out due to the different solubilities at the stationary phase, which can be solid (gas-solid chromatography GSC) or liquid (gas-liquid chromatography GLC).<sup>42,44</sup>

In HPLC, mainly UV-VIS, fluorescence (FLD), refractive index (RI), electron capture (ECD) and evaporative light scattering detectors (ELSD) are used.<sup>45</sup> Compared to that, often used detectors in GC are thermal conductivity (TCD), flame- (FID) or photoionization detectors (PID). A very powerful detector which can be used for HPLC but is especially often used in GC is the mass spectrometry detector.<sup>44</sup>

### 2.5.2.2 Exclusion Chromatography

Exclusion Chromatography is based on exclusion effects, like differences in molecular size and/or shape or in charge.<sup>42</sup>

When separation is based on the molecular size, the term *Size-Exclusion Chromatography* is used.<sup>42</sup> In SEC, molecules are sorted according to their size in solution. The stationary phase is a column filled with a rigid-structure, porous-particle packing. The mobile phase is liquid. Due to a repeated exchange of the sample with the mobile phase and with the liquid phase within the pores of the packing, the components are sorted according to their size. The

molecular size range is determined by the size of the pores. Thus, SEC retention can be seen as a “physical” interaction of the molecules with the packing pores. As seen in Figure 16, there are three possibilities: First, all molecules that are too big to penetrate the pores are totally excluded from the packing, showing very short or no retention. Thus, these molecules co-elute with the solvent (peak at  $KD = 0.0$ ) with the retention volume of the solvent, the exclusion volume  $V_0$ . Second, components with lower molar masses, thus being smaller, elute according to their decreasing size (peaks at  $KD = 0.4$  and  $0.8$ ) at volumes  $V_i$ , as smaller particles are retained for a longer time. Third, all molecules that are small enough to access all the pores, elute at the total permeation limit (peak at  $KD = 1.0$ ) with the total mobile-phase volume  $V_m$ . Due to the unknown number of compounds in the first and the last peaks, selectivity is only

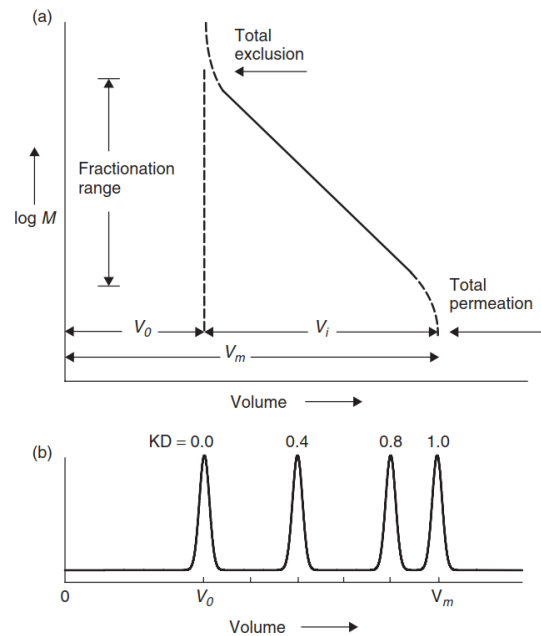


Figure 16: (a) Hypothetical SEC calibration curve and (b) chromatogram<sup>46</sup>

given between these two extreme cases. The detectors used in SEC are similar to the ones in HPLC and include UV/VIS, RI, FLD, ELSD and also viscometric detectors.<sup>46–48</sup>

### 2.5.3 Mass Spectrometry

In mass spectrometry, the molecular weight of a molecule is determined by measuring the mass of a charged ion. There are three main components in each mass spectrometer as can be seen in Figure 17: an ionization source, a mass analyzer and an ion detector.<sup>37</sup>

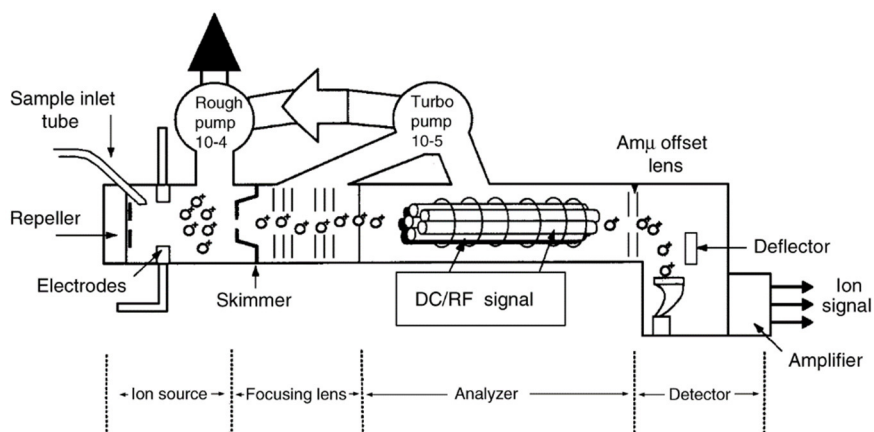


Figure 17: Schematic representation of a quadrupole mass spectrometer<sup>49</sup>

#### 2.5.3.1 Ionization sources

The ionization source converts the neutral molecule into cations, which can be detected. The most common ionization methods are electron (EI), chemical (CI) and electrospray ionization (ESI).<sup>37</sup>

Electron ionization is the mostly used ionization method in GC-MS analysis. In EI, the molecule is bombarded with highly energetic (70 eV) electrons, knocking a weakly bonded electron, for example from a lone pair, out of it. This leads to a positive charge due to an unpaired electron, giving unstable radical cations ( $M^+$ ). Due to that, these molecules fragment before they reach the detector, yielding specific fragmentation patterns with a “parent” molecular ion and lower-mass fragments. A drawback of this method is a possible total fragmentation of fragile molecules, after which no molecular ion can be detected which makes it hard to analyze.<sup>37,49–51</sup>

Chemical ionization mixes an ionization gas, for example  $NH_3$  or  $CH_4$ , with the vaporized sample. Here again, highly energetic electrons are introduced into the system. Now, the gas is preferentially ionized by electrons due to its much higher concentration than the sample, leading to the formation of cations, in this case  $NH_4^+$ . These cations react chemically via collision with the sample to charged complexes, which can later be detected, and uncharged gas molecules. Thus, in CI mostly masses with  $M + 1$  ( $+ H^+$ ) or  $M + 18$  ( $+ NH_4^+$ )/  $M + 17$  ( $+ CH_5^+$ ), where  $M$

is the mass of the compound, are observed. The ionization occurs at much lower energy than in EI, leading to more stable molecular ions without fragmentation.<sup>37,49–52</sup>

Electrospray ionization works in a similar way as CI, as a sample aerosol is ionized in the presence of sodium ions, leading to masses of  $M + 1$ ,  $M + 23$  ( $+ \text{Na}^+$ ) or  $M - 1$  ( $- \text{H}$ ) by the formation of anions. The sample aerosol is produced by applying a strong electric field to the liquid flowing through a capillary tube, generating highly charged droplets. As the solvent evaporates during the spraying process, a charge accumulation can be observed, leading to the formation of ions..<sup>37,51</sup>

Matrix-assisted laser desorption/ ionization (MALDI) is a method especially used for macromolecules like proteins, oligonucleotides, synthetic polymers and large inorganic compounds. In this method, the macromolecule is mixed with a matrix of an organic substance and an inorganic salt. Then the sample is radiated with an intense, pulsed laser over a short time, which knocks out charged ions from the matrix and neutral macromolecules from the sample. These macromolecules then complexate to ions with  $\text{H}^+$ ,  $\text{Na}^+$  or  $\text{Ag}^+$ .<sup>38,51</sup>

### 2.5.3.2 Mass analyzers

After the ions have been produced, they have to be separated according to their mass-to-charge ratio ( $m/z$ ). In GC-MS, a quadrupole mass analyzer was used, while LC-MS was coupled with a Time of Flight (TOF) mass analyzer.

A quadrupole mass analyzer is composed of four cylindrical (hyperbolic) quartz or metal rods clamped perfectly parallel in a pair of ceramic collars. On two rods, a direct current (dc) and on the other two rods an oscillating radio frequency (RF) is applied, so that adjacent rods have opposing charges. This combined dc/RF field is swept toward higher and lower field strength, up and down. At a given RF frequency, only a single-mass ion follows a stable path down the quadrupole to the detector, in a sinus curve due to the attraction and repulsion by the dc rods. All other ions follow unstable paths and end up within the walls of the quadrupole.<sup>49,51,52</sup>

In a TOF mass analyzer, ions with the mass  $m$  and the charge  $ze$  are accelerated through an electric field  $\epsilon$  over a distance  $d$ , after which a flight tube with the length  $l$  is passed to the detector in a time  $t$ .<sup>38</sup>

$$\frac{m}{z} = 2e\epsilon d \left(\frac{t}{l}\right)^2$$

This means, that the ions, which are given into the TOF in bundles, can be separated in the order of their increasing  $m/z$  ratio, as all parameters on the right side but the time are constants.

This makes the TOF analyzer very fast with still having very high sensitivity due to their high transmission efficiency and the possibility of separating same-time ions via the penetration depth after the flight. The biggest advantage of TOF is the much higher resolution compared to quadrupoles, which allows identification of the exact masses

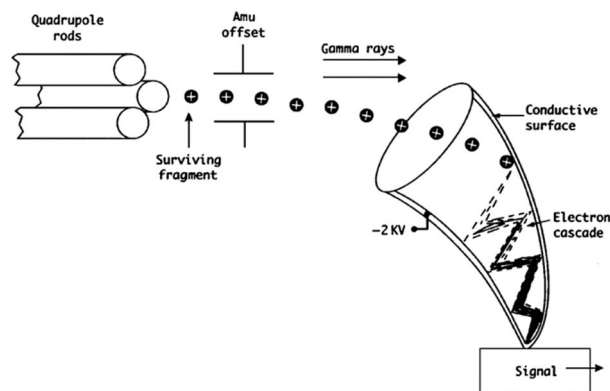


Figure 18: Schematic representation of an ion detector<sup>49</sup>

which can be used for elemental formula determination. Also, a TOF instrument has no upper limit regarding the mass range, as samples with masses >300 kDa have been observed. TOF mass analyzers can either be operated linearly or as a reflectron, which increases its resolution nearly without a loss of sensitivity<sup>50-52</sup>

### 2.5.3.3 Ion detectors

After the mass analyzer, the ions must be detected. This is done via generation of an electric current from the incident ions. The most widely used ion detector in MS is the electron multiplier (EM). In the EM, the fragments are deflected from a straight path by the amu offset, so that possible gamma particles from ionization, which would cause false signals, do not impact on the detector surface. The fragment ions hitting the detector are amplified via an electron cascade, so that a strong enough signal is generated, which can then be processed.<sup>49,51</sup>

## 2.6 Lignin depolymerization

Various methods for depolymerization of lignin to yield bulk and fine chemicals, especially aromatics and fuels<sup>4</sup>, have been investigated. These include the methods presented in chapters 2.6.1 to 2.6.7. The main depolymerization strategies used in this thesis are the electrocatalyzed oxidation and the reduction, which will be described in detail in chapters 2.6.6 and 2.6.7.

### 2.6.1 Base-catalyzed depolymerizations (BCD)

Base-catalyzed depolymerizations are mainly carried out with LiOH, NaOH or KOH at 250–650 °C (mainly ~ 300 °C).<sup>1,13,53,54</sup>

Beauchet et al.<sup>55</sup> depolymerized 10 wt% Indulin AT kraft lignin in a 5 wt% NaOH aqueous solution within a 30 m long continuous flow reactor with 0.66 cm internal diameter. The reactor was heated to 270, 290 or 315 °C and pressurized to 130 bar at flow rates of 1.4, 2.6 and 4 h<sup>-1</sup>. The products were recovered at the outlet at 20 °C and atmospheric pressure, separating the oligomers from the monomers via precipitation at pH 2 and subsequent filtration. The

monomer-fraction was then analyzed via GC-MS, quantifying the main monomers with GC-FID and external calibration. Products isolated after the reaction included 13–25 wt% gases, mainly CO<sub>2</sub> and 2.1–6.6 wt% small organic compounds, like methanol, formic acid and acetic acid. 49–72 wt% of the oligomers-rich fraction, containing polyaromatic compounds and non-converted lignin and finally 8–19 wt% of the monomer fraction were recovered, being the highest with 315 °C and 1.4 h<sup>-1</sup>. The main compounds identified and quantified in this fraction were pyrocatechol (up to 5 wt%), guaiacol (up to 2 wt%) and 4-methylcatechol (up to 1.2 wt%), while minor constituents identified were phenol, 3-methylcatechol, 4-ethylcatechol, vanillin, acetovanillone and 3-hydroxy-4-methoxy benzeneacetic acid, all with yields under 1 wt%. With that, Beauchet et al. reported a total yield of identified monomers of 8.4 wt% at 315 °C and 1.4 h<sup>-1</sup>.

Toledano et al.<sup>56</sup> carried out base-catalyzed depolymerizations on an organosolv olive tree pruning lignin in aqueous solutions of 4 wt% of various bases, including KOH, NaOH, Ca(OH)<sub>2</sub>, LiOH and K<sub>2</sub>CO<sub>3</sub>. Reactions were carried out in a batch reactor at 300 °C with 900 bar and mainly led to an oil product, with yields between 5 and 20 wt% depending on the base, and residual lignin, with contents up to 45 wt%. The oil was composed of monomeric phenols, mainly catechol with 0.1–2.4 wt% but also cresols, syringol and guaiacol. The main reason for the high residual lignin content were, according to this paper, repolymerization reactions during the BCD, thus limiting oil production.

### 2.6.2 Acid-catalyzed depolymerizations (ACD)

Acid-catalyzed depolymerizations are performed via various acids at temperatures of 78–380 °C.<sup>1,13,53</sup>

Forchheim et al.<sup>57</sup> reported the acid-catalyzed depolymerization of Protobind 1000 non-wood kraft lignin in 5 ml batch and 190 ml continuous stirred tank reactors (CSTR). For the batch reactor, 0.35 g lignin was used, while formic acid (1.1 g/g lignin) and ethanol (9 g/g lignin) were the catalyst and solvent, respectively, and the reaction conditions were 280 °C, 290–330 bar and 60–140 minutes. The gas-phase was analyzed via gas-phase GC-FID/TCD and the filtered and quantified liquids were analyzed via GC-FID and internal calibration, while the solids were weighed after drying. The gases mainly consisted of CO<sub>2</sub> (64–66 %), hydrocarbons (20–28 %) and CO (8–15 %). Up to 5.1 wt% total phenolics were extracted with the batch process, consisting of 2.0 wt% methoxyphenols, 1.7 wt% catechols and 1.4 wt% phenols. In the CSTR reactor, about 6.5 g lignin per hour were introduced, with formic acid and ethanol ratios of 1.2:1 g/g lignin and 9.5:1 g/g lignin, respectively. The temperature was the same as in

the batch reactions with 280 °C, while the pressures were between 200 and 300 bar at residence times of 60, 136 and 141 minutes. Samples were taken during and after the reaction, with a similar workup as described above. In these reactions, the gas-phase consisted of 34–38 % CO, 28–36 % CO<sub>2</sub>, 13–16 % H<sub>2</sub>. and 12–16 % hydrocarbons. A total of 4.4–6.9 wt% phenolic products were achieved with the CSTR, containing 2.8–3.3 wt% methoxyphenols, 1.3–2.1 wt% phenols and only 0.3–1.6 wt% methoxyphenols.

The Lewis acids NiCl<sub>2</sub> and FeCl<sub>3</sub> were used for the acid-catalyzed depolymerization of Alcell lignin in a 500 ml autoclave by Hepditch and Thring<sup>58</sup>. This reactor was charged with 15 g lignin, 250 ml water and 1.5 g of either NiCl<sub>2</sub> or FeCl<sub>3</sub>, carrying out the reactions at temperatures of 255–305 °C for 60 and 120 minutes. The product mixture was filtered, acidified to pH 1–2 and then extracted with diethyl ether to obtain the phenolic compounds in the ether phase. This ether phase was subsequently analyzed via capillary GC with an internal standard, while the aqueous phase was analyzed for water-soluble lignin with an UV-spectrophotometer and the solid residues were weighed. Ether soluble yields of 7.0–18 % were found by Hepditch for NiCl<sub>2</sub> and 6.3–14 % for FeCl<sub>3</sub>. Solid residues made up 68–87 % and 74–87 % for NiCl<sub>2</sub> and FeCl<sub>3</sub>, respectively. The water-soluble lignin was in the range of only 0.1–0.3 % for all experiments. After the reaction with NiCl<sub>2</sub>, the phenolic compounds with the highest percentage were catechol (up to 1.6 wt%), syringol (up to 1.0 wt%) and guaiacol (up to 0.6 wt%), while the other compounds, including phenol, vanillin, syringaldehyde, acetoguaiacone and acetosyringone, had contents of below 0.2 wt%. A similar result can be seen with FeCl<sub>3</sub>, where up to 2.5 wt% catechol, 0.4 wt% guaiacol and 0.3 wt% phenol were identified, with contents of the other compounds being again below 0.2 wt%. Hepditch sums up that low quantities of monomeric compounds were produced, while both catalysts favor condensation reactions, leading to the formation of solid reactor residues.

### 2.6.3 Pyrolysis

Lignin pyrolysis has been reported at temperatures of 450–600 °C either solely thermal or with the help of a catalyst.<sup>1,59</sup>

Kosa et al.<sup>60</sup> reported the pyrolysis of kraft lignin precipitated from pulping liquor with sulfuric acid (pH 3) and CO<sub>2</sub> (pH 10.5 and 9.5). 3 g of the sample were placed into a pyrolysis tube and pyrolyzed at 500 ° with nitrogen as inert gas. After the reaction, a solid residue called char and two liquid phases were retrieved, a light phase, acquired via decantation which contained over 80 % water, and a heavy fraction, recovered via washing with acetone and subsequent recovery by evaporation, also called product oil. Kraft lignin precipitated with CO<sub>2</sub> was reported to yield



less gas than the one precipitated with sulfuric acid (12 % vs. 18 %) and more of the product oil (32 % vs. 19 %). Char formation was in the range of 50–52 % for all three lignins. Elemental analysis of the oils showed higher carbon and lower sulfur contents for the CO<sub>2</sub> precipitated lignins, in the ranges of 66–69 % and 1.2–4.7 %, respectively. Hydrogen, with contents of 6.5–6.8 %, and oxygen, with 22–23 %, were about the same for all lignins. Via SEC in THF it was shown that, although the acid precipitated acid had lower M<sub>w</sub> and M<sub>n</sub> before pyrolysis, the molecular weights were about the same for the oils after all three reactions, with M<sub>w</sub> of 300–320 g/mol and M<sub>n</sub> of 140–160 g/mol. The educt lignins and the product oils were also analyzed via <sup>13</sup>C, <sup>1</sup>H and <sup>31</sup>P NMR. It was confirmed that the major inter-unit linkages in these lignins were β-5 and 5-5, while only small amounts of α-O- and β-O-ether linkages were found. The main cleavage products identified by Kosa were guaiacyl hydroxyls, aldehydes, toluols and styrenes, while p-hydroxy-phenols, catechols and cresols are products of further depolymerization. The biggest differences between the oils from acid and CO<sub>2</sub> precipitation were, that the latter lignin yielded more aliphatic compounds, like methyl and ethyl substituents on phenol and anisole, a higher amount of p-hydroxy phenols and catechols, while the acid precipitated lignin yielded a higher amount of guaiacol. Thus, Kosa identified CO<sub>2</sub> precipitated lignins as educt for pyrolysis with high yields, pointing out the possible utilization of the pyrolysis oils as liquid biofuels.

Jiang et al.<sup>61</sup> studied pyrolysis and its kinetic parameters for four different lignins, a commercial Protobind 1000 kraft lignin from wheat straw and sarkanda grass, a hydrolytic lignin from softwood, an organosolv and an Alcell lignin from hardwood and Klason lignins from softwood, hardwood and cassava. Jiang placed 2.5 mg of these samples in a thermogravimetric analyzer (TGA) and then heated the sample up to 900 °C with heating rates of 2–200 °C/minute, whilst using nitrogen as inert gas. With that, the Klason lignins showed char yields of 40–45 %, while alkali, Alcell and organosolv lignins had 30 % and the hydrolytic lignin only 22 % char yield. The determined activation energies were lowest for the alkali lignin, with 134 kJ/mol, in the range of 144–159 kJ/mol for hard- and softwood lignins and 172 kJ/mol with the cassava Klason lignin. Reaction orders were 1 for all lignins except the Klason lignins, which had an reaction order of 1.5.

#### 2.6.4 Depolymerization in supercritical solvents

Supercritical solvents used in lignin depolymerization include supercritical water, either alone or mixed with phenol or p-cresol, methanol/KOH and ethanol/KOH.<sup>53,59</sup>

Miller et al.<sup>62</sup> reported the base catalyzed depolymerization of an Alcell organosolv and an Indulin AT kraft lignin with KOH in supercritical methanol and ethanol in a microreactor. In these experiments, 0.43 g of the lignin were used together with 4.4 ml of a 10 % solution of KOH in methanol or ethanol for reactions at 290 °C for 0–60 minutes. The products of the reaction were precipitated via acidification (pH 2), the precipitate was recovered, washed, dried and weighed, giving the mass of unconverted lignin. The results showed greater conversion with Alcell lignin than with kraft lignin, by about 10 %. The total amount of insolubles in KOH/methanol for Alcell lignin was 14–17 %, while it was only 7 % in KOH/ethanol, thus ethanol was better suited for depolymerization. Most of the conversion occurred during the first 15 minutes. The BCD of the Alcell lignin in ethanol was also carried out with other strong (NaOH, CsOH) and weaker bases (LiOH, Ca(OH)<sub>2</sub>, Na<sub>2</sub>CO<sub>3</sub>). An excess of the base was required to reach maximum conversion, which was better for the strong bases (5–15 % insolubles) than for the weak bases (34–54 % insolubles). There were also synergistic effects reported by combining low amounts of a strong with a weaker base. Finally, Miller et al used various model compounds to verify that the primary reaction is solvolysis of ether linkages, while no evidence of C-C bond cleavage was found, resulting in phenols and ethyl ethers as products in ethanol.

In contrast to that, Wahyudiono and Goto<sup>63</sup> investigated the depolymerization of alkali lignin with supercritical water in a batch reactor. 0.1 g of the lignin were reacted with pure water, corresponding to densities of 0.16–0.67 g/ml, with argon as inert gas for 5–240 minutes at 350 or 400 °C. Via centrifugation, the product was separated into methanol soluble (MS) and methanol insoluble (MI) fractions. While the MI fraction was defined as solid residue or char and analyzed via FTIR, the MS fraction contained the products and was analyzed with GC-MS, HPLC and MALDI-TOF-MS. Catechol, phenol, m-/p-cresol and o-cresol were identified as the primary products of this reaction. With MALDI-TOF, the yield of these compounds was analyzed at different reaction times, temperatures and water densities. Catechol increased for the first 30 minutes, but decreased from that point, while the other compounds steadily increased up to 180 minutes, especially at 400 °C, where catechol was completely consumed at that time. At 350 °C, higher maximum amounts of catechol (~30 % vs. 26 %) and m-/p-cresol (~9 % vs. 7 %) were found, while phenol content (~12 % vs. 3 %) was higher at 400 °C. O-cresol showed amounts of ~4 % at both temperatures. With increasing water density, catechol decreased, while phenol and the cresols gradually increased. Meanwhile, FTIR analysis of the solid residue showed a disassembly of ether and carbon-carbon bonds.

### 2.6.5 Oxidation

Lignin oxidation is mainly carried out via metal salt catalysis, organometallic catalysis, metal-free organic catalysis, acid or base catalysis, enzymatic catalysis, photocatalysis or electrocatalysis, which is described in detail in chapter 2.6.6 Electrochemical oxidation.

Research in lignin oxidation is mainly focusing on model compounds, but there have also been papers which focus on (technical) lignin samples:<sup>1,13,15,53,54,59,64</sup>

Metal salt catalyzed oxidation has been reported by Voithl and von Rohr<sup>65</sup>, who used a polyoxometalate,  $\text{H}_3\text{PMo}_{12}\text{O}_{40} \cdot x \text{H}_2\text{O}$  in either water, methanol/water (40–80 vol%) or ethanol/water (40 vol%). The oxidation was carried out in a 500 ml autoclave, which was filled with 1 g kraft lignin, 5 bar of  $\text{O}_2$  or  $\text{N}_2$  and then heated to 170 °C, where the reaction was carried out for 20 minutes. The liquid product was filtered and extracted with chloroform, adding the internal standard n-decane before GC-MS analysis. The yield of monomeric products of the oxidations was greatly improved by using water/alcohol as solvent, from 0.1 % to 0.42 %, whilst using  $\text{N}_2$  inert gas. By using  $\text{O}_2$  as gas, the yield could even be increased to up to 2.92 % with the usage of 80 vol% MeOH/ $\text{H}_2\text{O}$ . This product mainly consisted of methyl vanillate (47 %) and vanillin (43 %), with low amounts of acetovanillone (2 %) and other products.

Crestini et al.<sup>66</sup> reported the oxidation of lignin model compounds, but also technical lignins, specifically hydrolytic sugar cane lignin (SCL), red spruce kraft lignin (RSL) and hardwood organosolv lignin (OSL) via acidic oxidation with  $\text{H}_2\text{O}_2$  and the help of the organometallic catalyst methyltrioxorhenium  $\text{MeReO}_3$  (MTO). The oxidation of 100 mg lignin sample was carried out in 5 ml acetic acid with 1 wt% MTO and 500  $\mu\text{l}$   $\text{H}_2\text{O}_2$  (35 %) for 24 hours, while the resulting reaction mixtures were evaporated, washed, centrifuged and freeze-dried, before phosphorylating them to analyze them via  $^{31}\text{P}$  NMR, where cholesterol was used as internal standard. Via that, it was shown that MTO oxidation yielded more soluble lignins with a high degree of degradation, as there was a decrease in aliphatic groups by 67 % (RSL), 43 % (SCL) and 14 % (OSL), indicating side-chain oxidation. Furthermore, there was a decrease in condensed OH groups by 67 % (SCL), 60 % (RSL) and 46 % (OSL), indicating a low amount of coupling processes. Meanwhile, the amount of carboxylic acid moieties increased through side-chain and aromatic ring cleavage.

TEMPO [(2,2,6,6-tetramethylpiperidine-1-yl)oxyl] was applied for alkaline oxidation of a thermomechanical pulp by Ma and Zhai<sup>67</sup>. They reported the precipitation of long fibers from this pulp, of which 30 g were used for oxidation with 0.05 g of TEMPO, sodium bromide (6 mmol/g fiber) and sodium hypochlorite (0.7–8 mmol/g fiber) at 21 °C for 50 minutes. After

draining, washing and filtering the product fibers, the carboxylic content, various fiber properties and, more importantly, Klason and acid-soluble lignin as well as the lignin aromatic and side-chain structures, analyzed by nitrobenzene oxidation and ozonation, were measured. The carboxylic content increased with increasing NaClO concentration, from 167 mmol/kg to 1444 mmol/kg fiber. With increasing carboxyl content, the lignin content decreased, being about 35 % at 167 mmol/kg and only about 25 % at 1444 mmol/kg. The lignin aromatic ring structures, determined via nitrobenzene oxidation, decreased with increasing carboxylic content, having values of 19.6–33.5 %, like the lignin side-chain structures, determined via ozonation, which decreased from 20.1 % to 15.7 %. This led to the conclusion, that both uncondensed and  $\beta$ -O-4 lignin contents decreased with increased oxidation.

For enzyme mediated oxidation, Wu and He<sup>68</sup> used two microbial consortia, called LI3 and LP3, for depolymerization of 1 g/l alkali lignin in serum bottles at a pH of 7.2 and a temperature of 35 °C for four weeks. The supernatant, taken at various sampling points, was acidified with HCl and then analyzed via HPLC-UV at 280 nm, while the methane produced in the headspace of the bottles was identified and quantified via GC-FID and standard samples. With that, it was found out that the methane amount steadily increased up to values of 152 ml/g lignin and 113 ml/g lignin for LI3 and LP3, respectively, while the structure of lignin changed from high to low molecular compounds via partial lignin depolymerization, as confirmed via HPLC. Wu also detected H<sub>2</sub> in trace levels, indicating that the bacteria break the ether or carbon-carbon linkages of the lignin to produce H<sub>2</sub>, which is immediately transformed into methane.

Ma et al.<sup>69</sup> reported the photocatalytic oxidation of alkali lignin with TiO<sub>2</sub> and Pt doped TiO<sub>2</sub> (Pt/TiO<sub>2</sub>). The lignin was dissolved in an aqueous solution with pH 11 to mimic lignin wastewater. The reaction was carried out in a reactor with sixteen vertical UV lamps (input energy 400 W, output energy 35 W). The synthetic lignin wastewater was used together with catalyst concentrations of 1, 5 and 10 g/l at pH values of 3, 7 and 11 and the reaction time was 60 minutes, taking samples at 5, 10, 15, 20, 30 and 60 minutes. The samples were analyzed for their dissolved organic carbon DOC with a TOC analyzer, the absorbance at 254 nm and the ADMI index by measuring transmittance at 590, 540 and 438 nm with a spectrophotometer. The results of this analysis show much better reaction rates with acidic pH, thus the following reactions were carried out at pH 7. The optimal dose of catalyst in reactions at pH 7 was found to be 1 g/l, as higher values did not lead to a higher DOC and ADMI decrease, while the same can be said for the time, where 30 minutes was found to be optimal. With the 1 g/l TiO<sub>2</sub> photocatalytic oxidation at pH 7 for 30 minutes, Ma could remove 21 % DOC and 41 % ADMI,

while the novel Pt/TiO<sub>2</sub>/UV method was able to remove 46 % DOC and 47 % ADMI, pointing out the better removal efficiency for future reactions.

### 2.6.6 Electrochemical oxidation

The reactions of the electrochemical oxidation of organic substances, described below, can be seen in Figure 19.<sup>70,71</sup>

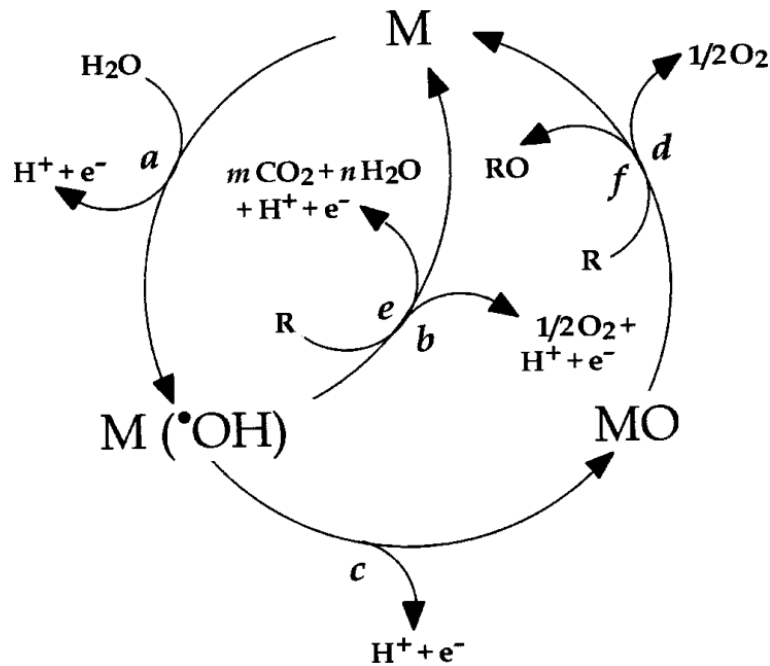
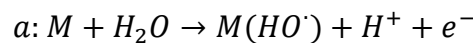


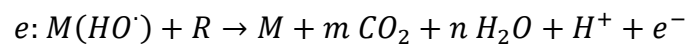
Figure 19: Reaction scheme of the electrochemical oxidation of organic substances (M: electrode surface, R: organic substance)<sup>70</sup>

In the first step, water molecules react to adsorbed hydroxyl radicals (reaction a):

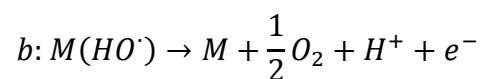


Now there are two possible cases:

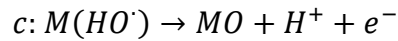
- 1) At inactive electrodes, like boron-doped diamond (BDD), used in this thesis, SnO<sub>2</sub> or PbO<sub>2</sub>, organic substances are completely/ terminally oxidized to CO<sub>2</sub> (reaction e):



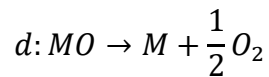
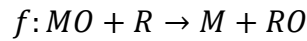
At too low concentration of the organic substance, oxygen formation occurs as a side reaction (reaction b):



- 2) At active electrodes, like graphite, platinum, IrO<sub>2</sub> or RuO<sub>2</sub>, metal oxides are generated on the electrode surface (reaction c):



Now, the oxidation of the organic substance (reaction f) competes with the oxygen formation (reaction d) at the metal oxide.



This means, that inactive electrodes oxidize organic substances completely to CO<sub>2</sub>, with only a small amount of generated oxygen (high oxygen overpotential), while active electrodes oxidize the substance R to RO, with a higher amount of oxygen generated (low oxygen overpotential).<sup>71</sup>

### 2.6.6.1 Literature overview of electrochemical lignin depolymerization

In literature, electrochemical lignin depolymerization is described with different lignins, mostly kraft lignin but also lignosulfonate, organosolv and enzymatic lignins, in various solvents and with many working electrodes.

Table 4 sums up the most important feedstocks and solvents for electrochemical oxidation of lignin with the working electrodes used in literature, while Table 5 sums up the main products of the oxidations, mainly substituted phenols and other aromatics. After that, the single papers are described in detail.

**Table 4: Electrode types, solvents and feedstocks used in lignin electrochemical oxidation**

Feedstock	Solvent	Working electrodes
Kraft lignin <sup>72-79</sup>	NaOH <sup>72,74,76-79</sup>	Ni plate, Pt mesh <sup>72</sup>
		Ni/C, Co/C, NiCo/C nanoparticles <sup>74</sup>
		Ti/TiO <sub>2</sub> -Nanotubes/PbO <sub>2</sub> <sup>76</sup>
		TiO <sub>2</sub> -IrO <sub>2</sub> , RuO <sub>2</sub> -IrO <sub>2</sub> , SnO <sub>2</sub> -IrO <sub>2</sub> , Ta <sub>2</sub> O <sub>5</sub> -IrO <sub>2</sub> <sup>77</sup>
		TiO <sub>2</sub> /Ti-Ta <sub>2</sub> O <sub>5</sub> -IrO <sub>2</sub> <sup>78</sup>
	Ni, DSA-O <sub>2</sub> , PbO <sub>2</sub> <sup>79</sup>	
	KOH <sup>73</sup>	Co core/ Pt partial shell alloy nanoparticles <sup>73</sup>
	Triethylammonium methanesulfonate <sup>75</sup>	RU <sub>0.25</sub> V <sub>0.05</sub> Ti <sub>0.7</sub> O <sub>x</sub> <sup>75</sup>
Lignosulfonate <sup>80,81</sup>	Water <sup>80</sup>	Ti/Sb-SnO <sub>2</sub> , Ti/PbO <sub>2</sub> <sup>80</sup>
	KOH <sup>81</sup>	Ni <sup>81</sup>
Organosolv lignin <sup>82</sup>	NaOH <sup>82</sup>	Ni <sup>82</sup>
Enzymatic lignin <sup>83,84</sup>	NaOH <sup>83,84</sup>	RuO <sub>2</sub> -IrO <sub>2</sub> /Ti mesh <sup>83,84</sup>

Table 5: Products obtained from lignin electrochemical oxidation

Products of lignin electrochemical oxidation		
Acetosyringone <sup>72,80,83,84</sup>	Acetovanillone <sup>72,73,75,82</sup>	Benzaldehyde <sup>75</sup>
p-Coumaric acid <sup>84</sup>	2,3-Dihydrobenzofuran <sup>83</sup>	2,5-Dimethyl-p-anisaldehyde <sup>83</sup>
Diphenylether <sup>75</sup>	3-Furaldehyde <sup>75</sup>	Gallic acid <sup>84</sup>
Guaiacol <sup>73,75,79</sup>	4-Hydroxybenzaldehyde <sup>72,79,82</sup>	Isovaleric acid <sup>80</sup>
Levulinic acid <sup>80</sup>	3-Methoxy-4-hydroxyacetophenone <sup>84</sup>	4-(4-Methoxyphenoxy)-acetophenone <sup>83</sup>
Phenol <sup>84</sup>	Phenylacetic acid <sup>84</sup>	Phthalic acid <sup>80</sup>
Piceol <sup>82,84</sup>	Syringaldehyde <sup>72,75,81,84</sup>	Syringic acid <sup>72,81,84</sup>
Syringol <sup>75</sup>	Vanillic acid <sup>72,75-77,79,81,82</sup>	Vanillin <sup>72,73,75-77,79,81-84</sup>

For kraft lignin, Stiefel et al.<sup>72</sup> presented a method to quantify the influence of five reaction parameters, the temperature, current density, lignin concentration, sodium hydroxide concentration and the electrode material, on the electrochemical oxidation of a technical kraft lignin, the alkali lignin from Sigma Aldrich also used in this thesis. A two-compartment reactor with an ion exchange membrane was used. For characterization, four methods were used, aqueous SEC for molecular weight determination and LC-MS to quantify monomeric compounds as well as acid-insoluble lignin and UV/VIS spectroscopy at 280 nm as fast and easy methods to quantify lignin cleavage. From the mentioned parameters, the NaOH concentration did not influence the outcome of the oxidation at all and the temperature showed very little influence at the investigated values of 1 or 4 mol/l and 30 or 80 °C as well, respectively. An increased yield of monomers can be seen with lower lignin concentration of 5 g/l than with 20 g/l and via the preferred usage of a Ni plate than a Pt mesh. The biggest influence can be seen from the current density, as a higher current density of 38.3 mA/cm<sup>2</sup> led not only to a higher yield in monomers, but also to a higher degree of depolymerization than with 2.1 mA/cm<sup>2</sup>, seeing changes with all four characterization methods. The oxidation yielded mainly vanillin, with 61–67 %, and vanillic acid, with 23–30 %, while lower amounts of acetovanillone (4–5 %), p-hydroxy-benzaldehyde, (3–4 %), syringic aldehyde, syringic acid and acetosyringone (all under 0.3 %) have been identified.

Pan et al.<sup>76</sup> investigated oxidation of a kraft lignin, extracted from Canadian black liquor via CO<sub>2</sub> precipitation for 16 hours. The electrochemical oxidation was carried out with a three-electrode setup with a Pt coil counter electrode, a Ag/AgCl reference electrode and a fabricated electrode consisting of lead dioxide nanoparticles supported on TiO<sub>2</sub> nanotubes (Ti/TiO<sub>2</sub>NT/PbO<sub>2</sub>). A 10 g/l solution of kraft lignin was oxidized in this system at a current of 100 mA and a temperature of 60 °C for four and eight hours, while FTIR and HPLC were used for characterization of the products. FTIR spectroscopy showed an increase in C=O groups, based on the increasing intensity of the peak at 1710 cm<sup>-1</sup>, and a decrease in C-O-C groups,

based on the intensity of the peak at  $1030\text{ cm}^{-1}$ . The two main products, identified with HPLC by comparison with standards, were vanillin and vanillic acid.

The same kraft lignin, precipitated from black liquor with  $\text{CO}_2$ , was also used for electrochemical oxidation in another paper, by Tolba et al.<sup>77</sup> Here, four  $\text{IrO}_2$ -based electrodes, namely  $\text{Ti/SnO}_2\text{-IrO}_2$ ,  $\text{Ti/RuO}_2\text{-IrO}_2$ ,  $\text{Ti/Ta}_2\text{O}_5\text{-IrO}_2$ , and  $\text{Ti/TiO}_2\text{-IrO}_2$ , were prepared and used as working electrodes for the electrochemical oxidation of the precipitated kraft lignin in  $\text{NaOH}$ . A saturated calomel electrode and a platinum wire coil were used as reference electrode and counter electrode, respectively. UV absorbance at 294 nm was used to monitor the changes during the oxidation of 100 ppm lignin for two hours, after which the lignin was completely degraded. The  $\text{Ti/RuO}_2\text{-IrO}_2$  electrode, which exhibited the longest lifetime and highest activity, was used for determination of the optimum temperature ( $60\text{ }^\circ\text{C}$ ) and current density ( $500\text{ mA/cm}^2$ ), again using UV absorption as characterization technique. After an oxidation with these parameters ( $\text{Ti/RuO}_2\text{-IrO}_2$ ,  $60\text{ }^\circ\text{C}$ ,  $500\text{ mA/cm}^2$ ) of 500 ppm kraft lignin in  $\text{NaOH}$  for 60 minutes, HPLC was used to identify the main intermediates and products by comparison with standards. These primary intermediates, vanillin and vanillic acid, increased linearly for the first 45 minutes, but only slightly in the following 15 minutes, resulting in an optimum oxidation time of 45 minutes under these conditions.

Another paper from the same working group<sup>78</sup> again used a prepared electrode, in this case a  $\text{Ti/TiO}_2$  nanotube electrode connected to a  $\text{Ti/Ta}_2\text{O}_5\text{-IrO}_2$  electrode ( $\text{TiO}_2/\text{Ti/Ta}_2\text{O}_5\text{-IrO}_2$ ), for electrochemical oxidation of kraft lignin precipitated from black liquor via  $\text{CO}_2$ . While a Pt coil and a  $\text{Ag/AgCl}$  electrode were used as counter and reference electrodes, a novel approach was applied by combining the electrochemical oxidation with UV irradiation of about  $20\text{ mW/cm}^2$  at 365 nm. UV absorption analysis at 295 nm showed 92 % degradation of 100 ppm lignin in 0.5 M  $\text{NaOH}$  over the course of the combined reaction, while only 66 % degradation was observed with electrochemical oxidation alone. FTIR and  $^{13}\text{C}$  NMR showed the formation of a carbonyl functionality during this combined reaction, while vanillin and vanillic acid were identified as the primary intermediates with HPLC, by comparison with standards, and GC-MS. Parpot et al.<sup>79</sup> investigated the electrochemical oxidation of a kraft lignin from Sigma Aldrich in a two-compartment filter press cell, separated by an ion exchange membrane. As electrodes,  $\text{DSA-O}_2$ ,  $\text{PbO}_2$  and Ni were used for three hours of oxidation, while analysis of the products was carried out via GC-MS, quantifying the compounds with a GC equipped with a capillary column. For  $\text{DSA-O}_2$ , oxidation of 2 % kraft lignin in 1 M  $\text{NaOH}$  was carried out at  $600\text{ A/m}^2$ , giving a conversion yield of 15 %. This yield consisted of 63 % vanillin, 15 % hydroxymethoxyphenyl ethanone (HMPE), 8 % guaiacol and hydroxymethoxybenzene acetic



acid (HMBAA) and low amounts of hydroxybenzaldehyde (HBA, 2 %) and vanillic acid. In the oxidation with the  $\text{PbO}_2$  electrode, the same current density of  $600 \text{ A/m}^2$  was used, but the lignin concentration was lowered to 0.2 % in 1 M NaOH, still yielding 2 % more conversion with 17 %. The product had a similar composition than the first oxidation, with 64 % vanillin, a lower amount of 11 % HMPE and a higher amount of 12 % guaiacol. The remainder was made up of 5 % HMBAA, 2 % HBA and a higher amount of vanillic acid with 4 %. Ni oxidation was carried out with the same lignin concentration as before, 0.2 %, but only at a halved current density of  $300 \text{ A/m}^2$ , which led to a much lower yield of only 7 %. This product consisted of a lower amount of vanillin (56 %) and similar HMPE (12 %), vanillic acid (5 %) and HMBAA (5 %) contents, but increased guaiacol, with 16 %, and HBA amounts, which has been doubled to 4 %.

The electrochemical oxidation of a Sigma Aldrich alkali lignin in another solvent, the protic ionic liquid triethylammonium methanesulfonate, was described by Reichert et al.<sup>75</sup> The oxidation was also carried out in a three-electrode setup, where the working electrode was a Ti-wire mesh coated with  $\text{Ru}_{0.25}\text{V}_{0.05}\text{Ti}_{0.7}\text{O}_x$ , and the counter electrode a Pt-wire mesh, while the third electrode was a Ag-quasi-reference electrode. The 5 wt% solution of alkali lignin in the ionic liquid was oxidized for eight hours at  $110 \text{ }^\circ\text{C}$  at potentials of 1, 1.3 and 1.5 V. By that, oxidative product yields of 3.1 % (1 V), 5.4 % (1.3 V) and 6.0 % (1.5 V) could be reached. HPLC-UV analysis at 274 nm of this product showed vanillin, vanillic acid and syringol as products at all three potentials. On the other hand, guaiacol was only detected at 1.0 and 1.3 V and syringol aldehyde only at 1.5 V. Via GC-MS analysis, mostly aldehydes and ketones have been identified with reference standards and the NIST database, as benzaldehyde, 3-furaldehyde, vanillin and acetovanillone were observed at all three potentials and m-tolualdehyde only at 1.3 and 1.5 V. Other compounds found at all three potentials were diphenylether, 2-methoxy-4-vinylphenol, syringol and 2-methoxybiphenyl, while guaiacol was again only identified at 1.0 and 1.5 V and 3-methylfuran was observed after electrochemical oxidation at 1.5 V. Vanillic acid could not unambiguously be confirmed by GC-MS analysis.

Movil-Cabrera et al.<sup>73</sup> reported the electrochemical oxidation of a sulfonated kraft lignin from Sigma Aldrich with an average molecular weight of 10,000 g/mol, the same sulfonated kraft lignin used in this master's thesis. In this paper, 10 g/l sulfonated kraft lignin in 1 M KOH were oxidized in a three-electrode beaker cell with a Co core/Pt partial shell alloy working electrode, a Hg/HgO reference electrode and a Pt ring counter electrode. The potential was held constant at 0.598 V vs. SHE for 2700 minutes, whereas GC-MS samples were taken out at 83 and 1200 minutes and after the reaction, identifying the oxidation products via the NIST database.

After 83 minutes, 8.45 ppm vanillin and 1.96 ppm acetovanillone were identified, while guaiacol, heptane, acetosyringone, 2,4-di-tert-butylphenol, 1,3-bis(1,1-dimethylethyl)-benzene, phenol, 2,4-dimethyl-1-heptene and 2,6-dimethyl-nonane were found in low concentrations of under 1 ppm. After 1200 minutes, the amounts of vanillin and acetovanillone dropped to 7.43 and 1.62 ppm respectively, while phenol, acetosyringone and 2,6-dimethyl-nonane could not be found and another compound, 4-methyl-benzaldehyde, could be identified, but only with a concentration of 0.17 ppm. The other compounds still had concentrations under 1 ppm. After the end of the oxidation, the concentrations of vanillin increased to 9.83 ppm and the one of acetovanillone to 2.49 ppm. The remainder of the product was like the product after 1200 minutes, the only difference being the vanishing of 4-methyl-benzaldehyde. The reason for the low overall concentrations in the product, compared to the initial lignin concentration (10,000 ppm), was attributed to the extremely low current in the beaker cell and the small electrocatalyst loading.

The same working group<sup>74</sup> also reported electrochemical oxidation of 10 g/l sulfonated kraft lignin in 1 M NaOH in a three-electrode beaker cell with a NiCo/C nanoparticle electrocatalyst working electrode and the same counter and reference electrodes as described above. Both educt and product after two hours of electrochemical oxidation at a potential of 0.42 V vs. SHE were analyzed via FTIR and UV-VIS spectroscopy. FTIR spectroscopy yielded lower intensities of peaks associated with methoxyl and guaiacyl units (1456, 1045 and 880  $\text{cm}^{-1}$ ), suggesting transformation of these units. Likewise, a characteristic carbonyl band appeared after the oxidation (1616  $\text{cm}^{-1}$ ), indicating oxidation of hydroxyl groups in the guaiacyl units to carbonyl containing products like quinones. UV-VIS spectroscopy of the educt showed a maximum absorbance peak at 235 nm, assigned to aromatic components in the lignin, whose intensity decreased after oxidation, suggesting destruction of aromatic rings during the electrochemical oxidation.

The electrochemical oxidation of lignosulfonate, in this case a sodium lignosulfonate, was reported by Shao et al.<sup>80</sup> 2000 ppm of the lignosulfonate in water were electrochemically oxidized at 0.8 A with either a titanium based antimony doped tin dioxide (Ti/Sb-SnO<sub>2</sub>) or a titanium based lead dioxide electrode (Ti/PbO<sub>2</sub>), each with 60  $\text{cm}^2$  effective area. The oxidations were performed at room temperature for 7 hours, taking samples before the reaction, after 1 and 3 hours and after the reaction. FTIR spectroscopy analysis of these samples showed only little differences after 1 hour of oxidation, but at longer oxidation times increased conjugated C=O in aromatic rings peaks (1675–1655  $\text{cm}^{-1}$ ), indicating quinone formation, and unsaturated bond peaks (1330–1400  $\text{cm}^{-1}$ ) were observed. In addition, a decrease in ether C-O-

C peaks (1130–1125  $\text{cm}^{-1}$ ), indicating cleavage of the ether groups connecting the lignin molecule, and in aromatic ring peaks, meaning destruction of these structures, was identified. The only difference between the two electrodes was a peak at 1388  $\text{cm}^{-1}$  visible after treatment with the Ti/PbO<sub>2</sub> electrode, indicating more carboxylic acids present with this electrode. GC-MS analysis of the educt with identification via NIST database showed several volatile fatty acids (VFAs) like butanoic acid, isovaleric acid and hexanoic acid and some low-molecular-weight aromatic compounds (LMWACs) like n-propylbenzene, 1,3-xylene and vanillin. These VFAs and LMWACs were degraded during the reaction, giving rise to intermediates, mainly quinones like 1,4-benzoquinone, 4-hydroxy-2-butanone, acetosyringone and 2,6-dimethoxy-2,5-cyclohexadiene-1,4-dione. Products after 7 hours of oxidation were short-chain carboxylic acids. According to Shao et al., these products indicate degradation of the lignin molecule during the depolymerization experiments, which was confirmed via COD and UV-VIS measurements. Both the COD and the absorption at 280 nm decreased during the reaction. The difference between the Ti/Sb-SnO<sub>2</sub> anode, a nonselective electrode, and the Ti/PbO<sub>2</sub> anode, a selective electrode, was the further oxidation of intermediates. While the Ti/Sb-SnO<sub>2</sub> electrode oxidized the untreated lignin and the intermediates equally, leading to low concentrations of intermediates and finally mineralized lignin to CO<sub>2</sub>, the Ti/PbO<sub>2</sub> electrode tended to oxidize the lignin rather than the intermediates, generating higher intermediate concentrations and making the lignin more biodegradable.

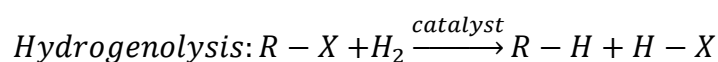
Smith et al.<sup>82</sup> carried out an electrochemical oxidation of an organosolv lignin, acetone-soluble spruce lignin (ASPPS). 10 g/l ASPPS in 3 M NaOH were oxidized in a reactor with a Ni anode and a Pb cathode at 170 °C and 4 mA/cm<sup>2</sup> for 4 hours. A yield of 36 % was reached, consisting of 51 % 4-hydroxybenzaldehyde, 19 % vanillic acid, 17 % vanillin, 9 % 4-hydroxyacetophenone and 4 % acetovanillone, detected by HPLC with UV detection at 280 nm.

Zhu et al.<sup>84</sup> reported an electrochemical depolymerization of a purified crude lignin derived from an enzymatic process for ethanol production from corn straw. The cell used was a cylindrical electrolytic cell with an outer RuO<sub>2</sub>-IrO<sub>2</sub>/Ti mesh anode and an inner porous graphite felt cathode. A 2 wt% solution of the lignin in 1 M NaOH was oxidized in this cell with 8 mA/cm<sup>2</sup> for 1 hour at room temperature. After the oxidation, diethyl ether was added, forming a three-phase-system with an upper ether phase, a middle lignin-fragments phase and a lower aqueous phase. The total yield was about 19–23 wt%, with the ether phase having a yield of 16–18 wt% and the aqueous phase 2–4 wt%. Ether phase analysis via GC-MS showed

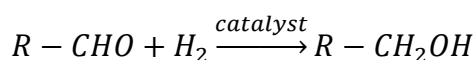
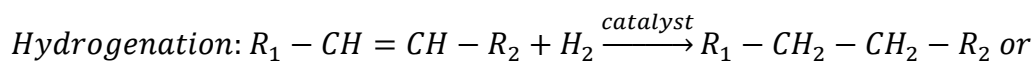
low-molecular-weight (LMW) products in this phase, such as vanillin, syringaldehyde, acetosyringone, 4-hydroxyacetophenone and 3-methoxy-4-hydroxyacetophenone. The aqueous phase mainly consisted of acids and phenols like phenol, phenylacetic acid, p-coumaric acid, gallic acid and syringic acid, determined by ESI-MS/MS analysis. The middle phase was analyzed via GPC, which yielded a  $M_w$  of about 1000 g/mol, much lower compared to 3000 g/mol in the lignin educt.

### 2.6.7 Reduction

The two main reactions in lignin reduction are hydrogenolysis, more specifically hydrodeoxygenation (HDO), and hydrogenation: <sup>1,4,13,54,59,64,85</sup>



Where -X is -OH (HDO), -OR, -SH or -NH<sub>2</sub> and R- the remaining lignin molecule



where R<sub>1</sub> and R<sub>2</sub> are the remaining lignin molecule

In this work, a NiMo catalyst is used for lignin reduction. This catalyst shows a higher HDO than hydrogenation reactivity, as reported in several references.<sup>13,54,64,85</sup> Regarding the different hydrogenation reactions, the C=O hydrogenation is the most prevalent in the used system due to the bimetallic catalyst NiMo used. The second possible reaction in this system is the C=C hydrogenation on the hydrocarbon chains between the aromatic structures of lignin, while nearly no reactivity is assumed in terms of C=C hydrogenation on the aromatic rings, as aliphatic alkenes are more easily hydrogenated.<sup>64</sup>

For both reactions, not only pressurized hydrogen, between 10 and 100 bar, and a suitable catalyst are needed, but also relatively high temperatures of up to 430 °C. Another limitation is the mostly relatively small yield to aromatics of under 10 %, although very good monomer yields in the products have been reported.<sup>13</sup>

#### 2.6.7.1 Literature overview of lignin reduction

Table 6 summarizes the feedstocks, solvents and catalysts used in lignin reduction and at which parameters it was carried out. The single papers are discussed in detail after Table 7, which shows important products of lignin reduction, mainly lignin fragments, especially substituted and non-substituted benzenes and phenols as well as dimers and oligomers of these.

Table 6: Summary of lignin reduction parameters

Feedstock	Solvent	Catalysts	Reaction conditions
Kraft lignin <sup>86-90</sup>	Methanol <sup>86</sup>	(Sulfided-)NiMo, (S-)CoMo, (S-)NiW, S-W, S-Ni <sup>86</sup>	320 °C, 35 bar H <sub>2</sub> , 8 h <sup>86</sup>
	NaOH <sup>89</sup>	5% Pd/C <sup>89</sup>	77–177 °C, 10–50 bar H <sub>2</sub> , 1–4 h <sup>89</sup>
	Tetralin <sup>87</sup>	NiMo <sup>87</sup>	350 °C, 37 bar H <sub>2</sub> , 5 h <sup>87</sup>
	Dodecane <sup>88</sup>	CoMo, Mo <sub>2</sub> C <sup>88</sup>	300 °C, 50 bar H <sub>2</sub> , 4 h <sup>88</sup>
	–	NiMo, S-NiMo, Cr <sub>2</sub> O <sub>3</sub> /NiMo 1/1 <sup>90</sup>	395–430 °C, 90–100 bar H <sub>2</sub> , 20–60 min <sup>90</sup>
Enzymatic lignin <sup>91</sup>	Dioxane/water <sup>91</sup>	5% Pd/C <sup>91</sup>	195 °C, 34.5 bar H <sub>2</sub> , 2–24 h <sup>91</sup>
Organosolv lignin <sup>88,92</sup>	Dodecane <sup>88</sup>	CoMo, Mo <sub>2</sub> C <sup>88</sup>	300 °C, 50 bar H <sub>2</sub> , 4 h <sup>88</sup>
	Tetralin <sup>92</sup>	NiW <sup>92</sup>	370–410 °C, 10 bar H <sub>2</sub> , 15–60 min <sup>92</sup>
	–	NiMo, S-NiMo, Cr <sub>2</sub> O <sub>3</sub> /NiMo 1/1 <sup>90</sup>	395–430 °C, 90–100 bar H <sub>2</sub> , 20–60 min <sup>90</sup>
Sugarcane bagasse lignin <sup>88</sup>	Dodecane <sup>88</sup>	CoMo, Mo <sub>2</sub> C <sup>88</sup>	300 °C, 50 bar H <sub>2</sub> , 4 h <sup>88</sup>
Steam exploded wood <sup>91</sup>	Dioxane/water <sup>91</sup>	5% Pd/C <sup>91</sup>	195 °C, 34.5 bar H <sub>2</sub> , 2–24 h <sup>91</sup>
Pine extracted wood <sup>91</sup>	Dioxane/water <sup>91</sup>	5% Pd/C <sup>91</sup>	195 °C, 34.5 bar H <sub>2</sub> , 2–24 h <sup>91</sup>

Table 7: Products obtained from lignin reduction

Products of lignin reduction		
Anisole <sup>86</sup>	Catechol <sup>92,93</sup>	Dihydroconiferyl alcohol <sup>91,94</sup>
Dimethylphenol <sup>86,90,93</sup>	Ethyl anisole <sup>90</sup>	Ethyl catechol <sup>92,93</sup>
1-Ethyl-2,3-dimethylbenzene <sup>88</sup>	Ethyl guaiacol <sup>86,88,91-94</sup>	Ethylmethylphenol <sup>86,90</sup>
Ethyl phenol <sup>86,88,90,92</sup>	Ethyl syringol <sup>88</sup>	Guaiacol <sup>86,88,91-94</sup>
Methyl catechol <sup>92,93</sup>	Methyl guaiacol <sup>86,88,91-94</sup>	Methylpropylphenol <sup>86,90</sup>
Methyl syringol <sup>88</sup>	o-/m-Xylene <sup>88</sup>	o-/p-/m-Cresol <sup>86-88,90,92,93</sup>
Propyl guaiacol <sup>86,91,93,94</sup>	Propyl phenol <sup>86,90,91</sup>	Phenol <sup>86-88,90,92,93</sup>
Syringaldehyde <sup>92</sup>	Syringol <sup>88,92</sup>	Tetramethylphenol <sup>86</sup>
Toluene <sup>88</sup>	Trimethylphenol <sup>86</sup>	Vanillin <sup>92</sup>

Not only the phenolic fragments, but also two building blocks of lignin, guaiacol and syringol, could be identified together with their alkane-chain substituted compounds. It is also clear that no hydrogenation reactions occurred at the aromatic structures, as all the reported compounds still contain aromatic rings. This means, that most of the reactivity came from the HDO reaction, with C=C hydrogenation happening at the hydrocarbon chains between the aromatic rings.

For kraft lignin, Narani et al.<sup>86</sup> carried out hydrotreatment reactions with Indulin AT pine kraft lignin in a 100 ml autoclave with NiMo, CoMo, NiWO<sub>x</sub>, W and Ni on activated charcoal (AC) support or NiW on AC, ZSM-5, MgO-La<sub>2</sub>O<sub>3</sub> (ML), MgO-CeO<sub>2</sub> (MC) and MgO-ZrO<sub>2</sub> (MZ) supports. The reactor was filled with 0.25 g respective catalyst, 1 g kraft lignin, 0.1 g dimethyl disulfide for in-situ sulfidation of the catalyst, and 30 ml methanol. It was pressurized to 35 bar H<sub>2</sub> and the reaction was carried out at 320 °C for 8 hours. After the reaction, solid residues, containing catalyst, unconverted lignin and char, and an oily product, called methanol soluble oil, were obtained via filtration and solvent evaporation. The solid residues were washed with DCM, yielding 2–22 % “DCM soluble solids”. The unconverted lignin was dissolved in DMSO, giving an amount of under 1 to 20 % “DMSO soluble solids”, while the remainder, solely char, was weighed and gave mostly amounts of 0–9 %, only reaching 30 % with the S-NiW/ZSM-5 catalyst. The yield of the methanol soluble oil, thus the product yield, was in the range of 40 % with the S-NiW/ZSM-5 catalyst up to 82 % with the S-NiW/AC catalyst, while the other catalysts on AC ranged from 41–70 %. The methanol soluble oil was further analyzed by GC-MS-FID, yielding about 30 main components. These compounds can be categorized either into alkylphenols, like phenol, anisole, cresols, dimethyl-, ethyl-, propyl-, ethyl-methyl-, methylated propyl-, tri- and tetra-methyl-phenols, or into guaiacols. Additionally, the two compound groups found in this analysis were quantified via GC x GC-FID, based on calibration of the various compound types and usage of di-n-butylether as external standard. Apart from alkylphenols and guaiacols, the total number of monomers was quantified, containing, besides the two groups mentioned before, naphthalenes, catechols, other aromatics and alkanes. The monomers yield ranged from 9 %, with S-CoMo/AC, up to 28.5 %, again with S-NiW/AC. Alkylphenols yield was also lowest with S-CoMo/AC (5.5 %) and highest with S-NiW/AC (16 %). The highest yield in terms of guaiacols was achieved with NiWO<sub>x</sub>/AC and S-NiW/ML with 7 %, while it was lowest after reduction with S-NiMo/AC with 2 %. Summing up, the S-NiW/AC catalyst was the most promising, achieving a product yield of 82 %. Further experiments with this catalyst at the same conditions as before, with reaction times up to 24 hours, gave monomer yields of 35 wt% and an alkylphenols content of up to 26 %.

Joffres et al.<sup>87</sup> reported the catalytic hydroconversion of a Protobind 1000 lignin from soda pulping of wheat straw with the usage of tetralin as solvent and a NiMo catalyst supported on alumina. Herein, a 0.3 l batch reactor was filled with 30 g lignin, 70 g tetralin, 3 g NiMo/Al<sub>2</sub>O<sub>3</sub> catalyst and 16 µl DMDS to maintain a sulfidation state to the catalyst. 37 bar of H<sub>2</sub> were introduced and the reaction was carried out at 350 °C for 5 hours. After the reaction, the gases were collected before opening the reactor and analyzed via µGC-TCD-MS to recover volatile

compounds. The reaction mixture was centrifuged to separate the liquids and the solids. The solids were extracted with THF in a Soxhlet apparatus, yielding a solid residue, the THF insolubles containing non-converted lignin, ashes and the catalyst, and a THF solubles fraction, obtained via subsequent evaporation of THF. The reaction liquids, mainly tetralin, were analyzed via 2D-GC-MS. After weighing all these residues, an ash-free conversion of 75 wt% to the initial lignin was reached, made up of 65.4 wt% liquids, 24 wt% THF solubles, 9.8 wt% gases and only 1 wt% THF insolubles. Characterization of the gases showed mainly methane and CO<sub>2</sub>, with low amounts of C<sub>2</sub>–C<sub>5</sub> alkanes and CO present. The liquids phase, containing 84 wt% tetralin, was apart from that made up of phenols, aromatics, naphthenes and C<sub>13</sub>–C<sub>18</sub> alkanes. The THF solubles fraction was analyzed with several techniques, including GPC, elemental analysis, FTIR, <sup>31</sup>P and HSQC NMR. GPC yielded a molecular weight of about 2300 g/mol, with a dispersity of 2.4, while elemental analysis showed, compared to the educt, a slight decrease in H/C ratio and a high decrease in O/C ratio. Per FTIR analysis, the product displayed a decrease in carboxylic acid C=O bonds (1700 cm<sup>-1</sup>), syringyl units (1334/1125 cm<sup>-1</sup>), guaiacol units (1183/838 cm<sup>-1</sup>) and hydroxyl aliphatic groups (1090 cm<sup>-1</sup>). <sup>31</sup>P NMR revealed similar results, with the disappearance of aliphatic and carboxylic OH groups, decrease of syringyl and guaiacyl groups and an increase in hydroxyphenyl units. HSQC NMR was in accordance to the previous results due to the exclusive appearance of guaiacyl and hydroxyphenyl units in the C-H aromatic region, while the signals of aliphatic chains, CH<sub>3</sub> and CH<sub>2</sub>, in the aliphatic region were even more intense after the reaction. Joffres used these results to identify five processes in soda lignin reduction: dehydroxylation of aliphatic OH groups to water, decarboxylation of carboxylic acids to CO<sub>2</sub>, saturation of aliphatic double bonds, demethoxylation of syringyl to guaiacyl and further to hydroxyphenyl units and ether linkage cleavage to phenols, present in the liquid phase.

The hydrogenation of a raw alkali lignin from alkaline pulping of wheat straw, reported by Jie-wang et al.<sup>89</sup>, were carried out in a 100 ml micro-autoclave at a low temperature of 117 °C and 40 bar H<sub>2</sub> pressure for 1–4 hours with a 5 wt% Pd/C catalyst. The sample after the reaction was precipitated with HCl at pH 2, getting the product via filtration. The yields reached with this reaction were in the range of 87 % after 1 hour to 84 % after 4 hours. Functional group analysis showed an increase of up to 64 % in total hydroxyl content, with an increase in phenolic hydroxyl groups of 37 % and of 90 % in aliphatic hydroxyl groups after 3 hours. Meanwhile, carbonyl and carboxyl groups decreased by 44 % and 53 %, respectively, indicating conversion of carboxyl to aliphatic hydroxyl groups. <sup>1</sup>H NMR analysis showed an increase in the number of aromatic protons, indicating a reduction of condensation and an increase in activity, in the

number of protons in  $\beta$ -ethenyl and benzyl, indicating oxygen reduction, and a decrease in methoxyl protons by 18 %, suggesting conversion into hydroxyl groups. Additionally, GPC analysis showed a decrease in  $M_n$  from 8750 g/mol to 5200 g/mol and of  $M_w$  from 16,800 g/mol to 13,900 g/mol, with the dispersity increasing from 1.92 to 2.68. Due to the higher contribution of low molecular weight to  $M_n$  and high molecular weight to  $M_w$ , Jie-wang thus reasoned that the alkali lignin was depolymerized to a large number of small molecules during the hydrogenation.

Oasmaa et al.<sup>90</sup> investigated the catalytic hydrotreatment of two kraft lignins, from pine and birch pulping, and a Organocell organosolv lignin, all precipitated from their corresponding black liquors. The catalysts used in this paper were NiMo on either aluminosilica or zeolite support, in their oxide and sulfide forms, and  $Cr_2O_3$  on alumina support in a 1:1 mixture. The hydrotreatment was carried out in a 1 l batch reactor by using 70 g lignin, 7 g catalyst, 90–100 bar  $H_2$  and 395–430 °C for 20–60 minutes. The oily residue after the reaction was collected in acetone, while the solid residue was separated from the catalyst and extracted with acetone in a Soxhlet apparatus, combining the resulting acetone phase with the one after the reaction. The acetone was evaporated at 40 °C, recovering the oil product. The yield of oil products ranged from 49–71 %, with the highest yields being achieved with the Organocell lignin, then with the pine kraft lignin and the lowest from birch kraft lignin. The sulfided catalyst increased the yield for the Organocell lignin, while no change was observed for the two kraft lignins. Elemental analysis of the products did not show bigger differences, as the molar ratio of H/C was in the range of 1.1–1.3 for all reactions, with C contents of about 80 %, H contents of about 8 % and nearly no N detectable. Only the reaction at higher temperature and longer time showed higher C content of 86.5 % and H content of 10.6 %, giving a molar ratio of 1.5. GLC-MS analysis gave detectable fractions of 14.6–20.9 % for all experiments except the one with longer reaction time and higher temperature, which had a detectable fraction of 38.4 %. The main groups detectable were monocyclic aromatics, including alkyl benzenes, phenols, ethylmethoxybenzene and dimethylbenzene, and polycyclic aromatics, including naphthalenes, phenanthrenes, anthracene and dimethylbiphenyl. Monocyclic aromatics were found in contents of 5.6–10.8 %, while only 1.3–2.2 % polycyclic aromatics were found, both being highest in the experiment with higher temperature and longer time.

A two-step process consisting of liquid phase reforming (LPR) and hydrodeoxygenation (HDO) to convert Indulin AT kraft, Alcell organosolv and sugarcane bagasse lignin into monoaromatic compounds is presented by Jongerius et al.<sup>88</sup> The first LPR step was conducted in a 100 ml high-pressure batch reactor with 1 g lignin, 0.5 g Pt/ $Al_2O_3$  catalyst and a mixture of 25 ml 1 M



NaOH and 25 ml ethanol as solvent. The reaction itself was carried out with 58 bar argon at 225 °C for 2 hours. After the reaction, a lignin-oil was recovered via acidification, filtration, extraction with DCM and evaporation of the solvents. After GC-FID and GPC analysis, 500–800 mg of this oil were loaded into a 25 ml high-pressure batch reactor, together with 50 mg of either CoMo/Al<sub>2</sub>O<sub>3</sub> or Mo<sub>2</sub>C/CNF catalyst, 0.35 g hexadecane internal standard and 7.5 of the solvent dodecane. After heating the reactor to 300 °C, it was pressurized to 50 bar H<sub>2</sub> and the reaction was conducted for 4 hours. The reaction mixture was then diluted with diethyl ether, precipitated lignin solids and catalyst were filtered off and the resulting product mixture analyzed via GC-MS. GPC analysis after the LPR step showed a decrease in molecular weight of 32 % for organosolv lignin, from 3900 to 2700 g/mol. For kraft lignin, a decrease of 57 %, from 5000 to 2200 g/mol and for sugarcane bagasse lignin a decrease of 27 %, from 3000 to 2200 g/mol, was observed. GC-FID analysis of organosolv and kraft lignin-oil after LPR demonstrate methyl-, ethyl-, propyl- and propanol-substituted guaiacols and syringol-type products, catechols, phenol and aromatic products, while the lignin-oil from sugarcane bagasse lignin only contains methyl- and ethylguaiacol, phenol and syringol. The total yield of monoaromatics detected in the lignin-oil after LPR were 11 % for organosolv, 9 % for kraft and 5 % for sugarcane bagasse lignin. Analysis of the liquid phase after HDO showed mainly formation of alkylated and non-alkylated syringol, guaiacol and other phenol-type molecules, also containing oxygen-free aromatics like benzene, toluene, xylenes and ethylmethylbenzenes, which were not identified after the first step. The total monoaromatics yields reached with the Mo<sub>2</sub>C/CNF catalyst, which was better suited than the CoMo catalyst, were 9 % for organosolv, 7 % for kraft and 6 % for sugarcane bagasse lignin, meaning lower yield for the first two lignins, but a higher one for sugarcane bagasse. In sugarcane bagasse lignin, 36 % of these monoaromatics were oxygen free, much higher than in organosolv (23 %) and kraft lignins (16 %). Thus, this two-step procedure can more effectively be used to produce oxygen-free products from lignins than the separate steps.

Another paper reporting the hydrocracking of Alcell lignin is the one by Thring and Breau<sup>92</sup>, where 20 g lignin were used with 250 ml of tetralin and 1 g of NiW catalyst on silica-alumina support. The 500 ml batch autoclave was pressurized with 10 bar H<sub>2</sub>, starting the reaction at 370–410 °C for 15, 30 or 60 minutes. After the reactions, the products were separated via extraction with ether and then dichloromethane, yielding solid residues consisting of char and catalyst, solids containing the residual lignin and a DCM-solubles fraction, containing the phenolic products. Total conversions, meaning all product solutions except the reactor residue and the residual lignin, only reached up to 50 %, with DCM-solubles being at a maximum of

7 %. The DCM-solubles fraction was analyzed via GC and yielded for the less severe reaction conditions, at lower temperatures and shorter time, relative abundances of 25.8 % catechols, 21.6 % syringol, 21.4 % guaiacols, 10.5 % aldehydes, including vanillin and syringaldehyde, and no phenols. At higher severities, with higher temperatures and times, 40.1 % catechols, 21.9 % guaiacols, 9.6 % phenols, including phenol, cresols and 4-ethylphenol, 6.8 % syringol and only 1.6 % syringaldehyde were identified. SEC-UV (277 nm) was used to analyze the molecular weight of the initial lignin and the residual lignin after the reaction. While  $M_w$  and  $M_n$  of the Alcell lignin were 3300 g/mol and 900 g/mol, respectively, these values dropped to 680–830 g/mol for  $M_w$  and 390–430 g/mol for  $M_n$ , indicating high depolymerization of the lignin during the hydrocracking experiment. Nevertheless, Thring states that, due to the high yield of reactor residue and residual lignin, the reaction conditions were not sufficient to effectively degrade lignin to liquid and gaseous products.

Torr et al.<sup>91</sup> investigated mild hydrogenolysis of native lignins, *Pinus radiata* extracted wood, steam exploded wood (SEW) and enzymatic mild acidolysis lignin (EMAL). 2.2 g extracted wood, 1.5–1.9 g SEW or 666 mg EMAL were put into a limbo autoclave, together with 0.18 g 5 % Pd/C and 50 ml dioxane/water 1/1. The autoclave was pressurized to 34.5 bar  $H_2$  and heated to 195 °C, then the reaction was carried out for 2, 5, 8 or 24 hours. The reaction products were filtered, extracted into DCM and then dried to constant weight, giving an oil product, which was analyzed via GC-MS, GPC with UV detection at 280 nm and ESI-MS. The hydrogenolysis yields, meaning conversion of lignin into oil products, after 24 hours were 79 % for extracted wood and 89 % for EMAL, while SEW only reached a yield of 51 %, mainly due to the steam explosion making it less reactive in hydrogenolysis. Analysis of the product via GPC showed an approximate ratio of monomers/dimers/oligomers of 1/1/2. The main monomeric products in the oil products were dihydroconiferyl alcohol (DCA) and 4-n-propyl guaiacol (PG) with maximum yields of 19–21 % and 2 %, respectively. Another 1.5–1.8 % were made up of guaiacol, substituted guaiacols and 4-n-propyl phenol. Dimeric products found mainly consisted of DCA units, in some cases PG units, connected via  $\beta$ -1, 5-5 or  $\beta$ -5 linkages. ESI-MS analysis of the oligomers suggested that the main units were DCA, PG and 4-ethyl guaiacol (EG), giving signals associated with  $DCA_2EG$ ,  $DCA_2PG$ ,  $DCA_3$ ,  $DCA_3EG$ ,  $DCA_3PG$  and  $DCA_4$  trimers and tetramers, while oligomers greater than four could not be detected in this work. The main linkages were  $\beta$ -5, 5-5 and 4-O-5, with a lower amount of  $\beta$ -1 and  $\beta$ - $\beta$  linkages. Thus, mild hydrogenolysis reported by Torr is a method to convert native lignins into low molecular weight phenolic compounds in high yields, consisting of 75 % dimeric and oligomeric compounds.

## 3 Experimental Section

### 3.1 Chemicals

#### 3.1.1 Samples

- Alkali lignin
  - Sigma Aldrich 370959; Lot # MKBV5831V
- Sulfonated kraft lignin
  - Sigma Aldrich 471003; Lot # 04414PEV
- Thin liquor
  - Thin liquor with 14.8 % dry matter, fresh out of the paper mill, supplied from Sappi Gratkorn Mill, Austria (23.6.2016)
- Black liquor
  - Fresh black liquor with 42 % dry matter, supplied from Zellstoff Pöls AG, Austria (28.11.2016)

#### 3.1.2 Reagents

- Acetic acid, 96 %, Acros Organics 295320025
- Calcium hydroxide, Merck 102110
- Hydrochloric acid, fuming 37 %, Merck 1.00317.2500
- Sulfuric acid, 95–98 %, Carl Roth X994.2

#### 3.1.3 Solvents

- Acetone, techn., Brenntag
- Acetonitrile, HPLC-grade, VWR Chemicals 83639.320
- Chloroform, VWR Chemicals 22706.361
- Cyclohexane, ROTISOLV HPLC, Carl Roth 7333.1
- Dichloromethane, VWR Chemicals 23367.321
- Diethyl ether (techn.), Institute of Chemistry, University of Graz
- Dimethylformamide, VWR Chemicals 23466.323
- Dimethyl sulfoxide,  $\geq 99.0$  %, Fluka Analytical
- Dioxane, Institute of Chemistry, University of Graz
- Ethanol, 96 %, VWR Chemicals 84836.360
- Ethyl acetate, ULTRA RESI-ANALYZED, J.T.Baker 9260-03

- Ethylene glycol,  $\geq 99.5$  %, Carl Roth 6881.2
- Methanol, HPLC-grade  $\geq 99.8$  %, VWR Chemicals 20864.320
- n-Heptane,  $\geq 99$  %, Carl Roth 8654.3
- Hexane, HPLC-grade, Fischer Scientific H/0406/17
- n-Propanol, ROTISOLV HPLC, Carl Roth T177.1
- Isopropyl alcohol, HPLC-grade, VWR Chemicals 20880.320
- Petroleum ether, 40–60 °C, Carl Roth CP44.3
- Pyridine,  $\geq 99$  %, VWR Chemicals 27194.295
- Sodium hydroxide,  $\geq 97$  % pellets, Acros Organics 42433
- Tetrahydrofuran (THF), HPLC-grade  $\geq 99.5$  %, VWR Chemicals 28559.320
- Toluene, HPLC-grade, VWR Chemicals 83625.320

### 3.1.4 Other chemicals

- Butylated hydroxytoluene (BHT),  $\geq 99.5$  %, Vulkanox, Lanxess 56820977
- Cholesterol, Sigma Aldrich C8503
- Silicone antifoaming emulsion, Carl Roth 0865.2
- Sodium sulfate, anhydrous, Merck 6649
- Catalyst: NiMo catalyst on kaolin support<sup>95</sup>
  - Catalyst loading: 6.1 % Ni and 3.5 % Mo
  - Support: Kaolin PS 450 HP

## 3.2 Instruments

- GC-MS: HP 6890 series GC system
  - Autosampler: HP 7683
  - Detector: HP 5973 Mass Selective Detector
  - Column: Agilent J&W DB-5ms Ultra Inert capillary column (-60–325 °C, 30 m x 0.25 mm x 0.25  $\mu$ m)
  - Software: MSD Chemstation D.03.00.552
- LC-TOF-MS: Agilent 6230B TOF LC/MS
  - HPLC: Agilent 1260 Infinity
  - Autosampler: Agilent G1392B
  - Degasser: Agilent G4225A
  - DAD: Agilent G4212BA
  - Software: Agilent MassHunter Workstation

- Size Exclusion Chromatography:
  - HPLC: Agilent 1100 Series
  - Degasser: G1322A
  - QuatPump: G1311A
  - ALS: G1313A
  - RI Detector: KNAUER K-2301
- FTIR Spectrometer: Agilent Cary 630 FTIR Spectrometer
  - Sampling accessories: Diamond ATR (solids) and Dialpath Sample Interface (liquids)
- Reactor: Parr Instruments Company 4575A High Pressure/High Temperature batch reactor (max.: 350 bar, 500 °C), 500 ml, material: Hastelloy C-276; with 4848B reactor controller; Software: Specview Version 2.5
- Balance: Sartorius 3100 P, max. 3100 g, d=0.01– 0.05 g
- Analytical balances:
  - VWR 254i, max. 250 g, d=0.1 mg
  - Sartorius BP 210 S, max. 210 g, d=0.1 mg
  - Sartorius AZ214, max. 210 g, d=0.1 mg
- Digital contact thermometer: IKA IKATRON ETS-D4 fuzzy
- pH meter: Metrohm 691
- Autovortex: Stuart Scientific SA6
- Thermostat (VTU): Lauda RE207
- Rectifier (VTU): bolz electronic TG30-2T
- Peristaltic pump (VTU): Watson-Marlow 520S
- Multimeter (VTU): Thermo Scientific Orion 5-Star Plus
- Muffle furnace: Heraeus thermicon T
- Ultrasonic bath: Elma Transsonic T460/H
- Karl Fischer titration: Metrohm Titrando 808 with 801 Stirrer
- Centrifuge: Eppendorf Centrifuge 5702
- Rotavapor: IKA Works RV 10

### 3.3 Lignin precipitation

#### 3.3.1 Lignosulfonate precipitation

20 ml of thin liquor were mixed with an excess of solid  $\text{Ca}(\text{OH})_2$  under continuous stirring, resulting in a pH of about 12. The solution was heated to 75 °C. After 2 hours 5 ml of 37 % HCl were added. After 20 minutes of stirring, the solid residue was filtered off and dried in the drying oven at 105 °C overnight.

#### 3.3.2 Precipitation of black liquor lignin

##### 3.3.2.1 First precipitation

100 ml of black liquor (116.37 g) were weighed into a beaker and a magnetic stir bar was added. A temperature sensor and a pH sensor were dipped into the black liquor. It was heated to 45 °C while stirring on a magnetic stirrer and 96 % acetic acid was added dropwise with a pipette. Foam formation and  $\text{H}_2\text{S}$  smell was also observed. At a pH value of 10.4–10.5, lignin precipitation was observable and the color changed from dark brown to a brighter, reddish brown. After reaching the desired pH value of 9, the suspension was stirred for 10 minutes, then adding more acetic acid until again reaching a pH value of 9. After stirring for another 10 minutes, the precipitate was allowed to settle overnight.

The next day, the brown precipitate was filled into centrifuge vials and centrifuged at 4000 rpm for 10 minutes, resulting in the accumulation of the precipitate at the bottom of the vial and a brown, clearer supernatant above it. The supernatant was filtered off using a Büchner filter apparatus (Vacuum, 70 mm diameter red band filters) and the resulting solids from the filters were added to the precipitate in the vials. The filtered-off liquid was collected in a separate beaker. The solid precipitate was now resuspended in acidified distilled water (pH 3 with acetic acid). This process was repeated 2 times, leading to a brighter, clearer supernatant. After filtering this supernatant off, the solid precipitate was collected in a crystallizing dish and air dried for roughly 72 hours at room temperature. Then these pre-dried solids were put in the drying oven for 24 hours at 105 °C and weighed.

The remaining liquid was put into the fridge overnight and the next day into the freezer (−35 °C) for 20 minutes to yield a maximum of precipitate. After that, the liquid was filled into centrifuge vials and centrifuged at 4000 rpm for 10 minutes. The supernatant was decanted into the Büchner filter apparatus. The solids were resuspended in 10 ml acidified distilled water and centrifuged again. After decanting the supernatant off, the solid residues were resuspended in 25 ml distilled water and centrifuged. After repeating this process once more, the solids were

also collected in a crystallizing dish and air dried for 36 hours at room temperature before drying it in the drying oven at 105 °C for 48 hours. Finally, the precipitate was weighed.

### **3.3.2.2 Second precipitation**

As only a small amount of black liquor lignin was precipitated in the first attempt, a second precipitation was carried out. In this case, 1.03 kg black liquor were weighed in a beaker. The principal setup was like the first precipitation described above, with the difference that the acetic acid was added via a dropping funnel. The acidification was identical to the previous one, adding 60 ml of acetic acid in this case.

After letting the precipitate settle overnight, the suspension was filled into centrifuge vials (50 ml) and the same procedure as in the first precipitation was followed. In this case, the precipitate had to be resuspended in acidified distilled water for 5 times, as a considerable higher amount of precipitate was observed in the vials. Also, the remaining liquid was not collected due to a small amount of precipitate isolated from it in the first precipitation. As there was a high amount of precipitation solution, the centrifugation procedure was carried out in two batches of 8 centrifuge vials each and a third batch with 4 vials. The procedure was the same for all 12 vials, except that the first 4 vials were put in the drying oven directly after transferring the solids into the crystallization dishes. The other solids were air dried at room temperature and after this step dried in the drying oven at 105 °C before weighing it.

## **3.4 Characterization**

### **3.4.1 Dry matter determination of the thin liquor**

10.6 g of thin liquor were weighed in a round-bottomed flask and the water and other potential solvents were evaporated in the rotary evaporator for 1 hour. To ensure dryness of the sample, it was dried in the drying oven at 105 °C for 3 hours.

### **3.4.2 Solubility**

#### **3.4.2.1 Solubility of sulfonated kraft lignin**

The solubility in various solvents was tested by weighing in the needed amount of lignin and addition of solvent to reach concentrations of 5 and 1 g/l, when full solubility was not observed at 5 g/l. The samples were shaken by hand, mixed on the vortex and then mixed for another 15 minutes in the ultrasonic bath at 30 °C. The solubility was determined optically (color, residue).

The exact amount of lignin soluble in THF was determined by weighing in 0.10 g sulfonated kraft lignin into a vial, adding 10 ml of THF and mixing the solution for 15 minutes in the

ultrasonic bath. After that, the remaining residue was filtered off and placed in the drying oven at 105 °C for 38 hours, after which the residue was weighed.

The maximum solubility in water was determined by weighing sulfonated kraft lignin and adding distilled water to reach the desired concentrations between 24 and 286 g/l. After shaking and vigorous stirring on the vortex, the samples were mixed for 5 minutes in the ultrasonic bath at 30 °C. If the lignin was not completely dissolved, it was put for another 15 minutes in the ultrasonic bath.

#### **3.4.2.2 Solubility of thin liquor lignin**

The solubility in five different solvents was tested by adding 10 ml of the solvent to about 100 mg of evaporated product (~10 g/L) and mixing for 15 minutes on the ultrasonic bath at 30 °C.

#### **3.4.2.3 Solubility of alkali lignin**

The solubility of the alkali lignin in different solvents was tested with concentrations of about 5 g/l. About 0.01 g alkali lignin were weighed into 10 ml vials and 2 ml solvent was added. After that, the solution was mixed shortly on the vortex and then in the ultrasonic bath for 15 minutes at 25 °C.

The solubility in sodium hydroxide was then tested at different concentrations. If no complete miscibility was observed after vortexing, the samples were put into the ultrasonic bath for 5 to 10 seconds.

#### **3.4.2.4 Solubility of black liquor lignin**

The solubility of the black liquor lignin was tested by weighing in about 0.05 g of black liquor lignin into a 15 ml vial and adding 10 ml of solvent, giving concentrations of 5 g/L black liquor lignin. After mixing on the vortex for a few seconds, the solutions were mixed in the ultrasonic bath for 15 minutes at 25 °C.

#### **3.4.2.5 Solubility of lignosulfonate**

About 0.005 g of the brown product were mixed with 1 ml of solvent (5 g/l) in a vial. The solution was shortly mixed on the vortex and then mixed in the ultrasonic bath at 20 °C.



### 3.4.3 IR analysis

For the FTIR analysis, a Cary 630 FTIR from Agilent Technologies was used. For solid samples, the diamond ATR sampling accessory was used, while for liquid samples (products of electrochemical oxidation, lignosulfonate), the DialPath sampling accessory was used. The water in the liquid samples was evaporated and the samples were analyzed with the diamond ATR accessory.

### 3.4.4 Molecular weight distribution determination via preparative SEC

For the determination of the molecular weight distribution in aqueous environment, a dilution series of 5, 8, 10, 12 and 15 mg/ml sulfonated kraft-lignin in HPLC-grade water was prepared, which was then analyzed for its molecular weight:

**Table 8: Dilution series for molecular weight analysis of sulfonated kraft lignin**

Sample	Sample [g]	Water [ml]	Concentration [mg/ml]
LTH1	0.0502	10	5.02
LTH2	0.0800	10	8.00
LTH3	0.100	10	10.0
LTH4	0.120	10	12.0
LTH5	0.150	10	15.0
LTH6 (blank)	–	10	–

For the determination of the molecular weight of the thin liquor, the thin liquor was neutralized by adding 25 ml of 0.1 M NaOH to 25 ml of thin liquor, which was monitored via a pH electrode. During that, the color changed from brown to black. Then again, a dilution series was prepared with HPLC-grade water:

**Table 9: Dilution series for molecular weight analysis of thin liquor**

Sample	Sample [ml]	Water [ml]	concentration [mg/ml]
LS1	10	0	74
LS2	8	2	59
LS3	6	4	44
LS4	4	6	30
LS5	2	8	15
LS6 (blank)	–	10	–

The product of the electrochemical oxidation of sulfonated kraft lignin was also analyzed via molecular weight analysis, for which a dilution series was prepared as follows:

**Table 10: Dilution series for molecular weight analysis of electrochemically oxidized sulfonated kraft lignin**

Sample	Sample [ml]	Water [ml]	Concentration [mg/ml]
TH_Lox1	10	0	20
TH_Lox2	7.5	2.5	15
TH_Lox3	5.0	5.0	10
TH_Lox4	2.5	7.5	5.0
Blank	–	10	–

The same applied to the electrochemically oxidized thin liquor, where no neutralization was needed before preparing the dilution series:

**Table 11: Dilution series for molecular weight analysis of electrochemically oxidized thin liquor**

Sample	Sample [ml]	Water [ml]	Concentration [mg/ml]
TH_LSox1	10	0	20
TH_LSox2	7.5	2.5	15
TH_LSox3	5.0	5.0	10
TH_LSox4	2.5	7.5	5.0
Blank	–	10	–

### 3.4.5 Elemental analysis

Three samples, the alkali lignin, the sulfonated kraft lignin and the black liquor lignin which were dried beforehand at 105 °C for an hour, were analyzed for their C, H, N and S contents at the Institute of Inorganic Chemistry at Graz University of Technology.

### 3.4.6 Moisture content determination

About 1 g of lignin was exactly weighed into a previously weighed crystallizing dish on the analytical balance; two times for each lignin. Then, the samples were put into the drying oven at a temperature of 105 °C. After 3 hours of drying, the samples were taken out of the oven and immediately weighed. The samples were put back in the oven for another 3 hours of drying. After this, the samples were again immediately weighed out of the oven. Next, all samples were put in the drying oven overnight, for about 17 hours. The samples were again weighed immediately after taking them out of the oven.

### 3.4.7 Ash content determination

For the ash content determination, the empty crucibles were cleaned with acetone and then put into the muffle furnace at 525 °C for 45 minutes. After that, the crucibles were cooled shortly before putting them into a desiccator with calcium chloride as drying agent. When they had cooled to room temperature, the crucibles were weighed on an analytical balance.

About 1.5 g of the lignin was weighed into each crucible. Each sample was carbonized gently over a low Bunsen burner flame to ensure that the samples would not start to burn. When the smoking had ceased and only char was left, the samples were put into the muffle furnace at 525 °C for 4 hours.

The samples were taken out of the furnace, cooled slightly and put into a desiccator to cool to room temperature. When room temperature was reached, the samples with the crucibles were weighed on the analytical balance.

### 3.5 Soxhlet extraction of alkali lignin

A Soxhlet apparatus was set up. 3.54 g alkali lignin were weighed into the cellulose thimble and 200 ml methanol were filled into a 250 ml round-bottom flask. Then the flask was slowly heated with a heating mantle. The evaporated methanol was cooled with a condenser and the condensed methanol dripped directly on the lignin, extracting soluble components. After evaporating enough methanol to fill the soxhlet, the whole methanol is sucked into the flask, ending the cycle. Then the new cycle began. A total of ten cycles were carried out. Then, a GC sample was taken. Using a rotary evaporator, the methanol was removed to about 25 % of the initial volume, where another GC sample was taken out. Next, the methanol was evaporated until nearly nothing was left and another GC sample was taken. The remaining methanol was evaporated completely, leaving a brown, oily residue on the walls of the flask, which became solid after cooling down. Now the samples were analyzed via GC-MS.

For quantification of the phenols, 0.005 g BHT and 0.017 g brown residue were weighed into a GC-MS vial, mixed with 1.5 ml methanol and then analyzed via GC-MS

### 3.6 Electrochemical oxidation (VTU)

The setup for the electrochemical oxidation reactions can be seen in Figure 20. The used anode was BDD-Niob with an area of  $0.00175\text{ m}^2$ , while the cathode was made of stainless steel. A rectifier was attached to these electrodes to apply the desired current. The conductivity of the prepared solution of lignin in water was raised to a value of about  $10\text{ mS/cm}$  with  $\text{Na}_2\text{SO}_4$ . This solution was flowing from the reactor through the cooling thermostat into the cell containing the electrodes (from the bottom to the top) and back into the reactor. The temperature, pH value and the conductivity of the solution were measured with a multiparameter meter.

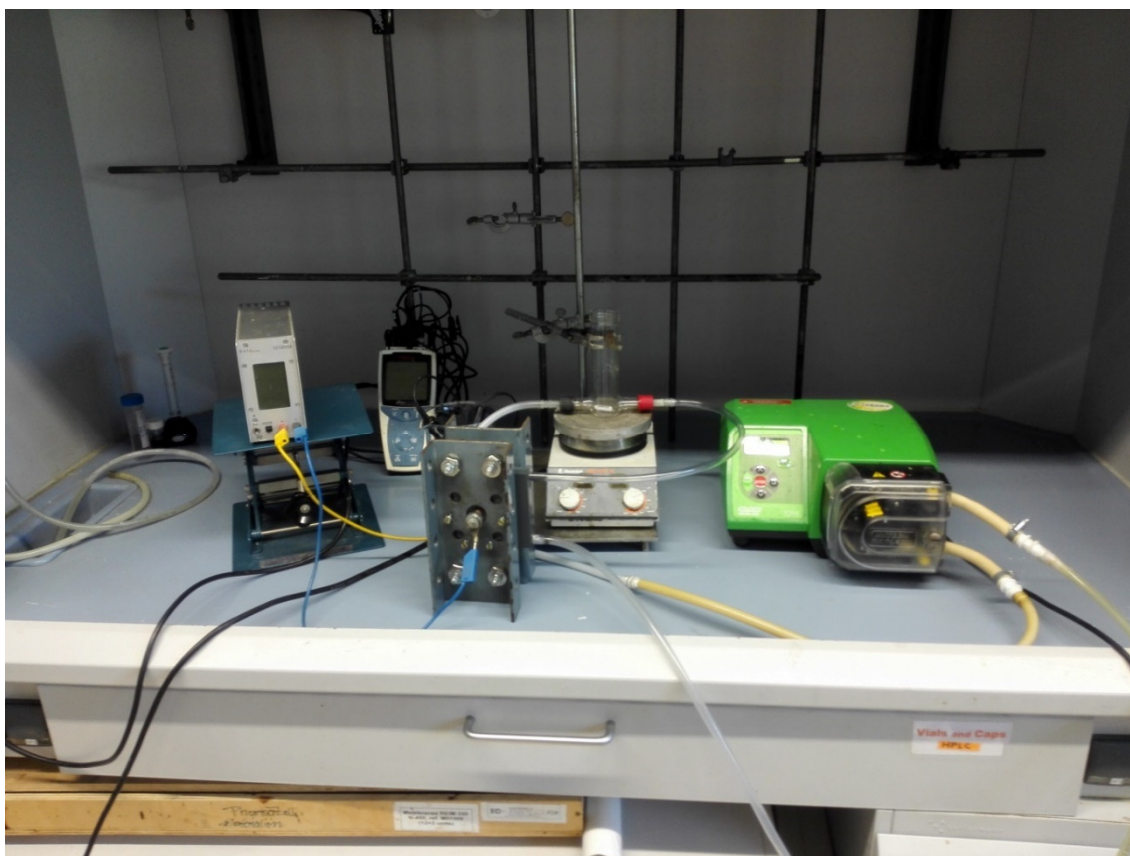


Figure 20: Setup of electrochemical oxidation reactions

In Figure 21, the setup for the second set of experiments is shown. In contrast to the previous setup there are two separated electrode rooms, one for the BDD-Niob anode, where the anolyte lignin solution flowed through, and one for the stainless steel cathode, where the catholyte  $\text{Na}_2\text{SO}_4$  solution was flowing through. These electrode rooms were separated by a membrane. Therefore, two separate cycles were present, one for the anolyte and one for the catholyte.

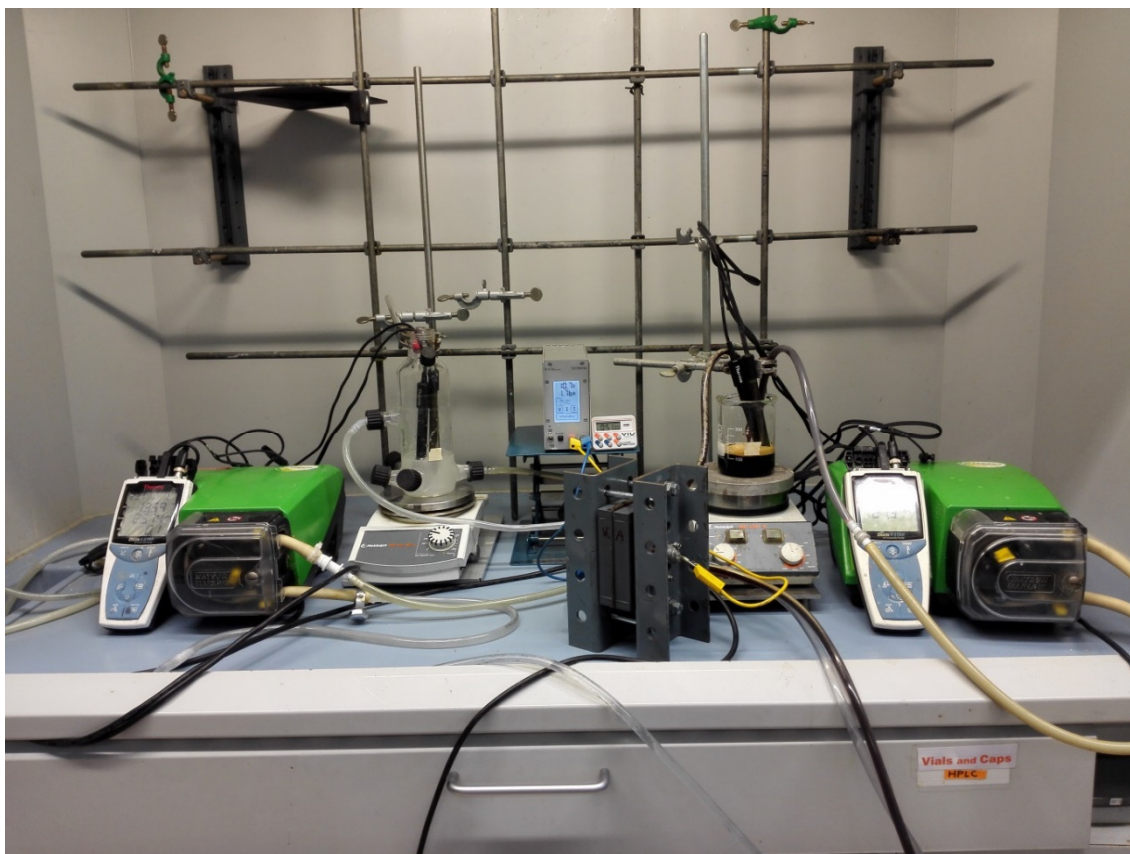


Figure 21: Setup of electrochemical oxidation reactions with membrane

Samples for subsequent analysis were taken out of the reactor before the reaction was started, several times during the reaction (every hour) and after the reaction has been terminated.

Apart from the temperature, pH value and conductivity, the chemical oxygen demand (COD) of every sample was also measured at VTU.

### 3.6.1 Sulfonated kraft lignin

#### 3.6.1.1 Electrochemical oxidation of sulfonated kraft lignin

6 g of sulfonated kraft lignin (20 g/l) were dissolved in 300 ml distilled water. The conductivity was adjusted to a value of 12.75 mS/cm with  $\text{Na}_2\text{SO}_4$  and the pump was set to 65 rpm. The used current was 1.75 A ( $1000 \text{ A/m}^2$ ). After the reaction started, foam started to build up, so 0.3 g of silicone antifoaming emulsion was added, leading to a strong decrease in foam. As the foam built up again after about two hours, another 0.25 g of antifoaming emulsion was added, after which no foam was observed until the end of the reaction. A total of 0.55 g foaming emulsion was added, giving a concentration of 1.83 g/l.

### 3.6.1.2 Electrochemical oxidation of sulfonated kraft lignin with membrane

For the anolyte, 6 g of sulfonated kraft lignin were dissolved in 300 ml distilled water and about 10 g/l  $\text{Na}_2\text{SO}_4$  were added to give a conductivity of about 10 mS/cm. For the catholyte, 5 g of  $\text{Na}_2\text{SO}_4$  were dissolved in 500 ml distilled water (10 g/l). Both pumps were set to 40 rpm ( $\sim 35$  l/min). The used current was 1.75 A ( $1000 \text{ A/m}^2$ ).

### 3.6.1.3 Electrochemical oxidation of sulfonated kraft lignin at lower current

This experiment was carried out analogous to the first electrochemical oxidation of sulfonated kraft lignin, with the difference that the current was set to 0.35 A ( $200 \text{ A/m}^2$ ). 6 g of sulfonated kraft lignin were dissolved in 300 ml distilled water and 3 g  $\text{Na}_2\text{SO}_4$  were added. The pump was set to 65 rpm. After 10 minutes, 0.22 g (0.73 g/l) antifoaming emulsion was added.

## 3.6.2 Alkali lignin

### 3.6.2.1 Electrochemical oxidation of alkali lignin

6 g alkali lignin were weighed into a beaker and filled up to 300 ml with 1 M NaOH, giving a concentration of about 20 g/l. The setup was again the same as in the electrochemical oxidation of the sulfonated kraft lignin.. The pump was again set to 65 rpm. The current was set to 0.04 A ( $\sim 23 \text{ A/m}^2$ ) for the first hour, with samples been taken out every 30 minutes. Then the current was set to 0.35 A ( $200 \text{ A/m}^2$ ) for another 5 hours.

## 3.6.3 Thin liquor

### 3.6.3.1 Electrochemical oxidation of thin liquor

For the thin liquor experiments, the same concentration (20 g/l) of the lignosulfonate was desired. Because only 15 % of the thin liquor are solids, 40 g of thin liquor were weighed in and 300 ml of distilled water were added. The conductivity was again set to 13.05 mS/cm with  $\text{Na}_2\text{SO}_4$ . The pump was set to 65 rpm. After 8 minutes, 0.53 g of antifoaming emulsion were added (1.75 g/l).

### 3.6.3.2 Electrochemical oxidation of thin liquor with membrane

This experiment was carried out analogous to the sulfonated kraft lignin experiment with the membrane. The catholyte was again prepared by weighing in 5 g of  $\text{Na}_2\text{SO}_4$  and dissolving it in 500 ml distilled water (10 g/l). The anolyte was prepared by mixing 41 g of thin liquor with 300 ml distilled water. The conductivity was increased to over 10 g/l with  $\text{Na}_2\text{SO}_4$ . The pumps were set to 40 rpm and a current of 1.75 A ( $1000 \text{ A/m}^2$ ) was used.

### 3.6.4 Work-up

To be able to analyze the samples via FTIR Spectroscopy, the product after 5 hours of oxidation had to be dried. 100 ml of the sulfonated kraft lignin oxidation and the thin liquor oxidation end products were dried at 90 °C in the drying oven for 3 days until only a solid residue was left. For the second experiments, 50 ml were dried at 90 °C for 3 days. After drying, the solid was analyzed via FTIR.

The samples at the beginning, after 3 hours and after 5 hours were analyzed via GC-MS as they were taken out of the reaction, with water as solvent.

To ensure a better analyzability via GC-MS, the products had to be extracted. Three solvents were tested: n-hexane, chloroform and chloroform:methanol 2:1.

#### 3.6.4.1 Extraction with n-hexane

25 ml of n-hexane were mixed with 25 ml sulfonated kraft lignin product (25.4 g) in a separating funnel. A picture of the mixture after shaking and reaching equilibrium can be seen in Figure 22. The upper phase is n-hexane, the middle phase is supposed to be a high-molecular lignin phase, while the third phase is the aqueous phase. The three phases were separated. The aqueous phase was extracted with n-hexane two more times, again yielding the three-phase-system seen in the picture. The three n-hexane phases were mixed and a GC-sample was taken out. Now the solvent was removed with the rotary evaporator. Samples were taken after 50 % of the solvent were removed and at the end of the evaporation.



Figure 22: Three-phase-system after extraction with n-hexane

For the thin liquor, 25 ml of n-hexane and 25.5 g of the product were mixed in a separating funnel. After shaking, a three-phase system like the one of the sulfonated kraft lignin was formed. The work-up was the same as for the kraft lignin and GC-MS samples were taken from the n-hexane phase after the extraction and at the end of the evaporation.



### 3.6.4.2 Extraction with chloroform

To ensure a better separation, chloroform was tested as solvent. 10 ml of sulfonated kraft lignin product (10.1 g) were mixed with 10 ml chloroform in the separating funnel and mixed. This procedure was repeated two times. Again, a three phase system was formed, but in this case the middle phase and the organic phase could not easily be separated, so a 0.22  $\mu\text{m}$  syringe filter was used to take out a sample for GC-MS.

### 3.6.4.3 Extraction with chloroform:methanol 2:1

For better analyzability with GC-MS, the so-called Foch extraction was used. 10 ml chloroform were mixed with 5 ml methanol. This mixture was added to 10 ml of sulfonated kraft lignin product. After shaking, again the three-phase system was formed. The aqueous phase was extracted with the Foch mixture a second time. The combined organic phases were washed with a 1:1 mixture of methanol and water until phase separation. The organic phase was evaporated in the rotary evaporator. Samples for GC-MS were taken after the first separation, after the second separation and after evaporation of the solvent.

### 3.6.4.4 GC-MS analysis

The following parameters were used for GC-MS analysis:

Table 12: GC-MS parameters for electrochemical oxidation analysis

<b>Column</b>	DB-5ms Ultra Inert capillary column
<b>Carrier gas</b>	Helium
<b>Carrier gas flow</b>	1.0 ml/min
<b>Mode</b>	Split 40:1
<b>Injection volume</b>	1.0 $\mu\text{l}$
<b>Initial temperature</b>	60 °C; hold 2 minutes
<b>Ramp 1</b>	10 °C/min to 310 °C
<b>Final temperature</b>	310 °C; hold 5 minutes



### 3.6.4.5 LC-TOF-MS analysis

The sulfonated kraft lignin educt and its product after 5 hours of electrochemical oxidation have been subjected to an analysis by LC-TOF-MS. The following parameters were used for this determination:

Table 13: LC-TOF-MS parameters for electrochemical oxidation analysis

<b>Injection</b>	0.01 $\mu$ l	<b>Ionization method</b>	APCI
<b>Flow</b>	0.3 ml/min, isocratic		positive/ <i>negative</i>
<b>Solvent</b>	10 %: H <sub>2</sub> O	<b>Gas Temp. (N<sub>2</sub>)</b>	350 °C
	90 %: 90 % ACN with 10 %	<b>Vaporizer</b>	375 °C
	H <sub>2</sub> O and 0.1 % 5 M	<b>Drying Gas</b>	10 l/min
	Ammonium formate	<b>Nebulizer</b>	40 psig
		<b>Fragmentor</b>	175 V
<b>Acquisition</b>	150–1100 m/z	<b>Skimmer</b>	65 V
	1 spectrum/s	<b>OCT 1 RF Vpp</b>	750 V
<b>Reference Masses</b>	922 m/z / 966 m/z	<b>Corona</b>	4 $\mu$ A/ 22 $\mu$ A

## 3.7 Reactor Reactions

For the reduction, a 500 ml Hastelloy C batch reactor from Parr instruments was used. After filling the reactor with the desired amount of sample, catalyst and solvent, the reactor was closed. The cuff was closed and the screws were tightened with a torque wrench in a crisscross fashion in the order of 2.1 kg, then 3.5 kg, next 4.9 kg and finally 5.6 kg. Then the heating mantle was positioned and the internal cooling system was turned on. After a check if everything was tight and all the valves were closed, the reactor was flushed with a small amount of hydrogen for the H<sub>2</sub> reduction reaction or nitrogen for the solely thermal reaction. Then the reactor was filled with the desired amount of either hydrogen or nitrogen. The heater and the stirrer were turned on. Now the temperature was set in the Specview program on the controlling PC. When the desired temperature was reached, the reaction time began. Figure 23 shows a typical temperature and pressure timeline during such an experiment:

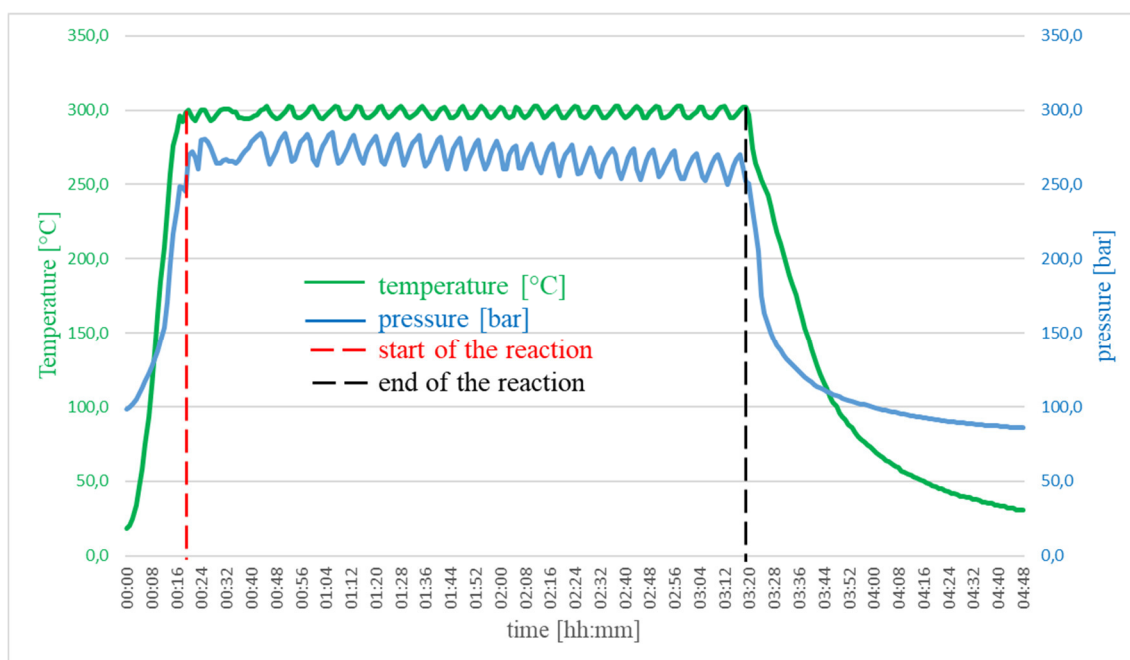


Figure 23: Typical temperature and pressure profile of a reduction experiment

After the reaction, the temperature was set to 20 °C and the heater was removed, so that the reactor could cool down faster. When a temperature of 40 °C or lower was reached, the outlet valve was slowly opened, so that the remaining hydrogen or nitrogen and formed gases were slowly released into the vent. Then the screws were untightened, the cuff was removed and the reactor opened. The liquids were transferred into an Erlenmeyer flask with as little as possible solids. The solids were taken out into another Erlenmeyer flask as complete as possible.

Table 14 sums up the important parameters during lignin reductions with hydrogen. Time, stirrer speed and solvent amount were the same in all experiments with 3 hours, 300 rpm and 100 ml methanol.

Table 14: Parameters of lignin reductions with hydrogen

Lignin	Experiment	H <sub>2</sub> pressure [bar]	Temperature [°C]	Starting material [g]	Catalyst [g]
Alkali lignin	V01	99.0	300	10.0	3.04
	V02	99.7	250	10.0	3.00
	V03	98.6	300	20.0	3.01
	V04	80.3	300	10.0	3.00
Sulfonated kraft lignin	V07	100	300	10.0	3.01
	V08	100	300	4.24	3.01
Black liquor lignin	V10	93.0	300	10.0	3.00

Important parameters of the lignin thermal reactions are presented in Table 15. Time, stirrer speed and methanol amount used were the same as in the reductions with hydrogen mentioned above.

Table 15: Parameters of lignin thermal reactions

Lignin	Experiment	N <sub>2</sub> pressure [bar]	Temperature [°C]	Starting material [g]
Alkali lignin	V05	8.6	300	10.0
	V06	8.7	300	5.20
Sulfonated kraft lignin	V09	8.8	300	10.0
Black liquor lignin	V11	9.2	300	5.02
	V12	8.8	300	10.0

### 3.7.1 Reactor reactions of alkali lignin

#### 3.7.1.1 Reductions of alkali lignin with hydrogen

##### Experiment V01

The table below shows the parameters of the first reduction with H<sub>2</sub>:

Table 16: Parameters of alkali lignin reduction with hydrogen V01

H <sub>2</sub> pressure beginning	99 bar	Time	3 hours
H <sub>2</sub> pressure end	94 bar	Temperature	300 °C
		Stirrer	300 rpm
Lignin	10.0 g alkali lignin		
Catalyst	3.04 g NiMo catalyst on kaolin		
Solvent	100 ml methanol		

The methanol phase derived from the reduction was collected in a flask and a GC-MS sample was taken out, which was filtered through a 0.22 µm syringe filter to ensure no solids were given onto the GC. Methanol was added to the solid residues to extract soluble compounds out of these residues. This mixture was stirred on a magnetic stirrer for 1 hour and then the solids were filtered off. The methanol phase was mixed with the methanol phase directly taken out of the reactor, while the solids were dried in the drying oven for 1 day, after which the solids were weighed.

The methanol phase was filled up to 200 ml and the water content was measured via Karl-Fischer titration, then the methanol was evaporated with a rotary evaporator. A viscous, methanol soluble oil remained, which was weighed. Then a small portion was dissolved in methanol to analyze it via GC-MS.

### Experiment V02

The temperature was set to 250 °C, all other parameters were the same as for the previous experiment.

Table 17: Parameters of alkali lignin reduction with hydrogen V02

<b>H<sub>2</sub> pressure beginning</b>	99.7 bar	<b>Time</b>	3 hours
<b>H<sub>2</sub> pressure end</b>	94.7 bar	<b>Temperature</b>	250 °C
		<b>Stirrer</b>	300 rpm
<b>Lignin</b>	10.0 g alkali lignin		
<b>Catalyst</b>	3.00 g NiMo catalyst on kaolin		
<b>Solvent</b>	100 ml methanol		

The solid residues of this experiment were stirred overnight and then filtered off as described before. The remainder of the work-up was like the previously described experiment.

### Experiment V03

For this experiment the amount of lignin was doubled from ten to twenty grams, all other parameters were the same as for the first experiment.

Table 18: Parameters of alkali lignin reduction with hydrogen V03

<b>H<sub>2</sub> pressure beginning</b>	98.6 bar	<b>Time</b>	3 hours
<b>Temperature</b>	300 °C	<b>Stirrer</b>	300 rpm
<b>Lignin</b>	20.0 g alkali lignin		
<b>Catalyst</b>	3.01 g NiMo catalyst on kaolin		
<b>Solvent</b>	100 ml methanol		

The work-up was similar as the one described in the previous experiment (V02)

**Experiment V04**

In this reaction, the hydrogen pressure was lowered to 80 bar, while all other parameters stayed the same.

**Table 19: Parameters of alkali lignin reduction with hydrogen V04**

<b>H<sub>2</sub> pressure beginning</b>	80.3 bar	<b>Time</b>	3 hours
<b>Temperature</b>	300 °C	<b>Stirrer</b>	300 rpm
<b>Lignin</b>	10.0 g alkali lignin		
<b>Catalyst</b>	3.00 g NiMo catalyst on kaolin		
<b>Solvent</b>	100 ml methanol		

The work-up was again similar to the previously described experiments.

**3.7.1.2 Thermal reactions of alkali lignin****Experiment V05**

The reactor was only filled with the desired amount of sample and solvent. Then the preparations for the reactor were the same as in the reactions with hydrogen, the only difference was that the reactor was filled with about 10 bar (pressure of the pipe) of nitrogen instead of hydrogen after closing the reactor. Then the reaction was started using the same parameters as in the first reduction reaction (experiment V01).

**Table 20: Parameters of alkali lignin thermal reaction V05**

<b>N<sub>2</sub> pressure</b>	8.6 bar	<b>Time</b>	3 hours
<b>Temperature</b>	300 °C	<b>Stirrer</b>	300 rpm
<b>Lignin</b>	10.1 g alkali lignin		
<b>Solvent</b>	100 ml methanol		

The work-up was also like the previous experiments.

**Experiment V06**

A second step of this treatment was carried out using the remaining solids from experiment V05. The same parameters as in the first step were used.

**Table 21: Parameters of alkali lignin thermal reaction V06**

<b>N<sub>2</sub> pressure</b>	8.7 bar	<b>Time</b>	3 hours
<b>Temperature</b>	300 °C	<b>Stirrer</b>	300 rpm
<b>Lignin</b>	5.25 g solids from experiment V05		
<b>Solvent</b>	100 ml methanol		

No changes were made to the work-up procedure

**3.7.2 Reactor reactions of sulfonated kraft lignin****3.7.2.1 Reductions of sulfonated kraft lignin with hydrogen****Experiment V07**

Following parameters were used for the first H<sub>2</sub> reduction of sulfonated kraft lignin:

**Table 22: Parameters of sulfonated kraft lignin reduction with hydrogen V07**

<b>H<sub>2</sub> pressure beginning</b>	100 bar	<b>Time</b>	3 hours
<b>H<sub>2</sub> pressure end</b>	~70 bar	<b>Temperature</b>	300 °C
		<b>Stirrer</b>	300 rpm
<b>Lignin</b>	10.0 g sulfonated kraft lignin		
<b>Catalyst</b>	3.01 g NiMo catalyst on kaolin		
<b>Solvent</b>	100 ml methanol		

The work-up was again similar to the experiments with alkali lignin, as a GC-MS sample was taken out right after the reduction. Again, the methanol phase was filled up to 200 ml and the water content was measured. After the evaporation of the methanol, a viscous, methanol soluble oil was left. This oil was weighed and then a portion was dissolved again in methanol and analyzed via GC-MS.

**Experiment V08**

A second reduction with the remaining solids from the first reduction was carried out:

**Table 23: Parameters of sulfonated kraft lignin reduction with hydrogen V08**

<b>H<sub>2</sub> pressure beginning</b>	100 bar	<b>Time</b>	3 hours
<b>H<sub>2</sub> pressure end</b>	~75 bar	<b>Temperature</b>	300 °C
		<b>Stirrer</b>	300 rpm
<b>Lignin</b>	4.15 g sulfonated kraft lignin	7.16 g total solids from the first reduction	
<b>Catalyst</b>	3.01 g NiMo catalyst on kaolin		
<b>Solvent</b>	100 ml methanol		

The work-up of this reduction experiment was like the first experiment, with the difference that the water content was not measured in this case. GC-MS samples were taken from the methanol phase directly after reduction and from the oil after the evaporation, dissolved in methanol.

**3.7.2.2 Thermal reactions of sulfonated kraft lignin****Experiment V09**

A solely thermal treatment of the kraft lignin was carried out with the following parameters:

**Table 24: Parameters of sulfonated kraft lignin thermal reaction V09**

<b>N<sub>2</sub> pressure</b>	8.8 bar	<b>Time</b>	3 hours
<b>Temperature</b>	300 °C	<b>Stirrer</b>	300 rpm
<b>Lignin</b>	10.0 g sulfonated kraft lignin		
<b>Solvent</b>	100 ml methanol		

The work-up was similar to the previous thermal experiments.

### 3.7.3 Reactor reactions of black liquor lignin

#### 3.7.3.1 Reductions of black liquor lignin with hydrogen

##### Experiment V10

Finally, a reduction reaction of the precipitated black liquor lignin was carried out:

Table 25: Parameters of black liquor lignin reduction with hydrogen V10

<b>H<sub>2</sub> pressure beginning</b>	93.0 bar	<b>Time</b>	3 hours
<b>H<sub>2</sub> pressure end</b>	61.8 bar	<b>Temperature</b>	300 °C
		<b>Stirrer</b>	300 rpm
<b>Lignin</b>	10.0 g black liquor lignin		
<b>Catalyst</b>	3.00 g NiMo catalyst on kaolin		
<b>Solvent</b>	100 ml methanol		

The work-up was also similar to the previous experiments.

#### 3.7.3.2 Thermal reactions of black liquor lignin

##### Experiment V11

Black liquor lignin was also subjected to a solely thermal reaction under inert gas atmosphere. As only a small amount of lignin was available at this time, the experiment was carried out with 5 g instead of 10 g lignin. The other parameters were like the experiments with the alkali and sulfonated kraft lignins.

Table 26: Parameters of black liquor lignin thermal reaction V11

<b>N<sub>2</sub> pressure</b>	9.2 bar	<b>Time</b>	3 hours
<b>Temperature</b>	300 °C	<b>Stirrer</b>	300 rpm
<b>Lignin</b>	5.02 g black liquor lignin		
<b>Solvent</b>	100 ml methanol		

The work-up was similar to the previous experiments.



**Experiment V12**

An experiment with 10 g black liquor lignin, this time from the second precipitation, was carried out. The other parameters were consistent with the other experiments.

**Table 27: Parameters of black liquor lignin thermal reaction V12**

<b>N<sub>2</sub> pressure</b>	8.8 bar	<b>Time</b>	3 hours
<b>Temperature</b>	300 °C	<b>Stirrer</b>	300 rpm
<b>Lignin</b>	10.0 g black liquor lignin		
<b>Solvent</b>	100 ml methanol		

The work-up was carried out according to the previous experiments.

**3.7.4 Quantification**

Next, dehydroabietic acid methyl ester (DHAAME) content and phenols content were determined. For this quantification, as internal standards cholesterol was chosen for DHAAME while for the phenols, butylated hydroxytoluene (BHT) was chosen.

An exact amount of sample was weighed into a GC-MS vial, then an exact amount of cholesterol or BHT was added. Then the vial was filled up with 1.5 ml of solvent. The vial was closed with the vial cap and stirred with a vortex mixer. Next, the vial was placed in the ultrasonic bath for 5 to 15 minutes until all components were completely dissolved. Then GC-MS measurement was conducted.

The following table shows the amount of cholesterol and sample for the quantification of DHAAME:

**Table 28: Amount of sample and cholesterol used for DHAAME quantification**

<b>Lignin</b>	<b>Experiment</b>	<b>Solvent</b>	<b>Amount of cholesterol [g]</b>	<b>Amount of sample [g]</b>
<b>Alkali lignin</b>	<b>V01</b>	Acetone	0.0051	0.0081
	<b>V03</b>	Acetone	0.0053	0.0095
	<b>V05</b>	Acetone	0.0062	0.051
<b>Sulfonated kraft lignin</b>	<b>V07</b>	Methanol	0.0017	0.011
	<b>V09</b>	Acetone	0.0018	0.015
<b>Black liquor lignin</b>	<b>V10</b>	Acetone	0.0023	0.0054
	<b>V11</b>	Acetone	0.0018	0.014
	<b>V12</b>	Acetone	0.0015	0.013

The response factor for DHAAME was determined by a colleague via preparing a calibration series with concentrations of 0.005, 0.01, 0.05, 0.1, 0.5 and 1.0 g/l abietic acid in acetone. To every solution, 0.1 g/l BHT and 0.1 g/l cholesterol were added and the solutions were thoroughly mixed. Then, GC-MS measurement was conducted.

The amounts of BHT and sample for the quantification of phenols are presented in the following table. As solvent, methanol was used:

**Table 29: Amount of sample and cholesterol used for phenols quantification**

<b>Lignin</b>	<b>Experiment</b>	<b>Amount of BHT [g]</b>	<b>Amount of sample [g]</b>
<b>Alkali lignin</b>	<b>V01</b>	0.040	0.046
	<b>V03</b>	0.014	0.058
	<b>V05</b>	0.012	0.071
<b>Sulfonated kraft lignin</b>	<b>V07</b>	0.0063	0.030
	<b>V09</b>	0.0034	0.047
<b>Black liquor lignin</b>	<b>V10</b>	0.0072	0.0095
	<b>V11</b>	0.0042	0.044
	<b>V12</b>	0.0045	0.042

For the determination of the response factors of phenolic compounds, a colleague prepared calibration series with concentrations of 0.005, 0.01, 0.05, 0.1, 0.5 and 1.0 g/l in THF of the following phenolic compounds: acetovanillone, catechol, eugenol, guaiacol, homovanillic acid, isoeugenol, methyl guaiacol and vanillin. After adding 0.1 g/l BHT to each of the solutions and mixing them thoroughly, GC-MS measurements were carried out.

### 3.7.5 GC-MS analysis

The following GC-MS parameters were used throughout all reactor reactions described in this chapter:

Table 30: GC-MS parameters for reduction analysis

<b>Column</b>	DB-5ms Ultra Inert capillary column
<b>Carrier gas</b>	Helium
<b>Carrier gas flow</b>	1.0 ml/min
<b>Mode</b>	Split 40:1
<b>Injection volume</b>	1.0 $\mu$ L
<b>Initial temperature</b>	50 °C; hold 5 minutes
<b>Ramp 1</b>	5 °C/min to 150 °C
<b>Ramp 2</b>	10 °C/min to 300 °C
<b>Final temperature</b>	300 °C; hold 20 minutes

## 4 Results and Discussion

### 4.1 Lignin precipitation

The samples used in this thesis were two commercial lignins from Sigma Aldrich, an alkali and a sulfonated kraft lignin, as well as two samples from pulping mills in the surrounding area, namely fresh thin liquor from a sulfite process of Sappi Gratkorn and a fresh black liquor from a sulfate process of Zellstoff Pöls AG. Before being able to analyze these samples, the lignin had to be precipitated from the liquors as described in this chapter.

#### 4.1.1 Lignosulfonate precipitation

After receiving the fresh thin liquor from Sappi Gratkorn, which had a solids content of about 15 %, it was directly put into the refrigerator at about 6 °C to avoid further reactions of possible celluloses or hemicelluloses in the batch. Then the lignosulfonate was precipitated from the thin liquor following the description in US Patent 1,981,176 by G. Howard<sup>96</sup> by mixing 20 ml of thin liquor with an excess of Ca(OH)<sub>2</sub> and heating the solution to 75 °C for two hours, yielding a solid product. After addition of HCl, a brown precipitate remained, which was filtered off and dried at 105 °C overnight.

Weighing of the brown product of the precipitation resulted in a yield of 2.40 g, which are 81 % of the dry matter in the thin liquor. This is in accordance to the precipitation yield from sulfite liquor as reported by Haars et al.<sup>97</sup>, where 76 % were precipitated, but still lower than the maximum amount possible for this precipitation, which are 95 %.<sup>98</sup>

#### 4.1.2 Precipitation of black liquor lignin

Analogous to the thin liquor, the fresh black liquor with a solids content of 42 % was stored in the refrigerator at 6 °C to avoid further reactions until precipitation. Generally, the precipitation method was developed according to the papers of Garcia et al.<sup>99</sup> and Kamble et al.<sup>100</sup> Thus, black liquor was acidified with acetic acid and lignin precipitation was observed at a pH of 10.5. However, the solution was acidified to a pH of 9 to ensure full precipitation. The precipitate was washed with acidified distilled water and separated from the water by centrifugation with subsequent filtration three to five times. The precipitated lignin was weighed after drying it in the open air at room temperature for 36 hours and in the drying oven at 105 °C for 48 hours.

#### 4.1.2.1 First precipitation

For the first precipitation, 116 g black liquor were used. The total yield of the precipitation, including the solids from the filtrations and the solids isolated from the filtered off liquid, is 10.9 g, which are 9.44 % of the used black liquor and thus 22.5 % of the solids in the black liquor.

#### 4.1.2.2 Second precipitation

To get more black liquor lignin for further reactions and as the yield of the first precipitation was low, a second precipitation was carried out with 1.03 kg black liquor. The yield of the second precipitation, only including the solids from the filtration, is 44.7 g, only 4.34 % of the used black liquor and 10.3 % of the solids.

The yield of this reaction could have most likely been improved by also isolating solids from the filtered off liquids, as some solids clearly went through the filter.

To sum up, there would be many possibilities to improve this precipitation process in different ways: Firstly, this method is quite time consuming, especially the centrifugation and filtration steps. Possibilities to speed up the centrifugation would be using a bigger centrifuge, more centrifuges at once or maybe lower centrifugation times. The filtration steps were even more time consuming, especially the ones directly after centrifugation, because the filter was blocked very rapidly. This could be circumvented by using higher porosity filters, but this would then again add the need to filter the liquid with a lower porosity, as a part of the lignin already was going through the filters used in this case. But maybe also the number of times the precipitate was resuspended in distilled water could be lowered to speed up this process.

The second problem, which is also competing with the time problem, is the problem of the relatively low yield. According to the datasheet given by Zellstoff Pöls AG, the black liquor had a solids content of 42 %, of which not all is lignin, but most certainly more than the maximum of 22.5 % reached with this method. To improve the yield with this method, mainly a better and more convenient filtration method should be used, as much lignin is lost due to the residues on the filter paper and the solids still present in the filtered off liquid.

Precipitation yields of lignin from black liquors reported in the literature, always calculated on the solids content of the black liquor, are 27–39 % with the usage of H<sub>2</sub>SO<sub>4</sub>, 43 % with acetic acid, while precipitation with CO<sub>2</sub> yielded 20 % and 26 %.<sup>7,32,100,101</sup> Thus, the result of the first precipitation, with 22.5 %, is not quite as high as the one reported for acetic acid in the literature,

but it is comparable to the percentages yielded with CO<sub>2</sub>. As the yield percentage of the second precipitation is only half of the first, it does not correlate with the literature values.

## **4.2 Characterization**

To get an overview of the properties of the four samples used in this thesis, the commercial alkali and sulfonated kraft lignins, the lignosulfonate and the black liquor lignin were characterized for their solubility in various solvents, their sulfur, moisture and ash contents were determined, while they were also analyzed via preparative SEC, FTIR and elemental analysis.

### **4.2.1 Dry matter determination of the thin liquor**

To test the amount of dry matter in the thin liquor and thus be able to later test the solubility of thin liquor lignin, the thin liquor solvents of 10.6 g thin liquor were evaporated in the rotary evaporator and the resulting product was dried in the drying oven for 3 hours at 105 °C. Weighing of the product showed a yield of 1.57 g (14.8 %), which equals the solids content of the sample and correlates with the results of the lignosulfonate precipitation.

### **4.2.2 Solubility**

The solubility of all four samples was determined to gain knowledge about which solvents can be used for further characterization and analysis, for example SEC and GC-MS, but more importantly for the electrochemical oxidation and reduction reactions.

#### **4.2.2.1 Solubility of sulfonated kraft lignin**

For the solubility testing of the sulfonated kraft lignin, an exact amount of lignin was weighed into a small beaker and such an amount of solvent was weighed in, that a concentration of 5 g/l was reached. After mixing the solutions the solubility was determined optically, regarding color of the solution and if any residues were visible on the ground of the beaker. If no residue was visible and a change in color was observed, indicating dissolution, the solubility in this solvent was marked “soluble”. If a change of color was observed but there was still a residue visible, the solubility was marked as “incomplete”. If still a high amount of residue was visible and no coloring of the solvent occurred, the solubility was marked as “insoluble”. For the samples, where no complete solubility could be observed, more solvent was added, so that a concentration of 1 g/l was reached, repeating the procedures for mixing and determining the solubility.

The results of the solubility tests of the sulfonated kraft lignin can be seen in the following table. When both concentrations were tested, the statement in the last column refers to the lower concentration.

**Table 31: Solubility of sulfonated kraft lignin in various solvents**

Solvent	Concentration 1	Concentration 2	Solubility
	[g/l]	[g/l]	
Acetone	5.02	1.01	insoluble
Acetonitrile	5.07	1.02	insoluble
Dichloromethane	5.22	1.00	insoluble
Diethyl ether	4.83	1.04	insoluble
Dimethyl sulfoxide	5.37	–	soluble
Dimethylformamide	5.02	1.01	incomplete
Dioxane	5.02	1.01	insoluble
Ethanol	5.22	1.05	insoluble
Ethyl acetate	5.22	1.05	insoluble
Isopropyl alcohol	4.98	1.03	insoluble
Methanol	5.32	1.07	incomplete
n-Propanol	5.12	1.03	incomplete
Pyridine	5.32	1.01	insoluble
Tetrahydrofuran	5.01	0.86	incomplete
Toluene	4.93	1.06	insoluble

Total solubility could only be achieved in DMSO at 5 g/l. Partial solubility was observed at 1 g/l in DMF, methanol, propanol and THF, of which methanol and THF are the most promising ones for future use as solvents due to their availability and already established usage in various methods.

To test the possibility of using GPC for lignin analysis for the sulfonated kraft lignin, its solubility in THF was determined. For this purpose, 10 g/l sulfonated kraft lignin in THF were mixed for 15 minutes in the ultrasonic bath and then dried in the drying oven at 105 °C for 38 hours. After weighing, the residue left from solving the kraft lignin in THF had a mass of 0.094 g, which means that only 6.2 mg (6.2 %) were dissolved in THF. This partial solubility made it impossible to analyze the sample even qualitatively via GPC.

The maximum solubility of sulfonated kraft lignin in water, needed for the electrochemical oxidation reactions which were carried out in aqueous medium, was determined by mixing the lignin with distilled water to reach various concentrations between 24 and 286 g/l. The samples were mixed in the ultrasonic bath for five minutes and if the lignin was not completely dissolved, the solution was mixed in the ultrasonic bath for another 15 minutes. The time needed to dissolve kraft lignin in distilled water increased from five minutes for concentrations of 24 g/l to 231 g/l to 20 minutes for 259 g/l and 286 g/l. Higher concentrations of lignin in water were not tested, as the dissolution of the 286 g/l sample was already very difficult to reach and was high enough for the wanted application in the electrochemical oxidation.

As the sulfonated kraft lignin was modified to better resemble the properties of a lignosulfonate than a kraft lignin<sup>17</sup>, the results of the solubility testing are as expected based on lignosulfonate solubility reported in literature: It is soluble in water and only one highly polar organic solvent, namely DMSO. It also showed low to no solubility in solvents which have been reported to dissolve non sulfonated kraft lignins, like dioxane, DMF, pyridine and THF.<sup>7,15-17</sup>

#### 4.2.2.2 Solubility of thin liquor lignin

To test the solubility of the precipitated product from the thin liquor, it was dissolved in five different solvents at a concentration of about 10 g/l, mixing it with the solvent in the ultrasonic bath for 15 minutes, determining the solubility optically. Three of these solvents were aqueous due to their usage in the electrochemical oxidation, while methanol was intended to be used in the reactor reactions and THF for GPC. The results can be seen in the following table:

Table 32: Solubility of thin liquor lignin in various solvents

Solvent	Sample [g]	Solvent [ml]	Concentration [g/l]	Solubility
0.1M HCl	0.100	10.0	9.94	complete
0.1M NaOH	0.101	10.0	10.0	complete
Methanol	0.100	10.0	9.91	incomplete
Tetrahydrofuran	0.100	10.0	9.91	insoluble
Water	0.101	10.0	9.99	complete

This solubility in aqueous solvents and the partial solubility in methanol corresponds very well to the solubility of the sulfonated kraft lignin, which was expected, as this particular commercial lignin was altered to resemble the properties of lignosulfonates. As previously stated, this also



corresponds with the solubility reported for lignosulfonates in literature, stating solubility in aqueous solvents on the whole pH scale.<sup>15,17</sup>

#### 4.2.2.3 Solubility of alkali lignin

The solubility of the alkali lignin was determined by mixing an exact amount of the lignin with the solvent in a vial, so that a concentration of about 5 g/l was reached. After mixing the solution on the vortex and in the ultrasonic bath for 15 minutes, solubility was determined optically. The following table shows the solubility of alkali lignin in various solvents:

Table 33: Solubility of alkali lignin in various solvents

Solvent	Sample [g]	Solvent [ml]	Concentration [g/l]	Solubility
Chloroform	0.010	2.0	5.1	incomplete
Diethyl ether	0.011	2.0	5.3	insoluble
Dioxane	0.010	2.0	5.2	complete
Dimethylformamide	0.012	2.0	5.7	complete
Dimethyl sulfoxide	0.011	2.0	5.6	complete
Ethyl acetate	0.011	2.0	5.6	incomplete
Ethylene glycol	0.012	2.0	6.2	complete
Hexane	0.012	2.0	5.9	insoluble
Isopropyl alcohol	0.011	2.0	5.7	insoluble
Methanol	0.0095	2.0	4.7	incomplete
NaOH 0.1%	0.0096	2.0	4.8	complete
Toluene	0.010	2.0	5.1	insoluble
Water	0.0098	2.0	4.9	insoluble

The greatest difference to the sulfonated kraft lignin was the insolubility in aqueous solvents, as expected because of the reported insolubility of alkali lignins in aqueous solvents with a pH lower than about nine, also indicated by the solubility in 0.1 % NaOH. Both lignins were soluble in DMSO, which also corresponds with the reported solubility of alkali lignins in strongly polar organic solvents.<sup>15</sup> The solubility of alkali lignin in dioxane was also previously reported in literature, even up to 7 g/l,<sup>7</sup> as was the solubility in DMF.<sup>17</sup> Solubility of alkali lignin in ethyl acetate has been reported to be 1 g/l, explaining the incomplete dissolution, while solubility in methanol has been found to be 6 g/l, which is in contrast to the findings in this thesis, where only incomplete solubility could be observed. Solubility in diethyl ether as well as chloroform

has been reported to be very low, with under 0.2 g/l.<sup>7</sup> This correlates with the observations above, as very low and no solubility was found for chloroform and diethyl ether, respectively.

To determine the possible concentrations of NaOH, which should be used as solvent for the electrochemical oxidation of the alkali lignin, different NaOH concentrations were tested for a lignin concentration of 20 g/l. After adding the NaOH to the lignin, the solutions were mixed on the vortex and, if no complete solubility was observed, for a few seconds on the ultrasonic bath. The solubility in sodium hydroxide at different concentrations can be seen in the following table:

**Table 34: Solubility of alkali lignin in NaOH at different concentrations**

<b>NaOH conc. [g/mol]</b>	<b>Sample [g]</b>	<b>Solvent [ml]</b>	<b>Concentration [g/l]</b>	<b>Solubility</b>	<b>Solubility after USB</b>
0.101	0.200	10.0	20.0	insoluble	complete
0.303	0.200	10.0	20.0	insoluble	complete
0.497	0.199	10.0	19.9	insoluble	complete
0.979	0.202	10.0	20.2	complete	complete

As already determined in the first solubility test, 20 g/L alkali lignin could be solved in 0.1 M NaOH after usage of the ultrasonic bath. Complete solubility without using the ultrasonic bath could be observed at a concentration of about 1 g/mol NaOH.

#### 4.2.2.4 Solubility of black liquor lignin

The solubility of the lignin precipitated from the black liquor was also tested by adding such an amount of solvent to the lignin in a vial to yield a concentration of about 5 g/l, mixing the solution on the vortex and in the ultrasonic bath for 15 minutes. The solubility of black liquor lignin in the tested solvents can be seen in the following table:

**Table 35: Solubility of black liquor lignin in various solvents**

<b>Solvent</b>	<b>Sample [g]</b>	<b>Solvent [ml]</b>	<b>Concentration [g/l]</b>	<b>Solubility</b>
Acetic acid 96%	0.0509	10.0	5.09	incomplete
Acetone	0.0506	10.0	5.06	incomplete
Acetonitrile	0.0506	10.0	5.06	incomplete
Chloroform	0.0492	10.0	4.92	insoluble
Cyclohexane	0.0514	10.0	5.14	insoluble
Dichloromethane	0.0485	10.0	4.85	insoluble
Diethyl ether	0.0513	10.0	5.13	insoluble
Dioxane	0.0514	10.0	5.14	incomplete
Dimethylformamide	0.0503	10.0	5.03	complete
Dimethyl sulfoxide	0.0509	10.0	5.09	complete
Ethanol	0.0507	10.0	5.07	incomplete
Ethyl acetate	0.0500	10.0	5.00	insoluble
Ethylene glycol	0.0492	10.0	4.92	incomplete
Heptane	0.0497	10.0	4.97	insoluble
Hexane	0.0514	10.0	5.14	insoluble
Isopropyl alcohol	0.0501	10.0	5.01	insoluble
Methanol	0.0509	10.0	5.09	incomplete
NaOH 0.1%	0.0502	10.0	5.02	complete
Petroleum ether	0.0494	10.0	4.94	insoluble
Pyridine	0.0490	10.0	4.90	incomplete
Tetrahydrofuran	0.0495	10.0	4.95	incomplete
Toluene	0.0501	10.0	5.01	insoluble
Water	0.0497	10.0	4.97	incomplete

After taking the samples out of the ultrasonic bath, black liquor lignin was completely dissolved in DMF, DMSO and NaOH. The different solvents could be ranked as follows (from mostly dissolved to nearly no solubility):

pyridine > methanol > acetic acid (suspension) > ethylene glycol > water (suspension) > acetonitrile (suspension) > dioxane > THF = acetone = ethanol (nearly no solubility)

Like the commercial alkali lignin from Sigma Aldrich, the black liquor lignin was soluble in DMSO, DMF and NaOH as expected. Interestingly, the solubility in dioxane and ethylene glycol was much lower for the black liquor lignin than for the alkali lignin. Also, the black liquor lignin was unexpectedly partially soluble in water, which normally does not apply for kraft lignins.<sup>15,17</sup> This lignin was not soluble in chloroform and ethyl acetate, while the alkali lignin was partially soluble in them. The fact that lignin is (nearly) soluble in pyridine is supported by literature, where a solubility of black liquor lignin in this solvent of up to 10 g/l has been reported. Another deviation from literature is the insolubility in dichloromethane, which was reported with a solubility of 2 g/l.<sup>7</sup>

To sum up, the black liquor lignin showed mostly the expected solubility for kraft lignins, with the biggest difference being the partial solubility in water and acetic acid, also the biggest difference to the alkali lignin.

#### 4.2.2.5 Solubility of lignosulfonate

For the solubility of the lignin precipitated from the thin liquor with  $\text{Ca}(\text{OH})_2$ , this sample was mixed with various solvents in the ultrasonic bath, so that a concentration of about 5 g/l was reached. The following table shows the results of this determinations:

Table 36: Solubility of lignosulfonate in various solvents

Solvent	Sample [g]	Solvent [ml]	Concentration [g/l]	Solubility
Acetone	0.0053	1.0	5.3	insoluble
Acetonitrile	0.0049	1.0	4.9	insoluble
Dichloromethane	0.0053	1.0	5.3	insoluble
Diethyl ether	0.0056	1.0	5.6	insoluble
Dioxane	0.0050	1.0	5.0	insoluble
Dimethylformamide	0.0053	1.0	5.3	insoluble
Dimethyl sulfoxide	0.0052	1.0	5.2	insoluble
Ethanol	0.0052	1.0	5.2	insoluble
Ethyl acetate	0.0054	1.0	5.4	insoluble
Isopropyl alcohol	0.0057	1.0	5.7	incomplete
Methanol	0.0049	1.0	4.9	insoluble
NaOH 0.1%	0.0055	1.0	5.5	incomplete
Pyridine	0.0057	1.0	5.7	insoluble
Tetrahydrofuran	0.0047	1.0	4.7	insoluble
Toluene	0.0056	1.0	5.6	incomplete
Water	0.0050	1.0	5.0	incomplete

There was no complete solubility observed in either of the solvents, with NaOH showing the best solubility, toluene, isopropyl alcohol and water showing at least partial solubility and the rest showing very small to no solubility. The insolubility in organic solvents is in accordance to the results found in literature as well as the thin liquor lignin, the difference being the insolubility in DMSO, while the thin liquor lignin was completely soluble in this solvent. Though, the low solubility in water is in contrast to literature and thin liquor lignin, as lignosulfonates should dissolve easily in aqueous solvent on the whole pH range.<sup>15,17</sup>

### 4.2.3 FTIR analysis

To be able to compare the products of the electrochemical oxidation to the educts, FTIR analysis was carried out with a Cary 630 FTIR from Agilent Technologies for the commercial sulfonated kraft lignin and alkali lignin samples as well as the thin liquor lignin and the liginosulfonate. As all the samples were in solid form, they were directly analyzed with the diamond ATR accessory.

The analysis of the absorption frequencies in the IR spectroscopy was done with the help of two IR spectroscopy absorption tables<sup>102,103</sup> and the “IR wizard”<sup>104</sup>.

#### 4.2.3.1 FTIR analysis of sulfonated kraft lignin

FTIR analysis of the commercial sulfonated kraft lignin from Sigma Aldrich yielded the following spectrum:

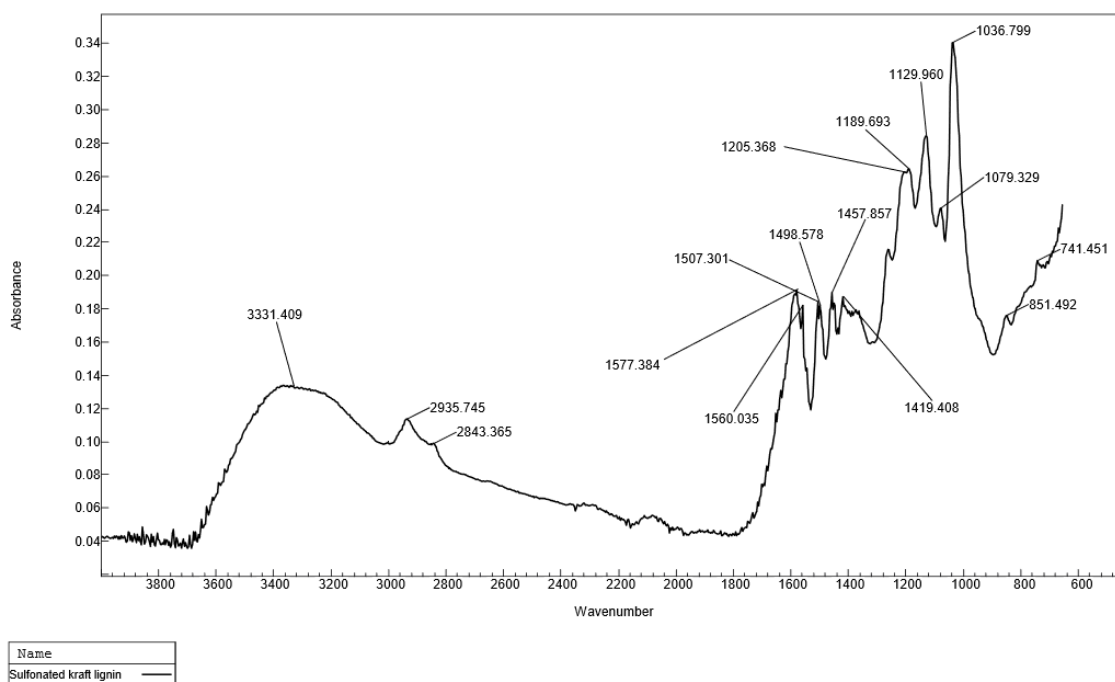


Figure 24: FTIR spectrum of sulfonated kraft lignin

The following table describes the bending and stretching vibrations assigned to the absorption frequencies of the sulfonated kraft lignin:

Table 37: FTIR absorption frequencies and assigned vibrations of sulfonated kraft lignin<sup>102-104</sup>

Wavenumber [cm <sup>-1</sup> ]	Bond	Type	Chemical class
3331	O-H	Stretching	Alcohol/ water
2936	C-H	Stretching	Arene/ alkane
2843	C-H	Stretching	Alkane
1577/1560	C=C	Stretching	Arene
1507/1499	C=C	Stretching	Arene
1457	C-H	Bending	Alkane
1419	O-H	Bending	Alcohol
~1320	O-H - S=O	Bending - Stretching	Phenol - Sulfonate
1205	C-O	Stretching	Alkyl aryl ether/ vinyl ether/ ester
1190	S=O	Stretching	Sulfonate
1130	C-O	Stretching	Aliphatic ether/ secondary-/ tertiary alcohol
1079	C-O	Stretching	Primary-/ secondary alcohol/ aliphatic ether
1037	C-O	Stretching	Alkyl aryl ether/ vinyl ether
851	C-H	Bending	Arene (di-, tri- or tetrasubstituted)
741	C-H	Bending	Arene (di- or tri-substituted)

The analysis of this FTIR spectrum shows various characteristics of the sulfonated kraft lignin, which was modified to show similarities to lignosulfonate. These characteristics, as previously described in the theoretical part of this thesis, are mainly arene moieties, connected by C-C and C-O-C ether bonds, with OH end groups, on the chain as well as the aromatic rings, or sulfonate end groups on the chain.

When looking at the table above, all these characteristics can be found in the IR spectrum. The aromatic ring vibrations show C-H stretching at 2936 cm<sup>-1</sup>, C=C stretching at 1499–1577 cm<sup>-1</sup> and C-H bending at 851 and 741 cm<sup>-1</sup>. Also, C-H stretching (2936 and 2843 cm<sup>-1</sup>) and C-H bending (1457 cm<sup>-1</sup>) of the alkane bonding between the rings and C-O stretching (1205, 1130 and 1037 cm<sup>-1</sup>) of the ether bonds can be characterized. Next, various alcohol moieties, phenolic and primary to tertiary ones, have been found with this characterization method. Finally, the

sulfonate end groups were also found in the IR spectrum ( $1320$  and  $1190\text{ cm}^{-1}$ ). The large broad peak between  $3700$  and  $3000$  corresponds to the moisture content of the sample.

Most of the bands found in this spectrum have also been reported in literature for lignosulfonates as well as kraft lignins. The biggest difference to the spectra in literature are the bands associated to the sulfonate end groups at  $1320$  and  $1190\text{ cm}^{-1}$ , which were not found in lignosulfonate FTIR characterization.<sup>80</sup> On the other side, neither unconjugated (at about  $1710\text{ cm}^{-1}$ ) nor conjugated (at about  $1690\text{ cm}^{-1}$ ) C=O vibrations have been found in this spectrum, while these have been reported for lignosulfonates as well as kraft lignins in literature.<sup>80,87,105</sup>

#### 4.2.3.2 FTIR analysis of alkali lignin

By FTIR analysis of the other commercial sample from Sigma Aldrich, the alkali lignin, the following spectrum could be obtained:

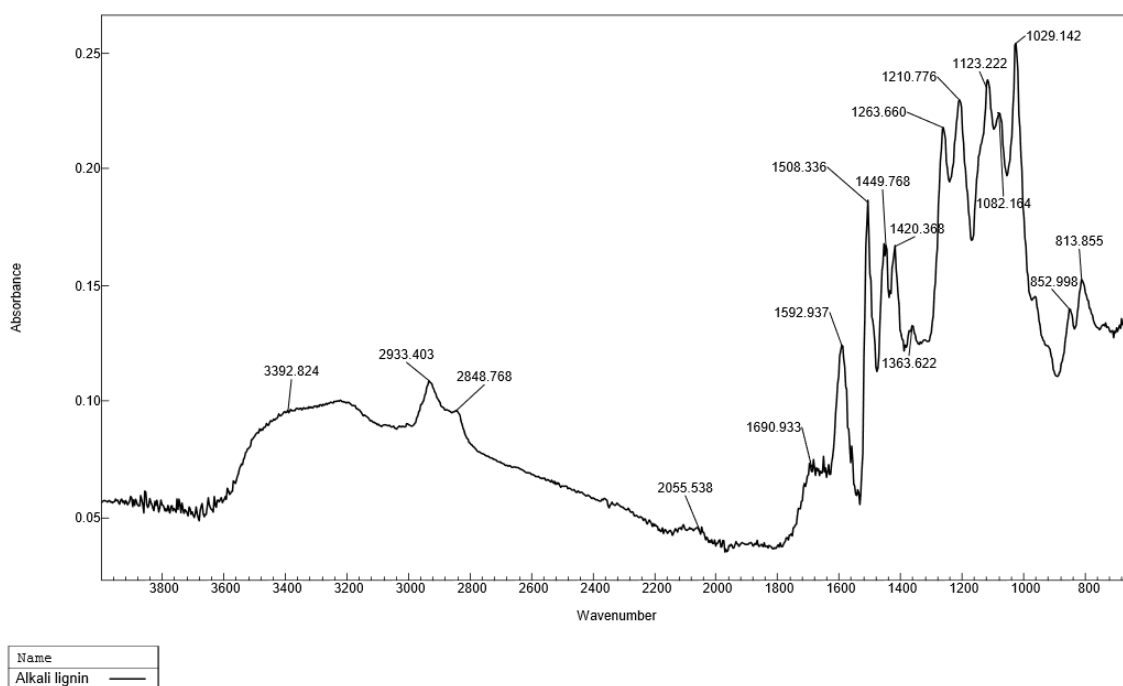


Figure 25: FTIR spectrum of alkali lignin



Table 38: FTIR absorption frequencies and assigned vibrations of alkali lignin<sup>102–104</sup>

Wavenumber [cm <sup>-1</sup> ]	Bond	Type	Chemical class
3392	O-H	Stretching	Alcohol/ water
2933	C-H	Stretching	Arene/ alkane
2849	C-H	Stretching	Alkane
1691	C=O	Stretching	Conjugated acid/ unsaturated aldehyde/ arylketone/ primary amide (free)
1593	C=C	Stretching	Arene
1508	C=C	Stretching	Arene
1450	C-H	Bending	Alkane
1420	O-H	Bending	Alcohol
1364	O-H	Bending	Phenol
1264	C-O	Stretching	Aromatic ester/ alkyl aryl ether
1211	C-O	Stretching	Alkyl aryl ether/ vinyl ether/ ester
1123	C-O	Stretching	Aliphatic ether/ secondary-/ tertiary alcohol
1082	C-O	Stretching	Primary alcohol/ secondary-/ tertiary alcohol
1029	C-O	Stretching	Alkyl aryl ether/ vinyl ether
853	C-H	Bending	Arene (di-, tri- or tetrasubstituted)
814	C-H	Bending	Arene (di-, tri- or tetrasubstituted)

Overall, the spectrum of alkali lignin is very similar to the one of the sulfonated kraft lignin, which was also supplied from Sigma Aldrich. The most obvious difference is the peak at 1691 cm<sup>-1</sup> in the spectrum of the alkali lignin, which can be assigned to conjugated acids or aldehydes, arylketones or even primary amides. The most probable of these, according to the models of alkali lignin presented in the theoretical part, would be the acid. Nevertheless, as many reactions in the lignin can occur in the production process, unsaturated aldehydes and ketones are also a possibility. Another big difference is the absence of S=O stretching bonds in the alkali lignin, which was expected as these are a feature of sulfonated kraft lignin or lignosulfonate. Interestingly, no thiol (S-H) bonds, usually indicated by a weak but sharp peak at 2550–2600 cm<sup>-1</sup>, were found with the FTIR analysis, which is a bit of a surprise as these are expected to be a part of the alkali lignin molecule. But when looking at alkali lignin FTIR spectra reported in literature, the S-H bond has not been found in any of these papers, which means that the S-H bond in lignins cannot be detected with this method.<sup>7,87,105–107</sup>

A minor difference would be the appearance of a C-O stretching band at  $1264\text{ cm}^{-1}$ , which can be assigned to either aromatic esters or alkyl aryl ethers. When looking at the expected structures of lignin, the alkyl aryl ether bond is more probable than the aromatic ester, but again, an alteration of the assumed carboxylic acid groups in the molecule could have also led to ester groups. Another minor difference is the second C-H bending band, which is at  $814\text{ cm}^{-1}$  in the alkali lignin, compared to  $741\text{ cm}^{-1}$  in the sulfonated kraft lignin. This does not only provide the possibility of this bond being a tetrasubstituted arene, but it also indicates, according to one of the used tables<sup>103</sup>, the presence of 1,2,4-trisubstituted aromatics. As the G-type monomer, coniferyl alcohol, a 1,2,4-trisubstituted aromatic, is a major building part in lignin, especially from softwood which is mostly used in paper industry, this gives a direct indication for the presence of this monomer. Apart from that it is unclear, why this specific distribution can only be seen in the alkali lignin and not in the sulfonated kraft lignin, which is believed to have the same building blocks.

Comparing the alkali lignin FTIR spectrum to spectra found in literature, no difference in the found bond vibrations can be detected, only the height of the individual peaks is differing.  
7,87,105–107

#### 4.2.3.3 FTIR analysis of thin liquor lignin

As the FTIR analysis of the thin liquor as it was retrieved only showed the peaks of the solvent water (not shown), the solid thin liquor lignin, obtained via evaporation before solubility testing, was used for this FTIR analysis:

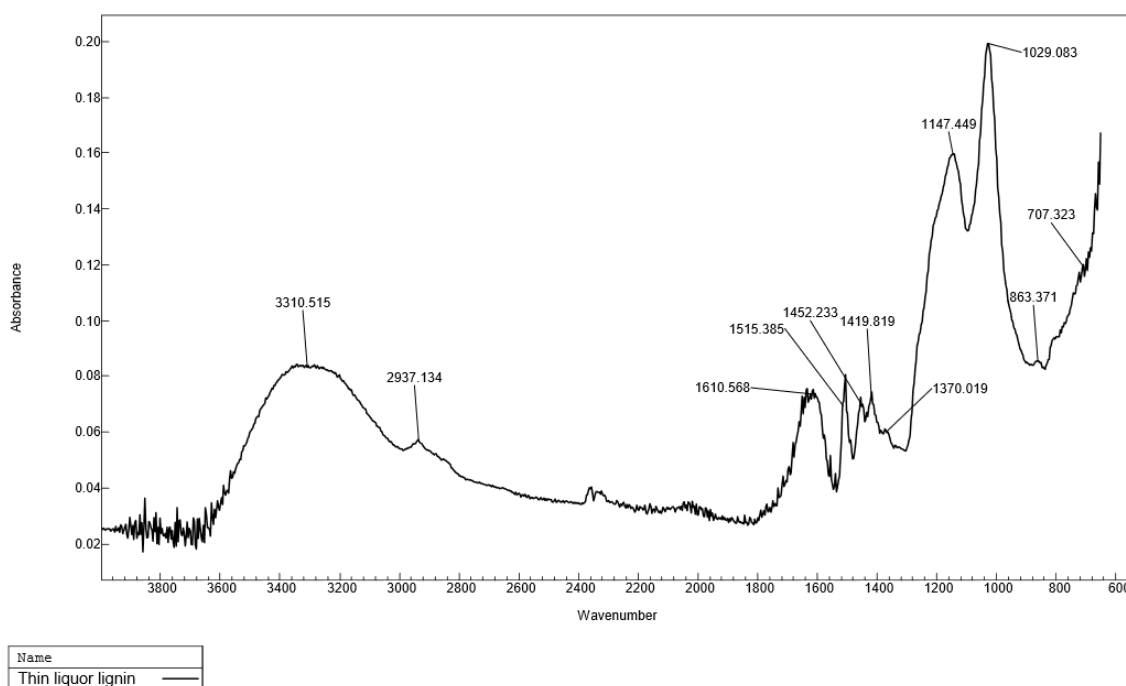
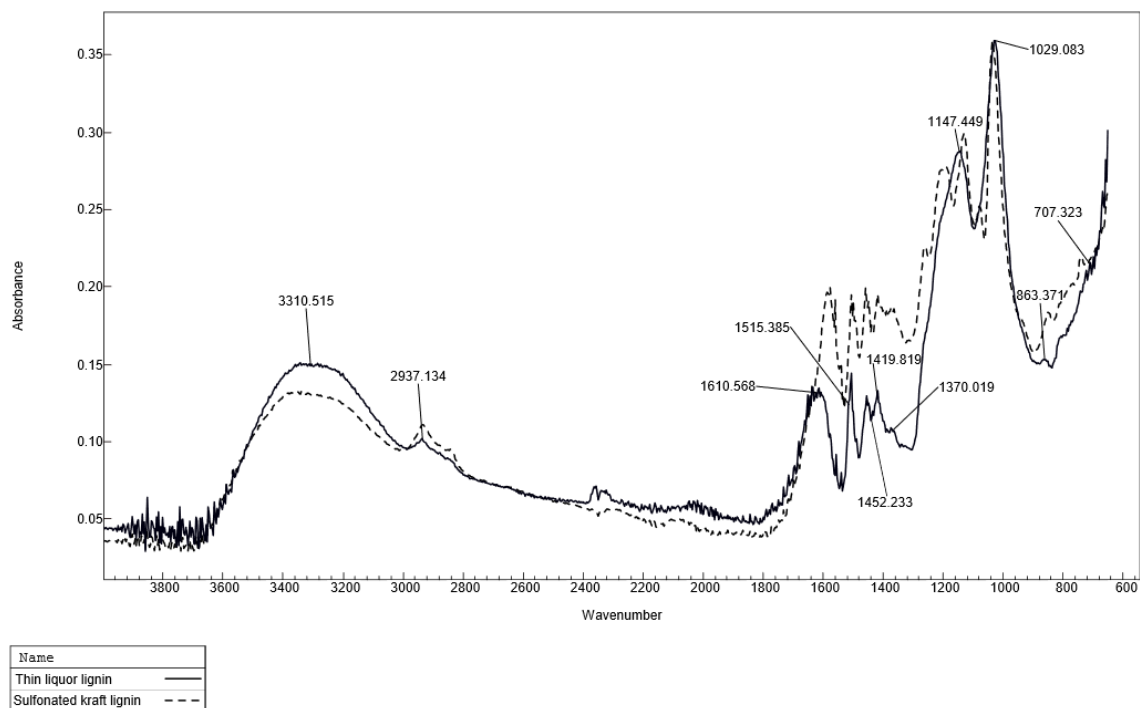


Figure 26: FTIR spectrum of thin liquor lignin

Table 39: FTIR absorption frequencies and assigned vibrations of thin liquor lignin<sup>102-104</sup>

Wavenumber [cm <sup>-1</sup> ]	Bond	Type	Chemical class
3311	O-H	Stretching	Alcohol/ water
2937	C-H	Stretching	Arene/ alkane
1611	C=C	Stretching	Arene
1515	C=C	Stretching	Arene
1452	C-H	Bending	Alkane
1420	O-H	Bending	Alcohol
1370	O-H - S=O	Bending - stretching	Phenol - sulfonate
1147	C-O - S=O	Stretching	Aliphatic ether/ tertiary alcohol - sulfonate
1029	C-O	Stretching	Primary alcohol
863	C-H	Bending	Arene (di-, tri- or tetrasubstituted)
707	C-H	Bending	Arene (di- or tri-substituted)

As this sample is a lignosulfonate and the sulfonated kraft lignin was modified to have similar characteristics than a lignosulfonate, there is not too much difference between the two spectra. The analysis of the spectrum shows the same characteristics than the sulfonated kraft lignin, with arene vibrations, ether and alkane bonds and alcohol and sulfonate end groups. Figure 27 shows a comparison of sulfonated kraft lignin and thin liquor lignin:



**Figure 27: FTIR spectra of thin liquor lignin and sulfonated kraft lignin**

The biggest difference is that there are more peaks from 1100 to about 1300  $\text{cm}^{-1}$  in the sulfonated kraft lignin, but it could also be possible that these vibrations are covered by the broad peak at 1147  $\text{cm}^{-1}$  in the thin liquor lignin. Another minor difference between the two spectra is the height of the peaks between 1370 and 1610  $\text{cm}^{-1}$ , where slightly stronger peaks in the sulfonated kraft lignin can be seen.

#### 4.2.3.4 FTIR analysis of lignosulfonate

Next, the lignosulfonate precipitated from the thin liquor via the Howard method was analyzed via FTIR:

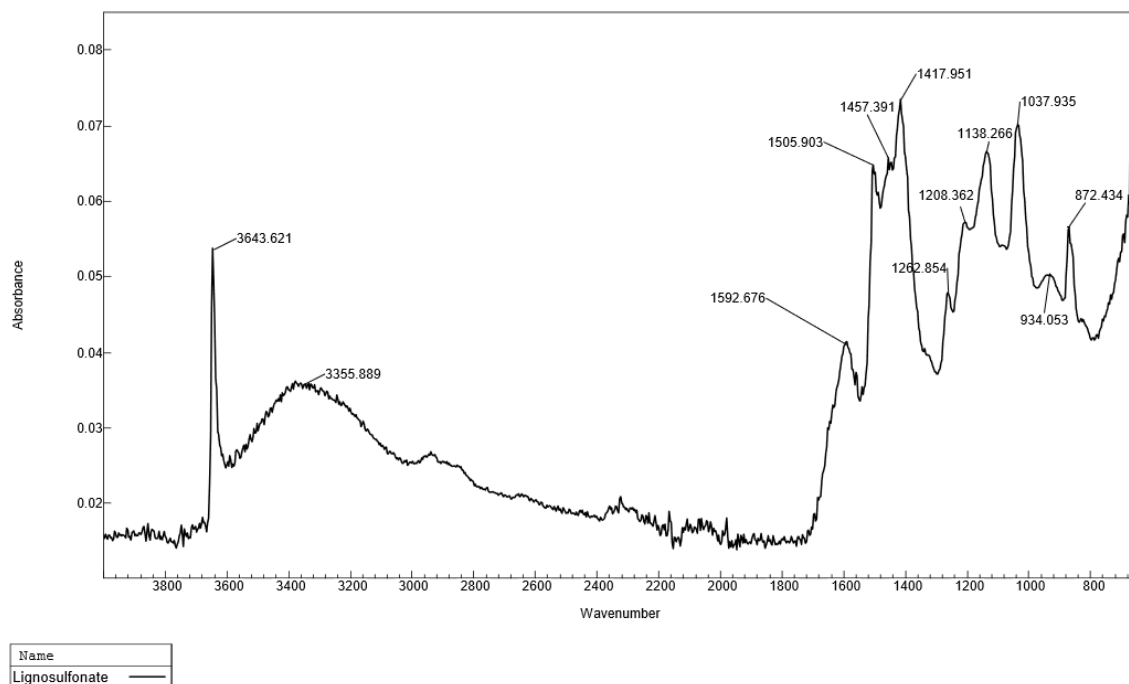
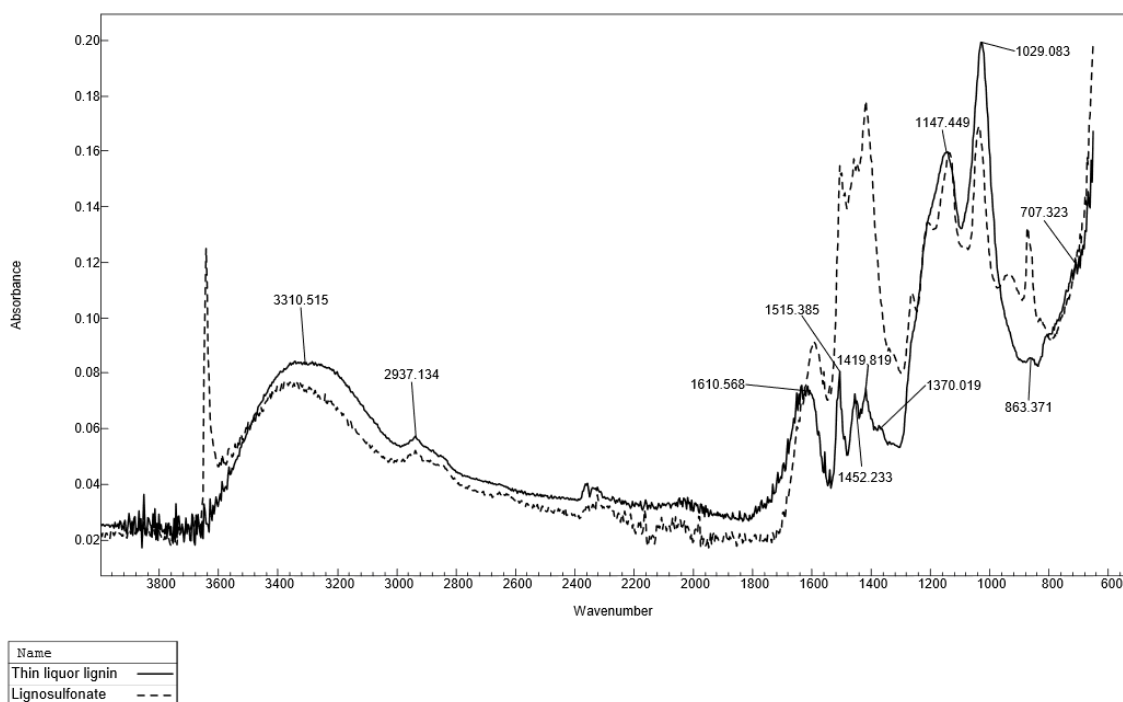


Figure 28: FTIR spectrum of lignosulfonate

Table 40: FTIR absorption frequencies and assigned vibrations of lignosulfonate<sup>102–104</sup>

Wavenumber [cm <sup>-1</sup> ]	Bond	Type	Chemical class
3644	O-H	Stretching	Alcohol (free)
3356	O-H	Stretching	Alcohol/ water
(~2940)	C-H	Stretching	Arene/ alkane
(~2843)	C-H	Stretching	Alkane
1593	C=C	Stretching	Arene
1506	C=C	Stretching	Arene
1457	C-H	Bending	Alkane
1418	O-H	Bending	Alcohol
1263	C-O	Stretching	Alkyl aryl ether/ aromatic ester
1208	C-O	Stretching	Alkyl aryl ether/ vinyl ether/ ester / tertiary alcohol
1138	C-O	Stretching	Aliphatic ether/ secondary-/tertiary alcohol
1038	C-O	Stretching	Alkyl aryl ether/ vinyl ether
872	C-H	Bending	Arene (di-, tri- or tetrasubstituted)

The found chemical classes in the FTIR of the liginosulfonate are mostly the same as the ones in the thin liquor lignin, which is not surprising as this is the same lignin, just with different precipitation methods. Apart from that, there are some differences, where the Howard precipitation method obviously has changed the structure of the sample. The following figure compares the spectra of the two liginosulfonates, thin liquor lignin and with the Howard method:



**Figure 29: FTIR spectra of thin liquor lignin and liginosulfonate**

The biggest difference is the strong, sharp peak at  $3644\text{ cm}^{-1}$ , which can be assigned to free alcohol groups. This free OH are derived most likely from  $\text{Ca}(\text{OH})_2$ , which was added in excess, so there are still OH groups present in the sample.<sup>108,109</sup> Like in the sulfonated kraft lignin, the peaks from about  $1400$  to  $1500\text{ cm}^{-1}$  are much higher in the liginosulfonate than in the thin liquor lignin. Additionally, the peak at  $860$  to  $870\text{ cm}^{-1}$  is much higher in the liginosulfonate than in the thin liquor lignin. Although, these differences are not believed to have any impact on the structure and reactivity of the lignin molecules, so these two samples are believed to be identical except the free OH groups present in the liginosulfonate sample.

#### 4.2.4 Elemental analysis

After drying the alkali, sulfonated kraft and black liquor lignins at 105 °C, they were analyzed for their elemental composition at the Institute of Inorganic Chemistry at Graz University of Technology. The following table sums up the results of this elemental analysis:

**Table 41: Elemental analysis of alkali and black liquor lignin**

	%C	%H	%N	%O*	%S
<b>Alkali lignin</b>	61.09	5.79	0.92	30.44	1.76
<b>Black liquor lignin</b>	63.60	5.55	<0.1	29.23	1.62
<b>Sulfonated kraft lignin</b>	50.69	4.67	<0.1	40.52	4.12

*\*determined by difference*

From these results, it can easily be seen that the alkali and black liquor lignin are mostly similar in their composition, as all the values are in about the same range, the only difference being the lack of nitrogen in the black liquor lignin, which instead showed a slightly higher carbon content. The main source of nitrogen in industrial lignins is the plant resource itself, from which the lignins are derived, which could explain the difference between the alkali and black liquor lignin. Another possible source of nitrogen is the addition of amino compounds to commercial lignins to make it more compatible with polymeric systems, which could be the case for the alkali lignin.<sup>90,110</sup>

In contrast to that, the sulfonated kraft lignin showed a completely different elemental composition. It consists of about 10 % less carbon and about 1 % less hydrogen, while the oxygen content is about 10 % and the sulfur content is about 3.5 % higher than in the two other lignins, which indicates the presence of sulfonate groups in the sulfonated kraft lignin. There is also no nitrogen in this sample.

Elemental analysis of kraft lignins done by different researchers yielded results comparable to the ones of the alkali and black liquor lignins.<sup>7,72,86,87,110,111</sup>

Especially the values of hydrogen are reported in a narrow range, between 5.6 and 6.4 %. Thus, the values determined for alkali and black liquor lignin perfectly fit this area. Additionally, the nitrogen content for all samples correlate very well with literature, where values between 0 and 1.1 % were reported. Although the values for sulfur showed a slightly higher variation, from 0.1 to 2.5 %, the values above also are in this range. For carbon and oxygen, the values showed a wider variation, with 59.1 to 66.5 % for carbon and 25.3 to 32.0 % for oxygen. The oxygen content is calculated and not measured in all the papers, so the deviation can be explained through the variation in the other parameters and through the fact, that in some papers also ash

and water contents were taken into account. The carbon as well as the oxygen contents found in the analysis of the alkali and black liquor lignins correlate very well with the papers, being in between the lowest and highest values found.

For lignosulfonates, which are best compared with the sulfonated kraft lignin, carbon contents of 37.2–40.0 % and oxygen contents of 51.8–53.7 % have been reported, which means that the sulfonated kraft lignin has a higher carbon and a lower oxygen content than lignosulfonates, with 50.7 and 40.5 %, respectively. Since the C and O contents of sulfonated kraft lignin are in between the lignosulfonates and the alkali lignins, it seems that this is an effect of the sample being only a sulfonated kraft lignin and not a lignosulfonate. For hydrogen content, values between 4.4 and 4.9 % were found in literature, while nitrogen content was found to be from 0.02–0.99 % and sulfur content 3.5–8 %. Thus, the values for these three elements determined in this thesis, 4.7 % H, <0.1 % N and 4.1 % S, fit the values from literature very well.<sup>7,110,112,113</sup>

#### 4.2.5 Moisture content determination

According to the method used for the ash content determination (TAPPI method T211 om-02<sup>114</sup>), the moisture content of the samples had to be determined beforehand, which was carried out as stated in TAPPI method T210 cm-03<sup>115</sup>.

After drying the samples at 105 °C for a total of 23 hours, when all samples were in the area of 0.1 % variation from the initial moist weight, the moisture content was determined for two alkali lignin batches, the sulfonated kraft lignin and the black liquor lignin, with the following formula after weighing the dry lignins:

$$\text{moisture content}[\%] = \frac{\text{mass}_{\text{moist lignin}}[\text{g}] - \text{mass}_{\text{dry lignin}}[\text{g}]}{\text{mass}_{\text{moist lignin}}[\text{g}]} * 100\%$$

The following table shows the results of the moisture content determination:

Table 42: Results of moisture content determination

	mass <sub>Moist</sub> [g]	Mass <sub>Dry</sub> [g]	Moisture content [%]	Moisture content mean [%]
<b>Alkali lignin 1</b>	1.02	0.957	5.74	5.37
<b>Alkali lignin 2</b>	1.00	0.952	4.99	
<b>Sulfonated kraft lignin 1</b>	1.03	0.910	11.6	10.6
<b>Sulfonated kraft lignin 2</b>	1.04	0.939	9.54	
<b>Black liquor lignin 1</b>	1.06	1.04	1.45	1.60
<b>Black liquor lignin 2</b>	1.04	1.02	1.75	



These results show a very high deviation in moisture contents of the samples, as the black liquor lignin only showed 1.6 %, while the sulfonated kraft lignin showed a moisture content of 10.6 %. This is surprising, as this lignin is a commercial one from Sigma Aldrich and should be somewhat dried. But also, the other commercial lignin, the alkali lignin, showed a much higher moisture content than the lignin precipitated from black liquor. This most likely means, that no extensive drying step was involved in the precipitation of the commercial lignins, as it was in the precipitation method used in this thesis. The high moisture content in sulfonated kraft lignin may also arise from other instable or volatile moieties present in this lignin.

In literature examples for the moisture content in kraft lignin, different values were reported: Sameni<sup>7</sup> reported moisture contents of only 1.13 to 2.39 % for different kraft lignins, while Oasmaa et al.<sup>90</sup> reported much higher moisture contents of 5.9 to 7.7 %. Interestingly, the value for the black liquor lignin fits very well in the values of the first work, while the results for alkali lignin are like the ones of the second paper. The sulfonated kraft lignin showed higher values than found in literature. Although, these results are likely dependent on the batch of kraft lignin for the commercial lignins and on the drying time for the precipitated lignin.

#### 4.2.6 Ash content determination

Following TAPPI method T211 om-02<sup>114</sup>, the alkali, sulfonated kraft and black liquor lignin samples were carbonized on a low Bunsen burner flame and then put in the muffle furnace at 525 °C for 4 hours.

After that time, the alkali and black liquor lignins turned colorless with no black particles seen, indicating complete combustion. The sulfonated kraft lignin still showed a distinct black color. The samples were cooled to room temperature in a desiccator and then the ash was weighed.

After weighing of the ash, the ash content was determined via the following formula:

$$\text{ash content}[\%] = \frac{\text{mass}_{\text{ash}}[\text{g}]}{\text{mass}_{\text{lignin}}[\text{g}]} * 100\%$$

The table below sums up the masses of educt weighed in, of ash weighed out and the ash content according to the formula above. The mass of the lignin educt was calculated to dry mass with the results of the moisture determination described above:

Table 43: Results of ash content determination

	Mass lignin [g]	Mass ash [g]	Ash content [%]
<b>Alkali lignin</b>	1.44	0.0458	3.19
<b>Sulfonated kraft lignin</b>	1.34	0.923	68.7
<b>Black liquor lignin</b>	1.49	0.0854	5.72

Firstly, it seems that this method is not suitable for the determination of the ash content of the sulfonated kraft lignin, as a value of 68.7 % was found. Thus, some moiety in the sulfonated kraft lignin seems to prevent it from getting burned completely, like the much higher sulfur content of this lignin, with over 4 % compared to under 2 % in the alkali lignin samples, indicating sulfonate groups.

Normally, ash contents in lignosulfonates have been reported in the range of 4 to 8 %<sup>116,117</sup>, while also values up to 25 % have been found by Jablonsky et al.<sup>118</sup> Jablonsky also analyzed the ash content of a commercial sulfonated kraft lignin, from Mestvaco, resulting in an ash content of 23.7 %.

For the other two samples, alkali and black liquor lignin, results of 3.2 and 5.7 % were found, respectively. To be able to discuss this percentages, the amounts had to be compared to ash contents described in literature<sup>7,90,119,120</sup>:

In these papers, kraft lignins from various resources have been analyzed for their ash content, including eucalyptus, bamboo, straw, hemp, flax, pine and birch. The ash contents of these lignins vary between a maximum of 5.35 and 5.2 % in bamboo<sup>119</sup> and pine kraft lignin<sup>90</sup>, respectively, and a minimum of 0.1 % in birch kraft lignin<sup>90</sup>. This means, that the value found for the commercial alkali lignin, with 3.19 %, correlates very well with some of the values found in the literature, right in between two commercial kraft lignins, Indulin AT, a pine kraft lignin, and Protobind 1000, a non-wood kraft lignin, which had values of 4.25 and 2.04 %, respectively<sup>7</sup>. The precipitated black liquor lignin showed an ash content of 5.72 %, which is a bit higher than the values reported for black liquor lignin. But the values for the bamboo and pine kraft lignins, as previously stated, are only 0.35–0.5 % higher than the values found in this work. Thus, the black liquor lignin also corresponds with the values in the literature. The values of hemp and flax lignin ash contents are 1.3–1.7 % higher than the alkali lignin and only 0.8–1.2 % lower than the black liquor lignin, so also lignins from other, non-wood sources show comparable ash contents.<sup>120</sup>

### 4.3 Soxhlet extraction of alkali lignin

Soxhlet extraction should be used to extract valuable compounds, especially phenols, from the untreated commercial alkali lignin sample to determine if these compounds were formed during the pulping process. For this, a Soxhlet apparatus was set up with methanol as extraction solvent. After ten cycles of soxhlet extraction, the color of the methanol around the thimble, containing the extracted compounds, was yellow and clear, in contrast to the methanol fraction during the first cycle, which was brown and slightly opaque, as seen in Figure 30. This indicates a much lower amount of extracted compounds and as the goal was mainly to see if, and which, compounds were already present in the lignin educt, the reaction was stopped after this cycle.



Soxhlet extraction during  
first cycle

Soxhlet extraction during  
tenth cycle

**Figure 30: Comparison of soxhlet reaction solvents during first and tenth cycle**

The solvent was evaporated via rotary evaporation, yielding 0.60 g of brown residue. This equals 17 % of the educt. This yield could almost certainly be increased by running more cycles of the soxhlet extraction. After resuspending the product in methanol, GC-MS analysis showed the following chromatogram:

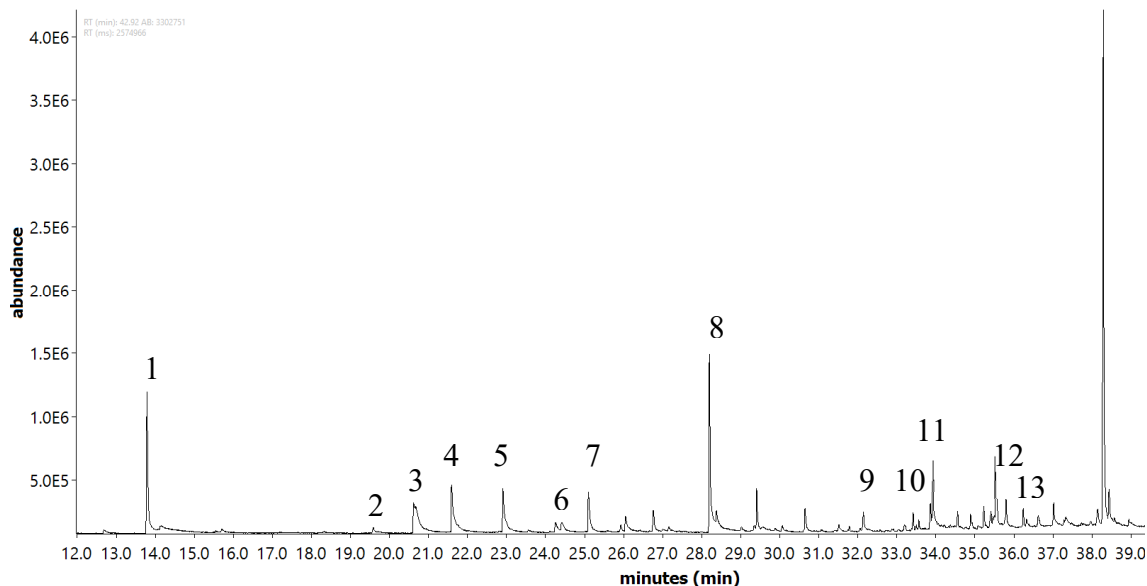


Figure 31: Gas chromatogram of alkali lignin soxhlet extract

Table 44: Identified peaks of the chromatogram (Figure 31)

Peak	Retention time [min]	Substance
1	13.79	Guaiacol
2	19.58	4-ethylguaiacol
3	20.62	2-methoxy-4-vinylphenol
4	21.59	Syringol
5	22.91	Vanillin
6	24.26	Isoeugenol
7	25.10	Acetovanillone
8	28.20	Homovanillic acid
9	32.14	Hexadecanoic acid
10	33.86	Octadecadienoic acid
11	33.92	Octadecenoic acid
12	35.80	Dehydroabietic acid methyl ester
13	36.24	Abietic acid methyl ester

Interestingly, already some phenolic compounds could be identified in the lignin educt. This also includes vanillin, which is often described in literature as a part of lignin and its products, but was only found after the soxhlet extraction of the educt alkali lignin. In addition to that, some fatty acids, which were found after the reduction as fatty acid methyl esters, could be

identified. Abietic and dehydroabietic acid methyl esters were also found in the educt. Another possibility would be that some of these products are released from the lignin molecule due to the temperature applied during the extraction, as part of the lignin is also dissolved in methanol, which leads to the appearance of lignin and lignin oligomers in the product of the soxhlet extraction.

The peak at about 38.5 minutes could not be unambiguously identified, but the mass spectrum suggests that its structure consists of two or more connected benzene rings.

To get an idea of how much phenols could be extracted from the alkali lignin educt, a quantification of the phenolic compounds via GC-MS with BHT as internal standard was carried out, like the one described in chapter 4.5.4 Quantification. Response factors were considered to factor in the differences between BHT and the various phenolic compounds. This yielded the following results:

**Table 45: Results of phenolic compounds quantification in soxhlet extracted alkali lignin**

<b>Soxhlet extracted alkali lignin</b>	
<b>Amount phenols<sub>MeOH soluble oil</sub> [mg]</b>	8.00
<b>Amount phenols<sub>MeOH soluble oil</sub> [%]</b>	1.33
<b>Amount phenols<sub>lignin</sub> [%]</b>	0.23

The quantification of the soxhlet extracted alkali lignin led to a result of 8.00 mg of phenolic compounds in the methanol soluble residue. This equals 1.33 % in this product. When looking at the lignin educt, 0.23 % were extracted by the soxhlet extraction. This means, that already a specific amount of free phenolic compounds is present in the alkali lignin. However, the major part of the phenols found after the reactor reactions was still released from the lignin by the conditions inside the reactor. This can easily be seen when looking at the total amount of phenols in milligrams, as even in the relatively ineffective thermal reaction of alkali lignin more than 100 times more phenolic compounds were found.

## 4.4 Electrochemical oxidation

In this chapter, the potential of generating valuable low molecular products like phenols via electrochemical oxidation was investigated. For that purpose, a boron-doped diamond (BDD) anode, an inactive electrode with an area of  $0.00175 \text{ m}^2$ , was used with a stainless steel cathode.

The general setup, built at VTU<sup>3</sup> where all of the oxidation reactions were carried out, consisted of a cell containing the BDD and stainless steel electrodes, and a rectifier attached to them to apply a fixed current, a reactor vessel, a peristaltic pump and a cooling thermostat. A solution of 20 g/l lignin in water was filled into the reactor vessel, from where it was pumped through the cooling thermostat into the cell from bottom to top and then back into the reactor. For the experiments carried out with a membrane, two separate cycles had to be set up due to the separated electrode rooms of BDD and stainless steel electrodes. While for the BDD cycle an anolyte solution of 20 g/l lignin was prepared as described above, a similar cycle was set up for the other electrode room with a catholyte solution of 10 g/l  $\text{Na}_2\text{SO}_4$  in water. Temperature, pH and conductivity were tracked with a multiparameter meter, while before, during and after the experiments, 1 ml samples were taken out of the reactor to be able to see the changes in the solution over time. These samples were analyzed for their chemical oxygen demand (COD) directly at VTU and with FTIR spectroscopy, GC-MS, preparative SEC and LC-TOF-MS.

The samples used for the electrochemical oxidation with and without membrane were the sulfonated kraft lignin, which was oxidized at two different currents, and the thin liquor, both dissolved in water. Also, such an amount of  $\text{Na}_2\text{SO}_4$  was added that a conductivity of about 10 mS/cm was reached. The alkali lignin, which was dissolved in NaOH in contrast to the other two lignins, was oxidized at lower currents.

### 4.4.1 Sulfonated kraft lignin

#### 4.4.1.1 Electrochemical oxidation of sulfonated kraft lignin (V01)

In this first electrochemical oxidation reaction a solution of 20 g/l sulfonated kraft lignin in water was used at a current of 1.75 A, which equals  $1000 \text{ A/m}^2$ . As foam formation was observed during the reaction, 1.83 g/l silicone antifoaming emulsion was added.

The following table sums up the parameters measured during and directly after the electrochemical oxidation of sulfonated kraft lignin:

Table 46: Parameters of sulfonated kraft lignin electrochemical oxidation V01

Sample [#]	Time [h]	Temperature [°C]	pH	Conductivity [mS/cm]	Voltage [V]	Current [A]	COD [mg/l O <sub>2</sub> ]
00	0	24.9	6.36	12.8	8.6	1.75	2.55*10 <sup>4</sup>
01	1	24.6	4.88	12.3	8.7	1.75	2.38*10 <sup>4</sup>
02	2	24.9	4.26	12.1	8.6	1.75	2.22*10 <sup>4</sup>
03	3	25.0	3.96	12.6	8.5	1.75	2.12*10 <sup>4</sup>
04	4	25.2	3.80	12.3	8.4	1.75	1.93*10 <sup>4</sup>
05	5	25.2	3.71	13.6	8.4	1.75	1.79*10 <sup>4</sup>

As the solution was flowing through a cooling thermostat, not much difference can be seen in the temperatures during the whole reaction.

The current was set with the rectifier, so this parameter should and did not change. The voltage also was only in a range of 0.3 V. The conductivity was adjusted to 12.8 mS/cm with Na<sub>2</sub>SO<sub>4</sub> and did not change very much during this reaction, which is no surprise as this parameter is correlated to the current and the voltage, as described in the theoretical part of this thesis.

The change of the remaining two parameters, the pH value and the COD, was visualized in the following figure:

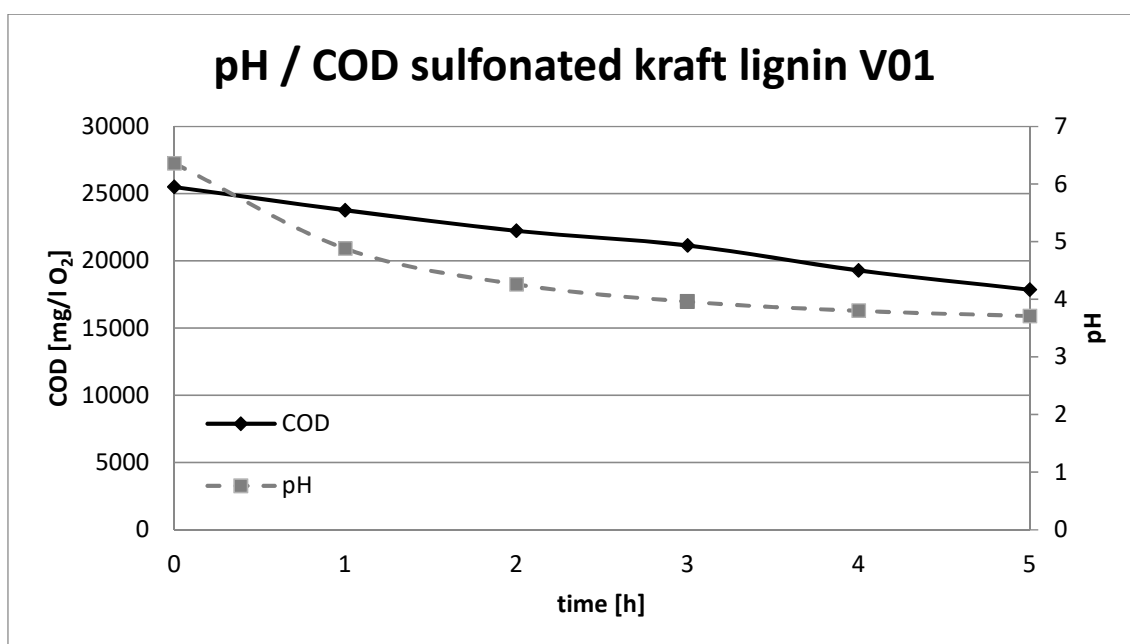


Figure 32: pH and COD change during sulfonated kraft lignin electrochemical oxidation V01

The pH value decreased strongly in the first hour of the reaction, by about 1.5, and by only about 1 in the next four hours. This decrease indicates a change in the lignin sample leading to this decrease. The most likely explanation for that would be that certain end groups of the lignin molecule reacted directly or through other moieties like acetic and formic acid to  $\text{CO}_2$ , which is often the case with the BDD-Niob anode. This tendency is highly desirable as the main application of this electrode is waste water treatment.<sup>70,71</sup>

Another indication for this reaction pathway is the steady decrease of the COD during the reaction. This COD degradation corresponds to a loss of organic substances, in the case of the BDD-Niob electrode most likely through the evolution of  $\text{CO}_2$ . This decrease is near the optimal line of COD degradation for waste water treatment.

The third indication for this theory is the quite strong foam formation directly after the start of the reaction which did not lessen until antifoaming emulsion was added. As the reaction itself was carried out in a closed reaction room,  $\text{CO}_2$  evolution in the form of bubbles could not be directly observed.

### FTIR analysis

For FTIR analysis, the product after 5 hours of oxidation was dried at  $90\text{ }^\circ\text{C}$  in the drying oven for three days, so that a solid product remained. This solid product was then directly analyzed via the diamond ATR accessory of the FTIR spectrometer. The result of this measurement can be seen in the following figure:

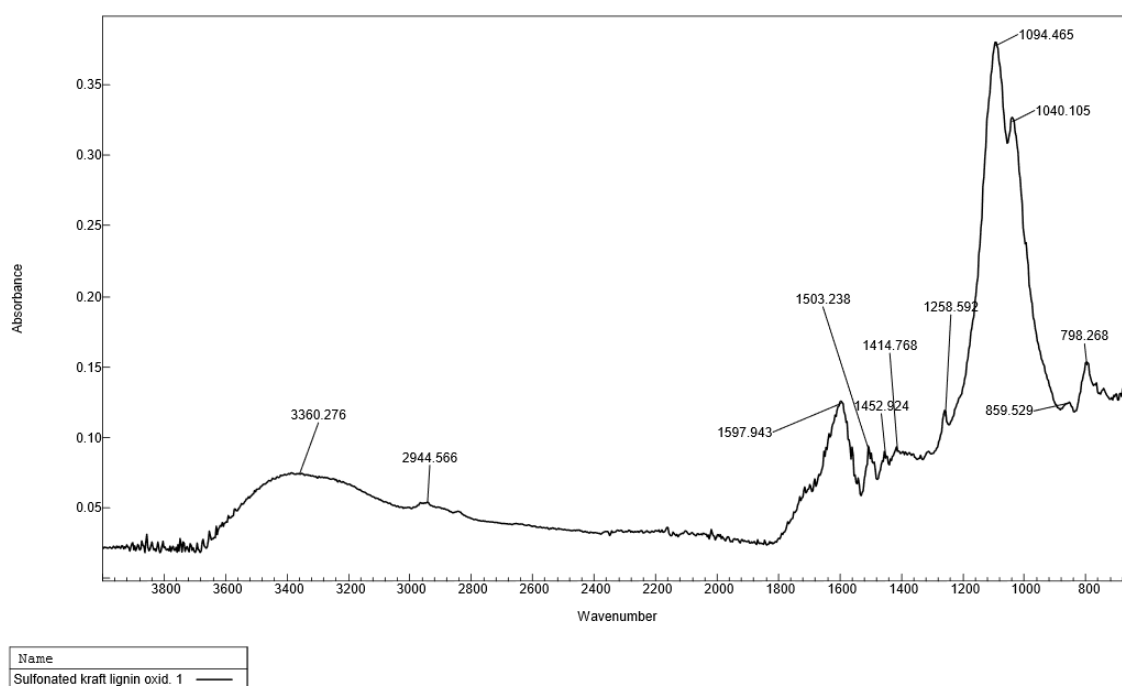


Figure 33: FTIR spectrum of oxidized sulfonated kraft lignin (V01)



**Table 47: FTIR absorption frequencies and assigned vibrations of oxidized sulfonated kraft lignin (V01)<sup>102-104</sup>**

Wavenumber [cm <sup>-1</sup> ]	Bond	Type	Chemical class
3360	O-H	Stretching	Alcohol/ water
2945	C-H	Stretching	Arene/ alkane
1598	C=C	Stretching	Arene
1503	C=C	Stretching	Arene
1453	C-H	Bending	Alkane
1415	O-H	Bending	Alcohol
1259	C-O	Stretching	Aromatic ester/ alkyl aryl ether
1094	C-O	Stretching	Secondary alcohol/ aliphatic ether
1040	C-O	Stretching	Alkyl aryl ether/ vinyl ether
860	C-H	Bending	Arene (di-, tri- or tetrasubstituted)
798	C-H	Bending	Arene (di-, tri- or tetrasubstituted)

When looking at the table above, there is not much difference between the electrochemically oxidized kraft lignin and the educt, the sulfonated kraft lignin. The only differences between the chemical classes found in these spectra are the peaks at 1190 and 1320 cm<sup>-1</sup>, as the peaks visible in the spectra of the educt cannot be seen in the oxidized lignin. These two peaks can be assigned to sulfonate groups, which means that these sulfonate groups are cleaved off from the lignin molecule either by the electrochemical oxidation or the acidic environment.

Like in the FTIR of the alkali lignin, the C-H bending vibrations at 860 and 798 cm<sup>-1</sup> indicate an 1,2,4-trisubstituted arene, which, as previously described, would be the G-type monomeric building block of lignin molecules.

Apart from that, there are some differences in the height of the various peaks to each other, as can be seen in the following figure:

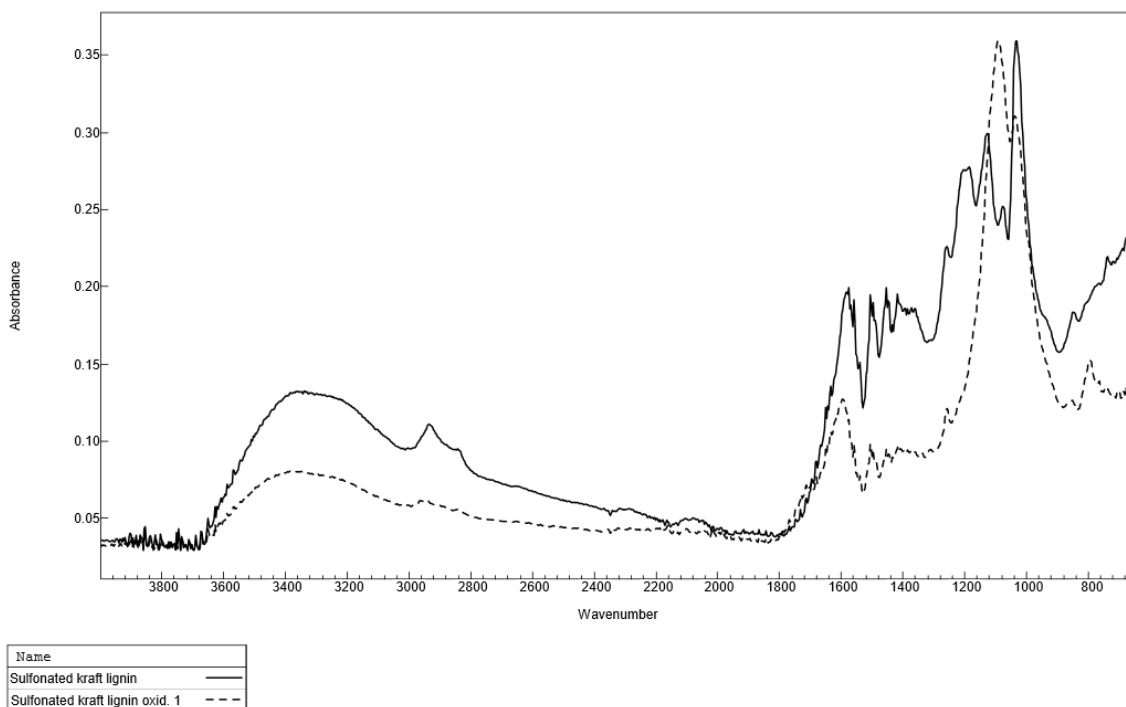


**Figure 34: FTIR spectra of sulfonated kraft lignin, unoxidized and oxidized (V01)**

In the area up to about  $1400\text{ cm}^{-1}$ , not much difference can be seen, except the slightly lower height of the educt spectrum, but no quantitative statements about the water content or alkane groups can be made from that. More interesting are the peaks between  $1200$  and  $1000\text{ cm}^{-1}$ . In the sulfonated kraft lignin educt, three peaks can be seen, the first one having an absorbance of about 0.30, the second one 0.25 and the third one 0.35. In contrast to that, the spectrum of the oxidation product shows only two peaks, the first one with an absorbance of 0.35 and the second one with 0.30. This means, that the alcohol or aliphatic ether vibrations are more intense after the oxidation, while the alkyl aryl ether vibrations have been stronger before the oxidation. Apart from that, the ratios between some peaks are also different. For example, the ratio of the peak at about  $1600\text{ cm}^{-1}$  to the one at about  $1100\text{ cm}^{-1}$  is much higher for the oxidized lignin, speaking for a higher relative abundance of secondary alcohols in the oxidized lignin.

### GC-MS analysis

The samples before the oxidation, after three hours and after five hours were injected into the GC-MS as they were taken out of the reaction chamber, with water as solvent. The chromatograms of the unoxidized sulfonated kraft lignin and after three hours of electrochemical oxidation can be seen in Figure 35

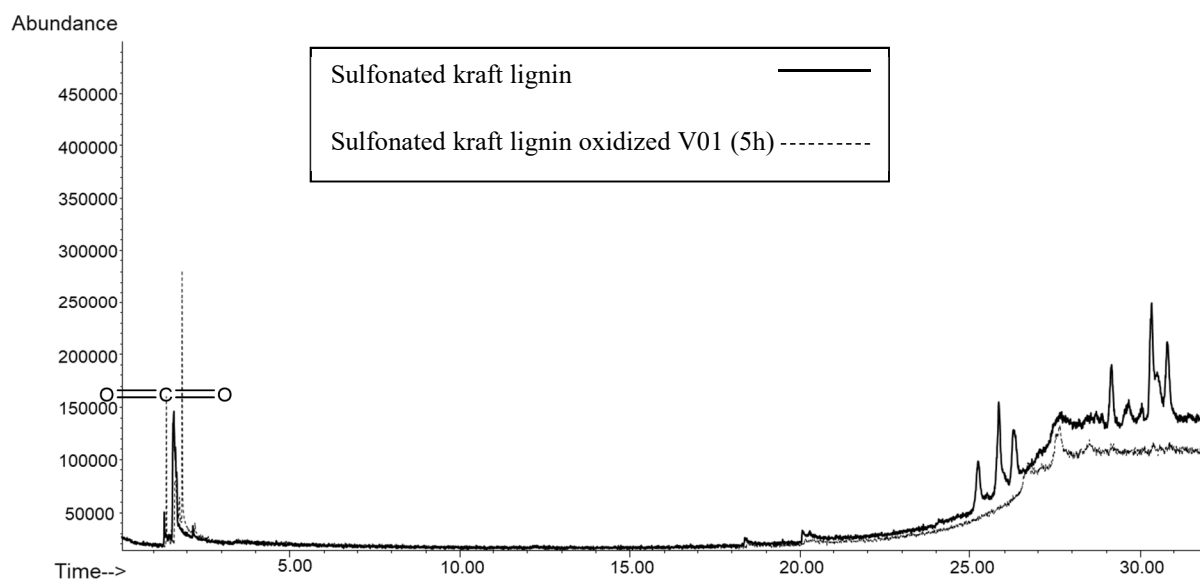


Figure 35: Gas chromatograms of sulfonated kraft lignin educt (solid) and electrochemically oxidized V01 after 5h (dashed)

Unfortunately, the only peak unambiguously identifiable in both chromatograms is the one at 1.34 minutes, which can be assigned to  $\text{CO}_2$ . The formation of  $\text{CO}_2$  was expected, as the BDD anode used is an inactive electrode, which oxidizes organic substances completely to  $\text{CO}_2$ , as described in chapter 2.6.6 Electrochemical oxidation. The other peaks at  $>18$  minutes are also visible in the chromatogram of the blanks and thus coming from previous analyses or the column itself. As this observation was made for all the chromatograms of sulfonated kraft lignin and the thin liquor, before and after the electrochemical oxidations, from now on only the first few minutes of the chromatograms, where differences were visible, will be shown:

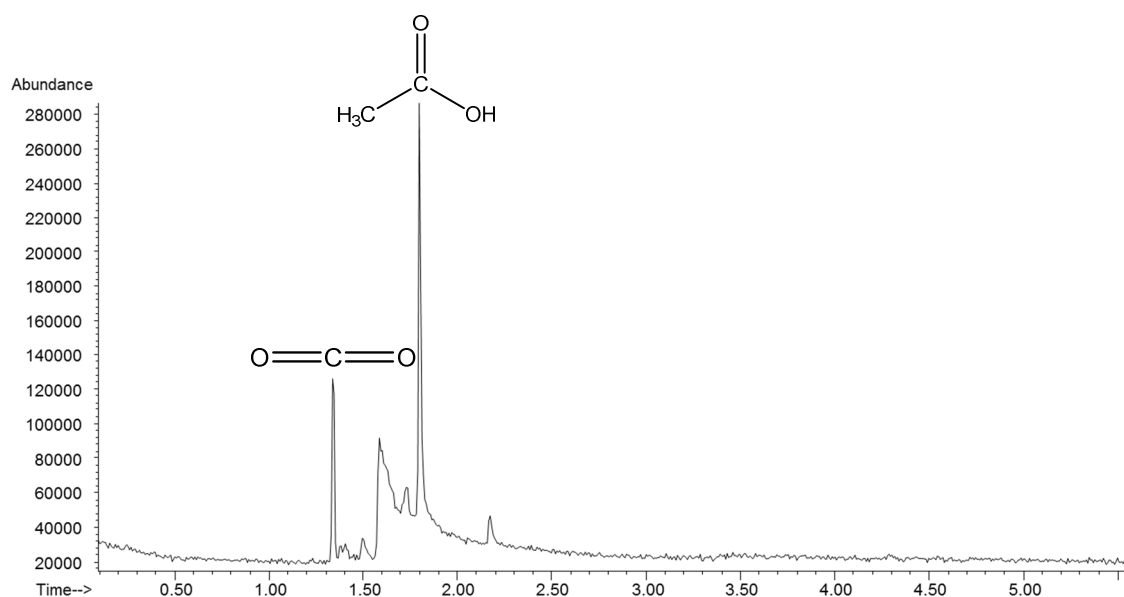


Figure 36: Gas chromatogram of sulfonated kraft lignin, electrochemically oxidized V01 (5h), first 5 minutes

The major difference between the chromatogram after five hours and the one before the oxidation is the second peak at 1.81 minutes. This peak can be assigned to acetic acid, which is then oxidized to CO<sub>2</sub> and further bubbles out.

To be able to better analyze the product mixtures and maybe see compounds in the products except CO<sub>2</sub> and acetic acid, the product of the oxidation was extracted with three different solvents, namely n-hexane, chloroform and chloroform:methanol 2:1. The solvents were mixed 1:1 with oxidized sulfonated kraft lignin product in a separating funnel. After reaching equilibrium, three-phase systems formed, with an upper organic phase, a middle lignin phase and a bottom aqueous phase. After separation of the three phases and repeating the extraction of the aqueous phase two more times, the mixed organic phases were evaporated in the rotary evaporator, taking out the last bit of solvent as GC-MS samples. Unfortunately, with neither solvent a difference in the area over three minutes could be seen just like with the usage of water as solvent, while the area under three minutes was mainly composed of solvent peaks. Thus, no products of the electrochemical oxidation of sulfonated kraft lignin except CO<sub>2</sub> and acetic acid can be detected with GC-MS in this case.

### Molecular weight analysis

Preparative SEC was carried out by Prof. Anton Huber (Polysaccharides & Hydrocolloids, Institute of Chemistry, University of Graz) as seen in Figure 37.<sup>121</sup>

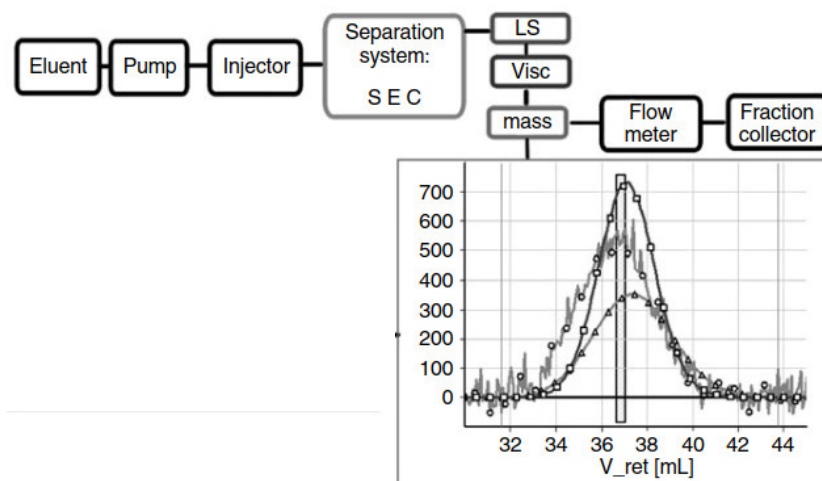


Figure 37: Determination of excluded volume distribution by SEC with triple detection (adapted from Huber & Praznik)<sup>121</sup>

The analysis is done by injecting the sample into the system, where it is pumped into the SEC section, consisting of 2–5 columns with different pore size in series. Size exclusion is achieved as described in chapter 2.5.2.2 Exclusion Chromatography. After this section, there is a detection section consisting of three different detection systems: a mass detector, a light scattering detector and a viscosity detector. From this SEC experiment, two molecular weight

distribution parameters are obtained: the distribution of mass fractions  $m\_MWD\_d$  and the distribution of molar fractions  $n\_MWD\_d$ . The difference between these two parameters is, that low-molecular components dominate the molar fractions, while the mass fractions are dominated by high-molecular components. From these values, the number average molecular weight  $M_n$  and the weight average molecular weight  $M_w$  are calculated according to following formulas:

$$M_n = \frac{\sum n_i M_i}{\sum n_i} \text{ and } M_w = \frac{\sum n_i M_i^2}{\sum n_i M_i}$$

where  $M$  is the molecular weight (g/mol),  $n$  the mol number (mol/l) and  $i$  are the indices of the SEC-separated fractions.

For the analysis, dilution series had to be prepared for the sulfonated kraft lignin educt as well as the product of its electrochemical oxidation after five hours. For the educt, concentrations of 5, 8, 10, 12 and 15 mg/ml were prepared, while the product, having a concentration of 20 mg/ml, was diluted to 15, 10 and 5 g/ml

The molecular weight analysis of the sulfonated kraft lignin solution before and after five hours of oxidation can be seen in Figure 38.

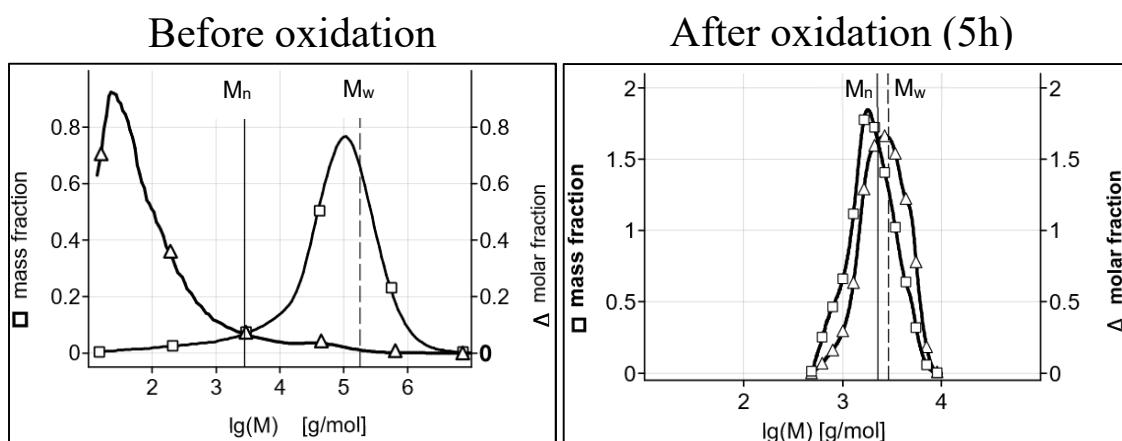


**Figure 38: Molecular weight distribution of sulfonated kraft lignin before and after electrochemical oxidation**

For the educt, most of the mass fraction is centered between 10,000 and 1,000,000 g/mol, likely mainly lignin molecules in different sizes since the mass fraction is dominated by high-molecular compounds as stated above. In contrast to that, the molar fraction, which mainly shows low-molecular compounds, is centered below 1000 g/mol. The number average molecular weight is about 2800 g/mol, while the mass average molecular weight  $M_w$  is about 185,000 g/mol, leading to a dispersity  $\mathcal{D}$  ( $\mathcal{D}_M = M_w/M_n$ ) of 66, meaning that the sample is highly non-uniform, as a value of 1 characterizes a uniform sample.<sup>33,34</sup>

After oxidation, the molecular weight is centered between 500 and 10,000 g/mol for both the molar and mass fractions, meaning that the molecular weight distribution is not dominated by either low-molecular or high-molecular compounds. This can also be seen for the molecular weights, as  $M_n$  is about 2250 g/mol, while  $M_w$  is about 2870 g/mol, giving a dispersity of 1.27, which means that this sample became nearly uniform during the electrochemical oxidation. With this, it can clearly be said that the lignin molecule in the solution has been split by the electrochemical oxidation reaction and low molecular weight compounds have been oxidized to  $\text{CO}_2$ .

It should be noted, that fragments under about 500-1000 g/mol cannot be conveniently detected with this method.

#### **LC-TOF-MS analysis**

The LC-TOF-MS analysis of the sulfonated kraft lignin educt, did not yield useful information about any compounds in this sample as the peaks in the MS could not be assigned to specific compounds. This leads to the conclusion, that the lignin molecule, as expected, is bigger than 1000 m/z and that no specific building blocks from the lignin, like the G-type monomer, can be detected with this method. Also, no compounds derived from these building blocks, like guaiacol, which could have been released from the lignin molecule during the kraft process, can be assigned to the peaks. The most probable hypothesis is, that the peaks found are oligomers of the lignin building blocks, either directly connected or through ether bonds, like in the lignin molecule. The compounds found with lower m/z ratios could also represent split off aromatic rings with different end groups.

#### **4.4.1.2 Electrochemical oxidation of sulfonated kraft lignin with membrane (V02)**

As described above, this experiment was carried out with two electrode rooms, separated by a membrane. Through the anolytic side, where the BDD electrode was located, a 20 g/l anolyte solution of sulfonated kraft lignin in water, set to a conductivity of 13.7 mS/cm with  $\text{Na}_2\text{SO}_4$ , was flowing, while 10 g/l  $\text{Na}_2\text{SO}_4$  was used as catholyte solution. A current of 1.75 A ( $1000 \text{ A/m}^2$ ) was applied.

Table 48 sums up the parameters of this experiment:

Table 48: Parameters of sulfonated kraft lignin electrochemical oxidation with membrane V02

Sample [#]	Time [h]	Temperature (A) [°C]	pH (A)	Conductivity (A) [mS/cm]	Voltage [V]	Current [A]	COD [mg/l O <sub>2</sub> ]
00	0	24.7	8.74	13.7	14.6	1.75	2.52*10 <sup>4</sup>
01	1	24.5	1.59	22.5	10.3	1.75	2.30*10 <sup>4</sup>
02	2	24.5	1.40	29.7	8.8	1.75	2.19*10 <sup>4</sup>
03	3	24.6	1.29	34.3	8.4	1.75	1.99*10 <sup>4</sup>
04	4	24.6	1.23	37.5	8.1	1.75	1.85*10 <sup>4</sup>
05	5	24.7	1.17	40.0	8.0	1.75	1.67*10 <sup>4</sup>

(A) indicates that these values are for the anolytic side of the membrane, where the lignin solution was flowing through. The values for the catholytic cycle are not shown.

As already discussed for the first electrochemical oxidation of sulfonated kraft lignin., the temperature and the current are constant. There is more change in the voltage compared to the first oxidation, especially during the first two hours of the reaction, where a change of about 6 V can be observed. This difference to the first oxidation is caused by the different setup in this experiment with the usage of a membrane. The different setup also leads to a greater variation in the conductivity, where an increase of about 26 mS/cm was observed from the start of the reaction to the end. This is also caused by the cation exchange between anolyte and catholyte and thus only a feature of the membrane design. The pH and the COD, like in the first experiment, can be seen in the following figure:

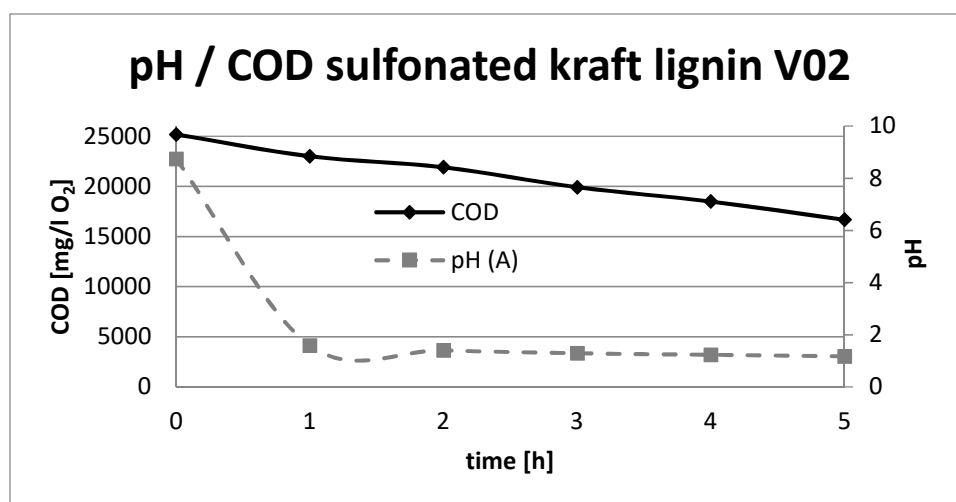


Figure 39: pH and COD change during kraft lignin electrochemical oxidation V02

There was a sharp pH decrease in the first hour of the experiment, much more distinct compared to the first experiment, from 8.74 to 1.59, which is lower than the value observed in the first experiment. This is again a particularity of the of the membrane setup, where most of the pH value change can be distributed to the ion exchange between the anolyte and catholyte and less can be said about the presence of acid groups or CO<sub>2</sub>.

Also like in the first experiment, the COD steadily decreased from about  $2.5 \cdot 10^4$  to about  $1.65 \cdot 10^4$  mg/l during the reaction time of five hours, again nearly following the optimal line for waste water treatment, indicating a loss of organic substances, most likely through degassing of CO<sub>2</sub>, which could be observed by the terms of bubbling.

### FTIR analysis

The dried product of the oxidation of sulfonated kraft lignin with membrane was analyzed by FTIR spectroscopy with the diamond ATR accessory, yielding the following chromatogram:

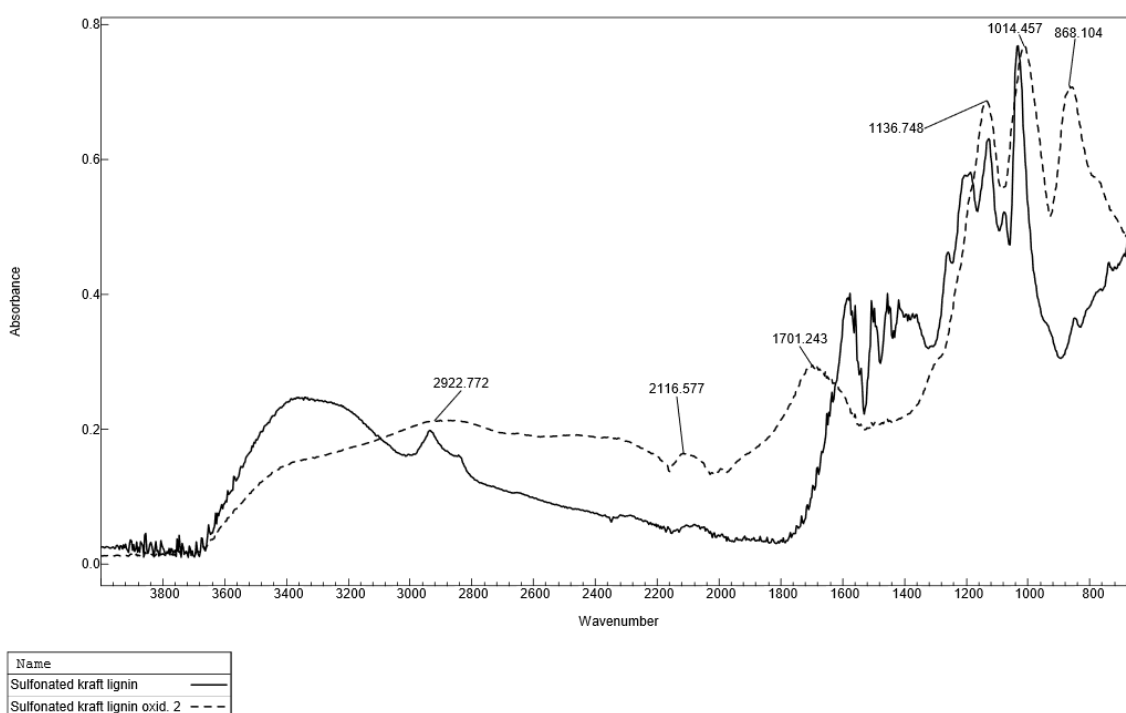


Figure 40: FTIR spectrum of oxidized sulfonated kraft lignin, unoxidized and oxidized (V02)



Table 49: FTIR absorption frequencies and assigned vibrations of oxidized sulfonated kraft lignin (V02)<sup>102-104</sup>

Wavenumber [cm <sup>-1</sup> ]	Bond	Type	Chemical class
2923	O-H	Stretching	Carboxylic acid/ intramolecular bonded alcohol
2117	C≡C	Stretching	Alkyne
1701	C=O	Stretching	Carboxylic acid/ saturated aldehyde/ saturated ketone
1137	C-O	Stretching	Aliphatic ether/ tertiary alcohol
1014	C-O	Stretching	Alkyl aryl ether/ vinyl ether
868	C-H	Bending	Arene (di-, tri- or tetrasubstituted)

The FTIR of the second kraft lignin oxidation product looks completely different compared to the educt and to the first oxidation. When looking at the table above and comparing it with the other two spectra, only the last three peaks, at 1137, 1014 and 868 cm<sup>-1</sup>, are similar. However, these peaks show a completely different characteristic, all three of them being very strong, broad and nearly of same height, which could not be observed for the educt. There, the last peak is significantly lower than the other two and the peaks themselves are rather sharp.

Generally, it can be observed that the other peaks are very broad, which is normally not the case except for the first peak at 2923 cm<sup>-1</sup>, representing a O-H stretching bond. This bond is not the same one as in the educt, which can be assigned to water or also alcohol groups, but it is more connected to carboxylic acids and bonded alcohol in the molecule. The second peak, at 2117 cm<sup>-1</sup>, could be an alkyne bond, which should normally not be present in the lignin molecule. This leads to three possibilities: First, that two end groups, for example hydroxyl groups, are split off at a linkage between two phenols, generating such a triple bond. Second, that the lignin molecule was changed greatly, and far more efficient, in the membrane reaction than in the normal reaction and that a bond rearrangement either of only C-C or of C-C and sulfonate groups had taken place. Third, that the IR vibration are somehow blocked or altered by features of the molecule or other moieties, which emerged during the reaction or were present in the solution.

The third peak, resembling C-O vibrations in carboxylic acids, aldehydes or ketones, is also much broader than normal carboxylic acid vibrations, again indicating that the spectrum is somehow altered by other contents of the analyzed solution, which are not detectable themselves.

### GC-MS analysis

Figure 41 show the gas chromatograms before and after one, two and three hours of oxidation, injected as taken out of the reaction with water as solvent. As there was no difference observable between the chromatograms from three to five hours of oxidation, only the former are shown.

As previously described for the first oxidation of the sulfonated kraft lignin, only the area of up to five minutes showed peaks, so the chromatograms will only be shown in this range.

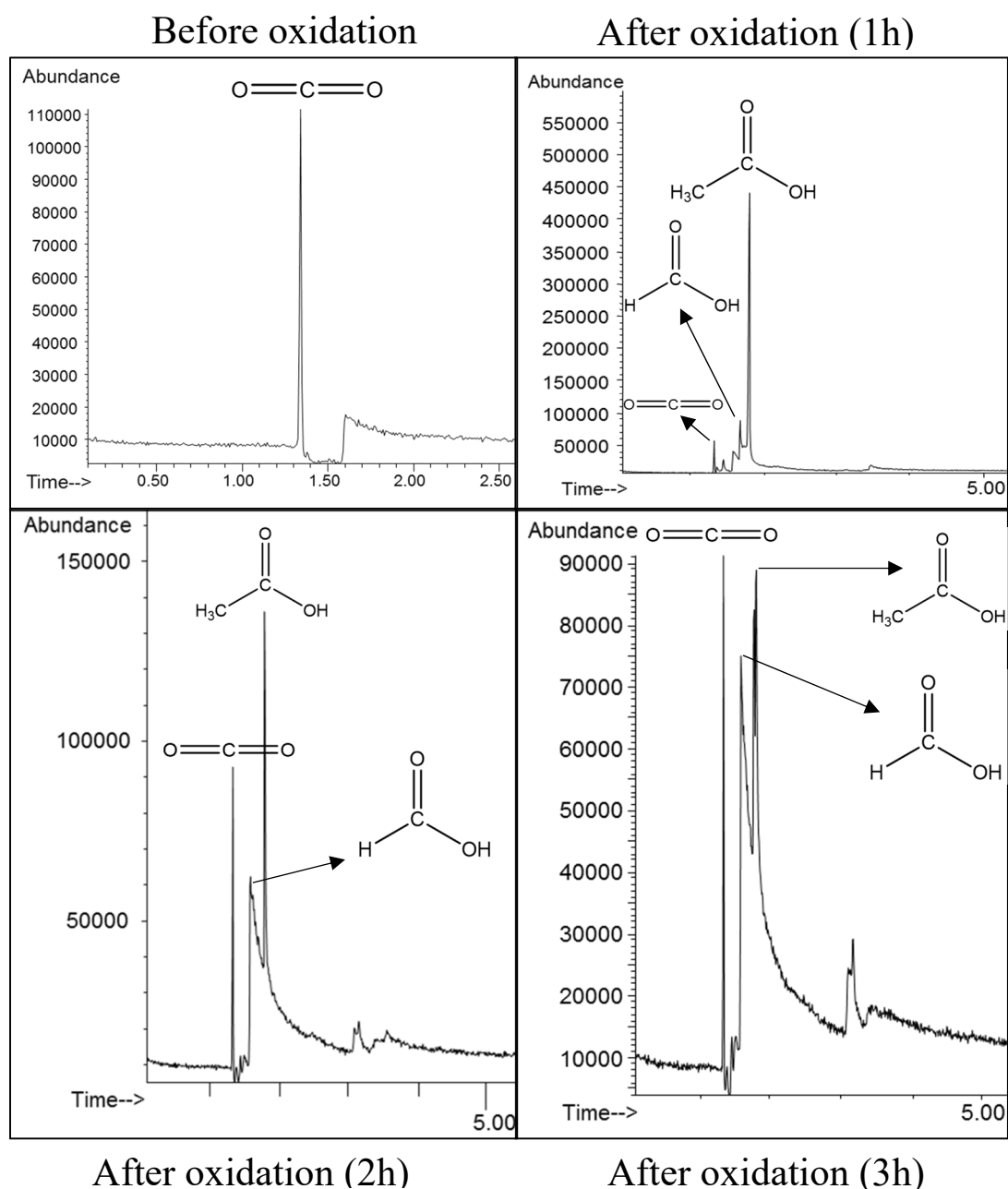


Figure 41: Gas chromatograms of sulfonated kraft lignin after 2h (left) and 3h (right) oxidation

The chromatogram of the sulfonated kraft lignin educt only showed CO<sub>2</sub>, showing no difference to the educt sample from the first experiment.

The chromatograms of the samples taken during the oxidation also showed acetic acid with the highest abundance, which was already discussed for the first experiment. In this case however, also formic acid was generated. This again suggests the mechanism of acetic acid splitting off from the lignin molecule and further oxidation to formic acid and finally to CO<sub>2</sub>, which then bubbled out. Another interesting part is the variation of the height of the peaks. The acetic acid peak strongly increased in the first hour up to an abundance of  $4.5 \cdot 10^5$ , but decreased again until it was even lower than the CO<sub>2</sub> peak after three hours. Also, the peak of the formic acid increased steadily until three hours of oxidation, where it was nearly as high as the other two peaks, indicating that not all of the acetic acid is oxidized directly to CO<sub>2</sub>, but also to formic acid, which is not completely oxidized at this point. Meanwhile, the CO<sub>2</sub> peak decreased from  $1.1 \cdot 10^5$  to  $6 \cdot 10^4$  in the first hour, but then stabilized at an abundance of about  $9 \cdot 10^4$ . As this does not correlate with the decrease of acetic acid, it most likely only shows the CO<sub>2</sub>, which is dissolved in the solvent water during the electrochemical oxidation and thus visible in the GC of the product, while most of the CO<sub>2</sub> bubbled out directly.

#### 4.4.1.3 Electrochemical oxidation of sulfonated kraft lignin at lower current (V03)

In this oxidation, a 20 g/l sulfonated kraft lignin solution analogous to the first two oxidations was used, but in this case, the current was set to a lower value of 0.35 A, equaling 200 A/m<sup>2</sup>. 0.73 g/l antifoaming emulsion had to be added. Table 50 sums up the parameters of this oxidation:

Table 50: Parameters of sulfonated kraft lignin electrochemical oxidation V03

Sample [#]	Time [h]	Temperature [°C]	pH	Conductivity [mS/cm]	Voltage [V]	Current [A]	COD [mg/l O <sub>2</sub> ]
00	0	23.9	9.25	14.3	5.0	0.35	$2.35 \cdot 10^4$
01	1	22.7	7.73	14.5	5.1	0.35	–
02	2	22.7	6.98	14.5	5.2	0.35	$2.25 \cdot 10^4$
03	3	22.7	6.73	14.6	5.2	0.35	–
04	4	22.8	6.46	14.6	5.2	0.35	–
05	5	22.8	6.21	14.7	5.2	0.35	$2.09 \cdot 10^4$

In this reaction, the current was set to just 0.35A, which results in a lower voltage of 5.0. This voltage only rose to 5.2 during this reaction, which is also reflected in the conductivity, which goes up to only 14.7 from the adjusted value of 14.3. The change of the pH value and the COD are again illustrated in the following figure:

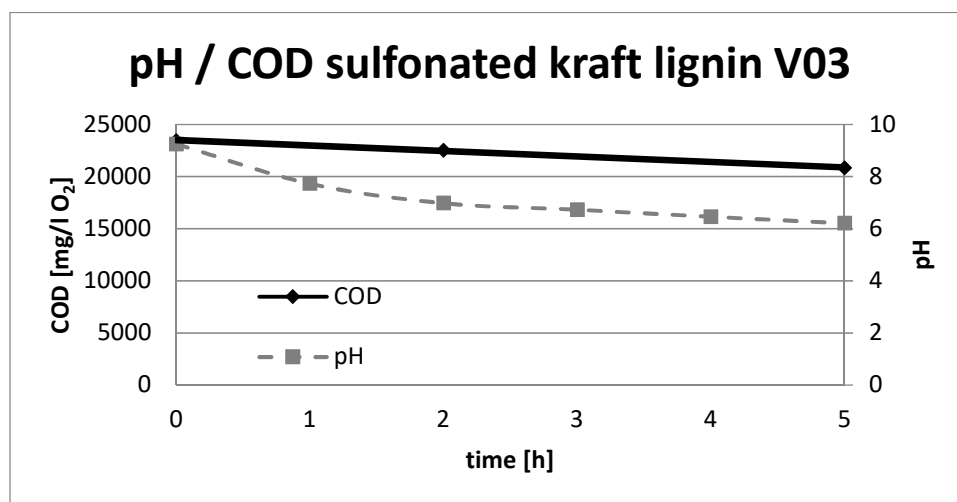


Figure 42: pH and COD change during sulfonated kraft lignin electrochemical oxidation V03

The pH value again decreased in a similar fashion as in the first experiment, by a value of about 3, although the difference was that in this case the starting pH was much higher, at a value of over 9 and reached only 6.2 at the end, while the first experiment showed a final pH of 3.7. Like in the first experiment, the pH decreased quite strongly in the first two hours of the reaction, but not as strong as in the reaction with the membrane. When looking at the results from the first experiment, this decrease is most likely due to the generation of CO<sub>2</sub> and acetic acid, which are dissolved in the reaction liquid.

There is also a COD degradation from  $2.4 \cdot 10^4$  to  $2.1 \cdot 10^4$  mg/l visible during this reaction, which indicates a degradation of organic substances to evolving CO<sub>2</sub>. This degradation again is near the optimal line for waste water treatment.

As GC-MS analysis proved to be more helpful in the analysis of the reaction products than IR, molecular weight and LC-TOF-MS analysis, only this method was used. After the analysis of the product after five hours of oxidation, no acetic acid was visible in the chromatogram and that was the case for all samples taken during the reaction. This either indicates a direct oxidation of the lignin to CO<sub>2</sub> or that the released acids, acetic or formic acid, are directly oxidized to CO<sub>2</sub> before the lignin molecule was attacked again.

To sum up, these results lead to the previously assumed conclusion, that a lower current yields the same products as the other reaction, just in a slower manner and not to the hoped outcome, that bigger parts are released from the lignin molecule due to the less harsh conditions.

## 4.4.2 Alkali lignin

### 4.4.2.1 Electrochemical oxidation of alkali lignin

With the same setup as the electrochemical oxidation of sulfonated kraft lignin, 20 g/l alkali lignin were dissolved in 1 M NaOH. Due to the high conductivity of this solution, no Na<sub>2</sub>SO<sub>4</sub> had to be added. To test a possible formation of valuable compounds at lower currents, it was set to 0.04 A, equaling about 23 A/m<sup>2</sup>, for the first hour, and then to 0.35 A, 200 A/m<sup>2</sup>, for five hours. The table below sums up the parameters of this experiment:

Table 51: Parameters of alkali lignin electrochemical oxidation

Sample [#]	Time [h]	Temperature [°C]	pH	Conductivity [mS/cm]	Voltage [V]	Current [A]	COD [mg/l O <sub>2</sub> ]
00	0	21.9	13.6	146	2.7	0.04	3.68*10 <sup>4</sup>
01	0.5	22.4	14.9	145	3.2	0.04	3.67*10 <sup>4</sup>
02	1	22.4	15.1	144	3.2	0.04	3.79*10 <sup>4</sup>
–	1	22.4	15.1	144	3.7	0.35	–
03	2	22.5	15.2	144	3.7	0.35	3.76*10 <sup>4</sup>
04	3	22.5	15.2	142	3.8	0.35	3.69*10 <sup>4</sup>
05	4	22.6	15.2	141	3.8	0.35	3.93*10 <sup>4</sup>
06	5	22.5	15.2	140	3.8	0.35	3.78*10 <sup>4</sup>
07	6	22.5	15.2	138	3.8	0.35	3.68*10 <sup>4</sup>

As 1 M NaOH in water was used as solvent in this reaction, the pH value was already very high at the beginning of the reaction and increased during this reaction to values over 14, mainly in the first 30 minutes of the reaction. Additionally, the conductivity already had a very high value of 146 mS/cm at the beginning of the reaction. The conductivity slowly decreased during the first hour of the reaction by about 1 mS/cm, then decreased by about 5 mS/cm in the following 5 hours. Interestingly, the voltage decreased by 0.5 V in the first 30 minutes and then decreased by only another 0.5 V after adjustment of the current to 0.35 A.

The COD increased and decreased over the course of the reaction between values of 3.67\*10<sup>4</sup> and 3.93\*10<sup>4</sup> mg/l O<sub>2</sub>. As no distinct trend is observable and the values are in the same range, the COD is assumed as constant over the course of the reaction.

The samples of this experiment were also only analyzed via GC-MS, as seen below:

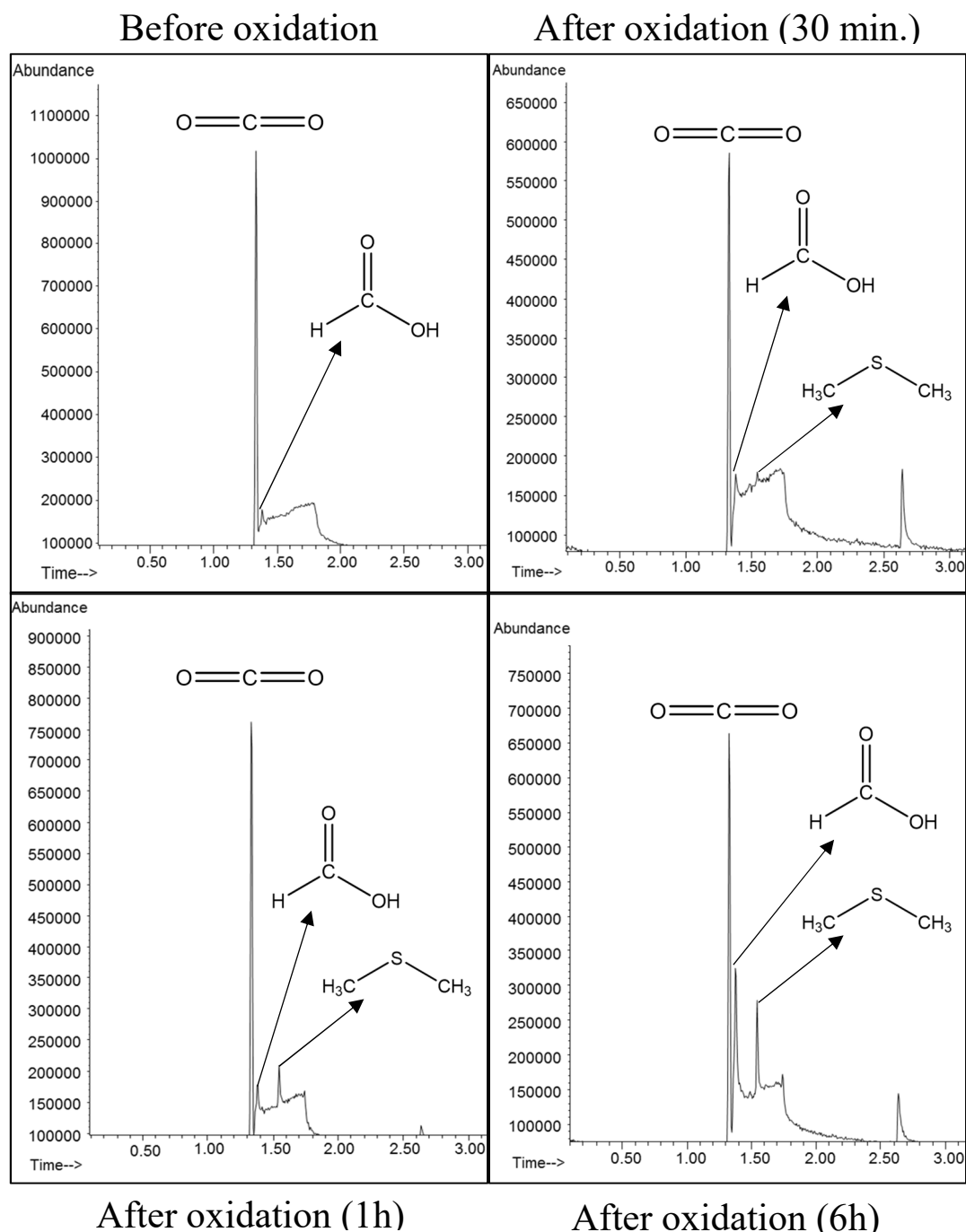


**Figure 43: Gas chromatograms of alkali lignin before, during and after electrochemical oxidation**

At the beginning of the reaction, this lignin already showed a very high amount of  $\text{CO}_2$ , compared to the other lignins. The amount of dissolved  $\text{CO}_2$  was nearly halved in the first 30 minutes, but stabilized at values between  $7 \cdot 10^5$  and  $8 \cdot 10^5$  after that until the end of the reaction.

In this lignin, a low amount of formic acid was visible before the reaction was started. The amount of the formic acid was constant during the first hour of the reaction, where a very low current was used. After another five hours of oxidation at a current of 0.35 A, the amount of

formic acid was doubled, indicating a much higher reactivity with the higher current, as expected.

What really stands out in GC-MS analysis of this lignin is the formation of dimethyl sulfide, which is already visible after 30 minutes and one hour of the reaction, but also doubles in the subsequent five hours at a current of 0.35 A, like formic acid. As described in the theoretical part of this thesis, the alkali lignin shows thiol end groups. These end groups seem to have reacted during the electrochemical oxidation in alkaline media, which yielded the not previously seen dimethyl sulfide group. Compared to that, the lignin in the thin liquor and the sulfonated kraft lignin show sulfoxide end groups, which cannot yield these dimethyl sulfide fragments.

### 4.4.3 Thin liquor

#### 4.4.3.1 Electrochemical oxidation of thin liquor (V01)

This experiment was carried out analogous to the electrochemical oxidation of the sulfonated kraft lignin, as a 20 g/l solution of thin liquor in water was prepared, with the conductivity set to 13.1 mS/cm with Na<sub>2</sub>SO<sub>4</sub>. Due to intense foaming, 1.75 g/l silicone antifoaming emulsion had to be added. The following table sums up the important parameters:

Table 52: Parameters of thin liquor electrochemical oxidation V01

Sample [#]	Time [h]	Temperature [°C]	pH	Conductivity [mS/cm]	Voltage [V]	Current [A]	COD [mg/l O <sub>2</sub> ]
00	0	24.6	3.90	13.1	8.5	1.75	1.97*10 <sup>4</sup>
01	1	24.2	2.83	13.5	8.5	1.75	1.84*10 <sup>4</sup>
02	2	24.3	2.50	14.3	8.4	1.75	1.68*10 <sup>4</sup>
03	3	24.4	2.33	14.8	8.2	1.75	1.52*10 <sup>4</sup>
04	4	24.4	2.22	15.5	8.0	1.75	1.32*10 <sup>4</sup>
05	5	24.2	2.16	16.4	7.8	1.75	1.13*10 <sup>4</sup>

Temperature and current were constant. The voltage did not change much during the first two hours, but then decreased by 0.2 V every hour, giving a total drop of 0.7 V. The conductivity was again set to a value slightly above 10 mS/cm, in this case 13.1 mS/cm. After three hours, the conductivity had increased by 3.33 mS/cm, most likely through formed moieties.

The two parameters with the most noticeable changes, the pH and the COD, are presented in the following figure:

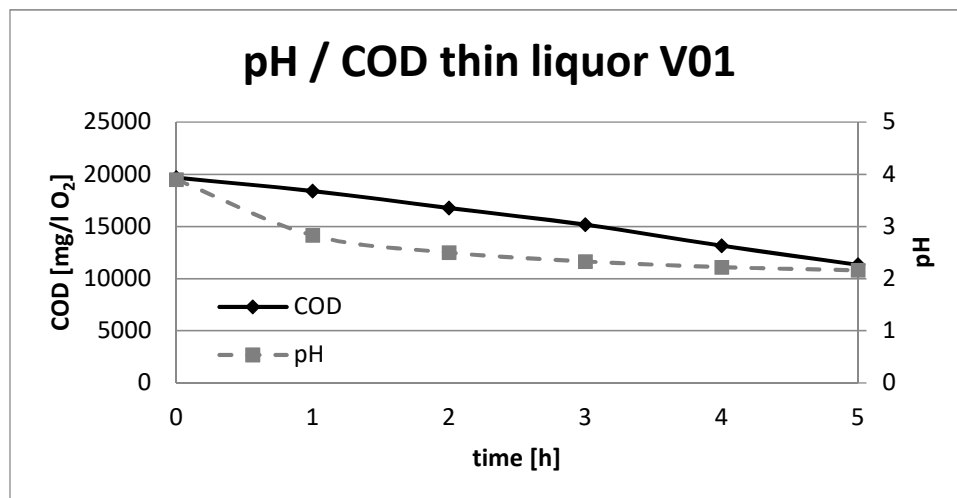


Figure 44: pH and COD change during thin liquor electrochemical oxidation V01

COD shows a similar behavior as in the first experiment with the sulfonated kraft lignin with a total drop of about 8000 mg/l O<sub>2</sub> over the course of the reaction. Thus, the course of the COD decrease again is very near to the ideal waste water treatment line, meaning that the lignin molecule is diminished and the organic substances are “lost” by degassing of CO<sub>2</sub>.

The decrease in the pH in the first hour is again the largest with 1 and only a decrease of 0.7 in the next 4 hours, representing a similar range as in the same experiment with the sulfonated kraft lignin. The difference between the thin liquor lignosulfonate and the sulfonated kraft lignin in this case is that the starting pH in this case was 3.9, while it was about 6.4 in the sulfonated kraft lignin. This leads to a lower decrease in pH, but still the final pH is about 1.5 under the final value in the other experiment, leading to the assumption that the pH of the reaction with kraft lignin would most likely have decreased further if the reaction were prolonged.

#### FTIR analysis

The product of the thin liquor electrochemical oxidation was dried and then analyzed via the diamond ATR accessory of the FTIR spectrometer. The resulting spectrum, compared with the unoxidized thin liquor lignin, can be seen in Figure 45:



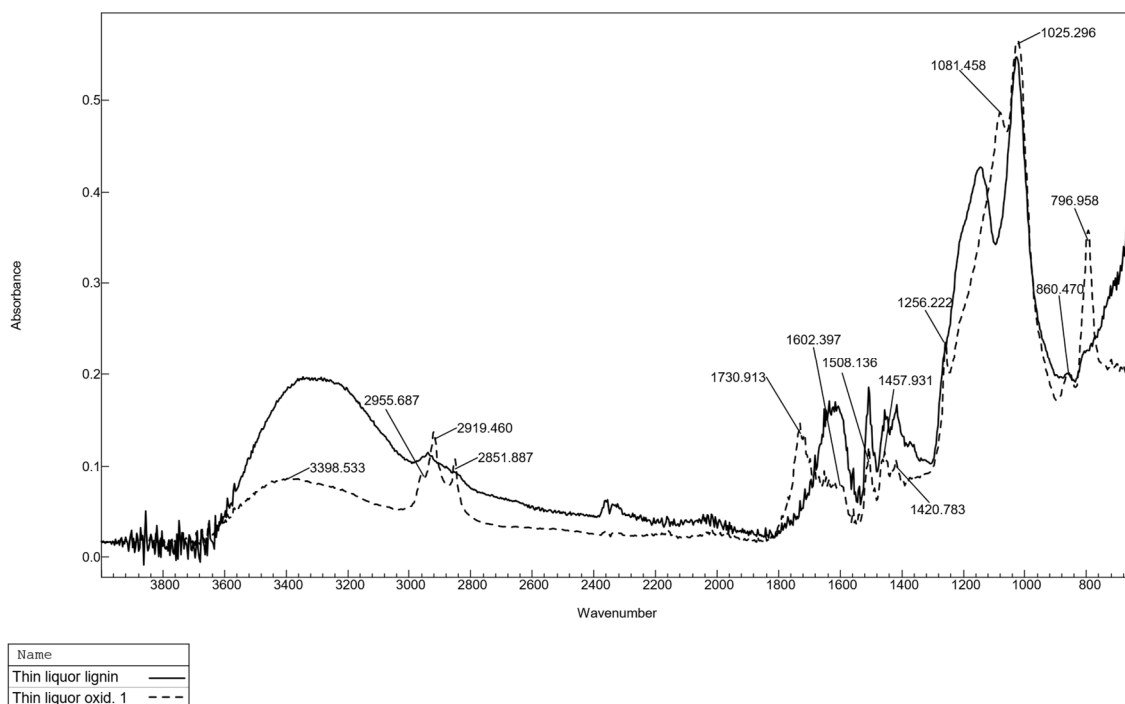


Figure 45: FTIR spectrum of thin liquor, unoxidized and oxidized (V01)

Table 53: FTIR absorption frequencies and assigned vibrations of electrochemically oxidized thin liquor (V01)<sup>102-104</sup>

Wavenumber [cm <sup>-1</sup> ]	Bond	Type	Chemical class
3399	O-H	Stretching	Alcohol/ water
2956	C-H	Stretching	Arene/ alkane
2919	C-H	Stretching	Alkane
2852	C-H	Stretching	Alkane
1731	C-H	Stretching	Aldehyde/ ester
1602	C=C	Stretching	Arene
1508	C=C	Stretching	Arene
1458	C-H	Bending	Alkane
1421	O-H	Bending	Alcohol
1256	C=O	Stretching	Alkyl aryl ether/ aromatic ester
1081	C-O	Stretching	Primary alcohol/ Secondary alcohol/ aliphatic ether
1025	C-O	Stretching	Alkyl aryl ether/ vinyl ether
860	C-H	Bending	Arene (di-, tri- or tetrasubstituted)
797	C-H	Bending	Arene (di- or tri-substituted)

When comparing the spectrum of the oxidized thin liquor with the one of the unoxidized thin liquor, many similarities can be seen, but also some differences:

The broad water peak on the left side of the spectrum has about the same intensity in both spectra, but the arene/alkane vibrations between 2950 and 2850  $\text{cm}^{-1}$  are much more intensive than in the unoxidized spectrum, where only one small peak could be found. The sharp peak at 1731  $\text{cm}^{-1}$ , which can be assigned to ester vibrations, was not found in both the unoxidized thin liquor and the oxidized sulfonated kraft lignin, speaking for a structural difference in this lignin, leading to the formation of ester or aldehyde bonds. The arene, alkane and alcohol vibrations between 1600 and 1400  $\text{cm}^{-1}$  are nearly equivalent to the unoxidized lignin, also regarding the intensity. Instead of the sulfonate vibrations, the oxidized thin liquor only showed alkyl aryl ether vibrations, which may have been superimposed by the broad peak at 1147  $\text{cm}^{-1}$  in the unoxidized spectrum. This may also be true for the C-O stretching at 1081  $\text{cm}^{-1}$ . The highest peaks in both spectra are in the area between 1025 and 1030  $\text{cm}^{-1}$ , which most likely is the C-O stretching of the alkyl aryl ether already discussed. For the arene vibrations under 1000  $\text{cm}^{-1}$ , the same C-H bending can be seen at 860  $\text{cm}^{-1}$ , with a very low intensity for both the unoxidized and oxidized thin liquor. While there was nearly no second arene peak visible in the spectrum before the oxidation, the spectrum after the oxidation showed a strong, sharp peak at 797  $\text{cm}^{-1}$ , like the one found after the oxidation of the sulfonated kraft lignin.

### GC-MS analysis

The following figure shows the comparison of the GC-MS of the unoxidized and the oxidized thin liquor after three hours of oxidation, injected into the GC-MS with water as solvent. There again was nearly no difference between the oxidation product after three and five hours.

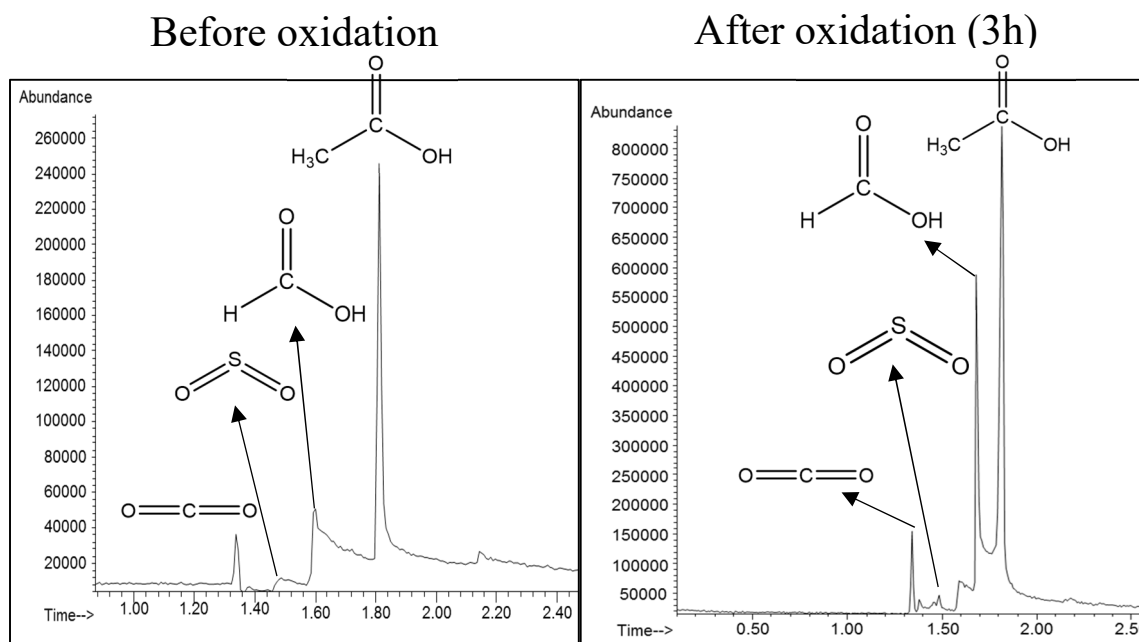


Figure 46: Gas chromatograms of thin liquor, before and after electrochemical oxidation V01 (3h)

What directly can be seen in the chromatogram of the educt is that there are much more compounds visible than in the sulfonated kraft lignin and the alkali lignin. Apart from the  $\text{CO}_2$ , which was found in every educt, and the formic acid, which has also been found in the alkali lignin educt, a very small peak clearly assignable to free sulfur dioxide has been found. Furthermore, a quite high content of acetic acid was already present in the thin liquor educt.

After three hours of oxidation, the amount of acetic acid and formic acid had increased strongly, with the difference in abundance still being about  $2 \cdot 10^5$ . This, like in the other lignins, indicates the process of acetic acid splitting off from the lignin molecule, reacting to formic acid and then to  $\text{CO}_2$ , which gassed out of the reaction reactor. The amount of solved  $\text{CO}_2$  also increased. For the sulfur dioxide, the abundance before and after oxidation is about the same, which could lead to the assumption that this compound did not react during the experiment and no new sulfur dioxide has been split off from the lignin molecule.

### Molecular weight analysis

The molecular weight analysis of the thin liquor before and after oxidation yielded the curves seen in Figure 47.

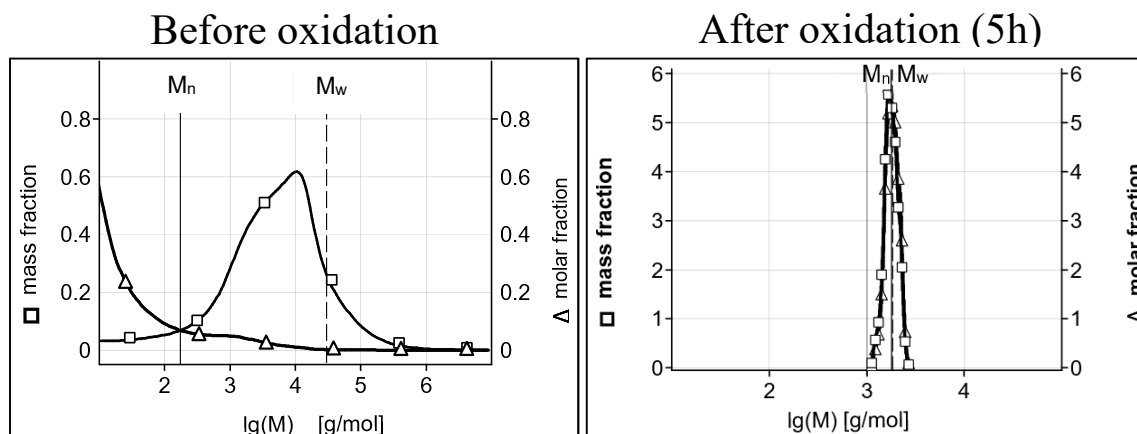


Figure 47: Molecular weight distribution analysis of thin liquor before and after electrochemical oxidation

The mass fraction, reigned by high-molecular compounds, before the oxidation shows a center between molecular weights of 500 and 100,000 g/mol, which is by a factor of ten smaller than the sulfonated kraft lignin, speaking for shorter lignin fragments in this sample than in the commercial lignin, which also was no liginosulfonate but only an alkali lignin with properties like a liginosulfonate. Most of the molar fraction, consisting of low-molecular compounds, can be found under 100 g/mol, again a factor of ten lower than in the sulfonated kraft lignin sample. The  $M_n$  is about 1740 g/mol, while the  $M_w$  is about 29,800 g/mol, both also about a factor ten lower than in the previous analysis. The dispersity  $\mathcal{D}$  in this case is even higher than in the sulfonated kraft lignin with a value of 171, being highly non-uniform. This does not correlate with the literature<sup>1,15,17</sup>, as liginosulfonates are normally associated with higher molecular weights than kraft liginins, but maybe the change in properties in the alkali lignin also includes interconnection of different lignin molecules, thus giving higher molecular weights.

After the oxidation, the molecular weight distribution narrowed, yielding mass fractions and molar fractions between about 1,000 and 2,500 g/mol, which again indicates a shortening of the lignin molecule as a whole. A  $M_n$  of 1780 g/mol and a  $M_w$  of 1830 g/mol yield a dispersity  $\mathcal{D}$  of 1.02, which means that the product of the thin liquor electrochemical oxidation is nearly uniform.

#### 4.4.3.2 Electrochemical oxidation of thin liquor with membrane (V02)

This second experiment with the thin liquor was analogous to the oxidation with membrane of the sulfonated kraft lignin. As catholyte, 10 g/l Na<sub>2</sub>SO<sub>4</sub> in water was prepared, while 20 g/l thin liquor in water, whose conductivity was adjusted to 12.1 mS/cm with Na<sub>2</sub>SO<sub>4</sub>, was used as anolyte. The following table sums up all parameters:

Table 54: Parameters of thin liquor electrochemical oxidation V02

Sample [#]	Time [h]	Temperature (A) [°C]	pH (A)	Conductivity (A) [mS/cm]	Voltage [V]	Current [A]	COD [mg/l O <sub>2</sub> ]
00	0	24.3	3.87	12.1	15.3	1.75	2.03*10 <sup>4</sup>
01	1	24.3	1.5	25.0	10.4	1.75	1.88*10 <sup>4</sup>
02	2	24.4	1.32	33.3	9.4	1.75	1.73*10 <sup>4</sup>
03	3	24.6	1.24	39.1	9.0	1.75	1.54*10 <sup>4</sup>
04	4	24.8	1.15	43.3	8.8	1.75	1.37*10 <sup>4</sup>
05	5	24.8	1.1	46.9	8.6	1.75	1.17*10 <sup>4</sup>

Like in the second experiment from the sulfonated kraft lignin, the voltage shows a big drop of 5 V in the first hour and then decreases by only 2 V in the following four hours. There also is a big change in conductivity visible, which increases from 12 to 25 mS/cm in the first hour and goes up to 47 mS/cm at the end. The change of pH and COD is again depicted in a figure:

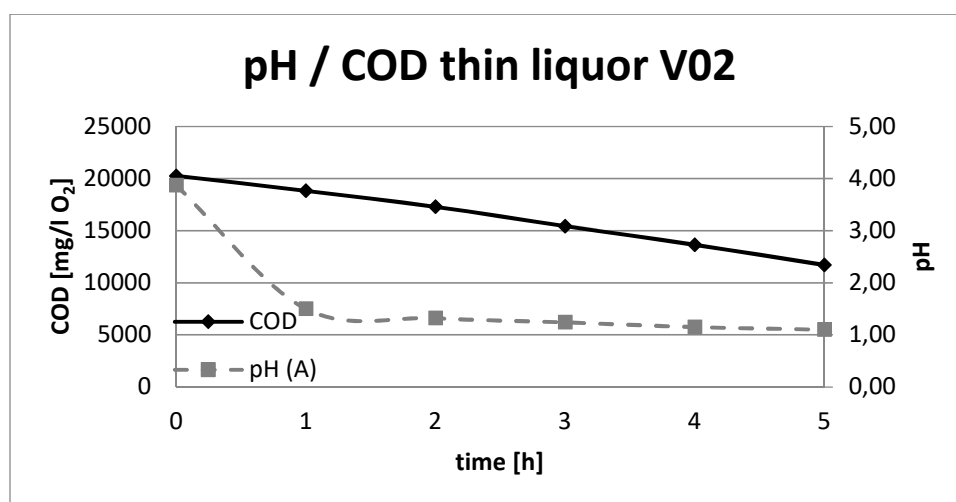


Figure 48: pH and COD change during thin liquor electrochemical oxidation V02

Although the pH was already low at the beginning with a value of nearly 4, it dropped to a similar value as in the membrane oxidation of the sulfonated kraft lignin during the first hour of the reaction. The pH at the end was 1.1, which cannot be described by the potentially formed compounds, but rather by the generated ions during these reactions, which are on the side of the membrane, where the pH was measured.

The decrease in COD again is near the optimal line for waste water treatment, with a decrease of about 8500 mg/l from  $2 \cdot 10^4$  to  $1.2 \cdot 10^4$  mg/l O<sub>2</sub> due to the loss of organic compounds, mainly CO<sub>2</sub>, during the course of the reaction.

### FTIR analysis

Like in the other electrochemical oxidation experiments, the product was dried three days at 90 °C and the dried product then applied on the diamond ATR accessory of the FTIR spectrometer. A comparison of the educt to the product can be seen in the following spectrum:

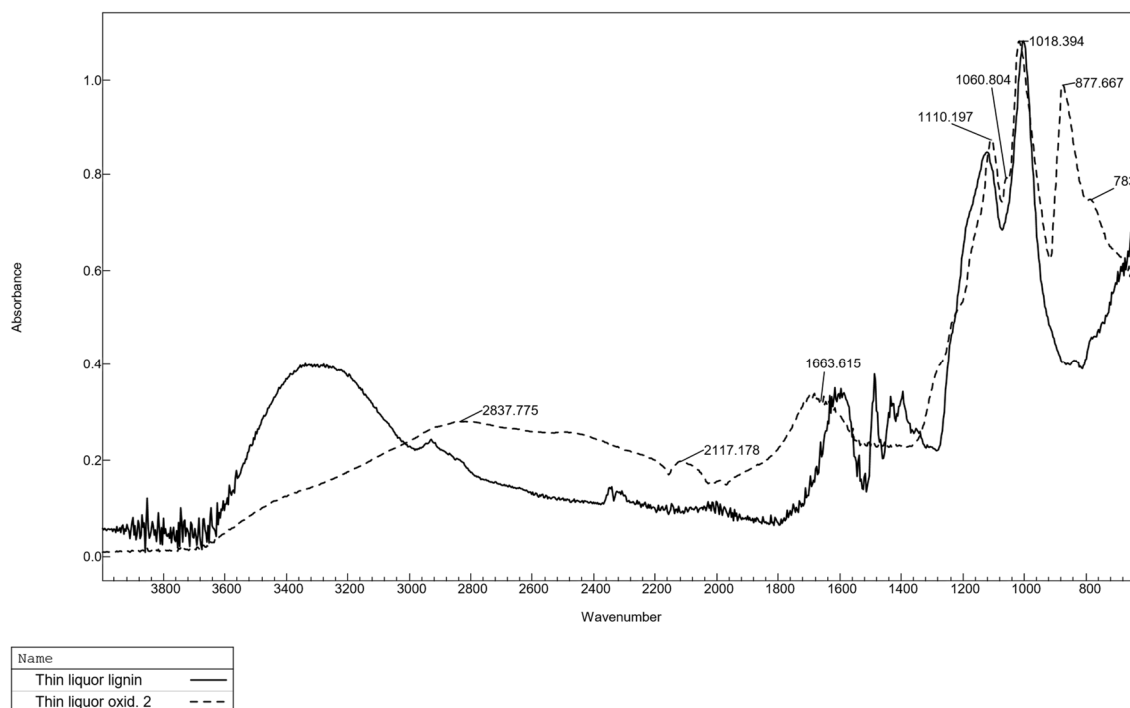


Figure 49: FTIR spectrum of thin liquor, unoxidized and oxidized (V02)

**Table 55: FTIR absorption frequencies and assigned vibrations of electrochemically oxidized thin liquor (V02)<sup>102-104</sup>**

Wavenumber [cm <sup>-1</sup> ]	Bond	Type	Chemical class
2838	O-H	Stretching	Carboxylic acid/ intramolecular bonded alcohol
2117	C≡C	Stretching	Alkyne - Isothiocyanate
~1700	C=O	Stretching	Carboxylic acid/ saturated aldehyde/ saturated ketone
1110	C-O	Stretching	Aliphatic ether/ secondary alcohol
1061	C-O	Stretching	Primary alcohol
1018	C-O	Stretching	Alkyl aryl ether/ vinyl ether
878	C-H	Bending	Arene (di-, tri- or tetrasubstituted)
783	C-H	Bending	Arene (di- or trisubstituted)

The IR spectrum of the oxidized thin liquor shows distinct differences compared to the unoxidized one. Only the two strong peaks between 1018 and 1147 cm<sup>-1</sup> correspond to similar chemical classes. The rest of the spectrum looks nearly like the spectrum of the oxidized sulfonated kraft lignin, with the very broad peak centered at about 2900 cm<sup>-1</sup>, the two smaller peaks afterwards and the broad carboxylic acid peak at around 1700 cm<sup>-1</sup>. In addition, the relative height of the three peaks between 850 and 1150 cm<sup>-1</sup> is the same, with the peak at 1110 cm<sup>-1</sup> being the lowest, the peak at 1018 cm<sup>-1</sup> being the highest and the peak at 878 cm<sup>-1</sup> being in between them. These peaks can therefore be associated to the same or at least similar compounds than in the oxidized kraft lignin.

This all leads to the assumption that either the membrane reaction changes the lignin or some lignin fragments in a typical way, giving very atypical IR spectra, or that some compounds are generated, which overlap with the other, unchanged fragments and thus give such spectra.

**GC-MS analysis**

For this analysis, there was again no difference between the chromatograms after three and five hours, so the following figure shows the comparison between the educt and the product after three hours, which were injected into the GC-MS as taken out of the reaction chamber:

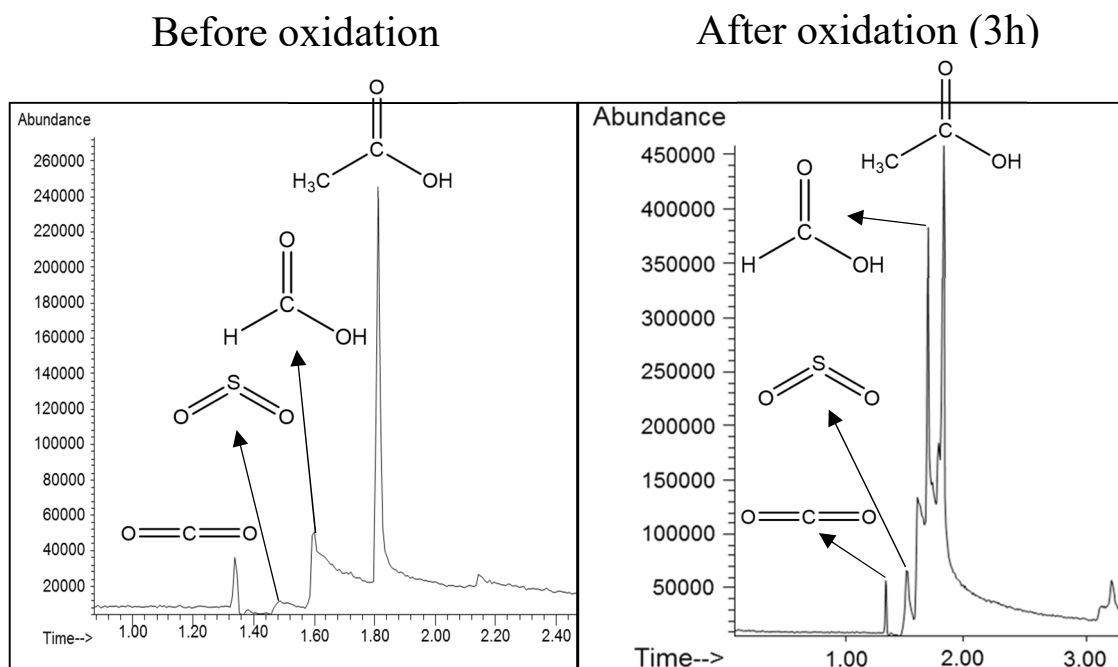


**Figure 50: Gas chromatograms of thin liquor, before and after electrochemical oxidation (3h), V02**

The same compounds as in the first experiment with the thin liquor can also be found after this reaction:  $\text{CO}_2$ ,  $\text{SO}_2$ , formic acid and acetic acid. The only real difference between the GC-MS of the second experiment and the first one is that the  $\text{CO}_2$  peak did not increase and that the increase of formic acid and acetic acid is not as big in this case. Apart from that, the formic acid is again the second largest peak after the oxidation and the peak height of sulfur dioxide did also not change, indicating no reactivity of this moiety.



## 4.5 Reactor reactions

The second method to yield potentially valuable compounds from lignins was a high-pressure reduction at elevated temperatures. The experiments were carried out in a 500 ml reactor from Parr instruments, either as reduction with the usage of hydrogen, which is solely referred to as “reduction” in this chapter, or as a solely thermal reaction, where the inert gas nitrogen was used to avoid any reactions with the gas.

Generally, the experiments were started by filling weighed amounts of one of the three lignin samples and, for the reductions, a NiMo catalyst on kaolin support into the reactor. After that, 100 ml methanol were added as solvent and the reactor was closed per the manufacturer’s instructions. Then, desired amounts of either hydrogen or nitrogen were filled into the reactor. The stirrer was set to 300 rpm for all reactions and then the desired temperature was set for the heater. The reaction started when reaching this temperature.

After three hours, the reactions were stopped and, after cooling down and releasing the gases, the solvent and the remaining solids were transferred into two Erlenmeyer flasks. The solids after the reaction were mixed with methanol and stirred for one hour to extract potential products from them. After filtering off the solids, the methanol phase was mixed with the methanol phase taken from the reactor. The solids, mainly consisting of lignin carbonized due to the drastic conditions, but also unreacted lignin fragments as well as the NiMo catalyst, which is assumed to not have changed during the reaction, were dried at 105 °C for one day and weighed afterwards. The water content of the methanol fraction, filled up to 200 ml with methanol to be able to compare all measurements, was measured via Karl-Fischer titration and then the methanol was evaporated with a rotary evaporator, leaving behind a viscous product, which is called “MeOH soluble oil” in this thesis. The product was weighed and a portion dissolved in methanol to analyze it via GC-MS. When adding up the mass of the solids and of the MeOH soluble oil, the remaining mass to the starting material is referred to as “losses”, containing losses through formed gases during the reactions, which are released after the reaction, as well as losses through transferring during the work-up of the reactions.

The lignin samples used for the reductions were the alkali lignin, the sulfonated kraft lignin and the black liquor lignin. Table 56 and Table 57 sum up the most important parameters and the amounts of starting material, catalyst as well as the product (MeOH soluble oil) of the reductions with hydrogen and the solely thermal reactions, which will be discussed in detail in the following chapters.

Table 56: Summary of lignin reductions with hydrogen

Lignin	Experiment	H <sub>2</sub> pressure [bar]	Temperature [°C]	Starting material [g]	Catalyst [g]	MeOH soluble oil [g]	MeOH soluble oil [%]*
Alkali lignin	V01	99.0	300	10.0	3.04	6.15	61.4
	V02	99.7	250	10.0	3.00	5.59	55.8
	V03	98.6	300	20.0	3.01	13.0	65.2
	V04	80.3	300	10.0	3.00	6.24	62.3
Sulfonated kraft lignin	V07	100	300	10.0	3.01	2.70	27.0
	V08	100	300	4.24	3.01	0.534	12.6
Black liquor lignin	V10	93.0	300	10.0	3.00	3.66	36.6

\* mass/ mass, calculated to starting material

Table 57: Summary of lignin thermal reactions

Lignin	Experiment	N <sub>2</sub> pressure [bar]	Temperature [°C]	Starting material [g]	MeOH soluble oil [g]	MeOH soluble oil [%]*
Alkali lignin	V05	8.6	300	10.0	2.14	21.3
	V06	8.7	300	5.20	0.130	2.49
Sulfonated kraft lignin	V09	8.8	300	10.0	1.09	10.9
	V11	9.2	300	5.02	0.830	16.6
Black liquor lignin	V12	8.8	300	10.0	1.04	10.4

\* mass/ mass, calculated to starting material

## 4.5.1 Reactor reactions of alkali lignin

As the kraft process is the most abundant process for commercial lignin production, the unmodified commercial alkali lignin was first used as sample to get a good overview of the possibilities to produce valuable compounds from lignin waste streams.

### 4.5.1.1 Reductions of alkali lignin with hydrogen

#### Experiment V01

This first experiment was carried out with 10 g of the commercial alkali lignin with about 100 bar H<sub>2</sub> at 300 °C, as this parameters have been found to be promising in previous works with this reactor.<sup>95</sup> The work-up was carried out according to the procedure described before.

Table 58 sums up the most important results of the gravimetric determination of the starting material before the reaction and of the solids, the MeOH soluble oil product and the losses after the reaction. As the catalyst is assumed to have the same mass after the reaction, its mass has been subtracted from the mass of the dried solids, so that the masses of the product add up to the mass of the starting material. The results are shown as absolute masses and as mass/ mass percentages calculated to the starting material.

Table 58: Mass balance of alkali lignin reduction V01

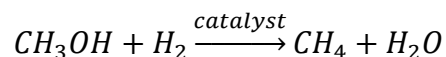
	Mass [g]	Mass/ mass [%]*
<b>Starting material</b>	10.0	100
<b>Solids (without cat.)</b>	1.42	14.1
<b>MeOH soluble oil</b>	6.15	61.4
<b>Losses</b>	2.45	24.5

\*calculated to starting material

This reaction showed a good yield of over 60 % to the oily product. The amount of losses is 25 %, while the amount of solid residues is only 14 %. These solid residues are, according to literature and also its appearance, mainly char generated during the reaction and also a small amount of not reacted lignin or shorter lignin-type fragments.<sup>86,87</sup>

The water content was quite high, with a mean value of 3.64 % in 200 ml of methanol, in which the product was dissolved. As HPLC-grade methanol was used, which only has a water content less than 0.1 %, this fraction can be neglected. Most likely, the water was generated during the reduction reaction and mixed with the solvent methanol.

A possible source for the water is also methanol itself, as it can react in a hydrogenolysis reaction with the hydrogen, as described in the theoretical part of this thesis:



With this, the water content can be used to get an estimate of how much dissolved water has been generated during the reaction, especially to compare it to the other reactions.

As previously stated, the GC-MS analysis of the alkali lignin educt did not show any peaks, except the solvent peak, in this case DMF, at the beginning of the chromatogram. As this was also the case for the sulfonated kraft lignin and the black liquor lignin, the chromatograms of these lignin educts will not be shown further on.

A small portion of the MeOH soluble oil of the first reduction was dissolved in methanol in a GC vial and then analyzed via GC-MS, yielding the following chromatogram:

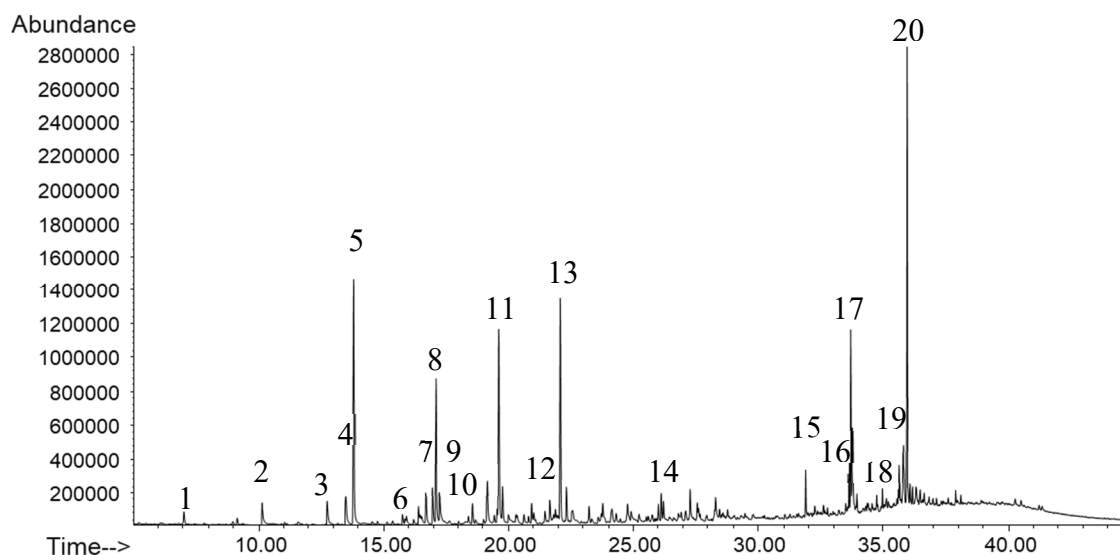


Figure 51: Gas chromatogram of alkali lignin reduction V01

Table 59 shows the identified substances of the GC-MS analysis of the hydrogenated alkali lignin:

Table 59: Identified peaks of the chromatogram (Figure 51)

Peak	Retention time [min]	Substance
1	7.03	Cyclohexanone
2	10.16	Phenol
3	12.75	o-/m-Cresol
4	13.50	p-Cresol
5	13.81	Guaiacol
6	15.77	Veratrole
7	16.97	1,4-Dimethoxy-benzene
8	17.11	4-Methylguaiacol
9	17.24	3,4-Xylenol
10	18.56	4-Methylveratrole
11	19.61	4-Ethylguaiacol
12	21.64	Syringol
13	22.06/22.31	4-Propylguaiacol
14	25.98	2,3,5-Trimethoxytoluene
15	31.86	Hexadecanoic acid methyl ester
16	33.59	Octadecadienoic acid methyl ester
17	33.66/33.72	Octadecenoic acid methyl ester
18	34.70	Methyl-8,15-pimaradien-18-oate
19	35.61/35.78	Dihydroisopimaric acid methyl ester
20	35.92	Dehydroabietic acid methyl ester

Mainly, the chromatogram can be divided into three parts. The first part, from the beginning of the chromatogram to about 22 minutes are the aromatics. The second part are mainly compounds, which could not be unambiguously identified, most likely highly substituted aromatics and aromatic dimers. This part is from about 22 to 31 minutes. The third part, being from 32 minutes to about 40 minutes, consists of fatty acid and resin acid methyl esters.

As already said, the first part comprises several aromatics. Especially interesting in the case of further usage as raw material for chemicals, for example, are the phenolic compounds. Several of these phenols have been found in this chromatogram.

The most interesting of these, because of the relatively high abundances compared to the other compounds, are guaiacol and its methyl, ethyl and propyl substituted derivatives, which can be seen in Figure 52:

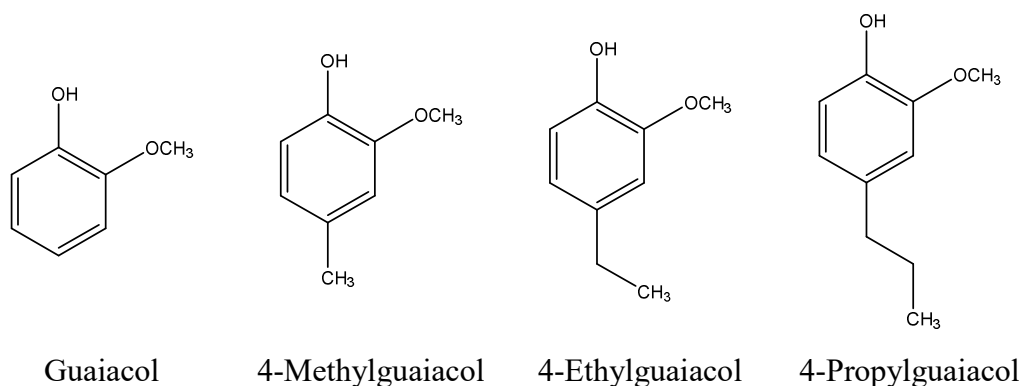


**Figure 52: Chemical structures of guaiacols found after alkali lignin reduction**

As can be clearly seen, these compounds are derived from the G-type monomer of the lignin molecule, coniferyl alcohol, as described in the theoretical part of this work the most abundant monomer in softwood. Thus, the lignin molecule is effectively split at the connections between the monomers, mainly at the  $\beta$ -O-4 motif, and this yields the guaiacols found. Interestingly, the propyl guaiacol showed nearly the same abundance as guaiacol, but a decrease in abundance was noted from the propyl to the ethyl and from the ethyl to the methyl moiety. This could either derive from a higher amount of longer alkane/alkene bonds and a lower amount of medium length alkanes/alkenes in the lignin molecule, leading mainly to propyl guaiacol and guaiacol, from propyl guaiacol groups being split off from the molecule which further react to the other guaiacols and not all the propyl guaiacol reacted or due to the used lignin or catalyst. Either way, this distribution should be noted for further comparison with other experiments and lignins.

In literature, these guaiacol compounds have also been reported: Narani et al.<sup>86</sup> reported GC-MS-FID chromatograms of methanol soluble fractions after hydrogenations at 320 °C with 35 bar H<sub>2</sub> for four hours. Here, guaiacol also showed a slightly lower abundance compared to methyl guaiacol, but in contrast to this work ethyl as well as propyl guaiacol showed the same abundance as guaiacol. Thring and Breau<sup>92</sup> investigated the found compounds at 10 bar H<sub>2</sub> with two different “severities”, meaning reaction time and temperature. At low severity, where the reaction was conducted at 390 °C for 15 minutes, the same amounts of guaiacol and methyl guaiacol were found, while the abundance of the ethyl moiety was far lower. At high severity, with a temperature of 410 °C for 60 minutes, ethyl guaiacol showed a higher abundance than guaiacol, while methyl guaiacol had the lowest abundance. This indicates, that the distribution of the guaiacols is strongly dependent on reaction temperature as well as the time. Olcay<sup>94</sup> found

the guaiacols after hydrogenation of two hardwood lignins at 225 °C for 47 hours with a H<sub>2</sub> pressure of 136 bar. After these harsh conditions, analysis showed the highest amount for propyl guaiacol, followed by methyl and ethyl guaiacol, while guaiacol itself showed the lowest abundance.

As expected, the other aromatics also have many similarities to the lignin monomers, mainly the G-type, but also the H-type (e.g. cresol) and the S-type (syringol).

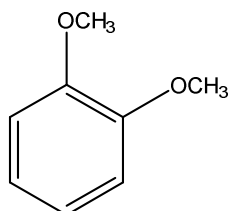


Figure 53: Chemical structure of veratrole

Another example for a compound split off from the lignin molecule is veratrole (Peak 6), whose structure is shown in Figure 53, where also its methyl substituted compound (Peak 10) was found.

All the phenolic compounds found in this spectrum have also been described in literature, as written in chapter 2.6.7 Reduction, the guaiacols also being main products. Interestingly, veratrole and its methyl derivative have not been found in any other literature reference. Thus, the formation of these compounds is most likely mainly due to the used temperature, pressure and time. Another possibility would be that the veratroles were formed due to the specific lignin used in this experiment or other compounds present in the lignin.<sup>86,90,92</sup>

For the second part only one peak, namely trimethoxytoluene, could be identified. As previously stated, the other peaks are also highly substituted aromatics, but these substances could not be unambiguously identified with the available NIST and Wiley libraries.

The third part can also be split into two parts: fatty acid methyl esters from 32 to 34 minutes and resin acid methyl esters from 34 to 40 minutes. Both, the fatty acid and the resin acid methyl esters, are most likely a remainder of resin, which should theoretically be separated from the lignin during the kraft process and is then used for tall oil production. It seems, that certain amounts of these resin and fatty acids were not completely separated from the lignin during lignin precipitation. Interestingly, dehydroabietic acid methyl ester (DHAAME), which can be seen in Figure 54, shows the highest abundance, not only from these compounds but for the whole chromatogram. It is unclear, how such a high amount of dehydroabietic acid methyl ester can be found in

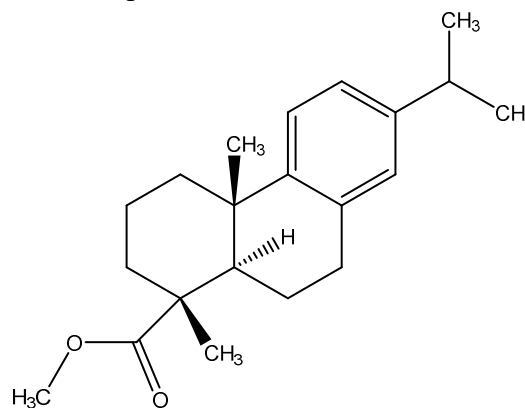


Figure 54: Chemical structure of dehydroabietic acid methyl ester

the lignin, especially after the reduction with hydrogen. One possibility for this would be, that dehydroabietic acid is somehow linked to the lignin, or maybe to oligomers with other resin acids, and that these bonds are broken during the reduction, which makes it possible to see it after the reduction, while not seeing it before. It is also unclear, why it is still found in its dehydrated form after the reduction rather than as abietic acid methyl ester, but it is suspected that this form is somehow energetically/ thermochemically favored after this reaction.

Reportage of dehydroabietic acid methyl ester was only found in one other literature example. Although, it was only reported in a lower quantity and has not been further explained in this reference.<sup>86</sup>

### Experiment V02

The second experiment with the commercial alkali lignin was carried out with the same amount of starting material and the same conditions as the first one, except that the temperature was lowered to 250 °C, to see if that changed the amount and composition of product.

Table 60 shows the mass determination results of the second experiment with alkali lignin:

**Table 60: Mass balance of alkali lignin reduction V02**

	Mass [g]	Mass/ mass [%]*
<b>Starting Material</b>	10.0	100
<b>Solids (without cat.)</b>	2.82	28.1
<b>MeOH soluble oil</b>	5.59	55.8
<b>Losses</b>	1.61	16.1

\*calculated to starting material

The reduction of the temperature to 250 °C led to a doubling of solid residues after the reaction. This further led to a decrease of 5 % of the methanol soluble oil product. As expected due to the lower reaction temperature, the amount of losses during the reaction also went down.

The water content significantly went down from 3.6 % to 1.46 % compared to experiment V01, speaking for less water generated at lower temperatures.

GC-MS analysis showed nearly all the same peaks and distributions. In the first part of the chromatogram, the guaiacols also had the same distribution as in the first experiment.

In the second part, again most of the peaks could not be identified. But except 2,3,5-trimethoxytoluen also a peak at 28.25 minutes could be identified as homovanillic acid, which also has structural similarities to the G-type monomer of the lignin molecule.



The third part also showed mainly the same peaks, with dehydroabietic acid methyl ester being the most prominent of them. However, in contrast to the first reaction, a peak shortly after DHAAME, at 37.89 minutes, with about a fifth of the abundance of dehydroabietic acid methyl ester could be identified as abietic acid methyl ester. This leads to the conclusion that dehydroabietic acid methyl ester is thermochemically preferred at 300 °C so that no abietic acid methyl ester can be seen, while at 250 °C also a certain amount of abietic acid is present.

### Experiment V03

To test the repeatability and linearity during upscaling of the alkali lignin reduction with hydrogen, an experiment with 20 g of alkali lignin, the double amount of experiment V01, and the same parameters as in experiment V01 regarding temperature, time, H<sub>2</sub> pressure and catalyst material, was carried out. The results of this experiment can be seen Table 61:

**Table 61: Mass balance of alkali lignin reduction V03**

	Mass [g]	Mass/ mass [%]*
<b>Starting material</b>	20.0	100
<b>Solids (without cat.)</b>	2.85	14.3
<b>MeOH soluble oil</b>	13.0	65.2
<b>Losses</b>	4.10	20.5

\*calculated to starting material

The expected effect of the doubling of the lignin mass, which were the same percentages in mass balance and water content, occurred. The percentage of the solids is nearly the same, while the amount of the oily product is slightly higher with 65 %, leading to a slightly lower amount of losses, with 21 %, in this reaction. The water content is also in the same range as in the first experiment, with 3.47 % compared to 3.64 %.

Additionally, the chromatogram of the product of this reduction showed the same substances already found in the first experiment, so this will not be once more discussed for this experiment.

To conclude, the doubling of the educt mass yielded about the double amount of product oil, which nearly had the same water content and did also yield the same products in the same distribution, according to GC-MS analysis. This speaks for a good upscale ability of the reduction of this lignin, as it is expected to have similarly good yields in even larger experiments. This also suggests, that methanol is used in excess for the reaction with 10 g, and

mainly also for this reaction, as the reaction showed the same yields with doubled educt, while the amount of methanol was the same as in the previous experiments.

#### Experiment V04

For this experiment, a lower hydrogen amount of 80 bar was used while leaving the other parameters and the amount of starting material the same as in experiment V01, to see if comparable results could be achieved with lower hydrogen consumption. The mass balance of this reaction is shown in Table 62:

**Table 62: Mass balance and of alkali lignin reduction V04**

	<b>Mass [g]</b>	<b>Mass/ mass [%]*</b>
<b>Starting material</b>	10.0	100
<b>Solids (without cat.)</b>	2.07	20.6
<b>MeOH soluble oil</b>	6.24	62.3
<b>Losses</b>	1.71	17.1

\*calculated to starting material

The most important fact is that the amount of oily products is in the same range as in the experiments with 100 bar of hydrogen. A difference can be seen in the amount of solid residues after the reaction, which is about 6 % higher than in the experiment with 20 bar of H<sub>2</sub> more. Thus, the amount of gas losses is at only 17 %.

The water content of the methanol fraction after the reaction was 1.89 %, suggesting that the water content is nearly halved compared to the first experiment, speaking for a lower amount of produced water during this reaction as expected due to the lower amount of hydrogen in the reactor.

The GC-MS measurement also showed no differences to the first experiment with 100 bar, in the substances found as well as in the distribution of these substances.

These results lead to the conclusion, that the reduction of lignin is also efficiently possible at a hydrogen pressure of 80 bar, with only an increased amount of solid residues compared to 100 bar of H<sub>2</sub> pressure, which can most likely be assigned to a higher degree of condensation reactions due to the lower hydrogen amount. Nevertheless, all the following experiments were performed at 100 bar H<sub>2</sub> pressure, to ensure better comparability.

#### 4.5.1.2 Thermal reactions of alkali lignin

To better be able to distinguish the effect of hydrogen and the drastic conditions, experiments were carried out where the reactor was filled with about 9 bar of the inert gas nitrogen, instead of hydrogen. This also dismissed the need for the NiMo catalyst, which was thus not used in this experiments.

##### Experiment V05

In this first solely thermal experiment, 10 g alkali lignin were used while the other parameters were equal to experiment V01. Table 63 sums up the results of this thermal reaction:

Table 63: Mass balance of alkali lignin thermal reaction V05

	Mass [g]	Mass/ mass [%]*
<b>Starting material</b>	10.1	100
<b>Solids</b>	5.20	51.7
<b>MeOH soluble oil</b>	2.14	21.3
<b>Losses</b>	2.71	27.0

\*calculated to starting material

The biggest difference to experiment V01, where hydrogen was used, is the relatively high amount of black, solid char residues recovered after the reaction. This also leads to a comparably low amount of MeOH soluble oil. Due to a high amount of losses (27 %), only 21 % of the initial lignin was converted into the product oil, compared to over 60 % in the same experiment with the usage of hydrogen. This means that the reduction process is far more effective in converting the lignin into the product oil than the thermal reaction, where mostly solid residues can be found.

The results of the water content determination via Karl-Fischer titration, carried out analogous to the previous experiment, led to a mean value of 1.53 %. Thus, the water content is less than half as high as in the experiment with hydrogen. However, this is no surprise, as in this case no hydrogen was used which could react to water, and maybe also the low percentage of product oil could be a factor.

The GC-MS analysis of the oily product showed the following chromatogram:

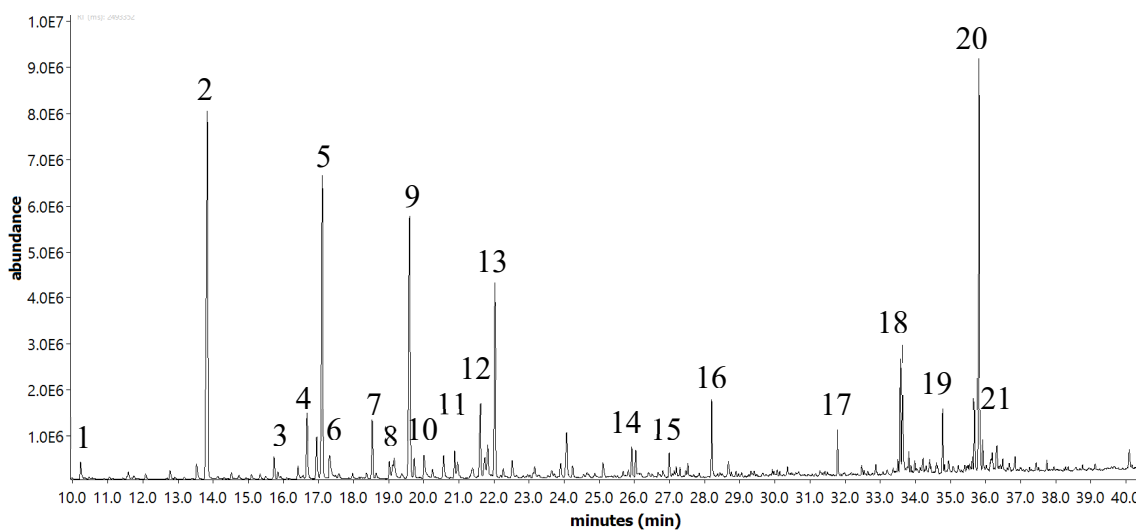


Figure 55: Gas chromatogram of alkali lignin thermal reaction V05

Table 64: Identified peaks of the chromatogram (Figure 55)

Peak	Retention time [min]	Substance
1	10.22	Phenol
2	13.84	Guaiacol
3	15.74	Veratrole
4	16.68	2-Methoxy-6-methylphenol
5	17.11	4-Methylguaiacol
6	17.31	Catechol
7	18.53	4-Methylveratrole
8	19.02	3-Methoxycatechol
9	19.60	4-Ethylguaiacol
10	20.01	4-Methylcatechol
11	20.88	4-Ethylveratrole
12	21.61	Syringol
13	22.03	4-Propylguaiacol
14	25.93	2,3,5-Trimethoxytoluene
15	26.99	Homovanillic acid methyl ester
16	28.20	Homovanillic acid
17	31.78	Hexadecanoic acid methyl ester
18	33.57	Octadecenoic acid methyl ester

19	34.78	Methyl-8,15-pimaradien-18-oate
20	35.82	Dehydroabietic acid methyl ester
21	36.33	Abietic acid methyl ester

The main features of this chromatogram are the same as in the experiment with hydrogen, again being able to identify most of the peaks in the first area up to 22 minutes. The area after this shows various smaller peaks, where only three of them could be identified. The last area, beginning at 32 minutes, again shows mainly fatty acid methyl esters and resin acid methyl esters.

In the area of the aromatics and phenols, only substances with smaller peaks in experiment V01 were not found, like cresol, dimethoxybenzene and 3,4-xylene. Instead of that, a methoxymethylphenol, catechol, substituted benzenediols and a dimethoxybenzene has been found. The other difference in this area is the difference in peak height from guaiacol to propyl guaiacol. Compared to the first experiments with hydrogen, where guaiacol was the highest, its methyl moiety the lowest and then the height increased up to the propyl moiety, in this experiment a decrease in peak height can be seen from guaiacol to methyl guaiacol, then from methyl to ethyl and further from ethyl to propyl guaiacol. It seems, that the thermal reaction leads directly to the simple guaiacol, contrary to the reduction, where still a large amount of propyl guaiacol was found.

In the second part, more peaks could be identified than in the H<sub>2</sub> reduction, namely trimethoxytoluene, also found in the reduction, but also homovanillic acid and its methyl ester.

In the third and final area, again the same substances were found, on one side fatty acid methyl esters and on the other side resin acid methyl esters, whereas dehydroabietic acid methyl ester had the highest peak in the chromatogram. There was also not much difference in the compared peak height between these peaks.

To conclude, the thermal reaction mainly led to the same compounds as the reduction with hydrogen, with only small differences in phenolic and other aromatic compounds found in lower abundances. The most important difference still is the very low product oil yield compared to the reduction, which may have an influence on the mass of this compound found in the product, determined in chapter 4.5.4 Quantification.

**Experiment V06**

As the amount of MeOH soluble oil obtained by the first thermal reaction of alkali lignin (experiment V05) was very low, especially compared to the reduction with hydrogen, the solids recovered after experiment V05, which have been dried afterwards, were used as starting material for this thermal reaction, giving a second similar step to experiment V05. The other parameters were analogous to experiment V05. The mass balance of this second step can be seen in Table 65:

**Table 65: Mass balance of alkali lignin thermal reaction V06 (2<sup>nd</sup> step of V05)**

	<b>Mass [g]</b>	<b>Mass/ mass [%]*</b>
<b>Starting material</b>	5.20	100
<b>Solids</b>	4.74	91.2
<b>MeOH soluble oil</b>	0.130	2.49
<b>Losses</b>	0.329	6.31

\*calculated to starting material

The second thermal reaction yielded over 90 % solid residues, speaking for the generation of char during the first part of the experiment, which could not react in the second experiment. From the 8.8 % of lignin, which were not recovered as solids, more than 6 % can be assigned to losses. Due to that, only 2.5 % of the solids retrieved after experiment V05 could be converted to the methanol-soluble oily product. Due to the low concentration, no peaks could be identified in the GC-MS of the product.

In Table 66, the mass balance of the whole two-step thermal reaction, experiments V05 and V06, can be seen:

**Table 66: Mass balance of alkali lignin thermal reactions V05+V06 (two-step reaction)**

	<b>Mass [g]</b>	<b>Mass/ mass [%]*</b>
<b>Starting material</b>	10.1	100
<b>Solids</b>	4.74	47.1
<b>MeOH soluble oil</b>	2.27	22.6
<b>Losses</b>	3.04	30.3

\*calculated to starting material

The second step of the reaction did not change much in terms of total conversion. The amount of solids went down by only 4 %, still having a value of 47 %. The amount of losses increased

by 3 % to 30 % in total. Only 1 % increase was seen in the product, which now has a percentage of 22.6 %.

Overall it can be said, that a similar second step in thermal treatment has nearly no effect on the outcome of the reaction, as most of the non-converted lignin is already reacting to char in the first step of the reaction, being unable to react in the second step. Due to the doubled amount of time and power needed for this second step and the very bad results of the second step, the future thermal reactions were only carried out in one step.

#### 4.5.2 Reactor reactions of sulfonated kraft lignin

After carrying out the reactions for the commercial alkali lignin, the other commercial lignin, the sulfonated kraft lignin, was used as a sample, as this lignin was modified to have properties like lignosulfonates from the sulfite pulping process, which is the second biggest process in the pulping industry. Thus, the possible production of valuable compounds from this lignin also needed to be addressed.

##### 4.5.2.1 Reductions of sulfonated kraft lignin with hydrogen

###### Experiment V07

This first experiment was carried out with similar parameters than experiment V01 (300 °C, 100 bar H<sub>2</sub>, 3 h) with the only difference being that 10 g of sulfonated kraft lignin were used instead of the alkali lignin. Table 67 shows the mass balance for this reduction:

Table 67: Mass balance of sulfonated kraft lignin reduction V07

	Mass [g]	Mass/ mass [%]*
<b>Starting material</b>	10.0	100
<b>Solids (without cat.)</b>	4.24	42.4
<b>MeOH soluble oil</b>	2.70	27.0
<b>Losses</b>	3.06	30.6

\*calculated to starting material

Interestingly, the amount of solids in this experiment is quite high with 42 %, significantly higher than in experiment V01, where the unchanged alkali lignin was used, and only 10 % lower than the thermal reaction with the alkali lignin. The amount of losses is also quite high with over 30 %, leading to only 27 % of the oily product. The water content, analyzed via Karl-Fischer titration, was also higher than in the alkali lignin, with 4.47 % compared to 3.6 % in the alkali lignin. This could again speak for a low conversion in this reaction.

GC-MS analysis of the product oil in methanol resulted in the following chromatogram:

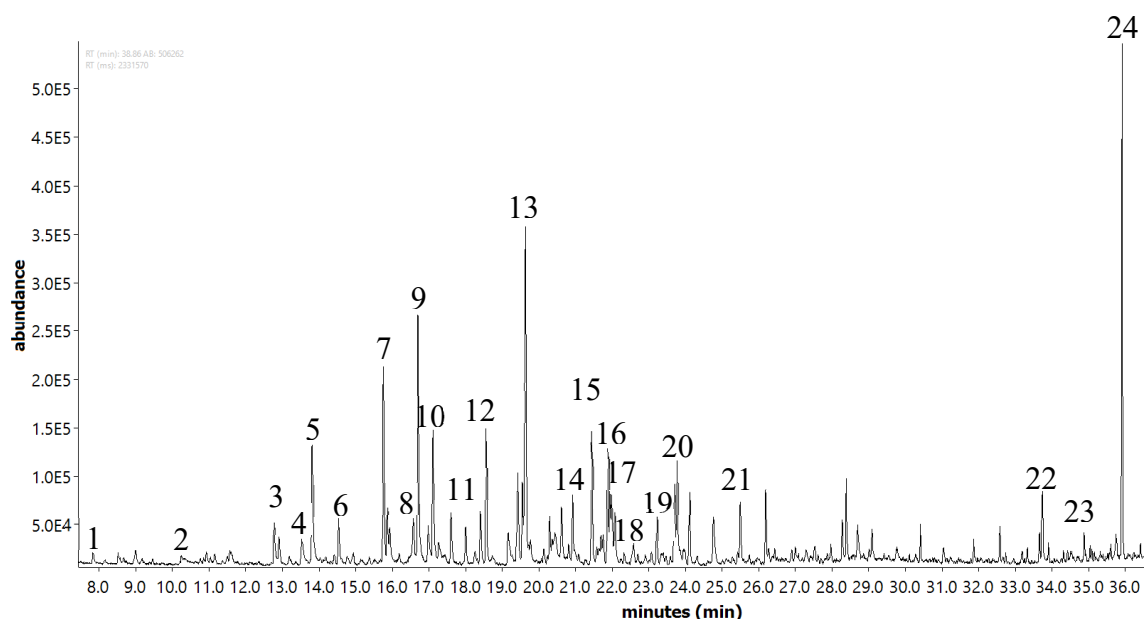


Figure 56: Gas chromatogram of sulfonated kraft lignin reduction V07

Table 68: Identified peaks of the chromatogram (Figure 56)

Peak	Retention time [min]	Substance
1	7.83	Methoxybenzene
2	10.25	Phenol
3	12.76	o-Cresol
4	13.53	p-Cresol
5	13.81	Guaiacol
6	14.54	2,6-Dimethylphenol
7	15.75	Veratrole
8	16.57	2,3-Dimethoxytoluene
9	16.70	4-Methylguaiacol
10	17.12	Methoxymethylphenol
11	17.60/ 18.40	Trimethylphenol
12	18.56	4-Methylveratrole
13	19.63	4-Ethylguaiacol
14	20.92	4-Ethylveratrole
15	21.44	Acetovanillone
16	21.86	Paeonol



17	21.93/ 21.99	Tetramethylphenol
18	22.07	4-Propylguaiacol
19	23.21	4-Propylveratrole
20	23.77	Carvacrol / Thymol
21	25.49	3,4-Dimethoxyacetophenone
22	33.73	7-Isopropyl-1-methyl-1,2,3,4-tetrahydrophenanthrene
23	34.88	Retene
24	35.91	Dehydroabietic acid methyl ester

The GC-MS of the sulfonated kraft lignin reduction products looks completely different from the one of the hydrogenated alkali lignin. The only similarity is the prevalence of most of the identifiable compounds in the area up to 25.5 minutes. After that, no compound could be clearly identified for 8 minutes, and then only three compounds could be identified. Furthermore, there are much more peaks with medium height visible than in the alkali lignin, where some bigger peaks and many small peaks were found.

In the first area from 8 to 25 minutes, as already said, many compounds were found in various intensities. The highest peak in this area can be assigned to 4-ethylguaiacol. But, in contrast to the reduction of alkali lignin with H<sub>2</sub>, where the other guaiacols were in about the same range of abundance, 4-methylguaiacol (Peak 9) had 2/3 and guaiacol (Peak 5) had only half the abundance of ethyl guaiacol. In addition, 4-propylguaiacol (Peak 18) can barely be seen in this chromatogram. Thus, the reduction of this sulfonated kraft lignin preferably split off the G-parts of the lignin molecule as ethyl guaiacol, then as the methyl moiety and guaiacol, but nearly nothing has been split off as the propyl guaiacol. This could also be due to the chemical modification of this lignin to have properties like lignosulfonates, which could have changed the structure of the lignin molecule to have less propyl bonds between the monomeric units, but more ethyl bonds.

The peak with the highest abundance apart from the guaiacols could be identified as veratrole (Peak 7), a dimethoxybenzene, which already was found in the alkali lignin, but with very low abundance. Here again, peaks 12 and 14 show the corresponding methyl and ethyl veratroles in descending abundance according to the length of the side chain. A reason for the detection of veratroles in this lignin, while only a small peak of veratrole was seen in the alkali lignin, could also be the chemical modification of this sulfonated kraft lignin. Another possibility would be

another feedstock of this sulfonated kraft lignin, which would also change the structure of the lignin molecule in different ways, mainly through a prevalence of other monomeric units.

Several conformers can be found in this chromatogram in addition to that. Examples for this would be peaks 3 and 4, two cresols, which also have been found in the alkali lignin. Then there are peaks 9 and 10, two methoxymethylphenols, where the higher peak was assigned to 4-methylguaiacol because of its known prevalence in the lignin molecule as part of the G-monomer. Number 11 shows two peaks, where several trimethylphenol conformers are possible, also valid for the peaks at number 17 for tetramethylphenol. Peaks 15 and 16 show two different hydroxymethoxyacetophenones with nearly the same abundance while at peak 20 carvacrol and thymol, two isopropylmethylphenols, were identified.

In the area between 25.5 and 33.7 minutes, no peak could be unambiguously identified, which also means that no fatty acid methyl esters, which can normally easily be identified due to their characteristic mass spectra, were found after the reduction of the sulfonated kraft lignin. This is a big difference to the alkali lignin, as the fatty acid methyl esters had quite high abundances there.

Except dehydroabietic acid methyl ester, which again represents the highest peak in this chromatogram, no resin acids could be identified after the reduction of sulfonated kraft lignin with H<sub>2</sub>. Instead, the two highest peaks in the area of dehydroabietic acid methyl ester (Peaks 22 and 23) were identified as phenanthrenes, namely retene and its tetrahydro-derivative. These compounds are, just like dehydroabietic acid, diterpenic substances. Retene is part of tar obtained from wood, so this compound was most likely formed due to a pyrolysis reaction in the solely thermal reaction. The structure of the two phenanthrenes can be seen in Figure 57:

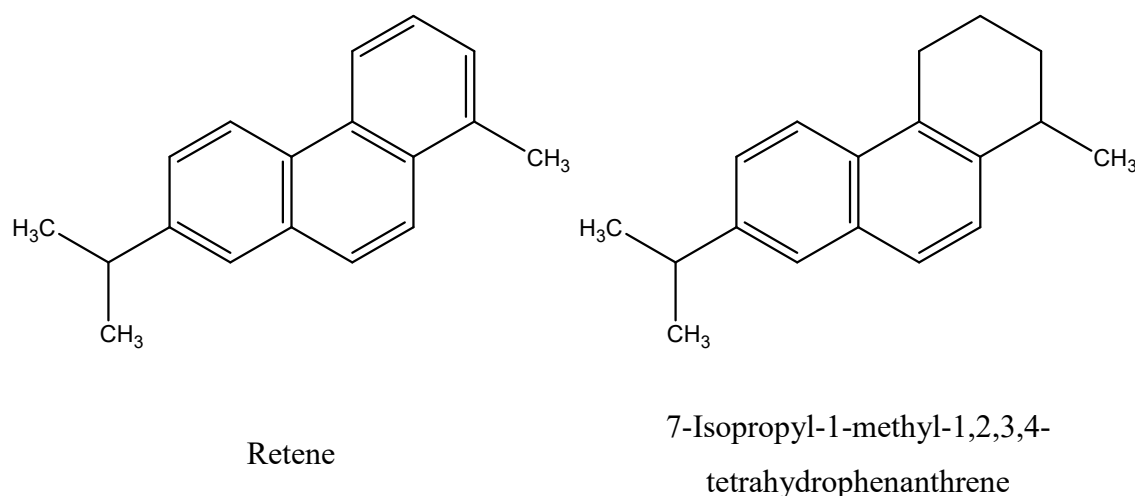


Figure 57: Chemical structures of retene and 7-isopropyl-1-methyl-1,2,3,4-tetrahydrophenanthrene

### Experiment V08

Just like for the thermal reaction of alkali lignin, a second step of the sulfonated kraft lignin reduction with hydrogen, for which the dried solids after experiment V07 were used as starting material, was carried out due to the relatively low conversion compared to alkali lignin reduction with hydrogen. The parameters were analogous to experiment V07 (300 °C, 100 bar H<sub>2</sub>, 3 h). The mass balance of this experiment can be seen in Table 69

**Table 69: Mass balance of sulfonated kraft lignin reduction V08 (2<sup>nd</sup> step of V07)**

	Mass [g]	Mass/ mass [%]*
<b>Starting material</b>	4.24	100
<b>Solids (without cat.)</b>	1.51	35.7
<b>MeOH soluble oil</b>	0.534	12.6
<b>Losses</b>	2.19	51.7

\*calculated to starting material

In this second step, a surprisingly low amount of solid residues after the reaction could be observed with 36 %, indicating that there was still potential for further reduction reactions. Unfortunately, most of the mass after the experiment can be assigned to losses with over 50 %, so that only 13 % of the final mass was oil product. When comparing the GC-MS after the first step and second step, various differences can be seen:

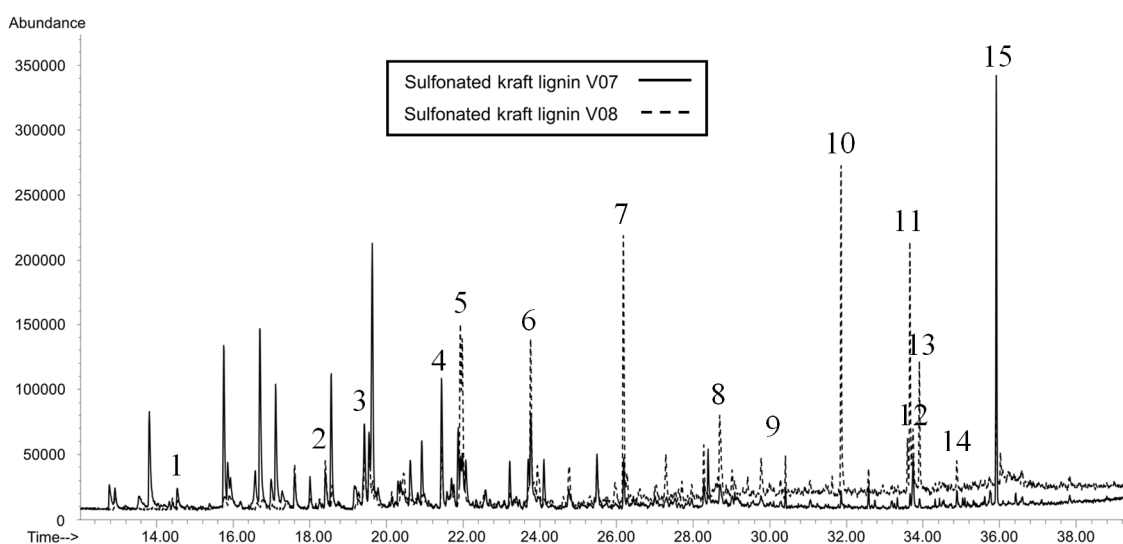


**Figure 58: Gas chromatogram of sulfonated kraft lignin reductions V07 vs V08**

Table 70: Identified peaks of the chromatogram (Figure 58)

Peak	Retention time [min]	Substance
1	14.54	2,6-Dimethylphenol
2	17.60/ 18.40	Trimethylphenols
3	19.43/ 19.55	Trimethylphenols
4	21.44	Acetovanillone
5	21.93/ 21.97	Tetramethylphenols
6	23.76	Carvacrol / Thymol
7	26.18	2-Isopropyl-1-methoxy-4-methylbenzene
8	28.70	1,2-Diethyl-3,4,5,6-tetramethylbenzene
9	30.41	Octadecane
10	31.86	Hexadecanoic acid methyl ester
11	33.60	Octadecadienoic acid methyl ester
12	33.66	Octadecenoic acid methyl ester
13	33.91	Octadecanoic acid methyl ester
14	34.88	Retene
15	35.91	Dehydroabietic acid methyl ester

What really stands out is the lack of most of the compounds in the area up to 22 minutes. In contrast to the product of the first step, no guaiacols were found after the second step and veratroles could not be identified. Several methyl substituted phenols, di- (Peak 1), tri- (Peaks 2 and 3) and tetramethylphenols (Peak 5) were found. A peak of small to medium abundance was identified as acetovanillone, which was also found after the first step. A medium height (peak 6) and a large peak (peak 7) were found between 23 and 26 minutes, being assignable to isopropyl substituted aromatics, namely carvacrol or thymol and isopropylmethoxymethylbenzene. The second compound, which resembled the larger peaks, was not found after the first step, while the first one has already been described after the first step.

Another big difference to the product from the first step is the abundance of fatty acid methyl esters, like the ones already seen after the reduction of alkali lignin. As described there, these fatty acid methyl esters are part of the resin and should normally not be found in lignin. The same can be said again for the resin acid dehydroabietic acid methyl ester. A difference to the alkali lignin can be seen in the height of the peaks, where in this case two fatty acid methyl

esters (Peaks 10 and 11) had even higher abundances than dehydroabietic acid methyl ester, whereas DHAAME was the highest peak after alkali lignin reduction. A similarity to the first step reaction can be seen in retene, which was also found after the second step, while the tetrahydro-derivative has not been found.

The following table now sums up the mass balance for both steps of sulfonated kraft lignin reduction:

**Table 71: Mass balance of sulfonated kraft lignin thermal reactions V07+V08 (two-step reaction)**

	<b>Mass [g]</b>	<b>Mass/ mass [%]*</b>
<b>Starting material</b>	10.0	100
<b>Solids (without cat.)</b>	1.52	15.2
<b>MeOH soluble oil</b>	3.23	32.3
<b>Losses</b>	5.25	52.5

\*calculated to starting material

With the second step of the reaction, the amount of solids recovered after the reaction was reduced from 42 % to only 15 %, which is a value very similar to the reduction of alkali lignin. Unfortunately, this step only increased the product yield by about 5 % to 32%, while the amount of losses increased to over 50 %.

This leads to the main conclusion, that the second step of the reaction is not necessary, as most of the remaining lignin is only converted into gases and cannot be recovered as product oil. The lack of phenols in the product also leads to this implication, meaning that most likely the main part of the phenols had already been extracted during the first step of the reaction. Instead, mainly higher substituted aromatics and phenols have been extracted in the second step of the reduction. The reason for this could be the preferred prevalence of condensation reactions in this second step compared to depolymerizations in the first step, where condensation products could serve as “initiators”.

The main fraction of the product of the second step are fatty acid methyl esters, which have not been found after the first step, interestingly. When looking at the alkali lignin reduction, one step with three hours was sufficient to find these compounds.

Thus, it looks like that firstly the phenols and aromatics, which can be split off from the lignin molecule, are extracted in the reduction of the sulfonated kraft lignin, while the higher-molecular-mass compounds, except DHAAME, are extracted afterwards. This might also be

true for the alkali lignin, but if that was the case, the extraction of fatty acid methyl esters and DHAAME had already begun.

#### 4.5.2.2 Thermal reaction of sulfonated kraft lignin

Although the solely thermal reactions of the alkali lignin (experiments V05 and V06) did not yield promising results, a thermal reaction with sulfonated kraft lignin was carried out to be able to compare possible differences or similarities between these reactions

##### Experiment V09

Just like in the first thermal reaction of alkali lignin, a temperature of 300 °C was used for a duration of three hours, while the N<sub>2</sub> pressure was again about 9 bar. The mass balance of the thermal reaction of 10 g sulfonated kraft lignin can be seen in Table 72:

Table 72: Mass balance of sulfonated kraft lignin thermal reaction V09

	Mass [g]	Mass/ mass [%]*
<b>Starting material</b>	10.0	
<b>Solids</b>	6.34	63.4
<b>MeOH soluble oil</b>	1.09	10.9
<b>Losses</b>	2.57	25.7

\*calculated to starting material

With a percentage of 63 % solid residues, the thermal reaction of sulfonated kraft lignin yielded even more solids than the thermal reaction of alkali lignin. The amount of losses is again in the same range between 25 and 30 %, like in the previous experiments. With this, only 11 % of the methanol soluble product were recovered, which is only half of what has been found after the thermal reaction of alkali lignin, making this reaction even more unsatisfactory yield-wise. On the other hand, the water content was with 1.56 % nearly the same as after the thermal reaction of alkali lignin, speaking for a similar result than with the alkali lignin, despite the low yield.

In the figure below, you can see the GC-MS of the product of the sulfonated kraft lignin thermal reaction:

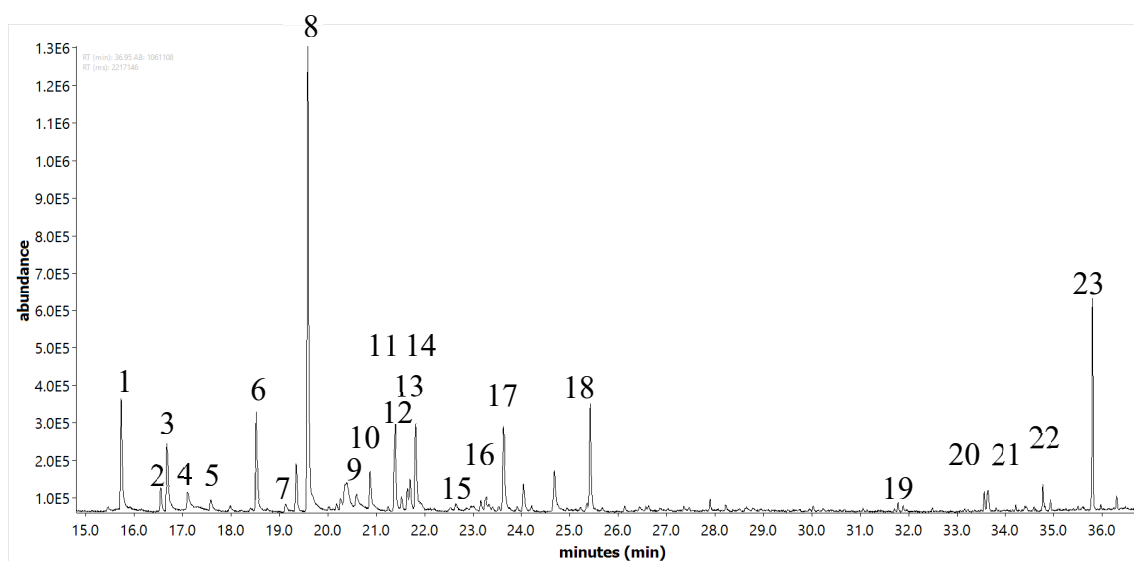


Figure 59: Gas chromatogram of sulfonated kraft lignin thermal reaction V09

Table 73: Identified peaks of the chromatogram (Figure 59)

Peak	Retention time [min]	Substance
1	15.73	Veratrole
2	16.55	2,3-Dimethoxytoluene
3	16.67	4-Methylguaiacol
4	17.11	Methoxymethylphenol
5	17.58	Trimethylphenol
6	18.52	4-Methylveratrole
7	19.14	2,5-Dimethoxytoluene
8	19.60	4-Ethylguaiacol
9	20.60	Dihydroxyacetophenone
10	20.88	4-Ethylveratrole
11	21.38	Acetovanillone
12	21.52	1-(Hydroxymethoxyphenyl)ethanone
13	21.70	1-(Hydroxymethoxyphenyl)ethanone
14	21.81	1-(Hydroxymethoxyphenyl)ethanone
15	22.64	1-(Hydroxymethoxyphenyl)ethanone
16	23.16	4-Propylveratrole

17	23.63	Methoxytrimethylphenol
18	25.42	3-tert-Butyl-4-hydroxyanisol
19	31.78	Hexadecanoic acid methyl ester
20	33.56	Octadecenoic acid methyl ester
21	33.64	7-Isopropyl-1-methyl-1,2,3,4-tetrahydrophenanthrene
22	34.77	Retene
23	35.79	Dehydroabietic acid methyl ester

Mostly, the same phenolic and aromatic compounds as after the reduction of the sulfonated kraft lignin and the thermal reaction of alkali lignin have been found. However, there are again differences in the relative abundances.

The highest peak, even higher than dehydroabietic acid methyl ester, can be assigned to 4-ethylguaiacol (Peak 8). The abundances of the other found guaiacol, methyl guaiacol (peak 3), are very low compared to ethyl guaiacol, so it seems that this reaction extracted the ethyl derivative quite selectively. Guaiacol itself and propyl guaiacol could not be found after this reaction. Other phenols found in lower abundances include another methoxymethylphenol, acetovanillone, and other hydroxymethoxyphenylethanones in various conformations and a methoxytrimethylphenol.

There have also been other aromatics identified after the thermal reaction, the most prominent of them being veratrole and its methyl, ethyl and propyl moieties (Peaks 1, 6, 10 and 16). Whereas the methyl veratrole has nearly the same abundance as veratrole, speaking for a similar concentration of these two substances, the height decreases with ethyl veratrole and is only very low for propyl veratrole. This speaks for the splitting off from units with shorter chains than with longer ones.

Interestingly, one of the two isomeric forms of the antioxidant butylated hydroxyanisole has been found after the thermal reaction of the sulfonated kraft lignin. It is unclear, why this substance has been found for the first time after this reaction and not in the reduction of the same lignin. As BHA is a synthetic compound and not a natural one and it is unlikely that the BHA was synthesized during the thermal reaction by lignin parts due to the complex nature of this compound, this substance is most likely a contaminant. The blank measurement of the solvent did not show any signs of BHA, meaning that BHA was not present in the methanol. Also, the measurement was repeated in other GC-MS vials, again showing the BHA peak. Other samples and blanks measured before and after this sample did not show any sign of a peak at



about 25.4 minutes, so a contamination in the GC-MS can also be excluded. Thus, it is unclear when and where the contamination could have happened.

In the area over 30 minutes, two fatty acid methyl esters already seen in various chromatograms can be seen, for example in the second step of the reduction or the alkali lignin thermal reaction. But in this case, also both phenanthrenes, which were identified after the first step of the reduction of this lignin, could also be seen. The highest peak in this area can again be assigned to dehydroabietic acid methyl ester.

### 4.5.3 Reactor reactions of black liquor lignin

After the reactions with the two commercial samples, the lignin precipitated from the black liquor from Zellstoff Pöls was used to see if there is a difference in yield and products between it and the commercial lignins.

#### 4.5.3.1 Reduction of black liquor lignin with hydrogen

##### Experiment V10

Here again, the same parameters as in experiments V01 and V07 were used with a temperature of 300 °C and about 100 bar H<sub>2</sub> pressure, with a relatively high amount of hydrogen lost during the reaction due to a small leakage in the graphite gasket. Reaction time was three hours, with 10 g of black liquor lignin sample and usage of the NiMo catalyst. The yield of this reaction can be seen in Table 74:

Table 74: Mass balance of black liquor lignin reduction V10

	Mass [g]	Mass/ mass [%]*
<b>Starting material</b>	10.0	100
<b>Solids (without cat.)</b>	3.57	35.7
<b>MeOH soluble oil</b>	3.66	36.6
<b>Losses</b>	2.77	27.7

\*calculated to starting material

The solids content after this reduction is lower than the one after the first step of the sulfonated kraft lignin reduction, but it is still 20 % higher than the amount of solid residues after the reduction of alkali lignin. This means, that the alkali lignin by far yields the lowest amount of these solid residues, while the black liquor lignin yields more than two and the sulfonated kraft lignin more than three times more of these solid residues.

When looking at the MeOH soluble oil, it makes up 36.6 % of the total mass after reduction, calculated to the starting material. This is again 10 % higher than in the reduction of the

sulfonated kraft lignin, while the yield is 25 % lower than the amount in the alkali lignin, which is due to the relatively high number of solid residues in the black liquor lignin.

The total losses are with 27 % in the same range as in all the reactor reactions and in between the alkali and the sulfonated kraft lignin.

The water content of the methanol phase before evaporating the solvent was again measured via Karl-Fischer titration, resulting in a mean value of 2.06 %. Thus, the water content of the product oil in 200 ml methanol is comparably lower than in the other reduction experiments with hydrogen with the same parameters, being 1.6 % lower than the one of alkali and even 2.5 % lower than the one of sulfonated kraft lignin. With that, the water content is more in the range of the reduction experiments of alkali lignin, where a lower temperature and a lower hydrogen pressure were used, which could also be an effect of the slightly lower hydrogen pressure in this experiment, with only 93 bar H<sub>2</sub> compared to 100 bar in the other experiments.

The results of the GC-MS analysis can be seen in the chromatogram below:

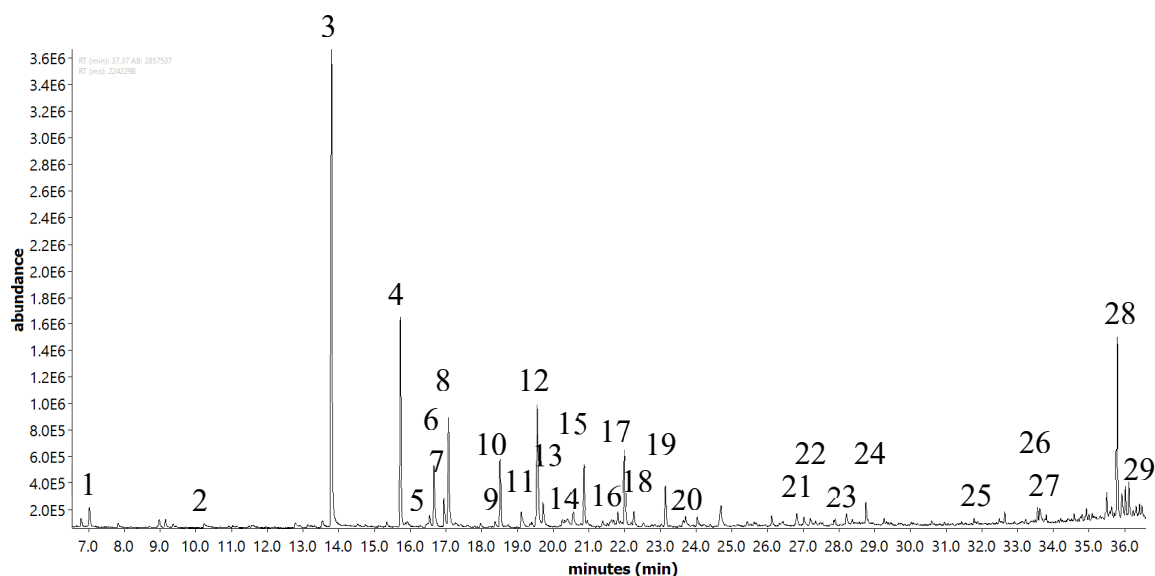


Figure 60: Gas chromatogram of black liquor lignin reduction V10

Table 75: Identified peaks of the chromatogram (Figure 60)

Peak	Retention time [min]	Substance
1	7.02	Cyclohexanone
2	10.23	Phenol
3	13.80	Guaiacol
4	15.73	Veratrole
5	16.54	Dimethoxytoluene
6	16.60	2-Methoxy-3-methylphenol
7	16.94	1,4-Dimethoxybenzene
8	17.07	4-Methylguaiacol
9	18.37	Trimethylphenol
10	18.51	4-Methylveratrole
11	19.11	2,5-Dimethoxytoluene
12	19.56	4-Ethylguaiacol
13	19.72	Ethylmethoxyphenol
14	20.25	3,4-Dihydroxyacetophenone
15	20.86	4-Ethylveratrole
16	21.81	4-Ethyl-2-methoxy-6-methylphenol
17	22.00	4-Propylguaiacol
18	22.26	Propylmethoxyphenol
19	23.14	4-Propylveratrole
20	23.70	Carvacrol/ Thymol
21	26.82	3,4-Dimethoxyacetophenone
22	27.02	3,4-Dimethoxyphenylacetone
23	28.20	Homovanillic acid
24	28.76	3-(3,4-Dimethoxyphenyl)-1-propanol
25	31.78	Hexadecanoic acid methyl ester
26	33.56	Octadecenoic acid methyl ester
27	33.81	Octadecanoic acid methyl ester
28	35.80	Dehydroabietic acid methyl ester
29	36.24	Abietic acid methyl ester

It was possible to identify 20 compounds in the area up to 24 minutes, which is as much as in the sulfonated kraft lignin and more than what was found in the alkali lignin. This area of the

chromatogram shows only compounds previously identified in the reactions with alkali lignin and sulfonated kraft lignin. The main peaks again show the guaiacols and the veratroles already described in the previous chapters. The peak with the highest abundance in this case is guaiacol itself (peak 3), being about 4 times higher than methyl and ethyl guaiacol (peaks 8 and 12), which have about the same abundance. Propyl guaiacol shows an even lower abundance than these.

The same can be said about the veratroles: Veratrole (peak 4) showed a much higher abundance than methyl and ethyl veratrole (peaks 10 and 15), while propyl veratrole (peak 19) had an even lower abundance.

The only other peak with an abundance higher than  $2.0 \cdot 10^5$  is another methoxymethylphenol (peak 6), a conformer of methyl guaiacol.

Interestingly, 4 peaks could be identified from 26.8 to 28.8 minutes. Two of these compounds have already been identified in the previous reductions, namely 3,4-dimethoxyacetophenone (peak 21) in the reduction of sulfonated kraft lignin and homovanillic acid (peak 23) in two reactions of the alkali lignin. The first one is structurally related to veratrole, having two methoxy substituents, while the second is related to guaiacol, with the hydroxyl group adjacent to the methoxy group. The other two compounds, 3,4-dimethoxyacetophenone (peak 22) and 3-(3,4-dimethoxyphenyl)-1-propanol (peak 24), the highest peak of the four, are also structurally related to veratrole.

The next three peaks (25 to 27) again show fatty acid methyl esters, most likely from the resin. However, compared to the other reduction reactions, especially the reduction of alkali lignin, the abundance of these peaks is low compared to the aromatic compounds in the first part of the chromatogram. This effect may be comparable to the one observed in the reduction of sulfonated kraft lignin, where a low amount of fatty acid methyl esters was found after the first step, but a much higher amount after the second step. A second step of this reaction might as well lead to a product rich in fatty acid methyl esters and resin acids, but short in aromatics.

At the end of the chromatogram, again dehydroabietic acid methyl ester has been found, like in every reactor reaction. This time, it showed a comparably low abundance, being only the second highest peak in this chromatogram. In addition, another resin acid derivative, abietic acid methyl ester, was identified shortly after the peak of DHAAME, but with much lower abundance than dehydroabietic acid methyl ester.

#### 4.5.3.2 Thermal reactions of black liquor lignin

Finally, thermal reactions of the black liquor lignin were carried out to be able to compare it to the results of the alkali and sulfonated kraft lignins.

##### Experiment V11

The first thermal reaction of black liquor lignin was carried out with only 5 g of starting material, due to the fact that the black liquor lignin used in this experiment was from the first experiment, which did not yield enough lignin for the usage of 10 g starting material. The parameters were again analogous to the thermal reactions of alkali lignin (experiment V05) and sulfonated kraft lignin (experiment V09), with a N<sub>2</sub> pressure of 9.2 bar. The mass balance of this experiment is shown in Table 76:

Table 76: Mass balance of black liquor lignin thermal reaction V11

	Mass [g]	Mass/ mass [%]*
<b>Starting material</b>	5.02	100
<b>Solids</b>	3.36	67.0
<b>MeOH soluble oil</b>	0.83	16.6
<b>Losses</b>	0.82	16.4

\*calculated to starting material

Due to the reduced amount of educt used, this reaction is not comparable to the other thermal reactions. Nevertheless, the thermal reaction of the first precipitated black liquor lignin showed yields comparable to the other thermal reactions, especially like the one of sulfonated kraft lignin. In this case, the amount of solid residues is even higher with 67 %. The amount of the product oil is lower than from the alkali lignin, but higher than in the thermal reaction of sulfonated kraft lignin, while the amount of losses is the lowest with only 16 %. The water content is also a little bit lower with 0.94 %, but this could also be due to the lower amount of educt used.

As GC-MS analysis of this experiment showed the same results than the next one, experiment V12, the chromatogram will not be shown here and the compounds will be discussed in experiment V12, which had a better comparability due to the same amount of sample used than in the other thermal reactions.

**Experiment V12**

As mentioned above, the second thermal reaction of black liquor lignin was carried out with 10 g of the second precipitation to get a better comparability to the thermal reactions of the alkali and sulfonated kraft lignins. Apart from that, the experiment was analogous to the previous one. The results of the thermal reaction can be seen in Table 77.

**Table 77: Mass balance of black liquor lignin thermal reaction V12**

	<b>Mass [g]</b>	<b>Mass/ mass [%]*</b>
<b>Starting material</b>	10.0	100
<b>Solids</b>	6.91	68.9
<b>MeOH soluble oil</b>	1.04	10.4
<b>Losses</b>	2.08	20.7

\*calculated to starting material

The solids content of the thermal reaction of the second black liquor lignin is nearly the same as in the previous experiment, when looking at the percentage calculated to the starting material. With this, it had the highest content of solid residues of all the experiments carried out. The remaining 31 % consisted of 2/3 losses, with 21 %, while only 1/3 of the converted lignin could be distributed to the MeOH soluble oil. Due to that, the total yield is as low as in the sulfonated kraft lignin with only about 10 %, which should again be subject to further investigations.

The water content is 1.61 %, which is only 0.08 % and 0.05 % higher than the ones of alkali and sulfonated kraft lignin thermal reactions, speaking for the same conversion in terms of water bound in the methanol during the reaction.

As last step, again GC-MS analysis was carried out, which yielded the following chromatogram:

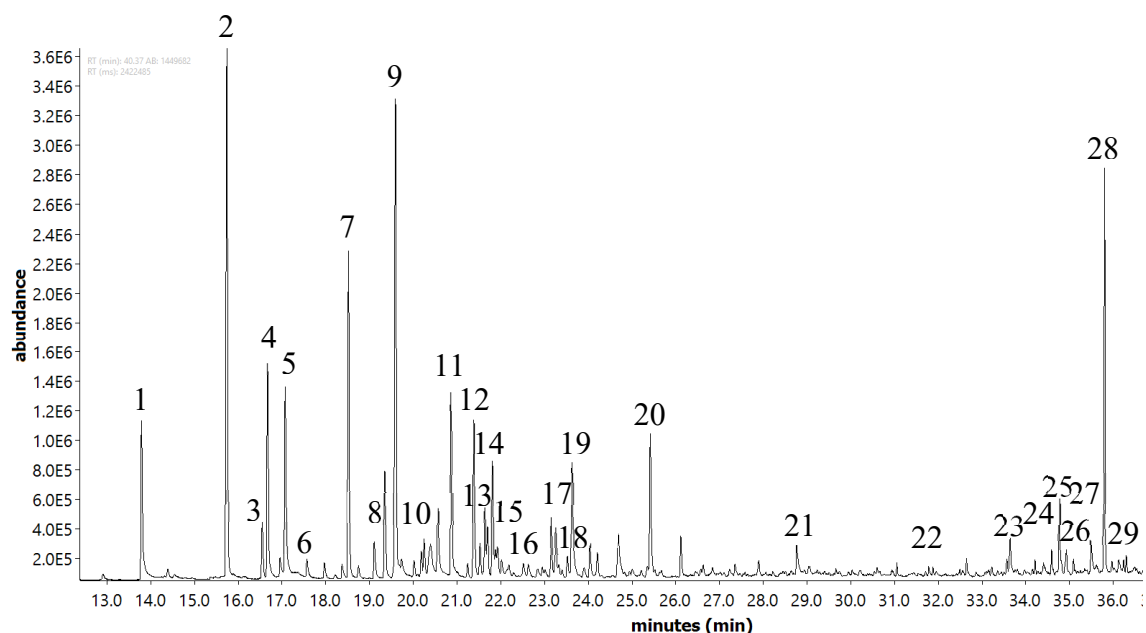


Figure 61: Gas chromatogram of black liquor lignin thermal reaction V12

Table 78: Identified peaks of the chromatogram (Figure 61)

Peak	Retention time [min]	Substance
1	13.79	Guaiacol
2	15.73	Veratrole
3	16.54	2,3-Dimethoxytoluene
4	16.67	Methoxymethylphenol
5	17.08	4-Methylguaiacol
6	17.57	Trimethylphenol
7	18.51	4-Methylveratrole
8	19.11	2,5-Dimethoxytoluene
9	19.60	4-Ethylguaiacol
10	20.24	2,5-Dimethoxytoluene
11	20.87	4-Ethylveratrole
12	21.38	Acetovanillone
13	21.52	3,4-Dimethoxyacetophenone
14	21.64/ 21.69/ 21.81	1-(Hydroxymethoxyphenyl)ethanones
15	21.88/ 21.93	Tetramethylphenols

16	22.63	1-(Hydroxymethoxyphenyl)ethanone
17	23.15	4-Propylveratrole
18	23.53	2,5-Dimethoxyacetophenone
19	23.64	Methoxytrimethylphenol
20	25.42	3-tert-Butyl-4-hydroxyanisol
21	28.76	3-(3,4-Dimethoxyphenyl)-1-propanol
22	31.78	Hexadecanoic acid methyl ester
23	33.64	7-Isopropyl-1-methyl-1,2,3,4-tetrahydrophenanthrene
24	34.59	Methyl-8,15-pimaradien-18-oate
25	34.77	Retene
26	34.92	Isodextropimaric acid methyl ester
27	35.50	Methyl isopimarate
28	35.80	Dehydroabietic acid methyl ester
29	36.24	Abietic acid methyl ester

Again, nearly 20 compounds could be identified in the area up to 20 minutes, where mostly phenols and other aromatics can be found. In this area, most of the prominent peaks can again be assigned to guaiacols and veratroles.

After this reaction, veratrole had the highest abundance (peak 2). This is surprising, as in all the previous reactions one of the four found guaiacols had a higher abundance than the highest veratrole. Methyl veratrole (peak 7) only shows 2/3 of the height of the veratrole peak, but still is the third highest peak in this chromatogram. Then the abundance is halved from the methyl to the ethyl veratrole (peak 11), which itself has about double the height of propyl veratrole (peak 17). But compared to the other reactor reactions, also the veratroles with longer side chain have high abundances, maybe indicating a high amount of these units in the precipitated lignin, or at least a preferred extraction of these compounds in the thermal reaction of this lignin

The second highest peak can be identified as ethyl guaiacol (peak 9). This phenolic compound has more than twice abundance than guaiacol (peak 1) and methyl guaiacol (peak 5), which have about the same abundance. Propyl guaiacol could not be identified in this chromatogram. An interesting detail in this area is the slightly larger peak directly next to methyl guaiacol, which is another methoxymethylphenol, thus a conformer of methyl guaiacol. This is the major difference to the other chromatograms, where a guaiacol had the highest abundance in this area every time. In other chromatograms, other substituted methoxyphenols were also found, but by



far not with a comparable abundance than the corresponding guaiacols, meaning that the guaiacols were the favored conformers. In this case, at least for methyl guaiacol, the two conformers each make up about 50% in this reaction. Compared to that, the veratrole peaks showed no conformers.

Two compounds with higher abundances are also acetovanillone (peak 12) and a methoxytrimethylphenol (peak 19), which were both already identified in comparable abundances in previous reactions.

Like in the thermal reaction of the sulfonated kraft lignin, a peak at about 25.5 minutes was identified as BHA (peak 20). As already discussed after the thermal reaction of the sulfonated kraft lignin, it is unlikely that this compound had formed during the reaction. With the finding in this sample, it is also unlikely that the BHA was introduced through a contamination of the lignin, as the sources are completely different ones, with the black liquor lignin being derived from Pöls directly and the sulfonated kraft lignin from Sigma Aldrich. As the solvent, the GC-MS vials and the GC-MS itself were already excluded after the thermal reaction of sulfonated kraft lignin, only a contamination of the reactor would be possible, but while the reduction of the black liquor lignin (experiment V10) was carried out directly after these two reactions, with no major cleaning run in between them, no BHA was found there. The only two possibilities in this case would be a low amount of BHA in the reactor, which is unlikely when looking at the quite high abundances in the two thermal reactions, or that the reduction with hydrogen altered BHA, so that it was not found after this reaction. In either case, it is questionable how the BHA was introduced into the reactor if this was the case

Looking at the area over 30 minutes, only one fatty acid methyl ester (peak 22) was found, while much more resin acid methyl esters were found compared to the other reactions (peaks 24, 26-29). Of these, isodextropimaric acid methyl ester and methyl isopimarate have not been identified in previous experiments. Also, retene and its tetrahydro-derivative have again been found (peaks 25 and 23). DHAAME was also found and again showed the highest abundance in this region.

#### 4.5.4 Quantification

As reasonable amounts of dehydroabietic acid methyl ester as well as phenols have been found after the reactor reactions of the three tested lignins, the amount of these compounds has been quantified.

#### 4.5.4.1 Dehydroabietic acid methyl ester

For DHAAME, which was surprisingly found in all the reactions with high abundances, the quantification was carried out with cholesterol as internal standard, due to the structural similarity of these substances with its condensed ring structures:

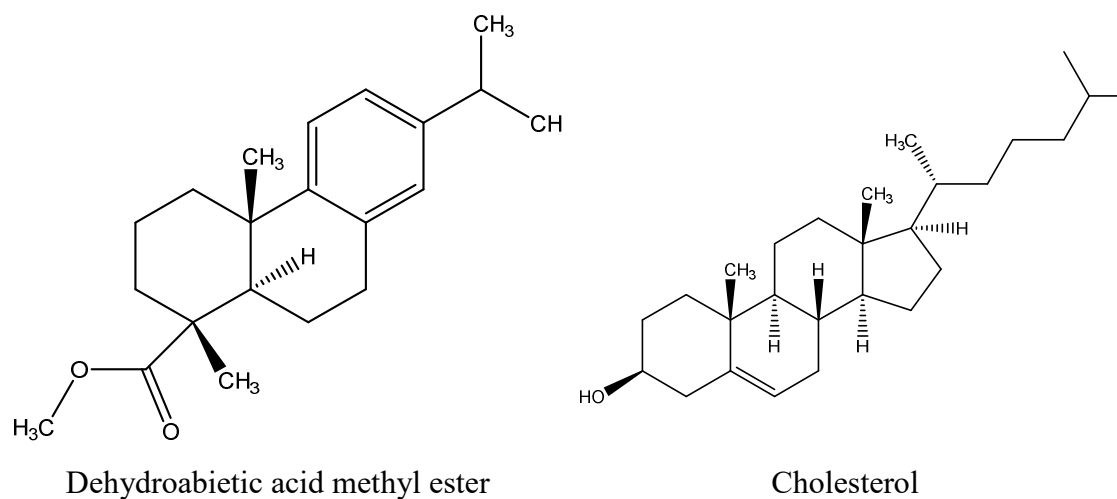


Figure 62: Chemical structures of dehydroabietic acid methyl ester and cholesterol

As the principle of GC-MS analysis was the same for all samples, only one example of a chromatogram after GC-MS analysis of the quantification mixtures will be shown:

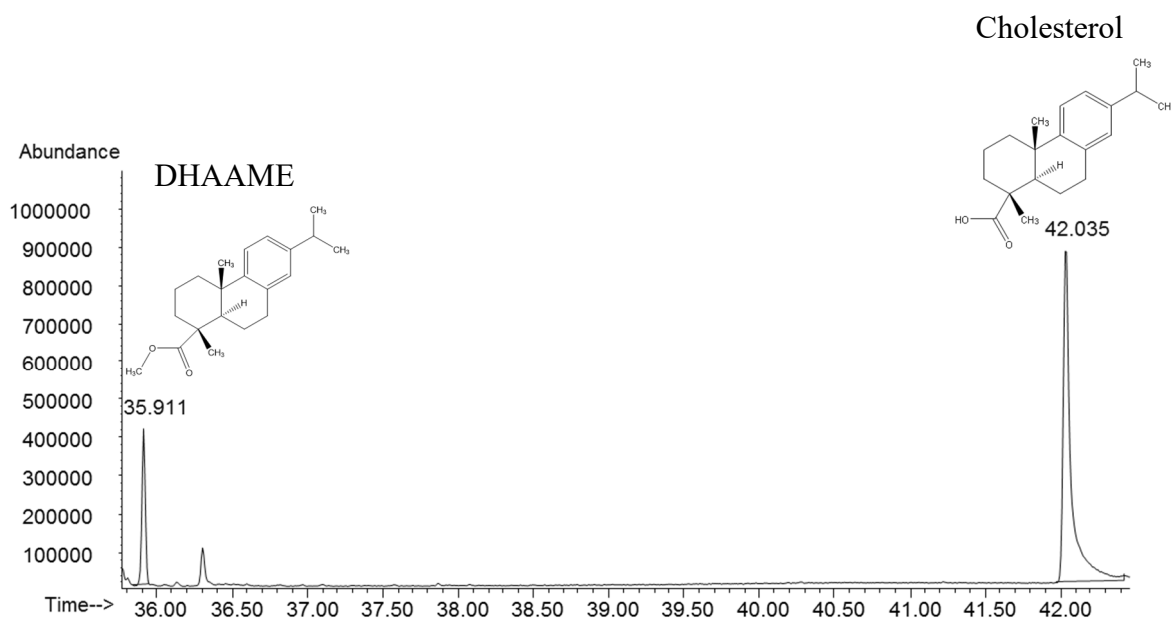


Figure 63: Gas chromatogram of DHAAME quantification

From this chromatogram, the peak areas of DHAAME and cholesterol were determined with the GC-Software. From the peak areas, the masses of cholesterol and sample and the response factor, the amount of DHAAME in the MeOH soluble oil could be determined:

$$DHAAME_{MeOH\ soluble\ oil}[\%] = \frac{peak\ area_{DHAAME}}{peak\ area_{cholesterol}} * \frac{mass_{cholesterol}[g]}{mass_{sample}[g]} * RF * 100\%$$

The response factor RF is needed to be able to quantify DHAAME via GC-MS by accounting for differences between DHAAME and cholesterol. The response factor was determined by a colleague by analyzing a calibration series of 0.005–1 g/l abietic acid, which is structurally very similar to DHAAME, in acetone via GC-MS and using the formula for the response factor ( $RF_i = \frac{C_i}{A_i}$ )<sup>50</sup> to calculate the response factors for all concentrations. BHT and cholesterol in concentrations of 0.1 g/l were used as internal standards to verify these values. Thereby, the mean value for abietic acid was calculated to be 7.46, which was used as response factor for all quantifications. Though, as the factor was determined afterwards, this value and thus the percentages calculated for DHAAME can only be seen as a rough estimation rather than the exact amounts of dehydroabietic acid methyl ester present in the samples, as it cannot be assumed that the instrument parameters were constant over this time frame.

As the amount in the product oil was known, it was possible to calculate the amount of DHAAME to the educt lignin with the amount of MeOH soluble oil after the reaction in percent, calculated to the starting material.

$$DHAAME_{lignin}[\%] = DHAAME_{MeOH\ soluble\ oil}[\%] * \frac{mass/mass_{MeOH\ soluble\ oil}[\%]}{100\%}$$

For the black liquor lignin, the amount of DHAAME in the initial black liquor was calculated with the yield of the lignin precipitation:

$$DHAAME_{black\ liquor}[\%] = DHAAME_{lignin}[\%] * \frac{yield_{lignin\ precipitation}[\%]}{100\%}$$

Table 79 sums up the results of dehydroabietic acid methyl ester quantification, calculated on the product oil, the lignin educt and, for the black liquor lignin, on the black liquor itself.

Table 79: Results of dehydroabietic acid methyl ester quantification

Lignin	Experiment*	Mass <sub>lignin</sub> [g]	DHAAME <sub>MeOH</sub>	DHAAME	DHAAME
			soluble oil [%]	lignin [%]	black liquor [%]
Alkali lignin	V01 (reduction)	10	11.6	7.16	–
	V03 (reduction)	20	9.55	6.19	–
	V05 (thermal)	10	30.0	6.41	–
Sulfonated kraft lignin	V07 (reduction)	10	11.9	3.21	–
	V09 (thermal)	10	11.2	1.19	–
Black liquor lignin	V10 (reduction)	10	7.53	2.76	0.15
	V11 (thermal)	5	14.8	2.46	0.22
	V12 (thermal)	10	14.0	1.42	0.07

\* all experiments were carried out for 3 h at 300 °C with 100 ml methanol; reductions used ~100 bar H<sub>2</sub> and 3 g catalyst; thermal reactions used ~9 bar N<sub>2</sub>

A large variance in the results can be observed, as the amount of DHAAME extracted from the corresponding lignins is between 1.19 % and 7.16 %, depending on the lignin used and the type of reaction.

The highest yields in terms of dehydroabietic acid methyl ester could be achieved with the alkali lignin, with 7.16 %, 6.19 % and 6.41 %. The reduction of 10 g of alkali lignin can be identified as the most effective reaction, meaning it was possible to extract the highest amount of dehydroabietic acid methyl ester out of this lignin educt. It does not represent the real amount of dehydroabietic acid methyl ester in the alkali lignin, as it was not possible to identify DHAAME in the educt and quantify it. Thus, the extraction yield cannot be determined. Interestingly, the thermal reaction with the same amount of sample had only about 0.7 % less dehydroabietic acid methyl ester content to the lignin than the reduction reaction, so the extraction efficiency seems equal for both reactions. The much higher percentage of DHAAME in the methanol soluble oil after the thermal reaction can be explained by the much lower yield of the thermal reaction coupled with a comparable amount of dehydroabietic acid methyl ester in both. Therefore, the extraction is, in this case, not highly depending on the yield. From the alkali lignins, the lowest amount of DHAAME was found after the reduction with 20 g of sample, when looking at the yield to the educt. The experiment with 20 g of sample yielded a lower amount of DHAAME in the oil than of the 10 g reduction, which is surprising as nearly

the same chromatogram was found in GC-MS analysis. This could be due to a slightly different DHAAME content in the part of the sample taken in this case or just a normal deviation due to the reduction with hydrogen, yielding slightly different amounts of the found compounds in every reaction, which could only be proven by doing more reactions with the same parameters.

Due to the comparatively low amount of conversion into the oily product, the percentage of DHAAME in the oil after sulfonated kraft lignin reduction is nearly the same as in the alkali lignin, but when looking at the percentage calculated to the lignin, the sulfonated kraft lignin reduction was only able to extract half the amount of dehydroabietic acid methyl ester. One possibility is that this reduction is not only less proficient in terms of yield, but also in terms of DHAAME extraction efficiency. The other possibility would be a much lower total amount of dehydroabietic acid methyl ester in the sulfonated kraft lignin, but that cannot be validated due to the inability to characterize the educt for DHAAME. The amount of dehydroabietic acid methyl ester in the product of the thermal reaction is even lower, with only 11.2 %. This result is also consistent with the observation, that DHAAME was not the largest peak in the chromatogram. Calculated on the educt, sulfonated kraft lignin, this only yields to a percentage of 1.19 %. This means, that the thermal reaction is less efficient in extracting dehydroabietic acid methyl ester than the reduction in the sulfonated kraft lignin.

For the black liquor lignin, the percentage in the product oil is 4 % lower than the one of the sulfonated kraft lignin and alkali lignin, but when looking at the percentage in the lignin educt, they are nearly the same due to the much higher yield of the black liquor lignin reduction than the one of sulfonated kraft lignin. Due to the very low precipitation yield of below 5 %, the amount of DHAAME extracted only makes up 0.15 % of the initial black liquor. The other two reactions were both solely thermal reactions, and they both yielded nearly the same amount of dehydroabietic acid methyl ester, with 14.8 and 14.0 %, respectively. However, calculated to the educt, the percentage of DHAAME in experiment V11 is 1 % higher than the one of experiment V12. The reason for this is that experiment V11 had a much lower product yield than experiment V12. A similar effect can be seen in the calculation to the black liquor. Here, experiment V11 had even a higher percentage than the reduction in experiment V10, which is the case because of the different precipitation yields. For experiment V11, the first lignin precipitated from the black liquor was used, which had a precipitation yield of nearly 10 %. Compared to that, the second precipitation only yielded below 5 %.

To sum up, the alkali lignin showed the highest contents in DHAAME extracted from it. Here, the thermal reaction yielded about the same amount as the reduction. This was not the case in

the other two lignins, where the thermal reactions with the same parameters yielded less than half of the reduction reactions. In addition, the percentages of both reduction and thermal reactions are nearly the same when comparing these two lignins.

#### 4.5.4.2 Phenolic compounds

For the quantification of phenolic compounds, BHT was used as internal standard, due to its phenolic structure but still being positioned after the phenolic compounds in the chromatogram and its synthetic nature, not being abundant in nature.

Figure 64 shows an example for a chromatogram taken during this quantification:

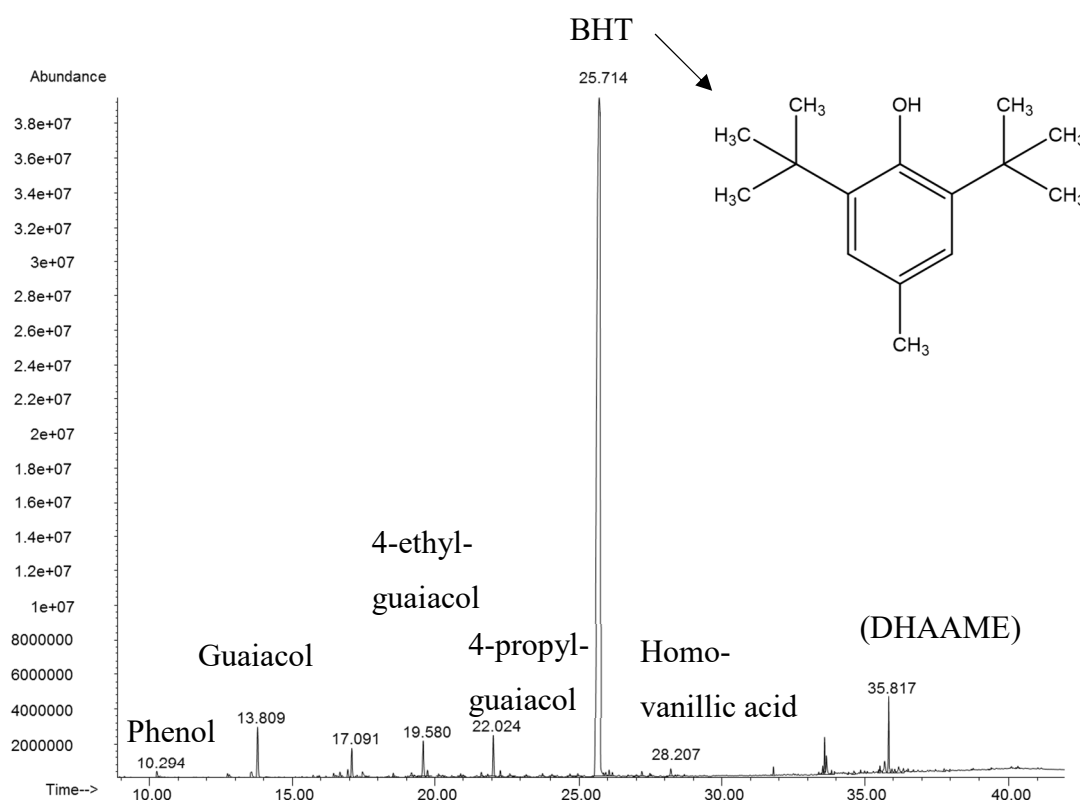


Figure 64: Gas chromatogram of quantification of phenolic compounds

In principal, the quantification of phenolic compounds is the same as the one of dehydroabietic acid methyl ester, using the same equations as in the last chapter. The only difference, apart from the usage of BHT instead of cholesterol, is that not only one, but many compounds had to be quantified. This was done by quantifying each single phenolic compound which was identifiable, meaning that the same equations described above were used. To consider the differences between BHT and the compounds, response factors had to be determined for the most important and abundant phenolic compounds. This was done by a colleague by analyzing calibration series of eight phenolic compounds in the range of 0.005–1 g/l in THF and calculating the response factors for each compound as it has already been described for

dehydroabietic acid methyl ester. BHT in a concentration of 0.1 g/l was used as internal standard to verify the calculated values. The response factors of the eight phenolic compounds are summed up in Table 80. Compounds similar in structure and/ or fragmentation to the ones in the table were assumed to have the same response factor. For example, ethyl- and propylguaiacol were adjusted with the same response factor than methyl guaiacol.

**Table 80: Determined response factors for several phenolic compounds**

Compound	Response factor
Acetovanillone	2.07
Catechol	5.65
Eugenol	2.06
Guaiacol	2.74
Homovanillic acid	2.71
Isoeugenol	2.24
Methyl guaiacol	2.21
Vanillin	2.50

As already stated in the previous chapter, these values as well as the percentages of phenols calculated below are rather rough estimations than the exact amounts present in the sample due to the possible and probable change of instrument parameters between the measurements of the samples and the response factors.

After quantifying every identifiable phenolic compound, the amount of them was added up to get the total amount of phenols in the sample, which will be represented in the table below:

**Table 81: Results of phenolic compounds quantification**

Experiment*	Mass <sub>lignin</sub>	Phenols <sub>MeOH</sub>	Phenols <sub>lignin</sub>	Phenols <sub>black</sub>	
	[g]	soluble oil [%]	[%]	liquor [%]	
<b>Alkali lignin</b>	<b>V01 (reduction)</b>	10	27.38	16.81	–
	<b>V03 (reduction)</b>	20	18.73	12.22	–
	<b>V05 (thermal)</b>	10	46.70	9.94	–
<b>Sulfonated kraft lignin</b>	<b>V07 (reduction)</b>	10	2.65	0.72	–
	<b>V09 (thermal)</b>	10	17.23	1.88	–
<b>Black liquor lignin</b>	<b>V10 (reduction)</b>	10	16.78	6.13	0.27
	<b>V11 (thermal)</b>	5	12.06	2.00	0.19
	<b>V12 (thermal)</b>	10	18.91	1.96	0.09

\* all experiments were carried out for 3 h at 300 °C with 100 ml methanol; reductions used ~100 bar H<sub>2</sub> and 3 g catalyst; thermal reactions used ~9 bar N<sub>2</sub>

A very high variation of values can be seen in the percentages of phenols in the lignin, ranging from only 0.72 % in the sulfonated kraft lignin reduction to 16.81 % in the alkali lignin reduction.

In the alkali lignin, a clear order in terms of percentage to the lignin educt can be seen: the reduction with 10 g yielded more than the reduction with 20 g and the thermal reaction had the lowest yield. The first reduction showed over 27 % of the product oil. When calculating the percentage in the lignin educt, 16.81 % can be assigned to phenolic compounds, which is the most for all reactions. The reduction reaction with 20 g of educt yielded 8.6 % and 4.6 % lower percentages in the oil and the lignin, respectively, due to the higher amount of educt used. The thermal reaction had only a percentage of 9.9 % on the lignin. The very high percentage in the oil, nearly 50 %, is due to the much lower amount of product oil recovered after the thermal reaction compared to the two reduction reactions, leading to accumulation of phenols in this low amount of oil.

The reduction of the sulfonated kraft lignin showed only 0.72 % phenols on the lignin educt, less than what was found in DHAAME in this sample. The main reasons for this are firstly the low overall yield and secondly the quite high amount of different substances after this reaction, most of them not being phenolic but other aromatic compounds or not identifiable. The thermal reaction of sulfonated kraft lignin yielded nearly 8 % less phenols, calculated to the lignin educt, than what was found after the thermal reaction of alkali lignin, making this lignin much less attractive in terms of further experiments for phenols extraction.

In contrast to the sulfonated kraft lignin, the black liquor lignin showed the same trend as the alkali lignin: the amount of phenols is higher in the product of the reduction than in the ones of the thermal reactions. Concerning the amount of phenols in the MeOH soluble oil, the black liquor lignin reduction product is in between the alkali and the sulfonated kraft lignin, which can also be seen when looking at the yield on the lignin. The yield calculated on the black liquor is only 0.27 %, meaning there are various other compounds present in the black liquor and only a small amount can be assigned to extractable phenols and DHAAME. The two thermal reactions showed a widely differing percentage of phenols in the product oil with 12 and 19 %. Due to the lower product yield in experiment V12, only a difference of 0.04 % in the amount of phenols on the lignin can be reported. The other great difference is also due to the precipitation yield, which was higher in the first precipitation and thus the amount of extracted phenols from the black liquors are 0.19 % in this case, higher than the other thermal reaction but lower than the reduction. This also means, that an increase in precipitation yield can increase



the percentage calculated on the black liquor, which increases the need for a more efficient precipitation method of the black liquor lignin.

The phenol contents found in literature correlate well with the ones from the reduction experiments described in this thesis. Narani et. al.<sup>86</sup> described phenol contents in the methanol soluble oil of Indulin AT lignin, a purified kraft pine lignin, of 8 % to 21.5 %, depending on the catalysts used. There were different catalysts used in this work, mostly sulfided ones and no solely thermal reactions were carried out, which makes them difficult to compare as the percentage in the oil is highly dependent on the yield. But there was also a sulfided NiMo catalyst on activated charcoal used, which is the most similar one to the NiMo catalyst used in this thesis. The comparison to the results of experiment V01 showed a much higher phenols content of the alkali lignin from Sigma-Aldrich, with 27 % compared to only 10 % in the paper of Narani, while the oil yield was only 4 % lower. Another difference is the amount of guaiacols in the oil: In the work of Narani, only up to 7 % guaiacols were found in the product oil, while a total of 15 % was found with experiment V01. The reason for this could be the difference in hydrogen pressure (100 bar vs. 35 bar H<sub>2</sub>) and time (3 h vs. 8 h). The black liquor lignin reduction showed a slightly lower oil yield as in the paper, but the reduction as well as the thermal reactions correlate very well to the values in this paper. Though, for the thermal reactions a much lower yield can be seen, with only 10 % and 16 % compared to 40 % to 80 % in the mentioned paper.

A second paper, which very well described the phenol contents after lignin reduction, but this time calculated in percentage to the dry lignin educt, is the one by Oasmaa et al.<sup>90</sup> Here, two pine kraft lignins were hydrogenated and a 1:1 mixture of a NiMo catalyst on aluminosilica and Cr<sub>2</sub>O<sub>3</sub> on alumina were used. Again, a very good correlation with the result of the reduction of the black liquor lignin can be seen, as total phenol contents of 5.3 % and 7.4 % are described by Oasmaa. These are nearly the same values like in the mentioned reduction, where a phenols content of about 6 % is reported. This is interesting, as a slightly different catalyst and parameters were used, with an equal hydrogen pressure of 100 bar but a reaction temperature of 395 °C and a reaction time of only 40 minutes. At the same time, the values found in the alkali lignin reductions are much higher than in this paper, with 16.8 % and 12.2 % found in experiments V01 and V02, which is about three times higher than the value reported by Oasmaa for experiment V01 and two times higher for experiment V02. The guaiacols were not separately quantified in this paper.

In summary, a high amount of phenolic compounds, up to 16.81% of the lignin educt, could be extracted, especially in the alkali lignin. Thus, the alkali lignin reduction seems to be the best

combination to extract phenols from lignins from the different feedstocks and reactor conditions tested in this thesis. Further research will be necessary to on one side increase the yield of phenols even further by adjusting hydrogen pressure, temperature and time. On the other side, it is necessary to extract the phenols from the product oil and separate them to be able to use these compounds as they are or to produce other, higher value products.

The black liquor lignin also showed promising yields of up to 6.13 % in the reduction reaction. The most important step in this case is, apart from adjusting pressure, temperature and time for optimal conditions, to find more convenient and effective methods for the precipitation of the lignin from the black liquor. This increases the amount of phenols extractable in the reduction reaction and thus the percentage of phenols extracted when calculating to the black liquor.

The sulfonated kraft lignin showed the worst amount of phenolic compounds, thus the commercial alkali lignin should be preferred over the commercial sulfonated kraft lignin for this application.

## 5 Conclusions and Outlook

The first aim of this thesis, the characterization of the different lignin feedstocks, was carried out with various techniques. The solubility of all lignins was as expected, as for the lignosulfonate samples complete solubility could be observed in aqueous solutions throughout the whole pH range. The kraft lignins were solely soluble in alkaline and some organic solvents, like dioxane, DMF and ethylene glycol, while all lignins were soluble in DMSO. FTIR spectroscopy showed the structural similarity of the commercial sulfonated kraft lignin and the lignosulfonate, while the commercial alkali lignin showed more differences to these two in its spectra. Nevertheless, it is hard to point out the real structural differences between the lignins just from the FTIR spectra. The values of C, H, N, O and S were all in the expected range, yielding results comparable to these found in the literature for all tested lignins. The same can be said for the moisture and ash contents, where the values of the kraft lignins fitted the expected values well, while the sulfonated kraft lignin yielded a higher moisture content and a very high ash content, which seems to indicate that the method is not applicable to this type of lignin.

The second aim of the present work was the depolymerization of lignin by two different ways, by electrochemical oxidation and by high-pressure reduction.

The electrochemical oxidation reactions, carried out with a BDD anode and at current densities of 200 and 1000 A/m<sup>2</sup>, led all to the same products, independent of the current density. These products, identified via GC-MS, were CO<sub>2</sub>, formic acid, acetic acid, dimethyl sulfide in alkali lignin and sulfur dioxide in lignosulfonate. Thus, the used anode cleaves off small groups from the molecule, so that acetic acid reacts through formic acid to CO<sub>2</sub>, which then goes out of the reactor. The same can be said for the dimethyl sulfide and sulfur dioxide groups, as these correlate with components of the respective lignins. This theory is also supported by the decrease in COD, which means a loss of organic matter, and the decrease in molecular weight seen after SEC.

The high-pressure reactions in the batch reactor yielded various compounds identifiable by GC-MS, of which the majority were phenols and other aromatic structures. Examples include phenol, guaiacol and veratrole as well as alkane substituted phenols, guaiacols and veratrols. Interesting and unexpected products of the reduction were dehydroabietic acid methyl ester and other components of the resin like fatty acids, which are in the lignin fractions mainly due to incomplete skimming during or the general absence of tall oil production. The amount of phenolic compounds extracted, quantified via BHT, were the highest in the commercial alkali

lignin with 9.9–16.8 %, while the other two samples only showed amounts of 0.7–2.0 %, with the black liquor lignin reduction between them with 6.1 %. Although dehydroabietic acid methyl ester (DHAAME) should only make up a small amount of the lignins, it was found out by quantification via cholesterol as internal standard that DHAAME amounts of up to 7 % are present. Another important factor was the usage of hydrogen, as these reactions yielded a much higher content of product oil and phenols, while the solely thermal reactions yielded a high amount of char. A variation in temperature by 50 °C and in H<sub>2</sub> pressure by 20 bar led to no significant differences.

Further experiments are needed regarding the characterization and determination of the molecular weight by SEC of the educts as well as the products from reduction reactions. Also, a more exact characterization, for example with LC-TOF-MS, NMR and pyrolysis-GC-MS should be subject to further insight. For the electrochemical oxidation, further experiments need to be conducted with different electrode materials, which are more suitable to produce valuable chemicals from the lignin feedstock. There is a wide range of optimization needed in the high-pressure reductions, regarding H<sub>2</sub> pressure, reaction temperature and time, reactor loading and the type of catalyst to maximize the yield of product oil and minimize the amount of char produced. Also, the amount of phenols could be optimized in that way. There are also experiments for the extraction of phenols from the product oil possible, as well as for the isolation and separation of DHAAME. Finally, experiments for lignin functionalization could dramatically increase desired properties of the lignins, for example enhance the solubility.

## List of Figures

Figure 1: Schematic representation of the location of lignocelluloses in a plant (Adapted from Zakzeski et al.) <sup>4</sup> .....	2
Figure 2: Molecular structure of cellulose (n = DP) <sup>5</sup> .....	3
Figure 3: Structures of the main hemicelluloses in wood <sup>5</sup> .....	3
Figure 4: Structures of the monolignols (adapted from Li et al.) <sup>1</sup> .....	4
Figure 5: Linkages between monolignol units <sup>1</sup> .....	4
Figure 6: Biosynthesis pathway of the three monolignols (adapted from Guragain et al) <sup>14</sup> .....	6
Figure 7: Structural model of lignin (Li et al.) <sup>1</sup> .....	7
Figure 8: Wood processing prior to pulping <sup>22</sup> .....	7
Figure 9: Kraft process (example: Zellstoff Pöls AG) <sup>22</sup> .....	8
Figure 10: Structures of black liquor hydroxy acids .....	9
Figure 11: Structures of the most common resin acids (adapted from Fiebach; Grimm) <sup>30</sup> .....	11
Figure 12: Model of kraft pine lignin (adapted from Zakzeski et al.) <sup>4</sup> .....	13
Figure 13: Model of lignosulfonate (Zakzeski et al.) <sup>4</sup> .....	13
Figure 14: Proposed mechanism for vanillin production from lignosulfonates (adapted from Fache et al.) <sup>36</sup> .....	18
Figure 15: Schematic representation of a FTIR spectrometer <sup>40</sup> .....	20
Figure 16: (a) Hypothetical SEC calibration curve and (b) chromatogram <sup>46</sup> .....	22
Figure 17: Schematic representation of a quadrupole mass spectrometer <sup>49</sup> .....	23
Figure 18: Schematic representation of an ion detector <sup>49</sup> .....	25
Figure 19: Reaction scheme of the electrochemical oxidation of organic substances (M: electrode surface, R: organic substance) <sup>70</sup> .....	32
Figure 20: Setup of electrochemical oxidation reactions .....	55
Figure 21: Setup of electrochemical oxidation reactions with membrane .....	56
Figure 22: Three-phase-system after extraction with n-hexane .....	58
Figure 23: Typical temperature and pressure profile of a reduction experiment .....	61
Figure 24: FTIR spectrum of sulfonated kraft lignin .....	81
Figure 25: FTIR spectrum of alkali lignin .....	83
Figure 26: FTIR spectrum of thin liquor lignin .....	85
Figure 27: FTIR spectra of thin liquor lignin and sulfonated kraft lignin .....	87
Figure 28: FTIR spectrum of lignosulfonate .....	88
Figure 29: FTIR spectra of thin liquor lignin and lignosulfonate .....	89
Figure 30: Comparison of soxhlet reaction solvents during first and tenth cycle .....	94

Figure 31: Gas chromatogram of alkali lignin soxhlet extract.....	95
Figure 32: pH and COD change during sulfonated kraft lignin electrochemical oxidation V01 .....	98
Figure 33: FTIR spectrum of oxidized sulfonated kraft lignin (V01).....	99
Figure 34: FTIR spectra of sulfonated kraft lignin, unoxidized and oxidized (V01).....	101
Figure 35: Gas chromatograms of sulfonated kraft lignin educt (solid) and electrochemically oxidized V01 after 5h (dashed) .....	102
Figure 36: Gas chromatogram of sulfonated kraft lignin, electrochemically oxidized V01 (5h), first 5 minutes.....	102
Figure 37: Determination of excluded volume distribution by SEC with triple detection (adapted from Huber & Praznik) <sup>121</sup> .....	103
Figure 38: Molecular weight distribution of sulfonated kraft lignin before and after electrochemical oxidation .....	104
Figure 39: pH and COD change during kraft lignin electrochemical oxidation V02 .....	106
Figure 40: FTIR spectrum of oxidized sulfonated kraft lignin, unoxidized and oxidized (V02) .....	107
Figure 41: Gas chromatograms of sulfonated kraft lignin after 2h (left) and 3h (right) oxidation .....	109
Figure 42: pH and COD change during sulfonated kraft lignin electrochemical oxidation V03 .....	111
Figure 43: Gas chromatograms of alkali lignin before, during and after electrochemical oxidation.....	113
Figure 44: pH and COD change during thin liquor electrochemical oxidation V01 .....	115
Figure 45: FTIR spectrum of thin liquor, unoxidized and oxidized (V01).....	116
Figure 46: Gas chromatograms of thin liquor, before and after electrochemical oxidation V01 (3h) .....	118
Figure 47: Molecular weight distribution analysis of thin liquor before and after electrochemical oxidation.....	119
Figure 48: pH and COD change during thin liquor electrochemical oxidation V02 .....	120
Figure 49: FTIR spectrum of thin liquor, unoxidized and oxidized (V02) .....	121
Figure 50: Gas chromatograms of thin liquor, before and after electrochemical oxidation (3h), V02 .....	123
Figure 51: Gas chromatogram of alkali lignin reduction V01 .....	127
Figure 52: Chemical structures of guaiacols found after alkali lignin reduction .....	129

Figure 53: Chemical structure of veratrole .....	130
Figure 54: Chemical structure of dehydroabietic acid methyl ester.....	130
Figure 55: Gas chromatogram of alkali lignin thermal reaction V05 .....	135
Figure 56: Gas chromatogram of sulfonated kraft lignin reduction V07.....	139
Figure 57: Chemical structures of retene and 7-isopropyl-1-methyl-1,2,3,4-tetrahydrophenanthrene .....	141
Figure 58: Gas chromatogram of sulfonated kraft lignin reductions V07 vs V08.....	142
Figure 59: Gas chromatogram of sulfonated kraft lignin thermal reaction V09.....	146
Figure 60: Gas chromatogram of black liquor lignin reduction V10.....	149
Figure 61: Gas chromatogram of black liquor lignin thermal reaction V12.....	154
Figure 62: Chemical structures of dehydroabietic acid methyl ester and cholesterol.....	157
Figure 63: Gas chromatogram of DHAAME quantification.....	157
Figure 64: Gas chromatogram of quantification of phenolic compounds.....	161

## List of Tables

Table 1: Biomass compositions of different plant resources .....	2
Table 2: Percentage of linkages in softwood and hardwood lignins <sup>1,4,7,18,19</sup> .....	5
Table 3: Regions of the IR spectrum (adapted from Clayden et al.) <sup>37</sup> .....	19
Table 4: Electrode types, solvents and feedstocks used in lignin electrochemical oxidation..	33
Table 5: Products obtained from lignin electrochemical oxidation .....	34
Table 6: Summary of lignin reduction parameters.....	40
Table 7: Products obtained from lignin reduction.....	40
Table 8: Dilution series for molecular weight analysis of sulfonated kraft lignin.....	52
Table 9: Dilution series for molecular weight analysis of thin liquor.....	52
Table 10: Dilution series for molecular weight analysis of electrochemically oxidized sulfonated kraft lignin .....	53
Table 11: Dilution series for molecular weight analysis of electrochemically oxidized thin liquor .....	53
Table 12: GC-MS parameters for electrochemical oxidation analysis.....	59
Table 13: LC-TOF-MS parameters for electrochemical oxidation analysis .....	60
Table 14: Parameters of lignin reductions with hydrogen .....	61
Table 15: Parameters of lignin thermal reactions.....	62
Table 16: Parameters of alkali lignin reduction with hydrogen V01 .....	62
Table 17: Parameters of alkali lignin reduction with hydrogen V02 .....	63
Table 18: Parameters of alkali lignin reduction with hydrogen V03 .....	63
Table 19: Parameters of alkali lignin reduction with hydrogen V04 .....	64
Table 20: Parameters of alkali lignin thermal reaction V05 .....	64
Table 21: Parameters of alkali lignin thermal reaction V06 .....	65
Table 22: Parameters of sulfonated kraft lignin reduction with hydrogen V07.....	65
Table 23: Parameters of sulfonated kraft lignin reduction with hydrogen V08.....	66
Table 24: Parameters of sulfonated kraft lignin thermal reaction V09 .....	66
Table 25: Parameters of black liquor lignin reduction with hydrogen V10.....	67
Table 26: Parameters of black liquor lignin thermal reaction V11 .....	67
Table 27: Parameters of black liquor lignin thermal reaction V12 .....	68
Table 28: Amount of sample and cholesterol used for DHAAME quantification.....	68
Table 29: Amount of sample and cholesterol used for phenols quantification.....	69
Table 30: GC-MS parameters for reduction analysis.....	70
Table 31: Solubility of sulfonated kraft lignin in various solvents .....	74



Table 32: Solubility of thin liquor lignin in various solvents .....	75
Table 33: Solubility of alkali lignin in various solvents .....	76
Table 34: Solubility of alkali lignin in NaOH at different concentrations.....	77
Table 35: Solubility of black liquor lignin in various solvents .....	78
Table 36: Solubility of lignosulfonate in various solvents.....	80
Table 37: FTIR absorption frequencies and assigned vibrations of sulfonated kraft lignin <sup>102-104</sup> .....	82
Table 38: FTIR absorption frequencies and assigned vibrations of alkali lignin <sup>102-104</sup> .....	84
Table 39: FTIR absorption frequencies and assigned vibrations of thin liquor lignin <sup>102-104</sup> ...	86
Table 40: FTIR absorption frequencies and assigned vibrations of lignosulfonate <sup>102-104</sup> .....	88
Table 41: Elemental analysis of alkali and black liquor lignin .....	90
Table 42: Results of moisture content determination.....	91
Table 43: Results of ash content determination .....	93
Table 44: Identified peaks of the chromatogram (Figure 31) .....	95
Table 45: Results of phenolic compounds quantification in soxhlet extracted alkali lignin....	96
Table 46: Parameters of sulfonated kraft lignin electrochemical oxidation V01.....	98
Table 47: FTIR absorption frequencies and assigned vibrations of oxidized sulfonated kraft lignin (V01) <sup>102-104</sup> .....	100
Table 48: Parameters of sulfonated kraft lignin electrochemical oxidation with membrane V02 .....	106
Table 49: FTIR absorption frequencies and assigned vibrations of oxidized sulfonated kraft lignin (V02) <sup>102-104</sup> .....	108
Table 50: Parameters of sulfonated kraft lignin electrochemical oxidation V03.....	110
Table 51: Parameters of alkali lignin electrochemical oxidation.....	112
Table 52: Parameters of thin liquor electrochemical oxidation V01 .....	114
Table 53: FTIR absorption frequencies and assigned vibrations of electrochemically oxidized thin liquor (V01) <sup>102-104</sup> .....	116
Table 54: Parameters of thin liquor electrochemical oxidation V02 .....	120
Table 55: FTIR absorption frequencies and assigned vibrations of electrochemically oxidized thin liquor (V02) <sup>102-104</sup> .....	122
Table 56: Summary of lignin reductions with hydrogen.....	125
Table 57: Summary of lignin thermal reactions.....	125
Table 58: Mass balance of alkali lignin reduction V01.....	126
Table 59: Identified peaks of the chromatogram (Figure 51) .....	128

Table 60: Mass balance of alkali lignin reduction V02.....	131
Table 61: Mass balance of alkali lignin reduction V03.....	132
Table 62: Mass balance and of alkali lignin reduction V04.....	133
Table 63: Mass balance of alkali lignin thermal reaction V05.....	134
Table 64: Identified peaks of the chromatogram (Figure 55) .....	135
Table 65: Mass balance of alkali lignin thermal reaction V06 (2 <sup>nd</sup> step of V05).....	137
Table 66: Mass balance of alkali lignin thermal reactions V05+V06 (two-step reaction)....	137
Table 67: Mass balance of sulfonated kraft lignin reduction V07 .....	138
Table 68: Identified peaks of the chromatogram (Figure 56) .....	139
Table 69: Mass balance of sulfonated kraft lignin reduction V08 (2 <sup>nd</sup> step of V07) .....	142
Table 70: Identified peaks of the chromatogram (Figure 58) .....	143
Table 71: Mass balance of sulfonated kraft lignin thermal reactions V07+V08 (two-step reaction).....	144
Table 72: Mass balance of sulfonated kraft lignin thermal reaction V09 .....	145
Table 73: Identified peaks of the chromatogram (Figure 59) .....	146
Table 74: Mass balance of black liquor lignin reduction V10 .....	148
Table 75: Identified peaks of the chromatogram (Figure 60) .....	150
Table 76: Mass balance of black liquor lignin thermal reaction V11 .....	152
Table 77: Mass balance of black liquor lignin thermal reaction V12 .....	153
Table 78: Identified peaks of the chromatogram (Figure 61) .....	154
Table 79: Results of dehydroabietic acid methyl ester quantification .....	159
Table 80: Determined response factors for several phenolic compounds.....	162
Table 81: Results of phenolic compounds quantification .....	162

## References

1. Li, C., Zhao, X., Wang, A., Huber, G. W. & Zhang, T. Catalytic Transformation of Lignin for the Production of Chemicals and Fuels. *Chemical reviews* **115**, 11559–11624 (2015).
2. McCoy, M. Has lignin's time finally come? *Chemical & Engineering News* **94**, 35–37 (2016).
3. VTU Engineering. Homepage. Available at <http://www.vtu.com/de/>.
4. Zakzeski, J., Bruijninx, P. C. A., Jongerius, A. L. & Weckhuysen, B. M. The catalytic valorization of lignin for the production of renewable chemicals. *Chemical reviews* **110**, 3552–3599 (2010).
5. Pu, Y., Kosa, M., Kalluri, U. C., Tuskan, G. A. & Ragauskas, A. J. Challenges of the utilization of wood polymers: how can they be overcome? *Applied microbiology and biotechnology* **91**, 1525–1536 (2011).
6. Calvo-Flores, F. G. & Dobado, J. A. Lignin as renewable raw material. *ChemSusChem* **3**, 1227–1235 (2010).
7. Sameni, J. K. Physico-chemical Characterization of Lignin Isolated from Industrial Sources for Advanced Applications. Doctoral Thesis. University of Toronto, Nov. 2015.
8. Ragauskas, A. J., Beckham, G. T., Biddy, M. J., Chandra, R., Chen, F., Davis, M. F., Davison, B. H., Dixon, R. A., Gilna, P., Keller, M., Langan, P., Naskar, A. K., Saddler, J. N., Tschaplinski, T. J., Tuskan, G. A. & Wyman, C. E. Lignin valorization. Improving lignin processing in the biorefinery. *Science (New York, N.Y.)* **344**, 1246843 (2014).
9. McKendry, P. Energy production from biomass (part 1). Overview of biomass. *Bioresource Technology* **83**, 37–46 (2002).
10. Hallac, B. B. & Ragauskas, A. J. Analyzing cellulose degree of polymerization and its relevancy to cellulosic ethanol. *Biofuels, Bioprod. Bioref.* **5**, 215–225 (2011).
11. Gibson, L. J. The hierarchical structure and mechanics of plant materials. *Journal of the Royal Society, Interface* **9**, 2749–2766 (2012).
12. Sjöholm, E. in *Handbook Of Size Exclusion Chromatography And Related Techniques*, edited by C.-s. Wu (CRC Press 2003).
13. Xu, C., Arancon, R. A. D., Labidi, J. & Luque, R. Lignin depolymerisation strategies: towards valuable chemicals and fuels. *Chemical Society reviews* **43**, 7485–7500 (2014).

14. Guragain, Y. N., Herrera, A. I., Vadlani, P. V. & Prakash, O. Lignins of bioenergy crops. A review? *Natural product communications* **10**, 201–208 (2015).
15. Lange, H., Decina, S. & Crestini, C. Oxidative upgrade of lignin – Recent routes reviewed. *European Polymer Journal* **49**, 1151–1173 (2013).
16. Saake, B. & Lehnen, R. in *Ullmann's Encyclopedia of Industrial Chemistry* (Wiley-VCH Verlag GmbH & Co. KGaA, Weinheim, Germany, 2000).
17. Holladay, J. E., White, J. F., Bozell, J. J. & Johnson, D. Top Value-Added Chemicals from Biomass. Volume II-Results of Screening for Potential Candidates from Biorefinery Lignin. PNNL-16983. Pacific Northwest National Laboratory, 2007.
18. Chakar, F. S. & Ragauskas, A. J. Review of current and future softwood kraft lignin process chemistry. *Industrial Crops and Products* **20**, 131–141 (2004).
19. Norberg, I. *Carbon fibres from kraft lignin* (Chemical Science and Engineering, Royal Institute of Technology (KTH), Stockholm, 2012).
20. Zellstoff Pöls AG. Sustainability Folder. Available at [http://files.starkraft.com/WEB\\_Starkraft\\_extended\\_2017.pdf](http://files.starkraft.com/WEB_Starkraft_extended_2017.pdf) (2017).
21. Ragnar, M. in *Ullmann's Encyclopedia of Industrial Chemistry* (Wiley-VCH Verlag GmbH & Co. KGaA, Weinheim, Germany, 2000).
22. Zellstoff Pöls AG. Innovative production of pulp & paper. Pulp production. Available at <http://www.zellstoff-poels.at/en/products/production/> (2017).
23. Bajpai, P. *Pulp and paper industry. Chemicals* (Elsevier, Amsterdam, 2015).
24. Niemelä, K., Tamminen, T. & Ohra-aho, T. Black liquor components as potential raw materials. *TAPPSA Journal - Technical Articles* (2008).
25. Kornhauser, A., Coelho, S. G. & Hearing, V. J. Applications of hydroxy acids: classification, mechanisms, and photoactivity. *Clinical, cosmetic and investigational dermatology* **3**, 135–142 (2010).
26. Gilbert/Commonwealth. Assessment of black liquor recovery boilers. United States Department Of Energy, 1979.
27. Parrish, D. Black Liquor Recovery Boilers. An Introduction. Available at <http://www.nationalboard.org/index.aspx?pageID=164&ID=231> (1998).

28. Norlin, L.-H. in *Ullmann's Encyclopedia of Industrial Chemistry* (Wiley-VCH Verlag GmbH & Co. KGaA, Weinheim, Germany, 2000).
29. Aro, T. & Fatehi, P. Tall oil production from black liquor. Challenges and opportunities. *Separation and Purification Technology* **175**, 469–480 (2017).
30. Fiebach, K. & Grimm, D. in *Ullmann's Encyclopedia of Industrial Chemistry* (Wiley-VCH Verlag GmbH & Co. KGaA, Weinheim, Germany, 2000).
31. Lin, S. Y. in *Methods in lignin chemistry*, edited by S. Y. Lin (Springer-Verlag, Berlin, Heidelberg, 1992), pp. 75–80.
32. Nagy, M., Kosa, M., Theliander, H. & Ragauskas, A. J. Characterization of CO<sub>2</sub> precipitated Kraft lignin to promote its utilization. *Green Chem* **12**, 31–34 (2010).
33. Nobbmann, U. Polydispersity – what does it mean for DLS and chromatography? Available at <http://www.materials-talks.com/blog/2014/10/23/polydispersity-what-does-it-mean-for-dls-and-chromatography/> (2014).
34. Stepto, R. F. T. Dispersity in polymer science (IUPAC Recommendations 2009). *Pure and Applied Chemistry* **81** (2009).
35. Stewart, D. Lignin as a base material for materials applications. Chemistry, application and economics. *Industrial Crops and Products* **27**, 202–207 (2008).
36. Fache, M., Boutevin, B. & Caillol, S. Vanillin Production from Lignin and Its Use as a Renewable Chemical. *ACS Sustainable Chem. Eng.* **4**, 35–46 (2016).
37. Clayden, J., Greeves, N. & Warren, S. G. *Organic chemistry*. 2nd ed. (Oxford University Press, Oxford, op. 2012).
38. Atkins, P. W., Trapp, C. A. & Zillgitt, M. *Physikalische Chemie*. 4th ed. (VCH, Weinheim [u.a.], 2012).
39. Griffiths, P. R. & Haseetha, J. A. de. *Fourier transform infrared spectrometry*. 2nd ed. (Wiley, Hoboken, NJ, 2007).
40. Sanchonx. Interferometer for FTIR. Available at [https://upload.wikimedia.org/wikipedia/commons/a/a1/FTIR\\_Interferometer.png](https://upload.wikimedia.org/wikipedia/commons/a/a1/FTIR_Interferometer.png) (2011).
41. Salzer, R., Thiele, S. & Suemmchen, L. Reflexionsmethoden in der IR-Spektroskopie. ATR-Spektroskopie - Einführung. Available at [http://www.chemgapedia.de/vsengine/vlu/vsc/de/ch/3/anc/ir\\_spek/ir\\_reflexion.vlu/Page/vs](http://www.chemgapedia.de/vsengine/vlu/vsc/de/ch/3/anc/ir_spek/ir_reflexion.vlu/Page/vs)

- c/de/ch/3/anc/ir\_spek/ir\_spektroskopie/reflexionsmethoden/ir\_6\_1/atr\_m14ht0300.vscml.html.
42. Ettre, L. S. Nomenclature for chromatography (IUPAC Recommendations 1993). *Pure and Applied Chemistry* **65**, 819–872 (1993).
43. Salzer, R., Thiele, S., Zuern, A. & Zimmerer, C. Chromatographie - kompakt. Trennprinzip. Available at <http://www.chemgapedia.de/vsengine/vlu/vsc/de/ch/3/anc/croma/chromakompakt.vlu/Page/vsc/de/ch/3/anc/croma/chromakompakt/trennprinzip/trennprinzip0104.vscml.html>.
44. Thet, K. & Woo, N. Gas Chromatography. Available at [https://chem.libretexts.org/Core/Analytical\\_Chemistry/Instrumental\\_Analysis/Chromatography/Gas\\_Chromatography](https://chem.libretexts.org/Core/Analytical_Chemistry/Instrumental_Analysis/Chromatography/Gas_Chromatography) (2015).
45. AlphaCrom. Chromatographie Grundlagen. Available at <http://www.alphacrom.com/de/hplc-grundlagen> (2017).
46. Snyder, L. R., Kirkland, J. J. & Dolan, J. W. *Introduction to modern liquid chromatography*. 3rd ed. (Wiley, Hoboken N.J., 2010).
47. Striegel, A. M., Yau, W. W., Kirkland, J. J. & Bly, D. D. *Modern Size-Exclusion Liquid Chromatography. Practice of gel permeation and gel filtration chromatography*. 2nd ed. (John Wiley & Sons, Inc, Hoboken, NJ, USA, 2009).
48. Phenomenex. A User's Guide to Gel Permeation Chromatography. Technical Notes 3. Available at [http://phx.phenomenex.com/lib/PEG19951\\_Gel%20Permeation%20guide.pdf](http://phx.phenomenex.com/lib/PEG19951_Gel%20Permeation%20guide.pdf) (2000).
49. McMaster, M. C. *GC/MS. A practical user's guide*. 2nd ed. (Wiley-Interscience, Hoboken N.J., 2008).
50. Hübschmann, H.-J. *Handbook of GC-MS* (Wiley-VCH Verlag GmbH & Co. KGaA, Weinheim, Germany, 2015).
51. Hoffmann, E. de & Stroobant, V. *Mass Spectrometry. Principles and Applications*. 3rd ed. (Wiley, Somerset, 2013).
52. Balogh, M. P. *The mass spectrometry primer* (Waters, Milford, MA, 2013).
53. Wang, H., Tucker, M. & Ji, Y. Recent Development in Chemical Depolymerization of Lignin. A Review. *Journal of Applied Chemistry* **2013**, 1–9 (2013).

54. Zhao, C. & Lercher, J. A. in *The role of catalysis for the sustainable production of bio-fuels and bio-chemicals*, edited by K. S. Triantafyllidis, A. A. Lappas & M. Stöcker (Elsevier, Amsterdam, 2013), Vol. 1, pp. 289–320.
55. Beauchet, R., Monteil-Rivera, F. & Lavoie, J. M. Conversion of lignin to aromatic-based chemicals (L-chems) and biofuels (L-fuels). *Bioresource Technology* **121**, 328–334 (2012).
56. Toledano, A., Serrano, L. & Labidi, J. Improving base catalyzed lignin depolymerization by avoiding lignin repolymerization. *Fuel* **116**, 617–624 (2014).
57. Forchheim, D., Gasson, J. R., Hornung, U., Kruse, A. & Barth, T. Modeling the Lignin Degradation Kinetics in a Ethanol/Formic Acid Solvolysis Approach. Part 2. Validation and Transfer to Variable Conditions. *Ind. Eng. Chem. Res.* **51**, 15053–15063 (2012).
58. Hepditch, M. M. & Thring, R. W. Degradation of solvolysis lignin using Lewis acid catalysts. *Can. J. Chem. Eng.* **78**, 226–231 (2000).
59. Pandey, M. P. & Kim, C. S. Lignin Depolymerization and Conversion. A Review of Thermochemical Methods. *Chem. Eng. Technol.* **34**, 29–41 (2011).
60. Kosa, M., Ben, H., Theliander, H. & Ragauskas, A. J. Pyrolysis oils from CO<sub>2</sub> precipitated Kraft lignin. *Green Chem* **13**, 3196–3202 (2011).
61. Jiang, G., Nowakowski, D. J. & Bridgwater, A. V. A systematic study of the kinetics of lignin pyrolysis. *Thermochimica Acta* **498**, 61–66 (2010).
62. Miller, J. E., Evans, L. R., Littlewolf, A. E. & Trudell, D. E. Batch Microreactor Studies of Lignin Depolymerization by Bases. 1. Alcohol Solvents. Sandia National Laboratories.
63. Wahyudiono, Sasaki, M. & Goto, M. Recovery of phenolic compounds through the decomposition of lignin in near and supercritical water. *Chemical Engineering and Processing: Process Intensification* **47**, 1609–1619 (2008).
64. Alonso, D. M., Wettstein, S. G. & Dumesic, J. A. Bimetallic catalysts for upgrading of biomass to fuels and chemicals. *Chemical Society reviews* **41**, 8075–8098 (2012).
65. Voitl, T. & Rohr, P. R. v. Demonstration of a Process for the Conversion of Kraft Lignin into Vanillin and Methyl Vanillate by Acidic Oxidation in Aqueous Methanol. *Ind. Eng. Chem. Res.* **49**, 520–525 (2010).

66. Crestini, C., Pro, P., Neri, V. & Saladino, R. Methyltrioxorhenium. A new catalyst for the activation of hydrogen peroxide to the oxidation of lignin and lignin model compounds. *Bioorganic & medicinal chemistry* **13**, 2569–2578 (2005).
67. Ma, P. & Zhai, H. Selective TEMPO-Mediated Oxidation of Thermomechanical Pulp. *Bioresources* **8**, 4396–4405 (2013).
68. Wu, Y.-R. & He, J. Characterization of anaerobic consortia coupled lignin depolymerization with biomethane generation. *Bioresource Technology* **139**, 5–12 (2013).
69. Ma, Y.-S., Chang, C.-N., Chiang, Y.-P., Sung, H.-F. & Chao, A. C. Photocatalytic degradation of lignin using Pt/TiO<sub>2</sub> as the catalyst. *Chemosphere* **71**, 998–1004 (2008).
70. Marselli, B., Garcia-Gomez, J., Michaud, P.-A., Rodrigo, M. A. & Comninellis, C. Electrogeneration of Hydroxyl Radicals on Boron-Doped Diamond Electrodes. *J. Electrochem. Soc.* **150**, D79 (2003).
71. Woisetschläger, D. Elektrochemische Abwasserreinigung. Dissertation. Technische Universität Graz, 2012.
72. Stiefel, S., Marks, C., Schmidt, T., Hanisch, S., Spalding, G. & Wessling, M. Overcoming lignin heterogeneity. Reliably characterizing the cleavage of technical lignin. *Green Chem* **18**, 531–540 (2016).
73. Movil-Cabrera, O., Rodriguez-Silva, A., Arroyo-Torres, C. & Staser, J. A. Electrochemical conversion of lignin to useful chemicals. *Biomass and Bioenergy* **88**, 89–96 (2016).
74. Movil, O., Garlock, M. & Staser, J. A. Non-precious metal nanoparticle electrocatalysts for electrochemical modification of lignin for low-energy and cost-effective production of hydrogen. *International Journal of Hydrogen Energy* **40**, 4519–4530 (2015).
75. Reichert, E., Wintringer, R., Volmer, D. A. & Hempelmann, R. Electro-catalytic oxidative cleavage of lignin in a protic ionic liquid. *Physical chemistry chemical physics : PCCP* **14**, 5214–5221 (2012).
76. Pan, K., Tian, M., Jiang, Z.-H., Kjartanson, B. & Chen, A. Electrochemical oxidation of lignin at lead dioxide nanoparticles photoelectrodeposited on TiO<sub>2</sub> nanotube arrays. *Electrochimica Acta* **60**, 147–153 (2012).
77. Tolba, R., Tian, M., Wen, J., Jiang, Z.-H. & Chen, A. Electrochemical oxidation of lignin at IrO<sub>2</sub>-based oxide electrodes. *Journal of Electroanalytical Chemistry* **649**, 9–15 (2010).



78. Tian, M., Wen, J., MacDonald, D., Asmussen, R. M. & Chen, A. A novel approach for lignin modification and degradation. *Electrochemistry Communications* **12**, 527–530 (2010).
79. Parpot, P., Bettencourt, A. P., Carvalho, A. M. & Belgsir, E. M. Biomass conversion: attempted electrooxidation of lignin for vanillin production. *J Appl Electrochem* **30**, 727–731 (2000).
80. Shao, D., Liang, J., Cui, X., Xu, H. & Yan, W. Electrochemical oxidation of lignin by two typical electrodes. Ti/SbSnO<sub>2</sub> and Ti/PbO<sub>2</sub>. *Chemical Engineering Journal* **244**, 288–295 (2014).
81. Moodley, B., Mulholland, D. A. & Brookes, H. C. The electro-oxidation of lignin in Sappi Saiccor dissolving pulp mill effluent. *WSA* **37** (2011).
82. Smith, C., Utley, J. H. P., Petrescu, M. & Viertler, H. Biomass electrochemistry. Anodic oxidation of an organo-solv lignin in the presence of nitroaromatics. *J Appl Electrochem* **19**, 535–539 (1989).
83. Zhu, H., Chen, Y., Qin, T., Wang, L., Tang, Y., Sun, Y. & Wan, P. Lignin depolymerization via an integrated approach of anode oxidation and electro-generated H<sub>2</sub>O<sub>2</sub> oxidation. *RSC Adv.* **4**, 6232 (2014).
84. Zhu, H., Wang, L., Chen, Y., Li, G., Li, H., Tang, Y. & Wan, P. Electrochemical depolymerization of lignin into renewable aromatic compounds in a non-diaphragm electrolytic cell. *RSC Adv.* **4**, 29917 (2014).
85. Mortensen, P. M., Grunwaldt, J.-D., Jensen, P. A., Knudsen, K. G. & Jensen, A. D. A review of catalytic upgrading of bio-oil to engine fuels. *Applied Catalysis A: General* **407**, 1–19 (2011).
86. Narani, A., Chowdari, R. K., Cannilla, C., Bonura, G., Frusteri, F., Heeres, H. J. & Barta, K. Efficient catalytic hydrotreatment of Kraft lignin to alkylphenolics using supported NiW and NiMo catalysts in supercritical methanol. *Green Chem* **17**, 5046–5057 (2015).
87. Joffres, B., Lorentz, C., Vidalie, M., Laurenti, D., Quoineaud, A.-A., Charon, N., Daudin, A., Quignard, A. & Geantet, C. Catalytic hydroconversion of a wheat straw soda lignin. Characterization of the products and the lignin residue. *Applied Catalysis B: Environmental* **145**, 167–176 (2014).

88. Jongerius, A. L., Bruijninx, P. C. A. & Weckhuysen, B. M. Liquid-phase reforming and hydrodeoxygenation as a two-step route to aromatics from lignin. *Green Chem.* **15**, 3049 (2013).
89. Jie-wang, Y., Gui-zhen, F. & Chun-de, J. Hydrogenation of Alkali Lignin Catalyzed by Pd/C. *APCBEE Procedia* **3**, 53–59 (2012).
90. Oasmaa, A., Alén, R. & Meier, D. Catalytic hydrotreatment of some technical lignins. *Bioresource Technology* **45**, 189–194 (1993).
91. Torr, K. M., van de Pas, D. J., Cazeils, E. & Suckling, I. D. Mild hydrogenolysis of in-situ and isolated *Pinus radiata* lignins. *Bioresource Technology* **102**, 7608–7611 (2011).
92. Thring, R. W. & Breau, J. Hydrocracking of solvolysis lignin in a batch reactor. *Fuel* **75**, 795–800 (1996).
93. Harris, E. E., Saeman, J. F. & Bergstrom, C. B. Lignin Hydrogenation Products. *Ind. Eng. Chem.* **41**, 2063–2067 (1949).
94. Olcay, A. Investigations on Lignin and Lignification. XXV. Hydrogenation of Milled-Wood Lignins from White Pine and Blue Spruce. *J. Org. Chem.* **27**, 1783–1786 (1962).
95. Meissner, M. Beiträge zur katalytischen Hydrierung und Isomerisierung von Fettderivaten. Masterarbeit. Technische Universität Graz, März 2016.
96. Howard, G. C. *Lignin derivatives and process of making same* (United States Patent Office, 1934), <https://www.google.com/patents/US1981176>.
97. Haars, A., Bauer, A. & Hüttermann, A. Precipitation of Lignosulfonates with Polyimines. - Effect of Structural Properties and Reaction Conditions on Quantitative Precipitation. *Holzforschung* **38**, 171–176 (1984).
98. Lange, H., Bartzoka, E. & Crestini, C. in *Biorefineries*, edited by M. Aresta, A. Dibenedetto & F. Dumeignil (de Gruyter, Berlin, 2015).
99. García, A., Toledano, A., Serrano, L., Egüés, I., González, M., Marín, F. & Labidi, J. Characterization of lignins obtained by selective precipitation. *Separation and Purification Technology* **68**, 193–198 (2009).
100. Kamble, S. V. & Bhattacharyulu, Y. C. Selective separation of biomass from black liquor waste by inorganic and organic acids. *International Journal of Advanced Research* **3**, 684–692 (2015).

101. Luong, N. D., Binh, N. T. T., Le Duong, D., Kim, D. O., Kim, D.-S., Lee, S. H., Kim, B. J., Lee, Y. S. & Nam, J.-D. An eco-friendly and efficient route of lignin extraction from black liquor and a lignin-based copolyester synthesis. *Polym. Bull.* **68**, 879–890 (2012).
102. OChemOnline. Infrared spectroscopy absorption table. Available at [http://www.ochemonline.com/Infrared\\_spectroscopy\\_absorption\\_table](http://www.ochemonline.com/Infrared_spectroscopy_absorption_table) (2011).
103. William Reusch. Infrared Spectroscopy. Available at <https://www2.chemistry.msu.edu/faculty/reusch/virttxtjml/Spectrpy/InfraRed/infrared.htm> (2013).
104. St. Thomas. Spectroscopic Tools. Available at <http://www.science-and-fun.de/tools/>.
105. Fițiḡău, I. F., Peter, F. & Boeriu, C. G. Structural Analysis of Lignins from Different Sources. *International Journal of Chemical, Molecular, Nuclear, Materials and Metallurgical Engineering*, volume = 7, 167–172 (2013).
106. El Mansouri, N.-E., Yuan, Q. & Huang, F. Synthesis and characterization of kraft lignin-based epoxy resins. *Bioresources* **6**, 2492–2503 (2011).
107. Derkacheva, O. & Sukhov, D. Investigation of Lignins by FTIR Spectroscopy. *Macromol. Symp.* **265**, 61–68 (2008).
108. Nasrazadani, S. & Eureste, E. Application of FTIR for Quantitative Analysis of Lime. University of North Texas, 2008.
109. Darroudi, M., Bagherpour, M., Hosseini, H. A. & Ebrahimi, M. Biopolymer-assisted green synthesis and characterization of calcium hydroxide nanoparticles. *Ceramics International* **42**, 3816–3819 (2016).
110. Sahoo, S., Seydibeyoḡlu, M.Ö., Mohanty, A. K. & Misra, M. Characterization of industrial lignins for their utilization in future value added applications. *Biomass and Bioenergy* **35**, 4230–4237 (2011).
111. Benigni, J. D. & Goldstein, I. S. Hydrogenation of kraft lignin. *J. polym. sci., C Polym. symp.* **36**, 477–488 (1971).
112. Leitner, S., Gratzl, G., Paulik, C. & Weber, H. Carbon Materials from Lignin and Sodium Lignosulfonate via Diisocyanate Cross-Linking and Subsequent Carbonization. *C* **1**, 43–57 (2015).
113. Klapiszewski, Ł., Zdarta, J., Szatkowski, T., Wysokowski, M., Nowacka, M., Szwarc-Rzepka, K., Bartczak, P., Siwińska-Stefańska, K., Ehrlich, H. & Jesionowski, T.

- Silica/lignosulfonate hybrid materials. Preparation and characterization. *cent.eur.j.chem.* **12**, 719–735 (2014).
114. TAPPI. *T 211 om-02 Ash in wood, pulp, paper and paperboard: combustion at 525°C* (Technical Association of the Pulp and Paper Industry, Peachtree Corners, Georgia, USA, 2002).
115. TAPPI. *T 210 cm-03 Sampling and testing wood pulp shipments for moisture* (Technical Association of the Pulp and Paper Industry, Peachtree Corners, Georgia, USA, 2003).
116. Leger, C. A., Chan, F. D. & Schneider, M. H. Fractionation and characterisation of technical ammonium lignosulphonate. *Bioresources* **5**, 2239–2247 (2010).
117. Vishtal, A. & Kraslawski, A. Challenges in industrial applications of technical lignins. *Bioresources* **6**, 3547–3568 (2011).
118. Jablonsky, M., Kocis, J., Haz, A. & Sima, J. Characterization and comparison by UV spectroscopy of precipitated lignins and commercial lignosulfonates. *Cellulose Chem. Technol.* **49**, 267–274 (2015).
119. Zhou, X.-F. Conversion of kraft lignin under hydrothermal conditions. *Bioresource Technology* **170**, 583–586 (2014).
120. Gosselink, R.J.A., Abächerli, A., Semke, H., Malherbe, R., Käuper, P., Nadif, A. & van Dam, J.E.G. Analytical protocols for characterisation of sulphur-free lignin. *Industrial Crops and Products* **19**, 271–281 (2004).
121. Huber, A. & Praznik, W. in *Renewable bioresources*, edited by C. V. Stevens & R. Verhé (Wiley, Chichester, West Sussex, England, Hoboken, NJ, 2004), pp. 138–159.